



University
of Glasgow

Pass, Chloe (2011) *The role of suppressor of cytokine signalling-2 in endochondral bone growth.*
PhD thesis.

<http://theses.gla.ac.uk/2832/>

Copyright and moral rights for this thesis are retained by the author

A copy can be downloaded for personal non-commercial research or study, without prior permission or charge

This thesis cannot be reproduced or quoted extensively from without first obtaining permission in writing from the Author

The content must not be changed in any way or sold commercially in any format or medium without the formal permission of the Author

When referring to this work, full bibliographic details including the author, title, awarding institution and date of the thesis must be given

THE ROLE OF SUPPRESSOR OF CYTOKINE SIGNALLING-2 IN ENDOCHONDRAL BONE GROWTH

Chloë Pass

BSc (Hons) The University of Edinburgh

This thesis is submitted for the degree of Doctor of
Philosophy at The University of Glasgow, Faculty of
Medicine

June, 2011



**UNIVERSITY
of
GLASGOW**



Abstract

Suppressor of Cytokine Signalling-2 (SOCS2) is a negative regulator of growth hormone (GH) signalling and bone growth via inhibition of the JAK/STAT pathway. This has been classically demonstrated by the overgrowth phenotype of SOCS2^{-/-} mice which have normal systemic IGF-1 levels. The local effects of GH on bone growth are equivocal and therefore this study aimed to understand better the SOCS2 signalling mechanisms mediating the local actions on epiphyseal chondrocytes and bone growth.

SOCS2, in contrast to SOCS1 and SOCS3 expression, was increased in cultured chondrocytes following GH challenge; and gain-and-loss of function studies indicated that SOCS2 acts to negatively regulate GH stimulated chondrocyte STAT phosphorylation. This was confirmed by the observation that GH stimulates the longitudinal growth of cultured SOCS2^{-/-} embryonic metatarsals and the proliferation of chondrocytes within. Consistent with this; bone growth rates, growth plate zone widths and chondrocyte proliferation were all increased in 6-week old SOCS2^{-/-} mice as was the number of phosphorylated STAT-5 positive hypertrophic chondrocytes. The results of these studies indicate that the SOCS2^{-/-} mouse represents a valid model for studying the local effects of GH and IGF-1 on bone growth.

Chronic paediatric inflammatory diseases are well accepted to lead to growth retardation and this is likely due to raised inflammatory cytokine levels and reduced GH/IGF-1 signalling. Whilst SOCS2 was not found to be increased in response to inflammatory cytokines, SOCS2^{-/-} mice were protected from LPS-induced growth retardation indicating that SOCS2 antagonists may help ameliorate the negative effects of chronic inflammation on growth.

Declaration

I declare that this thesis has been composed entirely by the candidate, Chloë Pass. This work has not previously been submitted for a Doctor of Philosophy, a degree or any professional qualification. I have done all the work, unless acknowledged otherwise. All sources of information have been acknowledged.

Chloë Pass

“Success is not final, failure is not fatal: it is the courage to continue that counts.”

Winston Churchill (1874-1965)

Acknowledgements

I would firstly like to thank my supervisors Professor Colin Farquharson, Professor Faisal Ahmed and Dr Vicky MacRae for their help and support throughout my PhD. I have been very fortunate to receive outstanding supervision, support and advice, and have been encouraged to present my work at many national and international meetings. This has made my PhD a challenging, fulfilling experience and a valuable education.

Thank you to everyone else in The Bone Biology Group at Roslin, the group has been so vibrant, friendly and helpful and I have enjoyed working with you all.

Thanks to the small animal unit at Roslin, in particular Tricia Mathieson who has been exceptional at organising the mice.

I would also like to thank the BBSRC for funding this project.

My friends and family have supported me throughout my degree and PhD. My parents have always supported and encouraged me in the choices I have made and I am deeply grateful to them for this. A special thank you to my husband Richard who is incredibly supportive, patient and understanding.

Refereed Publications

Pass C, MacRae VE, Ahmed SF, Farquharson C (2009) Inflammatory cytokines and the GH/IGF-1 axis: novel actions on bone growth. *Cell Biochemistry and Function* **27(3)**: 119-127. (Appendix 4).

Pass C, MacRae VE, Ahmed SF, Farquharson C (2011) SOCS2 is the critical regulator of GH action in murine growth plate chondrogenesis. **Under consideration with *Journal of Bone and Mineral Research*.**

Published Meeting Abstracts

Pass C, MacRae VE, Ahmed SF, Farquharson C (2008) The Potential Inhibitory Role of Suppressor of Cytokine Signalling-2 in Chondrocyte GH/IGF-1 Signalling via the JAK/STAT Pathway. *Calcified Tissue International* **83(1)**: 32.

Pass C, MacRae VE, Ahmed SF, Farquharson C (2009) The Potential Inhibitory Role of SOCS2 in Chondrocyte GH/IGF-1 Signalling During Chronic Inflammatory Diseases. *Endocrine Abstracts* **19**: P8.

Pass C, MacRae VE, Ahmed SF, Farquharson C (2009) The inhibitory role of suppressor of cytokine signalling-2 (SOCS2) on STAT signalling in the growth plate. *Calcified Tissue International* **85(2)**: 168.

Pass C, MacRae VE, Ahmed SF, Farquharson C (2009) Suppressor of cytokine signaling-2 inhibition of STAT signaling in the growth plate. *Hormone Research* **72(S3)**: 1-2.

Pass C, MacRae VE, Ahmed SF, Farquharson C (2009) Inhibition of chondrocyte STAT signaling by suppressor of cytokine signaling-2. *Journal of Bone and Mineral Research* **24**: S1.

Pass C, MacRae VE, Ahmed SF, Farquharson C (2010) SOCS2 Regulates Growth by Inhibiting GH Signalling in Chondrocytes. *Bone* **46**: S78-S79.

Pass C, MacRae VE, Ahmed SF, Farquharson C (2010) Does SOCS2 mediate inflammatory induced growth retardation? *Endocrine Abstracts* **21**: P125.

Pass C, MacRae VE, Ahmed SF, Farquharson C (2010) Reduced bone growth in chronic inflammatory conditions – a role for SOCS2? *Bone* **47(S1)**: S43.

Unpublished Meeting Abstracts

Pass C, MacRae VE, Ahmed SF, Farquharson C (2008) JAK/STAT Signaling in Chondrocytes and the Potential Inhibitory Role of SOCS2. *ENDO 2008: 90th Annual Meeting of the Endocrine Society, San Francisco, June 2008*.

Pass C, MacRae VE, Ahmed SF, Farquharson C (2008) The Potential Inhibitory Role of Suppressor of Cytokine Signalling-2 (SOCS2) in Chondrocyte GH/IGF-1 Signalling via the JAK/STAT pathway. *European Workshop on Growth Plate Research, Glasgow, July 2008*.

MacRae VE, Horvat S, Pells SC, **Pass C**, Dale H, Collinson RS, Pitsillides AA, Ahmed SF, Farquharson C (2008) Increased bone mass, altered trabecular architecture and modified growth plate organisation in the growing skeleton of SOCS2 deficient mice. *ESPE Growth Plate Working Group, Istanbul, September 2008*.

Pass C, MacRae VE, Ahmed SF, Farquharson C (2008) JAK/STAT Signalling in Chondrocytes and the Potential Inhibitory Role of SOCS2. *Yorkhill Children's Hospital Research Day, Glasgow, December 2008*.

Pass C, MacRae VE, Ahmed SF, Farquharson C (2010) SOCS2 is a Critical Regulator of GH Action in the Embryonic Metatarsal Model of Longitudinal Growth. *2nd European Workshop on Growth Plate Research, Stockholm, July 2010*.

Pass C, MacRae VE, Ahmed SF, Farquharson C (2011) SOCS2 is the Key Regulator of GH-Induced STAT Activation in Chondrocytes. *ENDO 2011: 93rd Annual Meeting of the Endocrine Society & Expo, Boston, June 2011.*

Achievements

Bone Research Society Diamond Jubilee Travel Award towards attendance at 37th ECTS Meeting, Glasgow, 2010.

Henning Anderson Prize for Best Abstract in Basic Science: 8th Joint LWPES/ESPE Meeting, New York, 2009.

Society for Endocrinology Conference Grant: £750 towards attending 8th Joint LWPES/ESPE Meeting, New York, 2009.

Roberts Travelling Fellowship (University of Glasgow): £816 towards attending ASBMR 31st Annual Meeting, Denver, 2009.

Bone Research Society Travel Grant towards attending 2nd Joint BRS/BSMB Meeting, 2009.

Society for Endocrinology Conference Grant: £500 towards attending SfE BES Meeting, 2009.

SHIL Innovation and Enterprise Award for oral presentation at Yorkhill Children's Hospital Research Day, Glasgow, 2008.

Bone Research Society Travel Grant towards attending BRS/BORS 2nd Joint Meeting, 2008

List of Abbreviations

-/-	Knockout
A₂₆₀	Absorbance read at 260nm
A₂₈₀	Absorbance read at 280nm
ALS	Acid-labile subunit
ANOVA	Analysis of variance
bp	Base pairs
BMD	Bone mineral density
BMPs	Bone morphogenetic proteins
BrdU	5-bromo-2'-deoxyuridine
BSA	Bovine Serum Albumin
°C	Degree Celsius
Ca	Calcium
cDNA	Complementary DNA
CIS	Cytokine-induced Src homology 2
cm	Centimetre
CO₂	Carbon dioxide
con	Control
Ct	Threshold cycle
DAB	3,3'-diaminobenzidine
dH₂O	Distilled water
DMEM	Dulbecco's modified Eagle's medium
DMSO	Dimethyl sulfoxide
DNA	Deoxyribonucleic acid
dNTP	Deoxyribonucleotide triphosphate

DPM	Depreciations per minute
DSS	Dextran sodium sulphate
ECL	Enhanced Chemiluminescence
<i>E. coli</i>	<i>Escherichia coli</i>
EDTA	Ethylenediamine tetra-acetic acid
ERK	Extracellular signal-regulated kinase
ES	Embryonic stem
FBS	Fetal bovine serum
FGF	Fibroblast growth factor
g	Gram(s)
GH	Growth hormone
GHR	Growth hormone receptor
H₂O	Water
H₂O₂	Hydrogen peroxide
HBSS	Hank's Buffered Salt Solution
HCl	Hydrogen chloride
HDAC4	Histone deacetylase-4
H&E	Haematoxylin and eosin
hg	High growth
HRP	Horseradish peroxidase
hrs	Hours
IBD	Inflammatory bowel disease
IFN-γ	Interferon-gamma
IGF-1	Insulin-like growth factor-1
IGF-1R	Insulin-like growth factor-1 receptor

IGFBP-1	IGF-1 binding protein-1
IGFBP-3	IGF-1 binding protein-3
IgG	Immunoglobulin G
Ihh	Indian hedgehog
IL	Interleukin
IL-1RI	Interleukin 1 receptor 1
IL-1RII	Interleukin 1 receptor 2
i.p.	Intraperitoneal
IRS-1	Insulin receptor substrate 1
ITS	Insulin transferring selenium
JAK	Janus Kinase
JIA	Juvenile idiopathic arthritis
kDa	Kilodaltons
kg	Kilogram
KO	Knockout
l	Litre
LB	Luria-Bertani broth
LIF	Leukemia inhibitory factor
LPS	Lipopolysaccharide
M	Molar
MAPK	Mitogen activated protein kinase
min(s)	Minute(s)
mg	Milligrams
MgCl₂	Magnesium chloride
ml	Millilitre

mm	Millimetre
mM	Millimolar
MMP	Matrix metalloproteinase
MOPS	4-Morpholinepropanesulfonic acid
n	Number (of samples)
NaCl	Sodium chloride
NaOH	Sodium hydroxide
NBF	Neutral buffered formaldehyde
NFW	Nuclease free water
ng	Nanograms
nm	Nanometres
OSE1	Osteoblast-specific cis-acting element 1
OSE2	Osteoblast-specific cis-acting element 2
P-	Phosphorylated
PBS	Phosphate buffered saline
PCR	Polymerase chain reaction
PI3K	Phosphatidylinositol 3-kinase
pmol	Picomoles
PTHrP	Parathyroid hormone-related peptide
P value (P)	Probability value
qPCR	Quantitative Polymerase Chain Reaction
RNA	Ribonucleic acid
rpm	Rotations per minute
RT-PCR	Reverse transcription PCR
Runx2	Runt-related transcription factor 2

SDS	Sodium dodecyl sulphate
sec(s)	Second(s)
SEM	Standard error of the mean
SH2	Src Homology 2
SOCS	Suppressor of cytokine signalling
Sox	Sry-type HMG box binding
STAT	Signal Transduction and Activators of Transcription
TAE	Tris-acetate-EDTA
TBE	Tris-borate-EDTA
TBS/T	Tris-buffered saline/Tween-20
TCA	Trichloroacetic acid
TE	Tris/EDTA
TGF-β	Transforming growth factor-beta
TNBS	Trinitrobenzenesulphonic acid
TNFα	Tumour necrosis factor-alpha
TRAP	Tartrate-resistant acid phosphatase
Tris	Tris (hydroxymethyl)aminomethane
U	Unit(s)
μCi	Micro -Curie
μCT	Micro computer tomography
UDG	Uracil DNA glycosylase
μg	Micrograms
μl	Microlitres
μm	Micrometre
μM	Micromolar

UV	Ultraviolet
V	Volts
VEGF	Vascular endothelial growth factor
vol.	Volume
wk	Week
WT	Wild-type
wt.	Weight

Table of Contents

1. INTRODUCTION	1
1.1. Bone Biology	1
1.1.1. Bone Structure and Function	1
1.1.2. Bone Growth	2
1.1.3. Bone turnover	2
1.1.4. Osteoclasts	4
1.1.5. Osteoblasts	4
1.1.6. Osteocytes	5
1.1.7. Chondrocytes	6
1.2. Endochondral Growth	6
1.2.1. The Growth Plate	6
1.2.2. Resting chondrocytes	9
1.2.3. Proliferating Chondrocytes	9
1.2.4. Hypertrophic chondrocytes	9
1.2.5. Terminal Differentiation	10
1.3. Regulation of Endochondral Growth Rate	11
1.3.1. Chondrocyte Proliferation and hypertrophy	11
1.3.2. Endocrine Factors	11
1.3.3. Autocrine and Paracrine Factors	14
1.4. GH and IGF-1 Signalling	17
1.4.1. GH Receptor Signalling	17
1.4.2. IGF-1 Signalling	20
1.4.3. GH and IGF-1 Regulation of Endochondral Growth	23
1.5. Inflammatory Cytokine Inhibition of Bone Growth	25
1.5.1. Paediatric Diseases Affecting Bone Growth	25
1.5.2. Inflammatory Cytokines and Endochondral Growth	26
1.6. Suppressor of Cytokine Signalling-2	27
1.6.1. SOCS Proteins	27
1.6.2. SOCS2 Knockout Mouse	31
1.6.3. Over-expression of SOCS2	33
1.6.4. SOCS2 and GH Signalling	33
1.7. Aims	35
2. MATERIALS AND METHODS	38
2.1. Materials	38
2.2. Cell Culture	38
2.2.1. ATDC5 Cells	38
2.2.2. Freezing/Thawing Cells	39

2.3.	In vivo Studies	39
2.3.1.	Animal Welfare	39
2.3.2.	Generation of SOCS2 Knockout Mice	39
2.3.3.	Tail/Ear Biopsies for Genotyping	40
2.3.4.	DNA Isolation for Genotyping	40
2.3.5.	Genotyping	41
2.3.6.	Growth Analysis	42
2.3.7.	Isolating Primary Chondrocytes	44
2.3.8.	Isolating Primary Osteoblasts	46
2.3.9.	Calcein Labelling	46
2.3.10.	BrdU Incorporation	47
2.3.11.	Isolating Embryonic Metatarsals	47
2.3.12.	LPS Model of Inflammation	49
2.3.13.	DSS Induced Colitis Model	49
2.4.	Proliferation Assays	50
2.4.1.	Cell [³ H]Thymidine Proliferation Assay	50
2.4.2.	Metatarsal [³ H]Thymidine Proliferation Assay	50
2.5.	Processing Tissue	51
2.5.1.	Paraffin Embedding Tissue	51
2.5.2.	Frozen Tissue	52
2.5.3.	Immunohistochemistry of BrdU	54
2.5.4.	Toluidine Blue Staining	55
2.5.5.	Von Kossa and H&E Staining	56
2.5.6.	Immunohistochemistry of Phosphorylated STAT5	56
2.6.	Transfecting ATDC5 Cells	58
2.6.1.	SOCS2 Over-expression and Control Plasmids	58
2.6.2.	Transformation of <i>E. coli</i>	59
2.6.3.	Preparing Glycerol Stocks	59
2.6.4.	Minipreparation of Plasmid DNA	61
2.6.5.	Restriction Digest	61
2.6.6.	EndoFree Maxipreparation of Plasmid DNA	62
2.6.7.	Transfection of ATDC5 Cells	63
2.6.8.	Growing Single Colonies of Transfected Cells	64
2.7.	PCR	66
2.7.1.	RNA Isolation	66
2.7.2.	Reverse Transcription	66
2.7.3.	Polymerase Chain Reaction (PCR)	67
2.7.4.	Quantitative PCR (qPCR)	68
2.8.	Western Blotting	72
2.8.1.	Extracting Protein	72
2.8.2.	Western Blot	72
2.8.3.	Stripping Nitrocellulose	75
2.9.	Statistical Analysis	75

3. ESTABLISHING GH, IGF-1 AND SOCS SIGNALLING IN THE GROWTH PLATE	78
3.1. Introduction	78
3.2. Aims and Hypothesis	81
3.2.1. Hypothesis	81
3.2.2. Aims	81
3.3. Materials and Methods	81
3.3.1. Cell culture	81
3.3.2. RT-PCR	82
3.3.3. Western Blotting	82
3.4. Results	82
3.4.1. Expression of GH, IGF-1 and IL-1 β Receptors in Chondrocytes	82
3.4.2. STAT Phosphorylation in Response to GH and IGF-1	84
3.4.3. The Effects of Inflammatory Cytokines on STAT Signalling	84
3.4.4. IGF-1 Signalling in Chondrocytes	86
3.4.5. The Expression of SOCS Proteins in Chondrocytes	88
3.4.6. The Expression of SOCS2 in Osteoblasts	90
3.5. Discussion	91
3.6. Conclusion	94
4. ANALYSING THE SOCS2^{-/-} GROWTH PHENOTYPE	96
4.1. Introduction	96
4.2. Aims and Hypothesis	98
4.2.1. Hypothesis	98
4.2.2. Aims	98
4.3. Materials and Methods	99
4.3.1. Growth Analysis	99
4.3.2. Analysis of Growth Plate Dynamics	99
4.3.3. μ CT Analysis	100
4.4. Results	100
4.4.1. SOCS2 ^{-/-} Growth Curves	100
4.4.2. Growth Plate Zone Widths in SOCS2 ^{-/-} Mice	101
4.4.3. Chondrocyte Proliferation in SOCS2 ^{-/-} Mice	104
4.4.4. SOCS2 ^{-/-} Endochondral Growth Rate	104
4.4.5. μ CT Analysis of SOCS2 ^{-/-} Mice	107
4.5. Discussion	110
4.6. Conclusion	113

5. THE EFFECTS OF SOCS2 ON GH SIGNALLING THROUGH STAT PROTEINS IN CHONDROCYTES	115
5.1. Introduction	115
5.2. Aims and Hypothesis	116
5.2.1. Hypothesis	116
5.2.2. Aims	117
5.3. Materials and Methods	117
5.3.1. Cell Culture	117
5.3.2. Western Blotting	118
5.3.3. PhosphoSTAT5 Immunohistochemistry	118
5.3.4. qPCR	118
5.4. Results	118
5.4.1. Temporal STAT Phosphorylation in SOCS2 ^{-/-} Chondrocytes in Response to GH	118
5.4.2. Temporal Expression of SOCS1 and SOCS3 in SOCS2 ^{-/-} Chondrocytes in Response to GH	119
5.4.3. The Effect of SOCS2 Over-Expression on STAT Signalling in Response to GH	121
5.4.4. Immunohistochemistry of Phosphorylated STAT5 in the Growth Plate	123
5.4.5. IGF-1 Expression in Primary Chondrocytes	123
5.5. Discussion	126
5.6. Conclusion	130
6. DIRECT EFFECTS OF INCREASED GH SIGNALLING IN SOCS2^{-/-} METATARSALS	132
6.1. Introduction	132
6.2. Aims and Hypothesis	134
6.2.1. Hypothesis	134
6.2.2. Aims	134
6.3. Materials and Methods	134
6.3.1. Cell Culture	134
6.3.2. Embryonic Metatarsal Culture	135
6.3.3. [³ H]Thymidine Proliferation Assay	135
6.3.4. Metatarsal Von Kossa and H&E Staining	135
6.4. Results	135
6.4.1. Chondrocyte Proliferation in Response to GH and IGF-1	135
6.4.2. Growth of WT and SOCS2 ^{-/-} Metatarsals in Response to GH and IGF-1	136
6.4.3. SOCS2 ^{-/-} and WT Metatarsal Proliferation in Response to GH and IGF-1	140
6.4.4. Zone Widths in SOCS2 ^{-/-} and WT Metatarsals	140
6.4.5. Investigating if GH Signals through IGF-1 in SOCS2 ^{-/-} Metatarsals	143
6.4.6. The Effects of IL-1β on Metatarsal Growth	145
6.5. Discussion	147

6.6.	Conclusion	150
7.	INDUCING INFLAMMATION IN SOCS2^{-/-} MICE	153
7.1.	Introduction	153
7.2.	Aims and Hypothesis	155
7.2.1.	Hypothesis	155
7.2.2.	Aims	155
7.3.	Materials and Methods	155
7.3.1.	LPS Model of Inflammation	155
7.3.2.	DSS Model of Colitis	156
7.3.3.	Analysis of Growth Plate Dynamics	157
7.4.	Results	157
7.4.1.	The Effects of LPS Challenge on Growth in WT and SOCS2 ^{-/-} Mice	157
7.4.2.	The Effect of LPS Challenge on Growth Plate Morphology and Endochondral Growth Rate	161
7.4.3.	DSS Induced Colitis Concentration Curve	164
7.4.4.	Main DSS Study	166
7.5.	Discussion	172
7.6.	Conclusion	175
8.	GENERAL DISCUSSION AND FUTURE WORK	177
8.1.	General Discussion	177
8.2.	Future Work	182
9.	REFERENCE LIST	186
10.	APPENDIX	209
10.1.	Appendix 1: Buffer Recipes	209
10.1.1.	Cell Culture	209
10.1.2.	<i>In Vivo</i> Studies	209
10.1.3.	Processing Tissue	210
10.1.4.	Transfecting ATDC5 cells	210
10.1.5.	PCR	211
10.1.6.	Western Blotting	211
10.2.	Appendix 2: Targeting for Construction SOCS2^{-/-} Mice	212
10.3.	Appendix 3: Plasmid Maps	213
10.3.1.	pEF-BOS Plasmid	213
10.3.2.	pEF-FLAG-I Plasmid	214
10.3.3.	pEF-FLAG-I/mSOCS2 Plasmid	215

10.3.4.	pcDNA3.1. ⁽⁺⁾ Plasmid	216
10.4.	Appendix 4: Published Paper	217

Figures

Figure 1.1	Bone turnover.	2
Figure 1.2	The location and cellular organisation of the growth plate.	7
Figure 1.3	Endocrine, autocrine and paracrine factors affecting endochondral bone growth.	11
Figure 1.4	GH signalling through the JAK/STAT pathway.	18
Figure 1.5	IGF-1 signalling.	21
Figure 1.6	SOCS regulation of cytokine signalling.	27
Figure 2.1	Genotyping.	42
Figure 2.2	Isolation of sternal primary chondrocytes.	44
Figure 2.3	Metatarsal culture.	47
Figure 2.4	The CryoJane tape transfer system.	52
Figure 2.5	Streaking agar plates.	59
Figure 2.6	Individual cell clones.	64
Figure 2.7	Primer optimisation.	70
Figure 3.1	Immunohistochemistry of SOCS2 expression.	79
Figure 3.2	Receptor expression.	82
Figure 3.3	STAT signalling.	82
Figure 3.4	STAT signalling with IL-1 β .	84
Figure 3.5	IGF-1 Signalling.	86
Figure 3.6	SOCS2 expression.	86
Figure 3.7	SOCS2 expression with inflammatory cytokines.	88
Figure 3.8	SOCS proteins in chondrocytes.	88
Figure 3.9	SOCS proteins in osteoblasts.	88
Figure 4.1	SOCS2 ^{-/-} phenotype.	95
Figure 4.2	Growth curves.	101
Figure 4.3	Toluidine blue stained growth plate sections from 3wk and 6wk old mice	102
Figure 4.4	BrdU labelling in 3- and 6-week old mice	104
Figure 4.5	Calcein labelling in 3- and 6-week old mice	105
Figure 4.6	μ CT analysis of 3- and 6-week old mice.	108
Figure 5.1	Temporal STAT signalling.	119
Figure 5.2	Temporal SOCS1 and SOCS3 expression.	119
Figure 5.3	SOCS2 over-expression cells.	121
Figure 5.4	STAT expression in SOCS2 over-expressing cells.	121
Figure 5.5	Phosphorylated STAT5 immunohistochemistry.	123
Figure 5.6	IGF-1 qPCR.	124
Figure 6.1	Proliferation assay.	136
Figure 6.2	Proliferation assay concentration curves.	137
Figure 6.3	Analysis of WT and SOCS2 ^{-/-} metatarsals growth.	138
Figure 6.4	Chondrocyte proliferation in metatarsals.	140
Figure 6.5	Metatarsals zone widths	141
Figure 6.6	Metatarsal growth curves with IGF-1 signalling inhibitor.	143
Figure 6.7	Metatarsal growth curves in response to IL-1 β .	145
Figure 7.1	Growth of mice treated with LPS.	157
Figure 7.2	Bone growth in mice treated with LPS.	159

Figure 7.3	Toluidine blue staining in growth plates from mice treated with LPS.	161
Figure 7.4	Calcein labelling in mice treated with LPS.	162
Figure 7.5	DSS concentration curve.	164
Figure 7.6	Main DSS study.	168
Figure 7.7	SOCS2 ^{-/-} and WT mice treated with DSS.	170

Tables

Table 2.1	Primers used for genotyping.	40
Table 2.2	PCR primer pairs.	66
Table 2.3	qPCR primer pairs.	68
Table 2.4	Western blot antibodies.	73
Table 4.1	μCT analysis of 3- and 6-week old mice.	107
Table 7.1	Main DSS study experimental design.	155

CHAPTER 1

INTRODUCTION

1. Introduction

This chapter summarises bone biology and in particular endochondral bone growth, and how the growth hormone/insulin-like growth factor-1 (GH/IGF-1) signalling pathway acts to regulate it. Mechanisms of inhibition of bone growth are discussed; in particular the negative effects of chronic inflammation on bone growth. Finally, the role of suppressor of cytokine signalling (SOCS) proteins in regulating GH signalling is examined, in particular the hypothesis that SOCS2 acts to regulate growth by inhibiting chondrocyte GH signalling. It should be noted that many sections of this introduction are based on the published review on the role of inflammatory cytokines and SOCS2 in GH signalling and bone growth (Pass *et al.*, 2009).

1.1. Bone Biology

1.1.1. Bone Structure and Function

Bone is probably thought of by many as a fairly dead and inert substance, whose main function is to provide support and protection to the body, whilst containing bone marrow that is essential for supplying immune cells. Although bone does provide vital functions as a supportive framework and organ protector, it is also a complex and dynamic tissue that provides a calcium and phosphorus reserve for the body.

There are two types of bone: trabecular (cancellous) and cortical (compact) bone. Cortical bone forms the thin outer layer of long bones, providing shape and support. It is designed to absorb weight-bearing stresses and strains on the bone (Sommerfeldt and Rubin, 2001). Trabecular bone is found within the cortical bone, and has a 'spongy' appearance as it is made up of rod and plate-like structures, giving it a higher surface area but a weaker structure than cortical bone. It is designed to distribute forces out to the cortical bone. Both types of mineralised bone are made up of hydroxyapatite [$\text{Ca}_{10}(\text{PO}_4)_6(\text{OH})_2$] crystals embedded in a collagenous rich matrix

1.1.2. Bone Growth

There are two forms of bone growth: endochondral (longitudinal, *e.g.* tibiae) and intramembranous (flat, *e.g.* skull) (Farquharson, 2003). The first of these increases bone length, occurs mainly postnatal and relies on the growth plate. This is discussed in more detail in Section 1.2. Intramembranous bone formation occurs when mesenchymal cells differentiate directly into osteoblasts which deposit bone, as described in Section 1.1.4.

1.1.3. Bone turnover

Bone remodelling, also known as bone turnover, is the dynamic process of bone resorption and bone formation that occurs throughout life. Bone remodelling is tightly regulated by autocrine, paracrine and endocrine factors and involves the actions of two cell types: osteoclasts (which resorb bone) and osteoblasts (which act to deposit bone on the surface) (Manolagas, 2000). A diagram depicting the process of bone turnover is shown in Figure 1.1. The process of bone turnover is not only important for repairing damage to the bone, following micro- or traumatic fractures, but also allows the bone to respond to changes in mechanical load, altered levels of calcium and a range of endocrine and paracrine factors (Sims and Gooi, 2008). Disrupted bone remodelling leads to bone diseases such as osteoporosis, Paget's disease and osteopetrosis; so that the understanding of the bone remodelling process has high biomedical importance.

This studentship has focused on endochondral bone growth and the actions of growth plate chondrocytes, so only brief descriptions of osteoblasts, osteoclasts and osteocytes (terminally differentiated osteoblasts) are given.

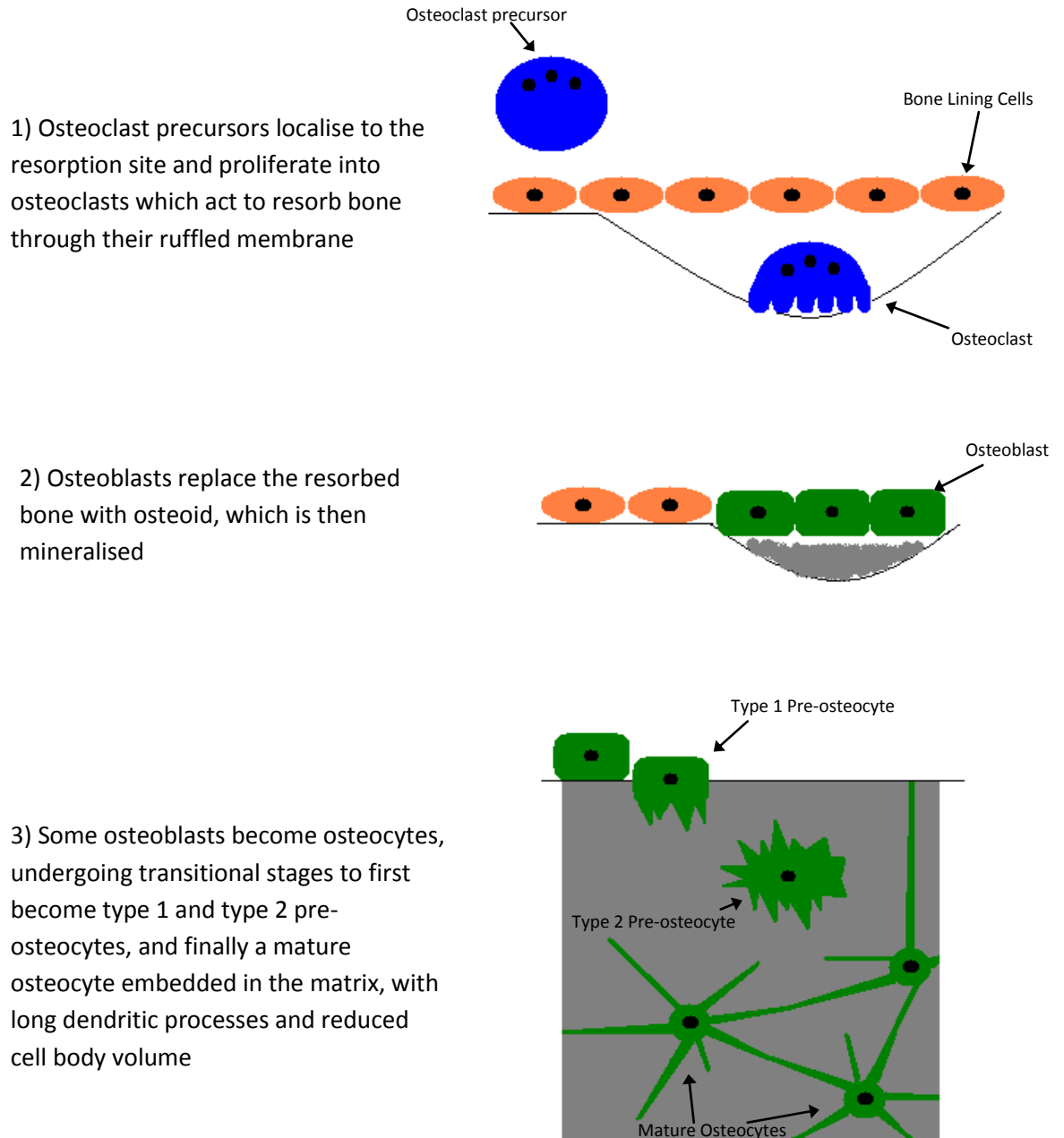


Figure 1.1. Bone turnover. Representation of resorption of bone by osteoclasts (1); osteoblast deposition of osteoid matrix (2); and osteoblast differentiation into an osteocyte (3).

1.1.4. Osteoclasts

Osteoclasts are found on the bone surface, where they resorb bone to form resorption pits. This is reviewed well by Teitelbaum (2000), and the key points are highlighted here. Osteoclasts are derived from haemopoietic myelomononuclear progenitors, and like macrophages are multinuclear, migratory and contain lysosomal enzymes (Sommerfeldt and Rubin, 2001). Osteoclastogenesis is stimulated by factors such as macrophage colony-stimulating factor (M-CSF), receptor for activation of nuclear factor kappa B ligand (RANKL) and osteoprotegerin; and requires contact with osteoblasts and stromal cells. Osteoclast precursors polarize to specific sites on bone for resorption, and upon maturation, the osteoclast attaches to the bone surface by the formation of a ruffled membrane surrounded by an actin rich podosomal ring. Bone resorption occurs at this site through demineralisation by acidification, where transporting events occur in the ruffled membrane leading to secretion of HCl, lowering the pH and activating enzymes such as tartrate-resistant acid phosphatase (TRAP) (Sommerfeldt and Rubin, 2001). The remaining organic components of bone are degraded by various proteases including cathepsin K, a lysosomal protease. This process forms a resorption pit known as lacunae, to which osteoblasts are then recruited to deposit new bone. With age, osteoclast bone resorption occurs at a greater rate than bone deposition by osteoblasts and this imbalance in bone remodelling leads to bone loss and osteoporosis.

1.1.5. Osteoblasts

Osteoblasts are bone-forming cells also found on the bone surface. During bone resorption osteoblasts act to replace bone that has been removed by osteoclasts, a process that is tightly regulated by both local and endocrine factors. Osteoblasts closely resemble fibroblasts, and differentiate from mesenchymal cells during endochondral ossification and intramembranous ossification (Ducy *et al.*, 2000). This differentiation occurs under transcriptional control by osteoblast-specific factors such as OSE1, OSE2 and Runx2 and by growth factors such as Indian

hedgehog (Ihh) (Ducy *et al.*, 2000). Differentiated osteoblasts act to deposit extracellular matrix, known as osteoid, and regulate its mineralisation (Ducy *et al.*, 2000; Sommerfeldt and Rubin, 2001). Osteoid mainly consists of collagen (94%), in addition to proteoglycans and other non-collagenous proteins such as osteocalcin (Sommerfeldt and Rubin, 2001). Mineralisation of this matrix occurs after its deposition, resulting in a mineralised bone (Sommerfeldt and Rubin, 2001). This process of osteoid deposition and mineralisation is controlled by Runx2 regulation of Osteocalcin, a gene expressed in terminally differentiated osteoblasts, and by endocrine factors such as Leptin, fibroblast growth factor (FGF) and IGF-1 (Hurley *et al.*, 1996; Ducy *et al.*, 2000). Following matrix deposition, osteoblasts either remain on the surface as inactive bone lining cells; undergo apoptosis; or become embedded in bone to transdifferentiate into osteocytes (Jilka *et al.*, 1998; Dallas and Bonewald, 2010).

1.1.6. Osteocytes

Osteocytes are found embedded in the bone matrix within lacunae, and are the most abundant bone cell, accounting for 90-95% of all bone cells (Bonewald, 2007b). Osteocytes are smaller than their osteoblast derivatives, with a higher nucleus to cytoplasm ratio (Sommerfeldt and Rubin, 2001). They have long dendritic processes that run through canaliculi tunnels to maintain contact with other bone cells; specifically other osteocytes, bone surface osteoclasts and osteoblasts, and bone marrow (Bonewald, 2007b). Osteocytes use these processes to send inhibitory signals to osteoclasts, and stimulatory signals to osteoblasts, thus controlling remodelling in response to mechanical stimuli (Bonewald, 2007a). Dying osteocytes, as a consequence of bone damage, are thought to send signals to osteoclasts to stimulate resorption and initiate the bone remodelling cycle (Bonewald, 2007b). It is thought that osteocytes extend dendrites in response to mechanical load, a process that is controlled by the transmembrane protein E11 (Bonewald, 2007b). E11, also called podoplanin and gp38, is a marker for early osteocytes while sclerostin is a marker for late osteocytes. Phosphate homeostasis is also regulated by osteocytes, which express Dmp1 (Dentin

Matrix Protein 1), PHEX (Phosphate Regulating Neutral Endopeptidases on Chromosome X) and FGF23 (Bonewald, 2007b).

1.1.7. Chondrocytes

Chondrocytes are found within growth plates, which are located at either end of long bones. Within the growth plate they are found organised in columns, embedded in a collagen rich matrix, and are responsible for controlling endochondral bone growth as they differentiate from a resting chondrocyte to a hypertrophic chondrocyte phenotype, as discussed in Section 1.2. There is a second type of chondrocyte within the body, named articular chondrocytes, which are found embedded in a collagen type-II and proteoglycan rich matrix forming the articular cartilage of synovial joints (Treadwell and Mankin, 1986). This cartilage is found at the end of long bones where it acts as a shock absorber and bone surface protector (Treadwell and Mankin, 1986). Unlike the growth plate, articular cartilage does not undergo the processes of vascular invasion and subsequent calcification to form bone.

1.2. Endochondral Growth

1.2.1. The Growth Plate

Embryonic long bone growth begins within limb buds, which consist of mesenchymal cells that are committed to differentiate into chondrocytes (cartilage cells) and osteoblasts from haemopoietic precursors (Kronenberg, 2003; Shimizu *et al.*, 2007). The mesenchymal cells increase in cell density to form pre-cartilage condensations, with cells held together in aggregates by adhesion molecules as they undergo transitions to pre-chondrocytes and begin to secrete an extracellular matrix (Dessau *et al.*, 1980; Cancedda *et al.*, 1995; Kronenberg, 2003; Shimizu *et al.*, 2007). Proteins in the early matrix produced by differentiating pre-cartilaginous limb-buds include collagen type-I, chondroitin sulphate proteoglycans, tenascin and fibronectin; which are replaced by collagen type-II and cartilage-specific proteoglycans (e.g. aggrecan) in the extracellular matrix

of the cells as they enter chondrogenic differentiation (Dessau *et al.*, 1980; Mackie *et al.*, 1987). As this process is occurring, mesenchymal cells on the outside of the condensations form a perichondrium, consisting of fibrous connective tissue, and then differentiate into osteoblasts that deposit bone and form a collar around the condensation (Farquharson, 2003; Kronenberg, 2003). The differentiation and cellular interactions of condensing mesenchymal cells leads to endochondral ossification, producing cartilage that is invaded by cells (osteoblast, osteoclasts and haemopoietic cells) to establish the primary and secondary centres of ossification, between which the growth plate is formed. This latter process takes place at birth in some species and after birth in others. As the skeleton matures, the ossification centres enlarge and replace the remaining cartilage and growth plates completely (Mackie *et al.*, 2008).

Postnatal endochondral bone growth occurs as a result of endochondral ossification at the epiphyseal growth plate (Figure 1.2) (Kember and Sissons, 1976; Farnum and Wilsman, 1987; Mackie *et al.*, 2008). Growth plates are thin layers of cartilage found situated near the ends of all long bones and it is at these regions that growth occurs (Kember and Sissons, 1976; Farnum and Wilsman, 1993). The growth plate cartilage consists of both chondrocytes and matrix. The matrix comprises of proteoglycans (including aggrecan), collagens (primarily collagen type-II) and a variety of other non- collagenous proteins (Ballock and O'Keefe, 2003). The chondrocytes, which are arranged in columns that parallel the longitudinal axis of the bone, proceed through a series of differentiation and maturation stages whilst maintaining their spatially fixed locations (Kember and Sissons, 1976; Hunziker *et al.*, 1987; MacRae *et al.*, 2006c). Each column is thought to represent the clonal expansion of one stem cell, and the chondrocytes are held in their distinct spatial locations by both longitudinal and transverse septa, which consist of an extracellular matrix rich in proteoglycans and collagens (Breur *et al.*, 1992).

THE GROWTH PLATE

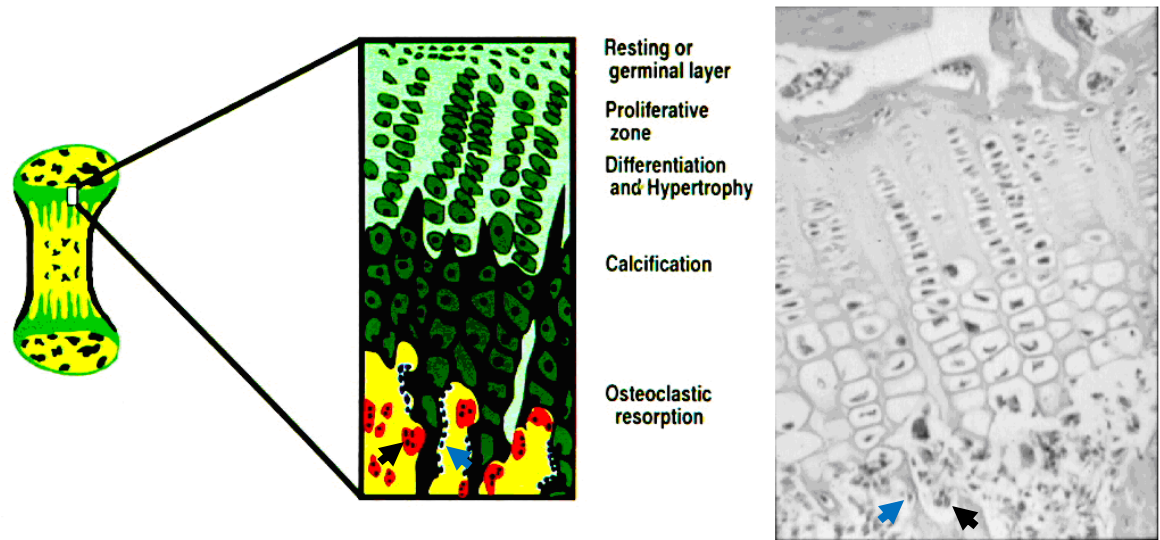


Figure 1.2. The location and cellular organisation of the growth plate. The position and organization of the growth plate can be seen in the schematic representation (left) and image of a mouse growth plate (right). The chondrocytes within the growth plate are shown going through the different stages of differentiation and maturation. Examples of osteoclasts are indicated by black arrows, while blue arrows point to osteoblasts. Schematic representation from Farquharson (2003).

1.2.2. Resting chondrocytes

The resting zone (Zone I or germinal layer) consists of resting chondrocytes and undifferentiated progenitors. Above the resting zone is the groove of Ranvier, which contains progenitor cells and stem cells. Resting chondrocytes have very low proliferation levels, synthesise small amounts of collagen type-II and proteoglycans, and are thought to store nutrients for later zones (Hunziker *et al.*, 1987; Mackie *et al.*, 2008). The resting chondrocytes are not found arranged in as distinct longitudinal columns found throughout the rest of the growth plate, but are found singly or in pairs surrounded by large volumes of extracellular matrix (Ballock and O'Keefe, 2003).

1.2.3. Proliferating Chondrocytes

The resting zone continues into the proliferative zone (Zone II) where the chondrocytes become flattened and undergo clonal expansion, forming clusters in longitudinal columns (Hunziker *et al.*, 1987; Hunziker and Shenk, 1989). The rate of proliferation is determined by many factors including endocrine signalling, circadian rhythm, age and cell kinetics (Farnum and Wilsman, 1993). The width of the proliferating zone is proportional to the rate of growth, with wider zones exhibiting increased growth rate (Farnum and Wilsman, 1993).

Following proliferation chondrocytes exit the cell cycle and enter the transition zone, where they begin to undergo terminal differentiation into hypertrophic chondrocytes. This zone consists of maturing chondrocytes with minimal DNA synthesis, which are post-mitotic and pre-hypertrophic, and they elongate in morphology to become tall spheres in the direction of growth (Buckwalter *et al.*, 1986; Breur *et al.*, 1994).

1.2.4. Hypertrophic chondrocytes

The chondrocytes then enter the hypertrophic zone (Zone IV), where they undergo hypertrophy to become rounded with increasing cell volume (up to 10 fold) and height (up to 5 fold) compared to proliferating cells, and greater synthesis of extracellular matrix (Hunziker *et al.*, 1987; Hunziker

and Shenk, 1989; Farnum and Wilsman, 1993). The height of chondrocytes in the direction of growth increases continuously throughout hypertrophy, towards terminal differentiation (Hunziker *et al.*, 1987). Hypertrophic chondrocytes have increased metabolic activity, associated with raised numbers of cytoplasmic organelles (rough endoplasmic reticulum, Golgi apparatus and mitochondria) (Hunziker *et al.*, 1987). Matrix components produced by hypertrophic chondrocytes include type X collagen, osteonectin, osteopontin and chondrocalcin, with a reduction in collagen type-II synthesis (Hunziker *et al.*, 1987; Farnum and Wilsman, 1987; Farnum and Wilsman, 1993). Late hypertrophic chondrocytes release matrix vesicles into the longitudinal septae and contain proteins and enzymes such as phosphate transporters, annexins, PHOSPHO1 and alkaline phosphatases which are responsible for establishing mineralisation nucleation sites for calcification (Hunziker *et al.*, 1987; Kirsch *et al.*, 1997; Mackie *et al.*, 2008).

1.2.5. Terminal Differentiation

The chondrocytes then enter the final terminal zone (Zone V) and the matrix of the longitudinal septa is mineralised by hydroxyapatite deposition through the actions of phosphatases such as PHOSPHO1 and alkaline phosphatase, which provide inorganic phosphate and hydrolyse extracellular pyrophosphate that otherwise acts to inhibit mineralisation (Anderson, 1969; Register *et al.*, 1986; Kirsch, 2006; Yadav *et al.*, 2011). This mineralised cartilage acts as a scaffold for deposition of osteoid by osteoblasts, which is then mineralised to form new trabecular bone (Hunziker *et al.*, 1987; Cancedda *et al.*, 1995). The transverse septa are resorbed by osteoclasts, along with terminal chondrocytes and remaining longitudinal septa (60%) during vascular invasion to allow invasion of blood vessels, osteoblast precursors and osteoclasts (Hunziker *et al.*, 1987; Farnum and Wilsman, 1987; Farquharson, 2003). The fate of the terminally differentiated chondrocyte is likely to involve both apoptosis and autophagy, however the transdifferentiation of chondrocytes into the osteogenic phenotype has yet to be established (Farnum and Wilsman, 1987; Roach *et al.*, 1995; Cancedda *et al.*, 1995; Shapiro *et al.*, 2005). The width of the growth

plate decreases with age, due to a decrease in cell proliferation, so that eventually growth stops completely and under oestrogen control the growth plate closes and cartilage is replaced by bone by the formation of bony bridges between the primary and secondary ossification centres (Kember and Sissons, 1976; Nilsson *et al.*, 2005).

1.3. Regulation of Endochondral Growth Rate

1.3.1. Chondrocyte Proliferation and hypertrophy

The rate of growth of long bones varies greatly, for example different species display large differences in growth rate. Chicken and rat proximal tibia growth plates grow at 0.86mm/day and 0.23mm/day respectively (Kember, 1972; Kirkwood *et al.*, 1989), while human bones grow considerably slower at 0.04 mm/day (distal femur) (Kember and Sissons, 1976). Several different factors influence growth rate, including chondrocyte specific changes. The rate of proliferation and the width of the proliferating zone are associated with bone growth rate, with increased cell cycle times and larger zones found in longer bone lengths (Farnum and Wilsman, 1993; Farquharson, 2003). The greatest influence on growth rate comes from the volume and height of hypertrophic cells, which is positively correlated with the rate of endochondral growth (Hunziker and Shenk, 1989; Breur *et al.*, 1991).

1.3.2. Endocrine Factors

The actions of chondrocytes are also influenced by several systemic (endocrine) and local (autocrine/paracrine) signalling molecules (Figure 1.3). The most significant endocrine factor to affect endochondral bone growth is GH, which is produced by somatotroph cells within the lateral wings of the anterior pituitary gland and is released in pulses to circulate in the blood and act on the liver, as well as other organs and tissue, to stimulate IGF-1 production and subsequent growth (Isaksson *et al.*, 1982; LeRoith *et al.*, 2001). The signalling pathways and effects of GH on growth are discussed in more detail in Section 1.4 below.

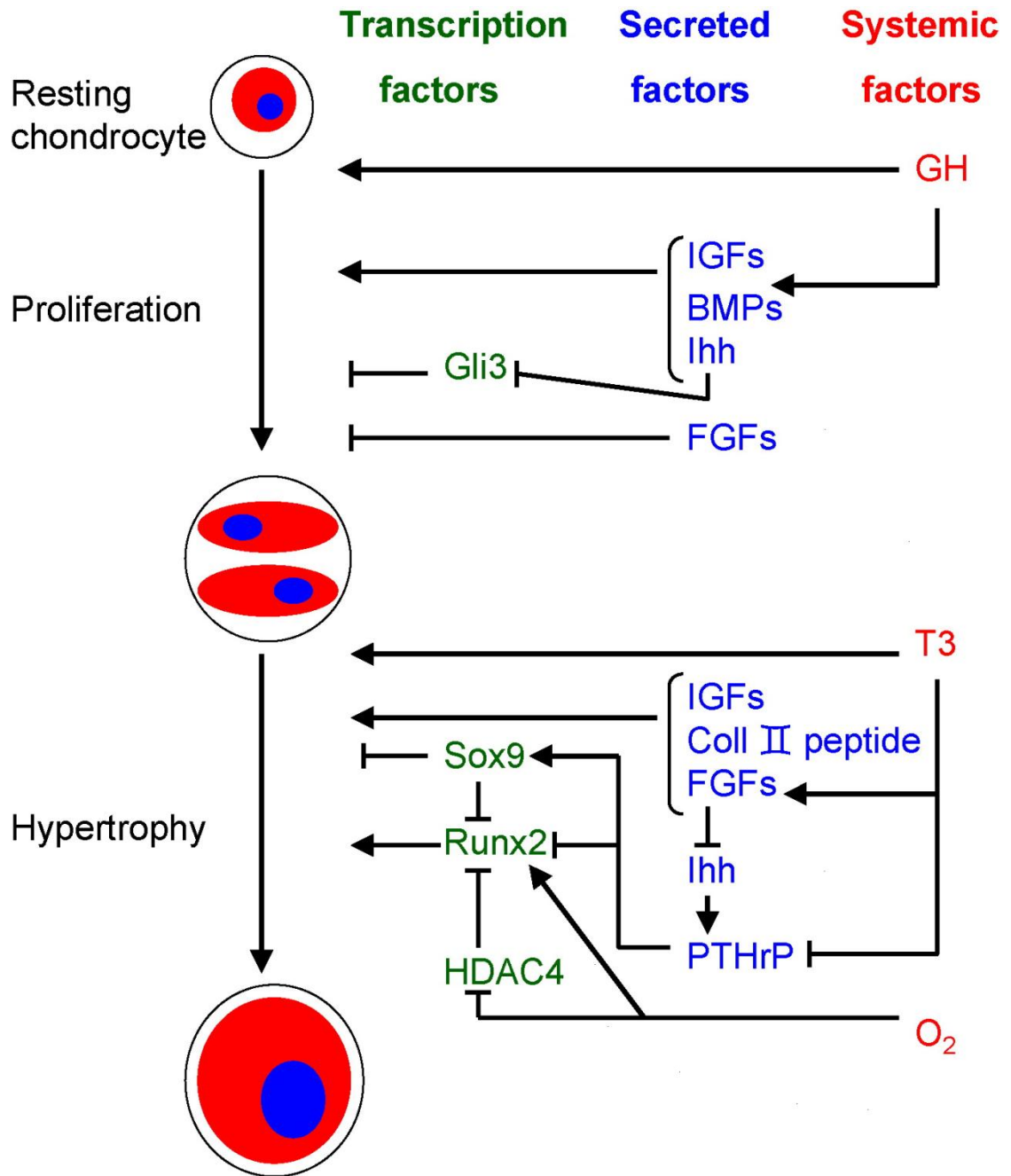


Figure 1.3. Endocrine, autocrine and paracrine factors affecting endochondral bone growth. Figure showing how various systemic factors, local secreted factors and transcription factors affect the different stages of chondrogenesis in the growth plate. Stimulation/activation is indicated by an arrow whereas inhibition is depicted by a crossed line. Only certain key molecules are shown here, more are discussed in the text. Image modified from Mackie *et al.* (2008).

Rising oestrogen levels are associated with increased mineralisation and bone formation at the growth plate, leading to eventual replacement of the growth plate by bone and epiphyseal fusion once adult height has been reached after a pubertal growth spurt (Kember and Sissons, 1976; Weise *et al.*, 2001). Premature oestrogen production seen during early puberty causes premature fusion of the growth plate and thus short stature, while oestrogen deficiency prevents epiphyseal fusion resulting in increased adult height (Smith *et al.*, 1994; Morishima *et al.*, 1995; Juul, 2001; Nilsson *et al.*, 2005). Oestrogen is thought to stimulate GH/IGF-1 signalling, as well as having direct effects on chondrocytes through oestrogen receptors α and β (Veldehuis *et al.*, 1997; Juul, 2001; Nilsson *et al.*, 2003; Börjesson *et al.*, 2010). Another group of sex steroids, androgens (e.g. testosterone), also act to stimulate longitudinal growth at puberty either through aromatase mediated conversion to oestrogen, or by acting directly on chondrocytes to stimulate proliferation, hypertrophic differentiation or both (Carrascosa *et al.*, 1990; Schwartz *et al.*, 1994; Öz *et al.*, 2001; Nilsson *et al.*, 2003).

Hypothyroidism is associated with reduced growth, thinner growth plates and inhibition of chondrocyte hypertrophy, demonstrating the role of thyroid hormone in stimulating bone growth (Rivkees *et al.*, 1988; Stevens *et al.*, 2000). Thyroid hormones (triiodothyronine and thyroxine) stimulate hypertrophy of chondrocytes through thyroid hormone receptor- α together with the expression of collagen type-X and alkaline phosphatase which are important for matrix mineralisation (Burch and Lebovitz, 1982; Böhme *et al.*, 1992; Ballock and Reddi, 1994).

Glucocorticoids, for example dexamethasone, are administered to children with chronic diseases such as Crohn's disease for their positive actions as immunosuppressant's and anti-inflammatories. Unfortunately, prolonged use of these drugs is associated with growth retardation, mediated by inhibition of chondrocyte proliferation and increased apoptosis (Simon *et al.*, 2002a; Heino *et al.*, 2008; Owen *et al.*, 2009). Glucocorticoids act indirectly on the growth

plate by inhibiting expression of GHR and IGF-1, and subsequently IGF-1 stimulation of proliferation (MacRae *et al.*, 2007a; Fernandez-Cancio *et al.*, 2008).

Rickets in mammals is a defect of bone growth as a result of vitamin D deficiency, with increased numbers of hypertrophic cells due to decreased apoptosis and abnormal mineralisation (Donohue and Demay, 2002). Vitamin D mediates absorption of calcium and phosphate which are critical for hydroxyapatite crystal formation; while vitamin D metabolites such as $1,25(\text{OH})_2\text{D}_3$, the active form of vitamin D_3 directly stimulates chondrocyte differentiation, proliferation and matrix production (Dean *et al.*, 2001; Boyan *et al.*, 2002).

1.3.3. Autocrine and Paracrine Factors

In addition to endocrine factors controlling endochondral bone growth, there are also a number of local molecules that act by autocrine and paracrine mechanisms which are also shown in Figure 1.3. Embryonic growth is largely controlled by IGF-1 and IGF-2 acting independently of GH. While postnatal IGF-1 production in response to GH is an important stimulator of chondrocyte proliferation as discussed in Section 1.4, IGF-2 is thought to be produced in response to GH and signals through the same receptor as IGF-1 but its role in growth plate function after birth is less clear and large species differences in growth plate IGF-2 expression have been reported (van der Eerden *et al.*, 2003). Parker and colleagues (2007) found increased IGF-2 in rat growth plates compared to IGF-1 in young animals, with its expression decreasing rapidly from 1- to 6-weeks of age (Parker *et al.*, 2007). One hypothesis is that, under GH control, IGF-2 acts to stimulate resting and proliferating chondrocytes while IGF-1 is important in the hypertrophic zone (LeRoith *et al.*, 2001). However many studies have demonstrated IGF-1 as important in stimulating proliferation, and IGF-1 mRNA has been found in proliferating chondrocytes (Nilsson *et al.*, 1986; Lupu *et al.*, 2001).

Prehypertrophic chondrocytes secrete Ihh, which acts to stimulate proliferation and inhibit hypertrophy of chondrocytes therefore regulating the rate of chondrocyte differentiation

(Vortkamp *et al.*, 1996; St-Jaques *et al.*, 1999). Ihh acts through the cell surface receptor patched-1 to inhibit activation of transcriptional repressors, Gli proteins (Ehlen *et al.*, 2006). Its effects on hypertrophy, but not proliferation, are mediated by Ihh stimulation of parathyroid hormone-related peptide expression (PTHrP) (St-Jaques *et al.*, 1999). Ihh secretion by prehypertrophic chondrocytes stimulates PTHrP production by periarticular chondrocytes in the perichondrium, which acts directly on late proliferating and transitional chondrocytes to keep the cells in a state of proliferation by delaying differentiation into hypertrophy (Vortkamp *et al.*, 1996; Kronenberg *et al.*, 1997). Ihh also stimulates perichondrial and periarticular cells to produce transforming growth factor- β (TGF- β), which in turn also stimulates PTHrP synthesis and inhibits chondrocyte hypertrophy (Serra *et al.*, 1999). The resulting increased levels of PTHrP act on late proliferating chondrocytes that express its receptor, delaying the production of Ihh secreting cells thereby completing a negative feedback loop that acts to control chondrocyte differentiation rate (Vortkamp *et al.*, 1996; Kronenberg *et al.*, 1997; Farquharson *et al.*, 2001). These signalling molecules are likely to exert their effects by adjusting cell cycle time (Ballock and O'Keefe, 2003).

One of the ways PTHrP mediates its actions is through signalling via its receptor to activate phosphorylation of the transcription factor Sox9 (Sry-type HMG box binding protein 9), which is important for chondrocyte differentiation and delays chondrocyte hypertrophy (Huang *et al.*, 2001; Akiyama *et al.*, 2002). Sox9 also acts independently of PTHrP, and is vital for the development of cells from mesenchymal condensations into chondrocytes before acting throughout chondrocyte proliferation and differentiation (Bi *et al.*, 1999; Akiyama *et al.*, 2002). Signalling through the PTHrP receptor also inhibits chondrocyte expression of Runx2, a transcription factor that acts to stimulate proliferating chondrocytes into hypertrophic differentiation and hypertrophy (Guo *et al.*, 2006). Runx2 is also inhibited by histone deacetylase-4 (HDAC4) and the activity of both Runx2 and HDAC4 is under regulation of oxygen tension, so that hypoxia leads to down regulation of Runx2 and stimulation of HDAC4 (Vega *et al.*, 2004; Hirao *et al.*, 2006).

Bone morphogenetic proteins (BMPs) are part of the TGF- β superfamily, and are capable of regulating growth rate independently of the PTHrP/Ihh loop. There are various BMPs, with some that are important for initiation chondrogenesis, and others that act to maintain chondrocyte proliferation (Pizette and Niswander, 2000; Minina *et al.*, 2001; Yoon *et al.*, 2006). BMPs have also been found to be important for stimulating hypertrophic chondrocytes to produce collagen type-X (Grimsrud *et al.*, 1999; Minina *et al.*, 2001). Ihh can stimulate production of BMPs, and BMPs can in turn induce Ihh expression, so that these two signalling pathways act in parallel to each other in both dependent and independent manners during bone growth (Grimsrud *et al.*, 1999; Minina *et al.*, 2001; van der Eerden *et al.*, 2003).

There are several members of the fibroblast growth factor (FGF) family that regulate various stages of chondrogenesis including proliferation and differentiation (Ornitz, 2005). For example, FGF receptor 3 is expressed by proliferating and pre-hypertrophic chondrocytes, and its signalling negatively regulates proliferation and differentiation (Naski *et al.*, 1998; Ornitz, 2005). FGF2 has been found to inhibit Ihh secretion, although inhibition of chondrocyte proliferation by FGFs can occur independently of Ihh (Minina *et al.*, 2002).

Vascular endothelial growth factor (VEGF) is expressed by hypertrophic chondrocytes and is important for mediating vascular invasion, terminal differentiation and chondrocyte apoptosis (Gerber *et al.*, 1999; Ferrara, 1999; Horner *et al.*, 1999). VEGF stimulates both the proliferation of vascular endothelial cells and vascular invasion of the mineralised hypertrophic chondrocyte matrix (Gerber *et al.*, 1999; Ferrara, 1999; Carlevero *et al.*, 2000). Its expression is regulated dependently and independently of hypoxia inducible factor-1 α , and expression of VEGF has been linked to Ihh through the transcription factor Runx2 (Schipani *et al.*, 2001; Zelzer *et al.*, 2001; Takeda *et al.*, 2001).

1.4. GH and IGF-1 Signalling

1.4.1. GH Receptor Signalling

GH exerts its actions on tissues through the GH receptor (GHR). Upon binding its receptor, GH can activate several different signalling pathways including: mitogen activated protein kinase (MAPK)/extracellular signal-regulated kinase (ERK); Insulin receptor substrate 1 (IRS-1)/phosphatidylinositol 3-kinase (PI3K); phospholipase C/protein kinase C/ Ca^{2+} (Argetsinger and Carter-Su, 1996). However, the majority of signalling occurs through the best characterised pathway Janus kinase (JAK)/signal transducer and activator of transcription (STAT) signalling, which is important for endochondral growth and is described here. The GHR is a member of the class I cytokine receptor super family, and contains an extracellular domain (ECD) consisting of two fibronectin type III sandwich domains, which is connected to a helical transmembrane domain leading to the intracellular domain (ICD) consisting of two Box motifs (Flores-Morales *et al.*, 2006; Brooks *et al.*, 2008). GH signalling follows GH activation of the GHR, which causes dimerisation of the ECD, leading to phosphorylation of the ICD (Waters *et al.*, 2006). This allows binding and phosphorylation of the tyrosine kinase JAK2 at Box 1 in the ICD, which, in turn, phosphorylates specific tyrosine (Tyr) residues on the associated ICD (Waters *et al.*, 2006; Uyttendaele *et al.*, 2007; Brooks *et al.*, 2008). These phosphorylated residues create binding sites for Src homology 2 (SH2) domain proteins, including STAT1, STAT3 and STAT5 proteins (Waters *et al.*, 2006; Brooks *et al.*, 2008). STAT proteins often have two isoforms, for example STAT5a and STAT5b, thought to have separate and related functions (Smit *et al.*, 1996; Herrington *et al.*, 2000). The identity of which GHR Tyr residues STAT5 preferentially binds is unclear, with evidence for stronger binding at Tyr534, Tyr566, and Tyr627, and weaker binding to Tyr595 and Tyr487 (Uyttendaele *et al.*, 2007). The STAT proteins are phosphorylated by JAK2 at the specific tyrosine and/or serine residues, leading to homo- or heterodimerisation and migration to the nucleus, activating gene transcription (Han *et al.*, 1996; Decker and Kovarik, 2000; Herrington *et al.*, 2000;

Waters *et al.*, 2006; Brooks *et al.*, 2008). Although GH signalling through STAT proteins is the primary signalling pathway (Figure 1.4), there are elements of this signalling cascade that are not yet fully defined, leading to different models. For example, the mechanisms by which GH activates its receptor is debated, and may involve GH activating GHR dimerisation as described above; GH binding causing GHR to internalise and auto-phosphorylate; or GH stimulating conformational change of a constitutively dimerised GHR (Uyttendaele *et al.*, 2007; Brooks *et al.*, 2008; Giustina *et al.*, 2008). The latter model is becoming more favoured, and it has been proposed that the two GHR subunits constitutively bind JAK2 kinases so that, upon GH activation, the receptor subunits rotate to allow the aligned JAK2 proteins to activate each other (Waters *et al.*, 2006).

GH may regulate the phosphorylation of a range of STATs and this may depend on the cell type; for example, STAT5 is activated by GH in adipocytes but not in adherent epithelial cells (Han *et al.*, 1996). To date, the specific STAT family member(s) involved in mediating GH signalling in chondrocytes has focussed on STAT5b and a role for STAT1 and STAT3 is, as yet, unknown (Gevers *et al.*, 2009). It has been shown that both GHR and STAT5 are localised to the resting, proliferating and pre-hypertrophic chondrocytes, and thus STAT5 phosphorylation in response to GH is likely to occur predominantly in these zones (Gevers *et al.*, 2009). STAT5 null mice show growth retardation, with narrower growth plate proliferating zones and reduced circulating IGF-1, but their phenotype is slightly different to GHR knockout mice (Sims *et al.*, 2000; Waters *et al.*, 2006).

GH Signalling via the JAK/STAT Pathway

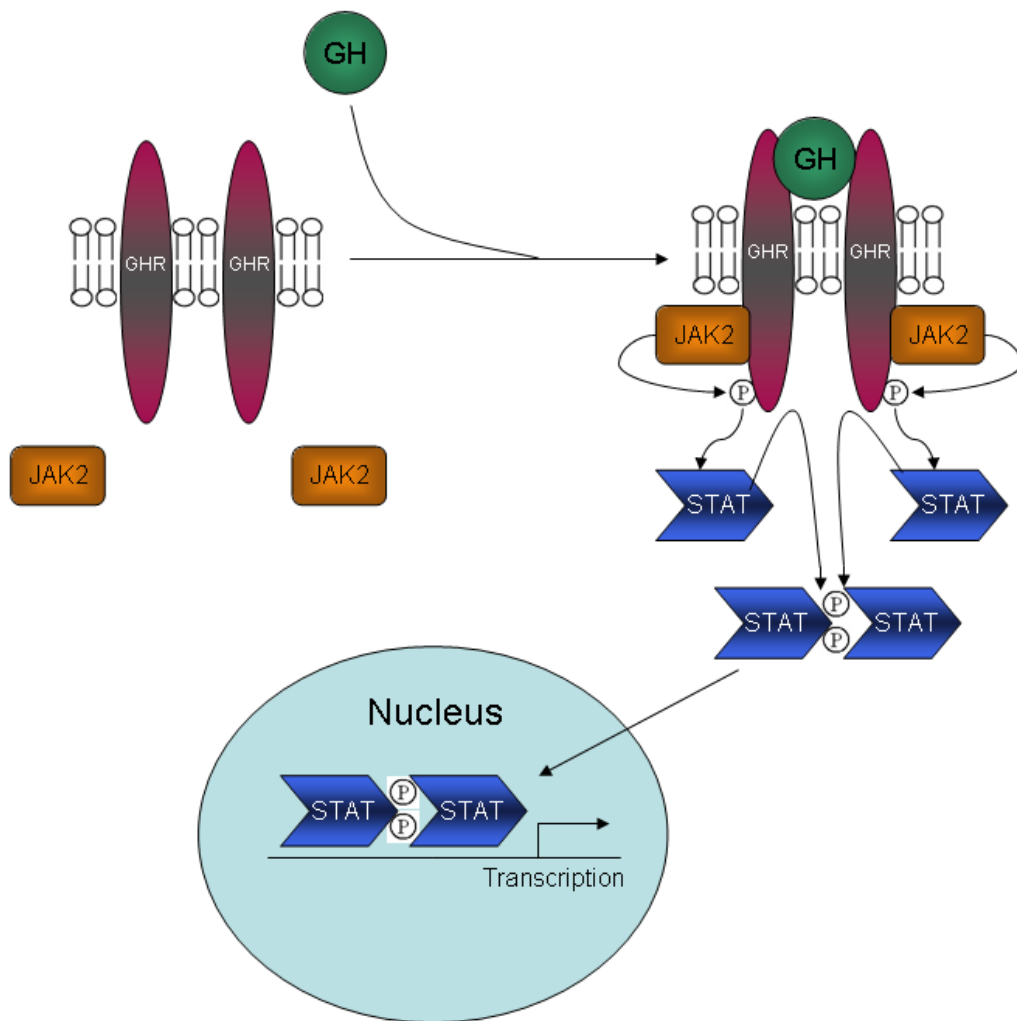


Figure 1.4. GH signalling through the JAK/STAT pathway. Upon binding its receptor, GH stimulates JAK2 and consequently STAT phosphorylation. Dimerised STAT proteins then translocate to the nucleus and activate gene transcription.

Growth retardation of STAT5 null mice appears earlier and is less severe than in GHR null mice, and appears to be due to an endochondral ossification fault as opposed to the premature growth plate senescence observed in GHR null mice (Sims *et al.*, 2000; Waters *et al.*, 2006). Also, STAT5 null mice show normal bone remodelling, whereas GHR null mice have lowered levels of bone remodelling (Giustina *et al.*, 2008). These different phenotypes suggest GH actions on chondrocytes have STAT5 independent effects. However, STAT5 null mice lack both STAT5A and STAT5B. Interestingly, growth retardation and reduced circulating IGF-1 are observed in STAT5b null mice but not STAT5a null mice, suggesting that STAT5b may be the important isoform in GH signalling in bones (Herrington *et al.*, 2000). STAT3 knockout mice are embryonic lethal, while STAT1 knockout mice are of normal size (Durbin *et al.*, 1996; Meraz *et al.*, 1996; Takeda *et al.*, 1997). In humans, mutations of GHR or STAT5b that result in the inhibition of STAT5b signalling but maintain STAT1 and STAT3 and MAPK-ERK signalling result in severe short stature (Kofoed *et al.*, 2003; Milward *et al.*, 2004; Rosenfeld *et al.*, 2005; Tiulpakov *et al.*, 2005).

1.4.2. IGF-1 Signalling

One of the outcomes of GH signalling is induction of IGF-1 gene expression, the mechanisms of which are poorly understood (Herrington *et al.*, 2000). Most evidence suggests that GH signalling through STAT5b leads directly to IGF-1 induction, although other transcription factors may also be involved (Herrington *et al.*, 2000; Woelfle *et al.*, 2003a; Woelfle *et al.*, 2003b). IGF-1 signalling can occur both dependently and independently of GH. Prenatally, IGF-1 signalling is considered to be GH independent whereas postnatally, IGF-1 signalling is partly or fully GH dependent (Klammt *et al.*, 2008). IGF-1 can be found in the circulation bound in a complex with IGF binding proteins, such as IGF binding protein-3 (IGFBP-3), and the acid-labile subunit (ALS) (Baxter and Martin, 1989; Firth and Baxter, 2002). These complexes increase the half-life of circulating IGF-1 and target the ligand to its receptor (Rajaram *et al.*, 1997). Other binding proteins, such as IGFBP-1,

inhibit IGF-1 bioactivity due to their greater affinity for IGF-1 than the IGF-1R (Jones *et al.*, 1991; Rajaram *et al.*, 1997).

In chondrocytes, IGF-1 signalling (Figure 1.5) involves IGF-1 binding a cell surface receptor tyrosine kinase (IGF-1R) with high affinity to induce IGF-1R conformational change (dimerisation) (Klammt *et al.*, 2008; Giustina *et al.*, 2008). Upon binding, the IGF-1R undergoes auto-phosphorylation of the receptor intracellular domains (β subunits), creating phosphorylated tyrosine residues that act as specific docking sites for various substrates important for downstream signalling cascades (LeRoith, 2000). This includes various insulin receptor substrate (IRS) proteins (such as IRS-1) and Shc proteins which activate downstream pathways important for inducing proliferation and inhibiting apoptosis (Hoshi *et al.*, 2004; Michaylira *et al.*, 2006a; MacRae *et al.*, 2007a). The main two downstream pathways of IGF-1 signalling that have been studied are the Shc mediated Ras/Raf/MAPK and the IRS-1 mediated PI3K/Akt/PKB pathways (LeRoith, 2000; Hoshi *et al.*, 2004).

It is worth noting that as IGF-1R does not contain specific tyrosine based motifs recognised by STAT proteins, IGF-1 is not thought to signal via the JAK/STAT pathway (Stahl *et al.*, 1995; Decker and Kovarik, 2000). Despite this, there is limited evidence of IGF-1 stimulation of STAT3 via JAK1, which clearly warrants further investigation (Zong *et al.*, 2000; Yadav *et al.*, 2005). IRS-1 has been shown to be vital to bone growth as chondrocytes in IRS-1 knockout mice have lower levels of proliferation, undergo faster apoptosis and the growth plate closes early (Hoshi *et al.*, 2004; Giustina *et al.*, 2008). This results in decreased bone turnover and reduced animal growth and weight (Hoshi *et al.*, 2004; Giustina *et al.*, 2008). IRS-1 null mice also show impaired fracture healing, which can be restored by over expression of IRS-1 in transgenic mice (Shimoaka *et al.*, 2004). Furthermore, the addition of the PI3K inhibitor, LY294002, restricts the IGF-1 mediated increases in chondrocyte proliferation and metatarsal growth, suggesting that the PI3K pathway is crucial in chondrocyte responses to IGF-1 (MacRae *et al.*, 2007a; Ulici *et al.*, 2008).

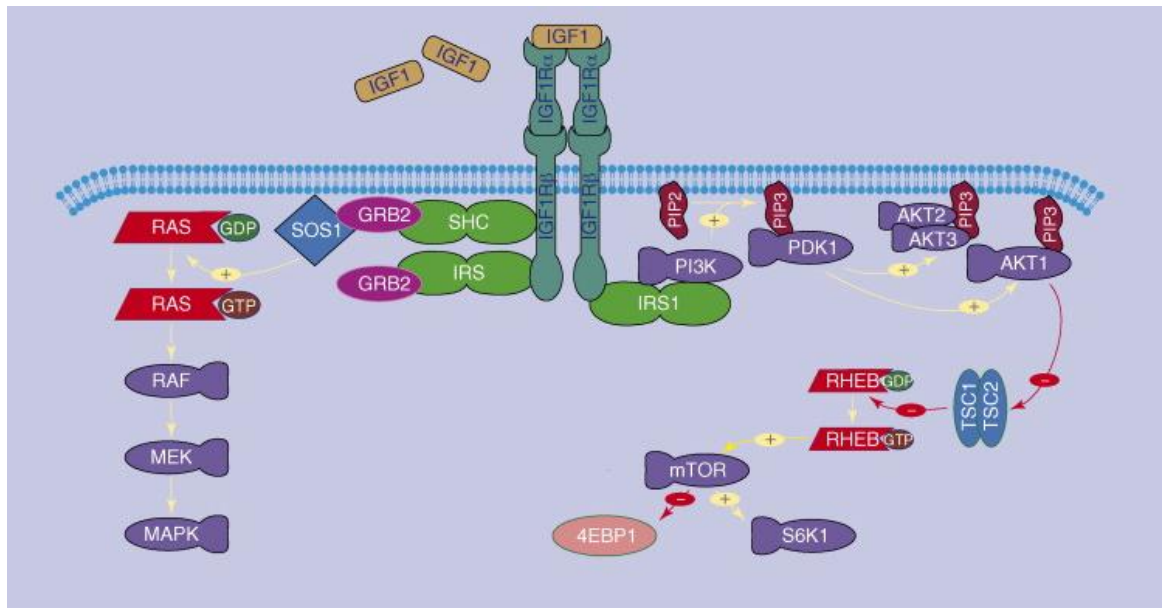


Figure 1.5. IGF-1 signalling. IGF-1 binds its receptor to stimulate signalling through a variety of pathways, mediated by SHC and IRS phosphorylation. + indicates activation and – indicates inhibition. Image from Klammt *et al.* (2008).

IGF-1 induces somatostatin which inhibits GH release and thereby forms a classical negative feedback loop (Giustina *et al.*, 2008).

1.4.3. GH and IGF-1 Regulation of Endochondral Growth

It has long been recognised that GH plays an important role in postnatal, but not embryonic, bone growth. GH deficiency results in impaired postnatal growth, with growth retardation in GHR knockout mice after 2-weeks of age, while excess GH causes gigantism (Cuttler *et al.*, 1989; Lupu *et al.*, 2001). Indeed, recombinant human GH (rhGH) is widely used to treat a diverse group of conditions that are associated with short stature and poor growth and range from GH deficiency to conditions such as Prader-Willi syndrome and Turner's syndrome (Hindmarsh and Dattani, 2006). Therapy with recombinant human GH has also been used in humans with chronic inflammatory diseases and has shown variable extent of improvement in growth and even disease (Slonim *et al.*, 2000; Mauras *et al.*, 2002; Wong *et al.*, 2007). IGF-1 deficiency inhibits growth both pre- and post-natal, with IGF-1 knockout mice exhibiting growth retardation and IGF-1 receptor (IGF-1R) deficient mice dying shortly after birth (Baker *et al.*, 1993; Lupu *et al.*, 2001). Furthermore, in humans with GH insensitivity due to a GH receptor defect, growth retardation and osteoporosis which are the result of IGF-1 deficiency are observed (Parks *et al.*, 1997). More recently, abnormalities of STAT5b, the IGF-1 receptor gene itself and the binding proteins that influence bioavailability of IGF-1 at the tissue level have all been reported to be associated with a variable extent of short stature in humans (Walenkamp and Wit, 2007). IGF-1 signalling is also thought to be critical for bone healing following fracture (Hoshi *et al.*, 2004).

The original model implicating GH and IGF-1 as central regulators of bone growth was termed the somatomedin hypothesis (Salmon and Daughaday, 1957; Daughaday *et al.*, 1972; Daughaday, 1989). It proposed that GH exerted its effects on the growth plate by stimulating production of hepatic IGF-1 (previously known as somatomedin), which would in turn stimulate target tissues including bone and the growth plate (Daughaday *et al.*, 1972; Daughaday, 1989; Lupu *et al.*,

2001). The somatomedin hypothesis has been questioned by experiments reporting that low concentrations of GH directly infused into the growth plate stimulates longitudinal growth in comparison to the contralateral limb (Isaksson *et al.*, 1982). The somatomedin hypothesis has been further challenged by studies showing that conditional liver-specific IGF-1 knockout mice exhibited body weights that were indistinguishable from wild-type littermates (Yakar *et al.*, 1999; Sjögren *et al.*, 1999; Liu *et al.*, 2000). These studies showed that, although the liver is the main source of circulating IGF-1, it is local IGF-1 that is important for regulating postnatal growth (Yakar *et al.*, 1999; Sjögren *et al.*, 1999). These findings have been challenged by Stratikopoulos and colleagues, who found that inducing hepatic IGF-1 production in IGF-1 knockout mice, which lacked IGF-1 in all other tissues, resulted in an increase of growth demonstrating that liver derived endocrine IGF-1 does in fact contribute to 30% of adult body size and sustains postnatal development (Stratikopoulos *et al.*, 2008).

It is now thought that GH can act independently on the growth plate to increase chondrocyte proliferation, as well as stimulating local production of IGF-1 (Nilsson *et al.*, 2005). Nilsson and colleagues found strong IGF-1 localisation in proliferating chondrocytes, with low levels of IGF-1 in hypertrophic cells, and they demonstrate that growth plate IGF-1 levels increased in response to GH (Nilsson *et al.*, 1986). Interestingly, more recent studies found that IGF-1 mRNA expression is predominantly found in the perichondrium with comparatively very low expression in any of the growth plate zones, indicating that IGF-1 may diffuse into the growth plate (Parker *et al.*, 2007). In combination with other similar studies, these observations have led to an alternative hypothesis termed the dual effector theory, where GH acts directly on germinal zone precursors of the growth plate to stimulate the differentiation of chondrocytes and the amplification of local IGF-1 secretion. This locally produced IGF-1, in turn, stimulates both chondrocyte clonal expansion and hypertrophy and consequently bone growth in an autocrine/paracrine manner (Isaksson *et al.*, 1982; Green *et al.*, 1985; Zezulak and Green, 1986; Wang *et al.*, 1999). Thus, although liver-derived IGF-1 is the main determinant of systemic IGF-1 levels, it is locally derived IGF-1 that

appears more important for postnatal growth (Yakar *et al.*, 1999; Yakar *et al.*, 2002). In fact, it seems likely that GH and IGF-1 have both dual and overlapping functions on chondrocytes, as both GH receptor (GHR) and IGF-1 mutant mice show reduced growth which is more severe in double GHR/IGF-1 mutants (Lupu *et al.*, 2001; Giustina *et al.*, 2008). There remain unanswered questions about the independent and combined relationships of GH and IGF-1 on the growth plate and bone growth, including whether or not GH mediates any IGF-1 independent effects on chondrocytes. Data on GH actions on chondrocyte proliferation have so far been largely conflicting; with some authors showing strong proliferative effects of GH while others show little or none (Madsen *et al.*, 1983; Livne *et al.*, 1997; Hutchison *et al.*, 2007).

1.5. Inflammatory Cytokine Inhibition of Bone Growth

1.5.1. Paediatric Diseases Affecting Bone Growth

Many chronic childhood inflammatory diseases, such as inflammatory bowel disease (IBD) and juvenile idiopathic arthritis (JIA), are associated with growth retardation coupled with elevated levels of inflammatory cytokines such as IL-6, TNF α , and IL-1 β (MacRae *et al.*, 2006a; MacRae *et al.*, 2006c; MacRae *et al.*, 2007a). Growth retardation in these patients is further exacerbated by the use of anti-inflammatory glucocorticoids such as dexamethasone which are known to inhibit bone growth and development (Ahmed *et al.*, 2002; Ahmed and Sävendahl, 2009). Patients with inflammatory conditions can have variable levels of GH but generally reduced levels of circulating IGF-1, indicating GH resistance (Davies *et al.*, 1997; De Benedetti *et al.*, 2001a; Wong *et al.*, 2010). They also show lower concentrations of IGFBP-3 (Davies *et al.*, 1997; De Benedetti *et al.*, 2001a). Treatment with relatively high doses of recombinant human GH has been shown to improve growth in children with JIA as well as IBD (Touati *et al.*, 1998; Bechtold *et al.*, 2001; Wong *et al.*, 2011).

Mice over-expressing IL-6 or TNF α exhibit growth retardation, with IL-6 over-expression resulting in reduced IGF-1 and IGFBP-3 levels, as observed in patients (Siegel *et al.*, 1995; De Benedetti *et*

al., 1997; De Benedetti *et al.*, 2001a; Li and Schwartz, 2003). The IL-6 growth defect can be completely abolished by IL-6 neutralization (De Benedetti *et al.*, 2001b). Treatment with IL-1 β results in reduced plasma levels of IGF-1 and ALS (Barreca *et al.*, 1998; Delhanty, 1998). There is also evidence that IL-1 β stimulates IGFBP-1 protein expression, which will inhibit IGF-1 activity (Lang *et al.*, 1996; Lang *et al.*, 1999; Frost *et al.*, 2000).

1.5.2. Inflammatory Cytokines and Endochondral Growth

Few studies have reported the effects of inflammatory cytokines on the growth plate. Elevated levels of IL-1 β , TNF α and IL-6 during inflammatory synovitis lead to local destruction of the growth plate (de Hooge *et al.*, 2003). IL-1 β and TNF α decrease both the width of the proliferating zone and the rate of endochondral bone growth; a possible consequence of altered chondrocyte proliferation and apoptosis rates (Aizawa *et al.*, 2001; Martensson *et al.*, 2004; MacRae *et al.*, 2006b). Furthermore, IL-1 β and TNF α reduce chondrocyte expression of proteoglycans including aggrecan and collagen types-II and -X (Goldring *et al.*, 1988; Horiguchi *et al.*, 2000; MacRae *et al.*, 2006b). IL-6, in combination with IL-6 receptor, has been shown to inhibit articular chondrocyte differentiation via the JAK/STAT pathway, but the addition of IL-6 alone appears to have little effect on growth plate chondrocytes (Legendre *et al.*, 2003; Martensson *et al.*, 2004). It therefore seems likely that IL-6 needs to be added in combination with soluble IL-6R to have an effect on chondrocyte proliferation and differentiation. Some of these effects, in particular those that result in destruction of the growth plate are likely to be a consequence of increased production of matrix metalloproteinase (MMPs) (Delhanty, 1998). The catabolic actions of MMPs on cartilage are well recognised and will counteract the anabolic actions of the GH/IGF-I axis (Reynolds *et al.*, 1994).

It is likely that one of the cellular mechanisms through which inflammatory cytokines act on the growth plate is the inhibition of IGF-1 signalling (Broussard *et al.*, 2004; Kenchappa *et al.*, 2004). Neither TNF α nor IL-1 β appear to affect IGF-1 signalling at its receptor level, although this has

been poorly investigated in chondrocytes (Matsumoto *et al.*, 1994; Shen *et al.*, 2002; Strle *et al.*, 2004; MacRae *et al.*, 2006c). Alternatively, inflammatory cytokines may disrupt signalling downstream of the IGF-1R, for example IRS phosphorylation, MAPK signalling or PI3K signalling. It has been suggested that IL-1 β is likely to inhibit the proliferative effect of IGF-1 on chondrocytes via the PI3K pathway (MacRae *et al.*, 2007a). TNF α and IL-1 β inhibit IRS-1 phosphorylation in myoblasts, and TNF α has been shown to inhibit Akt phosphorylation and MAPK-kinase phosphorylation in neuronal cells (Broussard *et al.*, 2004; Kenchappa *et al.*, 2004; Strle *et al.*, 2004). It is also possible that inflammatory cytokines act on GH signalling but to date little knowledge of the effects of inflammatory cytokines on STAT signalling in chondrocytes exists. IL-6 and oncostatin M have been shown to activate JAK2, STAT1 and STAT3 (IL-6 only) in chondrocytes, leading to down-regulation of matrix components (Li *et al.*, 2001; Legendre *et al.*, 2003). IL-1 β has been shown to antagonize GH signalling through STAT5 in hepatocytes whilst activating STAT3 in mouse kidney tumour cells (Boisclair *et al.*, 2000; Liu *et al.*, 2006). There is also evidence that IL-1 β , IL-6 and TNF α can induce the expression of SOCS proteins, which act to inhibit GH signalling (Denson *et al.*, 2003; Shi *et al.*, 2004).

1.6. Suppressor of Cytokine Signalling-2

1.6.1. SOCS Proteins

Cytokine signalling is negatively controlled by a variety of proteins, including protein tyrosine phosphatases and the SOCS proteins (Rico-Bautista *et al.*, 2006). There have been eight SOCS molecules identified to date, namely CIS and SOCS1-7, all of which are involved in negatively regulating cytokine signalling. SOCS proteins consist of a conserved C-terminal motif named the SOCS box, a central SH2 domain and a variable N-terminal domain (Tollet-Egnell *et al.*, 1999; Rico-Bautista *et al.*, 2006). They can bind through their SH2 domains to phosphorylated tyrosines within the cytokine receptor-JAK complex and inhibit JAK signalling and downstream STAT activation (Hilton, 1999; Rico-Bautista *et al.*, 2006; Pass *et al.*, 2009).

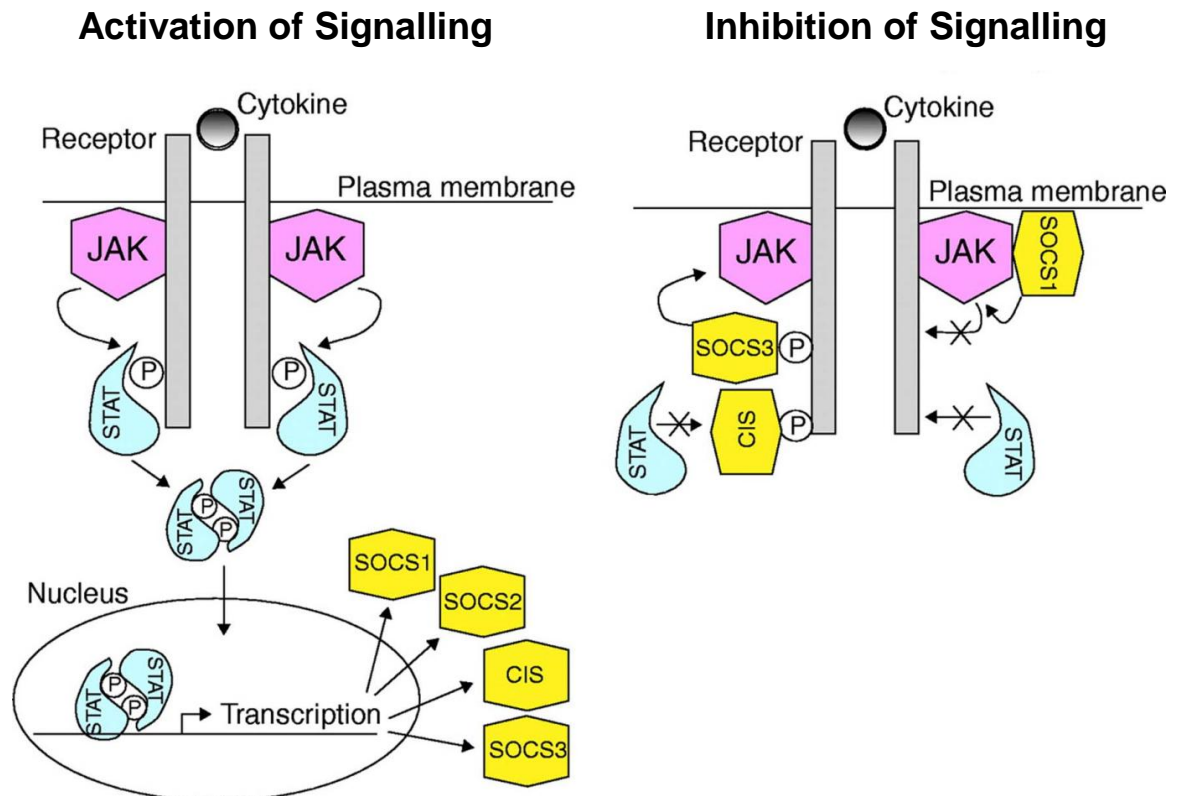


Figure 1.6. SOCS regulation of cytokine signalling. Once released downstream of cytokine signalling, SOCS proteins act in a negative feedback loop to regulate cytokine signalling through JAK proteins. Shown are the mechanisms of inhibition by CIS, SOCS1 and SOCS3. The mechanisms of SOCS2 are unknown. Image from Krebs and Hilton (2001).

The way in which SOCS proteins are thought to interact with cytokine signalling is depicted in Figure 1.6.

Expression of SOCS is normally stimulated by the very cytokines they inhibit, thereby creating a negative feedback loop (Turnley, 2005; Rico-Bautista *et al.*, 2006). GH signalling is inhibited by CIS and SOCS1-3. These four SOCS proteins can be induced by: IL-2, IL-3, IL-4, IL-6, prolactin, interferon- γ (IFN- γ), erythropoietin (Epo), granulocyte colony-stimulating factor (G-CSF), granulocyte macrophage colony-stimulating factor (GM-CSF), and leukemia inhibitory factor (LIF); although the relationship between the SOCS proteins and these cytokines varies from cell to cell and between SOCS proteins (Krebs and Hilton, 2001).

SOCS1 has been shown to inhibit signalling by IL-2, IL-3, IL-4, IL-6, GH, prolactin, erythropoietin, LIF, IFN- γ , IFN- α , oncostatin M (OSM), thymic stromal lymphopoietin (TSLP), thrombopoietin (TPO), thyrotropin and IGF-1 (Nicholson *et al.*, 1999; Krebs and Hilton, 2001; Greenhalgh and Alexander, 2004). It can directly bind phosphorylated JAK proteins via its SH2 domain (Greenhalgh and Alexander, 2004). SOCS1^{-/-} mice exhibit stunted growth and die young, before weaning, with immune cell infiltration of organs and liver fatty degeneration (Starr *et al.*, 1998). Upon examination the mice also have small thymus and reduced numbers of mature B lymphocytes (Starr *et al.*, 1998). Studies in SOCS1^{-/-} mice have found that it is a key regulator of IFN- γ signalling, as administration of IFN- γ to the mice can prevent the fatal organ degeneration (Alexander *et al.*, 1999). The perinatal lethality of SOCS1^{-/-} mice is also mediated by lymphocytes, so that SOCS1 seems to act to regulate T cell function and/or differentiation and to inhibit IFN- γ signalling (Marine *et al.*, 1999b).

Studies have found that SOCS3 can inhibit signalling by IL-2, IL-3, IL-4, IL-6, GH, prolactin, erythropoietin, LIF, IFN- γ , IFN- α , IGF-1, ciliary neurotrophic factor, leptin, oncostatin M, and insulin (Nicholson *et al.*, 1999; Pezet *et al.*, 1999; Krebs and Hilton, 2001). Like SOCS1, it can directly bind activated JAK proteins through its SH2 domain (Greenhalgh and Alexander, 2004).

SOCS3^{-/-} mice are embryonically lethal, dying between gestation days 11 and 13 (Roberts *et al.*, 2001). The premature death of SOCS3^{-/-} embryos occurs as a result of faults with placental development, caused by increased cytokine signalling (Roberts *et al.*, 2001). SOCS3^{-/-} lethality is also associated with erythrocytosis, demonstrating that SOCS3 acts to negatively regulate liver erythropoiesis, and with IL-6 hyper-responsiveness (Marine *et al.*, 1999b; Greenhalgh and Alexander, 2004).

CIS can inhibit signalling by IL-2, IL-3, prolactin, erythropoietin, IGF-1 and GH (Krebs and Hilton, 2001). CIS is thought to inhibit STAT signalling by interacting with the cytokine receptor to block STAT binding sites (Krebs and Hilton, 2001). CIS^{-/-} mice exhibit no obvious phenotype, although over-expression of CIS results in growth retardation (Greenhalgh and Alexander, 2004). Studies using transgenic mice have demonstrated that CIS is an important regulator of T cell activation mediated by the T cell receptor (Li *et al.*, 2000).

SOCS2 has been shown to inhibit signalling by GH, IL-6, LIF, IGF-1 and prolactin (Minamoto *et al.*, 1997; Dey *et al.*, 1998; Pezet *et al.*, 1999; Greenhalgh *et al.*, 2002b; Kamradt and Schubert, 2005). SOCS2^{-/-} mice are viable and exhibit an overgrowth phenotype from 3-weeks of age, as discussed below (Metcalf *et al.*, 2000). Inhibition of GH signalling by SOCS1 and 3 is complete whereas SOCS2 and CIS only cause partial inhibition and it is difficult to reconcile these actions with the observed growth of the transgenic mice (Adams *et al.*, 1998; Hansen *et al.*, 1999; Inaba *et al.*, 2005). Clearly, other interactions are important possibly involving the other SOCS proteins. The pathways inhibited by SOCS4, SOCS5, SOCS6 and SOCS7 are largely unknown, although SOCS5 has been shown to inhibit IL-6 and IL-4; SOCS6^{-/-} mice exhibit mild growth retardation due to an unknown mechanism; SOCS7 can associate with growth factor receptor-bound protein 2 (Grb2), non-catalytic region of tyrosine kinase adaptor protein (Nck) and phospholipase C-γ (PLCγ) (Krebs and Hilton, 2001; Greenhalgh and Alexander, 2004).

1.6.2. SOCS2 Knockout Mouse

The overgrowth phenotype of SOCS2 knockout (SOCS2^{-/-}) mice has led to confirmation that the key pathway regulated by SOCS2 is the GH/IGF-1 axis, although SOCS2 also regulates other pathways including prolactin signalling (Metcalf *et al.*, 2000; Rico-Bautista *et al.*, 2005; Rico-Bautista *et al.*, 2006). Adult male SOCS2^{-/-} mice are 40% heavier than their wild-type littermates and are more severely affected than females. However adult females still reach the same size as wild-type males (Metcalf *et al.*, 2000). The increased body weight of SOCS2^{-/-} is not as a result of any increase in fatty tissue, but rather a proportional increase in size of most internal organs, muscle and bones, due to hyperplasia and not hypertrophy (Metcalf *et al.*, 2000). Consistent with increased bone size, SOCS2^{-/-} mice have longer longitudinal bones (femur, tibia, radius and humerus) as well as increased body length (Metcalf *et al.*, 2000; MacRae *et al.*, 2009). Epiphyseal chondrocytes express SOCS2 and growth plates from SOCS2 null mice are enlarged with wider proliferative and hypertrophic zones (MacRae *et al.*, 2009). Some studies have shown reduced trabecular and cortical bone mineral density (BMD) in SOCS2^{-/-} bones, which is not consistent with the enhanced GH/IGF-1 signalling observed in the SOCS2^{-/-} mice (Lorentzon *et al.*, 2005; Rico-Bautista *et al.*, 2006). More recent studies using high resolution analyses of trabecular bone architecture and cortical bone geometry have found that SOCS2^{-/-} mice exhibit no difference in BMD compared to wild-type littermates, coupled with increased trabecular bone volume (MacRae *et al.*, 2009). This is consistent with the anabolic role of GH on the skeleton (Ohlsson *et al.*, 1998; Andreassen and Oxlund, 2001). SOCS2^{-/-} mice display elevated IGF-1 mRNA in some tissues (heart, lung, spleen but not liver, bone, fat, muscle), but interestingly circulating IGF-1 levels are not increased (Metcalf *et al.*, 2000; MacRae *et al.*, 2009). It is therefore likely that the increased bone growth and observed structural differences within SOCS2^{-/-} growth plates is a direct consequence of altered SOCS2 mediated GH/IGF-1 signalling at the growth plate (Alexander *et al.*, 1999; Turnley, 2005; MacRae *et al.*, 2009).

Greenhalgh *et al.* demonstrated firm evidence that SOCS2 acts on the GH pathway by crossing SOCS2^{-/-} mice with Ghrhr^{lit/lit} mice, which are GH deficient due to a point mutation in the GH-releasing hormone (LeRoith and Nissley, 2005; Greenhalgh *et al.*, 2005). Both the double knockout mice and the Ghrhr^{lit/lit} mice exhibited a similar 60% growth retardation (Greenhalgh *et al.*, 2005). Furthermore, administration of GH to these double knockout mice caused an increase of growth to a size indistinguishable from SOCS2^{-/-} mice (LeRoith and Nissley, 2005; Greenhalgh *et al.*, 2005). An interaction between SOCS2 and GH signalling in regulating growth is consistent with the temporal increased expression of the GHR and the overgrowth phenotype with both occurring at around 3-weeks of age (Metcalf *et al.*, 2000). Moreover, prolonged STAT5 activation in response to GH has been observed in hepatocytes cultured from SOCS2^{-/-} mice, which may result in increased IGF-1 activation (Greenhalgh *et al.*, 2002a; Turnley, 2005; LeRoith and Nissley, 2005). When SOCS2^{-/-} mice are crossed with STAT5b^{-/-} mice the overgrowth phenotype is attenuated, with normal growth observed demonstrating the importance of SOCS2 interactions of GH signalling (Greenhalgh *et al.*, 2002a; LeRoith and Nissley, 2005; Flores-Morales *et al.*, 2006).

Similar phenotypes to the SOCS2^{-/-} mice have been observed in high growth (hg) mice, a phenotype that occurs following a spontaneous mutation in mouse chromosome 10 that has been mapped to a genetic interval of 100 to 103 centimorgan from the top of human chromosome 12 (Horvat and Medrano, 1995; Horvat and Medrano, 1998; Horvat and Medrano, 2001). Again these mice demonstrate 30-50% increases in postnatal growth, and the identification of the SOCS2^{-/-} mouse phenotype has led to SOCS2 being mapped to the hg region (Horvat and Medrano, 1995; Horvat and Medrano, 2001). The only recognised difference between hg and SOCS2^{-/-} mice is that hg mice have high plasma IGF-1, levels possibly due to another gene deletion in the hg region (Horvat and Medrano, 2001).

1.6.3. Over-expression of SOCS2

Intriguingly, over-expression of SOCS2 using a human ubiquitin promoter does not limit growth as may be expected, but surprisingly results in a similar phenotype to SOCS2^{-/-} mice (Greenhalgh *et al.*, 2002b; Turnley, 2005). Transgenic expression of SOCS2 in male mice causes a 13-15% increase in body weight, with significant increases in female mice also (Greenhalgh *et al.*, 2002b). It is, therefore, likely that the effects of SOCS2 on GH signalling is dose dependant, with dual effects (Greenhalgh *et al.*, 2002b; Turnley, 2005; Flores-Morales *et al.*, 2006). It has been proposed that at physiological levels, SOCS2 inhibits GH signalling by blocking sites of STAT activation on the GHR, but at higher doses it inhibits signalling of other, more potent GH inhibiting SOCS (SOCS1 and 3) (Favre *et al.*, 1999; Greenhalgh *et al.*, 2002b; Turnley, 2005). This could be through association with SOCS3 binding sites on the GHR, thus blocking SOCS3 action, or by binding the other SOCS themselves and suppressing them through proteasomal degradation (Uyttendaele *et al.*, 2007).

1.6.4. SOCS2 and GH Signalling

Expression of SOCS is usually stimulated by the very cytokines they inhibit, so that they create negative feedback loops (Turnley, 2005; Rico-Bautista *et al.*, 2006). GH signalling is inhibited by CIS, SOCS1, SOCS2 and SOCS3, but this work in chondrocytes will focus on SOCS2. If the premature death of SOCS1^{-/-} mice is prevented by using IFN- γ antibodies the mice do not display overgrowth, the role of SOCS3 has been poorly examined as SOCS3^{-/-} mice are embryonic lethal and CIS^{-/-} mice do not exhibit any phenotype (Greenhalgh and Alexander, 2004; Turnley, 2005). Inhibition of GH signalling by SOCS1 and 3 is complete, with SOCS3 thought to be the primary inhibitor, whereas SOCS2 and CIS only cause partial inhibition (Adams *et al.*, 1998; Ram and Waxman, 1999; Hansen *et al.*, 1999). Incidentally, these four SOCS proteins (CIS, SOCS1, 2 and 3) are the only ones that have been widely studied and it is possible other SOCS family members may also inhibit GH signalling (Inaba *et al.*, 2005).

It has been well documented that GH signalling stimulates SOCS2 expression, in a dose and concentration dependant manner, with the maximum affect observed after 24hrs treatment with 0.5 - 5.0µg GH/ml (Tollet-Egnell *et al.*, 1999). Furthermore, it is thought that SOCS2 production is regulated by GH signalling through STAT5b, which is consistent with the importance of STAT5b for growth (Vidal *et al.*, 2007). This confirms the hypothesis that SOCS2 acts in a negative feedback loop to control and regulate GH signalling under physiological conditions and offers a plausible explanation for the overgrowth phenotype of SOCS2^{-/-} mice (Tollet-Egnell *et al.*, 1999). High SOCS2 expression has been found in the liver, a major source of circulating IGF-1, and in the heart (Tollet-Egnell *et al.*, 1999).

The precise mechanism by which SOCS2 regulates GH signalling is unclear. The strongest evidence indicates that SOCS2 may bind the SHP2-binding sites on the GHR (Tyr595 and Tyr487), which will prevent STAT5b activation (Greenhalgh *et al.*, 2005; Yoshimura *et al.*, 2007; Uyttendaele *et al.*, 2007). It has also been demonstrated that SOCS2 binds Elongins B and C, suggesting this complex may then bind cullin-2 and act as an E3 ubiquitin ligase to degrade the GHR or the GHR-JAK2 complex (Ram and Waxman, 1999; Greenhalgh and Alexander, 2004; Rico-Bautista *et al.*, 2006). Furthermore, it has been demonstrated that the SOCS2 SH2 domain directly binds a tyrosine in the activation loop of JAK2, inhibiting JAK2 tyrosine phosphorylation and activation of STATs (Rico-Bautista *et al.*, 2006; Flores-Morales *et al.*, 2006). Interestingly, SOCS2 actions may not be confined to regulating GH signalling. There is evidence that SOCS2 can directly bind the IGF-1R and therefore it is possible that SOCS2 also regulates IGF-1 signalling, although IGF-1 does not induce SOCS2 expression (Dey *et al.*, 1998; Greenhalgh and Alexander, 2004; Michaylira *et al.*, 2006b).

Glucocorticoids, including dexamethasone, are thought to desensitize GH signalling and thus suppress growth by up-regulating SOCS2 (Tollet-Egnell *et al.*, 1999; Rico-Bautista *et al.*, 2006). Oestrogen inhibition of GH signalling, through JAK2 inhibition, is also thought to be mediated by

SOCS2 (Leung *et al.*, 2003). The effects of inflammatory cytokines on SOCS2 have however been poorly investigated, with evidence that some interleukins induce SOCS2 gene expression in specific cell types (IL-2, -3, -4, -5, -6) (Starr *et al.*, 1997; Krebs and Hilton, 2001). For example, IL-1 β has been shown to stimulate SOCS2 in tonsillar cells and B-lymphoma cells, whereas it does not increase SOCS2 expression in hepatic liver cells (Dogusan *et al.*, 2000; Boisclair *et al.*, 2000). Furthermore, TNF α stimulates SOCS2 expression in chondrocytes (MacRae *et al.*, 2009). There is evidence that IL-1 β , TNF α and IL-6 induce expression of SOCS3 in certain cell types (Denson *et al.*, 2003; Shi *et al.*, 2004).

There are still many aspects on the actions of SOCS2 that have yet to be investigated. The precise mechanism by which SOCS2 alters GH/IGF-I signalling have yet to be fully determined as are the resultant cellular events that occur at the growth plate and are responsible for normal growth. It is also unclear if SOCS2 mediates the deleterious effects of inflammatory cytokines on linear bone growth.

1.7. Aims

The overgrowth phenotype of SOCS2^{-/-} mice occurs from 3-weeks of age, but the local cellular (chondrocyte) mechanisms behind the increased longitudinal growth from this age are largely unknown. Therefore, the aim of this studentship is to fully establish the role of SOCS2 on endochondral bone growth and the signalling pathways involved. This will be achieved both *in vitro* and *in vivo* using a range of cell and molecular biology techniques. The specific aims are:

- Establish the role of GH and IGF-I signalling on STATs1, 3 and 5 phosphorylation and SOCS1-3 expression in growth plate chondrocytes
- Conduct a detailed examination of the growth plate of SOCS2^{-/-} mice to help understand better the overgrowth phenotype

- Using in vitro chondrocyte cultures (wild-type, SOCS2 null and SOCS2 over-expressing cells) and metatarsal organ cultures (wild-type and SOCS2 null) determine if the overgrowth phenotype of SOCS2^{-/-} mice is a result of altered chondrocyte proliferation and STAT activation by GH
- Examine the role of SOCS2 in mediating the effects of inflammatory cytokines on growth

CHAPTER 2

MATERIALS AND METHODS

2. Materials and Methods

2.1. Materials

Unless stated otherwise: chemicals were obtained from Sigma (Poole, UK); cell culture reagents were purchased from Invitrogen (Paisley, UK); PCR oligonucleotides were generated by Eurofins MWG Operon (London, UK). All medium and buffer recipes are shown in Appendix 10.1.

2.2. Cell Culture

2.2.1. ATDC5 Cells

The murine chondrogenic ATDC5 cell line has been widely used throughout the field of growth plate research. The cells were derived by Atsumi *et al.* from AT805 teratocarcinoma cells, and have been shown to be a good model of chondrocyte differentiation (Atsumi *et al.*, 1990). Cultured ATDC5 cells can be used to study differentiation of mesenchymal cells into chondrocytes, followed by terminal differentiation from proliferating to hypertrophic chondrocytes (Mushtaq *et al.*, 2002).

ATDC5 cells were obtained from the RIKEN cell bank (Ibaraki, Japan), and maintained as described previously (Atsumi *et al.*, 1990). Cells were cultured in T175 flask (Costar, High Wycombe, UK) in maintenance medium until sub-confluent, and then passaged as follows. Cells were washed in serum free DMEM/F-12 and then incubated in trypsin-EDTA (Sigma) until cells were rounded and detached. Maintenance media (containing serum to inactivate the trypsin) was then used to wash the cells into a universal and the cells pelleted, resuspended and counted with a haemocytometer. This allowed cells to be plated at the required density (6000/cm²) in multi-well plates for experimentation. Once confluent, cells were induced to differentiate by addition of differentiation medium (which contained insulin). For serum deprivation, differentiation medium without FBS and ITS was used. Cells were first incubated in serum free medium for 15mins at 37°C

to rid cells of serum components, which was replaced over night with fresh serum free medium. Cells were incubated in a humidified atmosphere (37°C, 5% CO₂:95% air).

2.2.2. Freezing/Thawing Cells

For freezing, cells were first trypsinised and counted as described in 2.2.1. Cells were then re-suspended in 50/50 maintenance medium and freezing mix to give 3 million cells per ml. 1ml of this was added to each cryovial (Corning, Surrey, UK) and wrapped in cotton wool within a polystyrene box at -80°C for 3-5 days before transfer to -150°C.

To thaw cells, a cryovial (containing 3 million cells) was thawed from -150°C to 37°C and then had 5ml maintenance medium added in a slow, drop wise manner. Cells were pelleted by centrifugation, to remove toxic DMSO, and resuspended in maintenance medium before being transferred to a T175 flask to grow to sub-confluency prior to plating in multi-well plates (see 2.2.1.).

2.3. In vivo Studies

2.3.1. Animal Welfare

Animals were maintained under conventional housing conditions with a 12h light/dark cycle. All animal experiments were approved by The Roslin Institute's Animal Users Committee and the animals were maintained in accordance with Home Office guidelines for the care and use of laboratory animals.

2.3.2. Generation of SOCS2 Knockout Mice

The SOCS2 knockout mice were previously generated at The Roslin Institute by Dr. Simon Horvat, as described by MacRae *et al.* (2009). A summary taken from that paper is given here (MacRae *et al.*, 2009). A previously isolated BAC clone (520L19) which contains the *Socs2* locus was used to subclone a plasmid with a *Xba*I genomic fragment containing exons 2 and 3 of the *Socs2* transcript

(Ensembl ID ENSMUST00000020215; 7517bp long; positions 94841854 to 94849370 bp on chromosome 10; mouse genome Ensembl release 45 – June 2007; http://www.ensembl.org/Mus_musculus/) (Horvat and Medrano, 1998). The reporter-selection marker cassette from plasmid pGT1.8Ires β geo was inserted into exon 2 at the *KpnI* site (see Appendix 10.2), causing transcription to terminate prematurely and thus a lack of *Socs2* function. Embryonic stem (ES) cells from the strain 129Sv were electroporated with *NotI*-linearised construct (Magin *et al.*, 1992) and antibiotic resistant ES cell colonies selected using G418. Southern blot analysis of digested DNA was used to identify clones containing the expected fragment size of targeted and wild type alleles. Two karyotypically normal positively targeted ES clones were used to inject C57Bl/6J blastocytes and generate chimeras, which were then back-crossed with C57Bl/6J mice. Agouti-coloured potential founder offspring were identified using southern blot analysis as above, and subsequent generations tested by PCR analysis of DNA.

2.3.3. Tail/Ear Biopsies for Genotyping

Genotyping was performed on tissue taken from ear clips at weaning, also used for animal identification, or from 1-2cm tail biopsies taken under halothane anaesthetic. The tissue was digested in lysis buffer (150 μ l for ear; 750 μ l for tail) overnight at 37°C, and then frozen at -20°C.

2.3.4. DNA Isolation for Genotyping

Digested tissue isolated as described in Section 2.3.3 was thawed to 37°C, then washed in 0.75 volume phenol:chloroform:isoamyl alcohol (1 volume = 750 μ l for tail samples; 100 μ l for ear samples). Samples were vortexed and centrifuged to wash, then 0.75 volume of the supernatant transferred to a fresh Eppendorf. 0.025 volume of 20M sodium acetate and 0.75 volume of isopropanol were added, tubes inverted 15 times then left to stand for 15 minutes. DNA was pelleted by 1 minute centrifugation at 13,000rpm. The supernatant was removed and the pellet was washed in 1 volume 70% ethanol (Fisher Scientific, Leicestershire, UK), re-pelleted and air dried. The DNA was then re-suspended in 50-100 μ l dH₂O overnight at 4°C. DNA concentration and

quality was read on a Nanodrop spectrophotometer (ND-1000; Labtech International Ltd, East Sussex, UK). Quality was assessed by the A_{260}/A_{280} ratio, where 1.8 was considered optimum. Samples were finally diluted to 4ng/ μ l in dH₂O for PCR.

2.3.5. Genotyping

Two separate PCR reactions were carried out for genotyping to identify wild-type (WT; SOCS2) and knockout (KO; neo-cassette) bands. Primer pairs are shown in Table 2.1.

	Forward (5' to 3')	Reverse (5' to 3')	Band Size
SOCS2 (WT)	TGTTTGACTGAGCTCGCGC	CAACTTTAGTGTCTTGGATCT	569bp
Neo (KO)	ACCCTGCACACTCTCGTTTTG	CCTCGACTAAACACATGTAAAGC	100bp

Table 2.1. Primers used for genotyping. Sequences and band sizes for primers used to genotype SOCS2 knockout and wild-type mice.

For the WT PCR, each reaction contained: 3 μ l DNA (4ng/ μ l); 2.5 μ l 10X NH₄ buffer (Bioline, London, UK); 0.75 μ l 50mM MgCl₂ (Bioline); 2.5 μ l 2mM dNTPs (Invitrogen); 0.5 μ l 20pmol/ μ l forward and reverse SOCS2 primers; 16 μ l nuclease free H₂O; 0.25 μ l 5U/ μ l Biotaq DNA Polymerase (Bioline). The PCR reaction was performed on a DNA Engine Dyad machine (Peltier Thermal Cycler, Bio-Rad Laboratories, Hertfordshire, UK) under the following conditions: 3mins denaturing at 94°C; 35 thermocycles consisting of 20secs at 94°C (denaturing), 20secs at 54°C (annealing), and 45secs at 72°C (extension); 10mins extension at 72°C.

For the KO PCR, each reaction contained: 6 μ l DNA (4ng/ μ l); 1.68 μ l nuclease free H₂O; 1.2 μ l 10X PCR buffer (Invitrogen); 1.2 μ l 2mM dNTPs (Invitrogen); 1.2 μ l 25mM MgCl₂ (Invitrogen); 0.3 μ l 10pmol/ μ l Neo Forward primer; 0.3 μ l 10pmol/ μ l Neo Reverse primer; 0.12 μ l 5U/ μ l Platinum Taq DNA Polymerase (Invitrogen). The PCR reaction was performed on the DNA Engine Dyad machine under the following conditions: 2mins denaturing at 92°C; 35 thermocycles consisting of 1min at 92°C (denaturing), 1min at 55.7°C (annealing), and 1min at 72°C (extension); 10mins extension at 72°C.

The PCR products were diluted 5:1 with 5X blue loading buffer (WT; Bioline) or 6X orange loading buffer (KO; New England Biolabs, Herts, UK). 12µl was loaded per sample in separate wells in 1.8% Agarose/1XTBE (Ambion, Cambridge, UK) gels containing 0.5µg/ml Ethidium Bromide. Gels were run in TBE buffer in an electrophoresis tank at 160V. HyperLadders I and V (Bioline) were used as molecular weight markers. Gels were imaged under UV light using a Gel Logic 200 Imaging System and software (Kodak, Hemel Hempstead, Herts, UK). Figure 2.1 shows typical bands for wild-type and SOCS2 knockout samples.

2.3.6. Growth Analysis

Growth analysis was measured by staff in the small animal unit at The Roslin Institute. Weekly measurements were taken for both male and female mice in 5 SOCS2^{-/-} and 5 wild-type (WT) litters (33 WT and 40 SOCS2^{-/-} mice in total) from 2-weeks until 7-weeks of age. Body lengths were established by measuring the crown to rump distance using digital callipers. Body weight was determined by placing the animal in a container on scales.

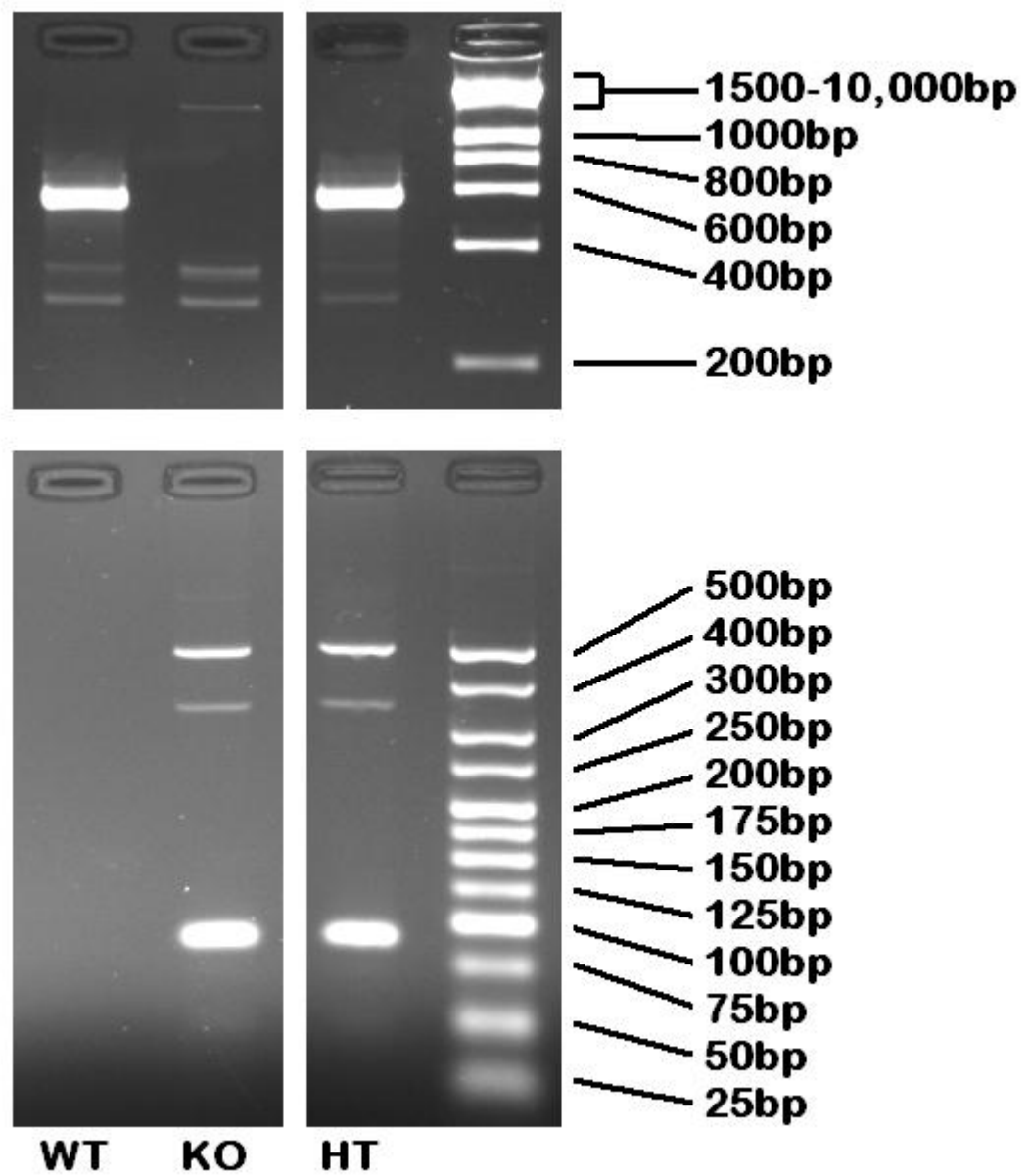


Figure 2.1. Genotyping. Typical bands gained for wild-type (WT), SOCS2 knockout (KO) and heterozygous (HT) samples, with molecular weight ladders. The bands are approximately 570bp (WT) and 100bp (KO).

2.3.7. Isolating Primary Chondrocytes

Sternal primary chondrocytes were isolated from 1- to 3-day old WT Swiss mice and C57/BL6 WT or SOCS2^{-/-} mice and cultured using a method previously developed by Lefebvre and colleagues (Lefebvre *et al.*, 1994; MacRae *et al.*, 2009). Mice were killed by decapitation and the rib cage and sternum were dissected, removing organs, the spine and excess tissue. Ribcages were washed in sterile phosphate buffered saline (PBS; 1X) and incubated at 37°C in 2mg/ml protease (from *Streptomyces griseus*) in PBS for 30mins, with shaking. The ribcages were then washed in PBS before being placed in sterile 3mg/ml collagenase type 2 (Worthington Biochemical Corporation, Lakewood, New Jersey, US) in DMEM (with 4.5g/l glucose and L-Glutamine) and incubated for 15mins at 37°C, with shaking. Muscle and soft tissue were then removed from the ribs and sternum by gentle pipetting, and bones washed in sterile PBS. Figure 2.2 shows an example of a rib cage at this stage.

The cartilage rods were then finally digested by incubation at 37°C in sterile collagenase type 2 (3mg/ml in DMEM) for 3 to 4hrs with regular agitation. Cells suspended in collagenase were filtered through a 45µm sieve, pelleted by centrifugation and re-suspended in DMEM. The cells were counted using a haemocytometer (typically 1×10^6 cells were isolated per mouse), and plated at a density of 100,000 cells per cm² in primary chondrocyte medium (supplemented with 50µg/ml L-ascorbic acid phosphate (Wako Pure Chemicals Ltd, North Rhine-Westphalia, Germany) for the first 48hrs of culture). Medium was changed every 2 days. For experiments requiring serum deprivation, cells were cultured without FBS for 24hrs prior to challenge with growth factors or cytokines. Cells were incubated in a humidified atmosphere (37°C, 5% CO₂). To ensure the chondrocytes did not de-differentiate, they were not typically cultured for longer than one week.

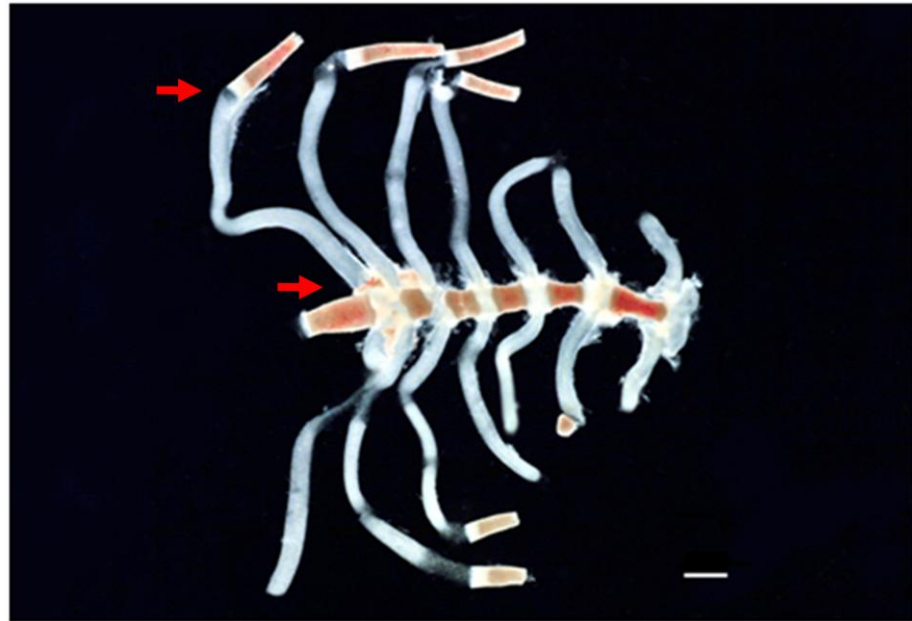


Figure 2.2. Isolation of sternal primary chondrocytes. Chondrocytes were isolated from the rib cage cartilage (the area between the red arrows) by collagenase digestion. Scale bar shows 1mm.

2.3.8. Isolating Primary Osteoblasts

Primary osteoblasts were isolated from 4-day old C57/BL6 WT mice that were killed by decapitation. Calvaria were dissected and washed in sterile HBSS. They were then digested in sterile 1mg/ml collagenase 2 (Worthington Biochemical Corporation) in HBSS at 37°C for 10mins with shaking. The supernatant was discarded and the calvaria were digested with fresh 1mg/ml collagenase for 30mins. The supernatant was retained as fraction 1. The calvaria were washed in sterile PBS and incubated in 4mM EDTA for 10mins at 37°C with shaking. The supernatant was retained as fraction 2. The calvaria were then washed in sterile HBSS, which was added to fraction 2. They were then digested in 1mg/ml collagenase at 37°C for 30mins, with shaking, and the supernatant removed as fraction 3. The calvaria were finally washed in sterile PBS which was added to fraction 3. The three fractions were pelleted by centrifugation and re-suspended in osteoblast medium. The cells were then distributed in T75 flasks (Costar) at a ratio of 3 calvaria per flask in 12ml osteoblast medium. Medium was refreshed following 3hrs culture to remove cell debris. Following 3-4 days of culture the osteoblasts were trypsinised and passaged as described in 2.2.1 and plated into multi-well plates at a density of 10,000/cm². For experiments requiring serum deprivation cells were incubated without FBS. Cells were incubated in a humidified atmosphere (37°C, 5% CO₂).

2.3.9. Calcein Labelling

C57/BL6 WT or SOCS2^{-/-} mice received an intra-peritoneal (i.p.) injection of 10mg/ml calcein in sodium bicarbonate (NaHCO₃; BDH Limited, Poole, UK) 4 days prior to sacrifice. Calcein aliquots were wrapped in foil to protect from the light and stored at 4°C prior to use. Calcein is incorporated into the mineralisation front and can be observed as green fluorescence under UV light and thus used to measure daily mineral apposition rate at the chondro-osseous junction (Owen *et al.*, 2009).

2.3.10. BrdU Incorporation

C57/BL6 WT or SOCS2^{-/-} mice received an i.p. injection of 10µl/kg of 20mM BrdU (5-bromo-2'-deoxyuridine) in 0.9% sterile saline (NaCl) 24hrs prior to sacrifice. BrdU is taken up by proliferating cells thus can be analysed by immunohistochemistry of tissue sections to assess proliferation (Farquharson and Loveridge, 1990).

2.3.11. Isolating Embryonic Metatarsals

Embryonic metatarsal cultures provide a well established ex vivo model of bone growth ((Mushtaq *et al.*, 2004); Figure 2.3). Plug dates were ascertained from matings of WT or SOCS2^{-/-} mice, after which mating pairs were separated to give an accurate date of conception. 17 day old embryos were killed by decapitation and the middle three metatarsals were isolated under a dissecting microscope. Throughout the dissection the bones were kept moist with preparation medium that had been warmed to 37°C (from aliquots stored at -20°C).

Metatarsals were cultured in 24-well plates (Costar) containing one bone in 300µl metatarsal medium per well. Metatarsals were cultured for up to 14 days, and medium changed every 2 days. Their lengths were measured at X4 magnification every 2 days using a Nikon eclipse TE300 microscope with a digital camera attached, using Image Tool (Image Tool Version 3.00, University of Texas Health Life Sciences Centre, San Antonio, TX). Bones were incubated in a humidified atmosphere (37°C, 5% CO₂).

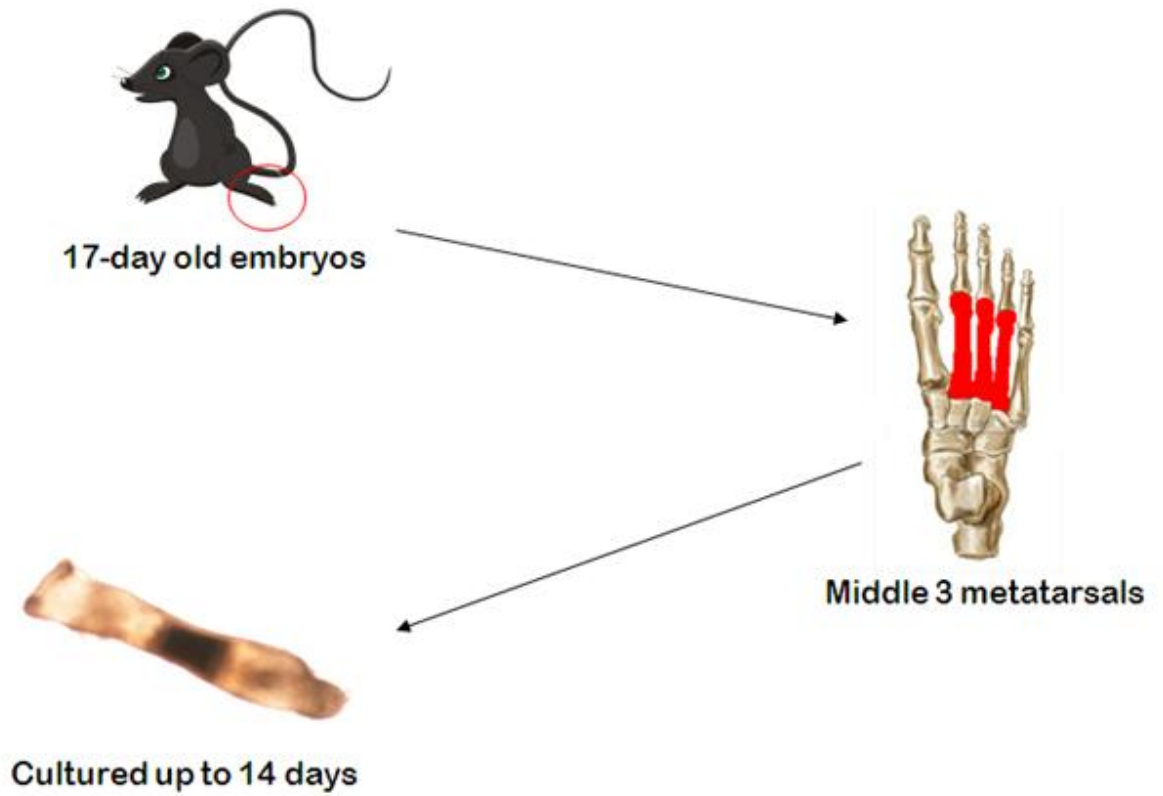


Figure 2.3. Metatarsal culture. The middle three metatarsals were dissected for 17-day old mouse embryos and cultured for up to 14-days to measure linear growth.

2.3.12. LPS Model of Inflammation

The systemic administration lipopolysaccharide (LPS), a bacterial endotoxin, is a widely accepted model of inflammation that results in a reproducible production of pro-inflammatory cytokines. The LPS model was used for a small pilot study investigating the inflammatory response in the absence of SOCS2. 4-week old C57/BL6 WT or SOCS2^{-/-} mice were weighed, measured crown to rump and anaesthetised by isoflurane gas to allow the acquisition of whole-body x-rays, which were then used to measure tibiae lengths. Twenty-four hours later they were injected i.p. with 50µg/kg LPS (Serotype 0127:B8) in sterile 0.9% saline. Age and genotype matched control mice received i.p. injections of an equal volume of sterile 0.9% saline. The mice received LPS/saline injections as above every 24hrs for 7 days to induce an inflammatory response. The mice were re-weighed after 4 days to ensure the dosage regime was correct, and crown to rump measured. Twenty-four hours following the final injection the mice were culled and weighed, measured from crown to rump, whole body x-rayed and the long bones dissected out.

2.3.13. DSS Induced Colitis Model

Oral administration of dextran sodium sulphate (DSS) has been shown to induce colitis in the distal colon, which slowly repairs upon removal of DSS. DSS is thought to have a toxic effect on intestinal cells, resulting in a breach of the mucosal barrier and exposure to luminal antigens which results in inflammation (Harris *et al.*, 2009). This leads to a systemic increase in pro-inflammatory cytokines, which in turn leads to decreased body weight associated with reduced bone length, growth plate width and bone mass (Williams *et al.*, 2001; Hamdani *et al.*, 2008; Harris *et al.*, 2009). Mice received DSS (molecular weight 36,000-50,000; MP Biomedicals, Solon, OH, US) typically 4%, in their drinking water (tap water). They were given DSS treated water ad lib for 5 days, which was refreshed daily, following which they received normal tap water for a 10 day recovery period. They were then culled by cardiac puncture, blood collected for serum analysis, and the long bones and distal colon dissected. The mice were weighed and the crown to

rump length was measured daily, as described in Section 2.3.6. Their health status was also scored daily, with particular attention paid to their coat condition, mobility, blood in stools and eye clarity. In accordance with Home Office legislation any mice that lost 25% of their starting body weight, or whose health severely deteriorated, were culled. The mice were anaesthetised with isoflurane gas and x-rayed at days 1, 8 and 15. To establish the weight loss that was due to inflammation and not lowered food intake, the quantity of food consumed daily (fed *ad lib.*) was weighed and then administered to pair-fed control animals the following day (who received no DSS). Control mice were also weighed and measured daily, x-rayed as above, and scored for health. All mice were housed individually to allow accurate measurement of food intake and health status.

2.4. Proliferation Assays

2.4.1. Cell [³H]Thymidine Proliferation Assay

To assess proliferation (ATDC5 cells; primary chondrocytes and primary osteoblasts) cells were plated in 48-well plates. During the last 2hrs of culture the cells were incubated with 0.2 μ Ci/ml [³H]-thymidine (Amersham, Buckinghamshire, UK). The cells were then washed in DMEM and fixed in ice-cold trichloroacetic acid (5%; TCA) for 15mins. They were then washed twice in PBS (5mins) and lysed in 0.1M NaOH for up to 20mins. The lysed cells were then added to a scintillation vial along with 3ml scintillation fluid (OptiPhase HiSafe 2; Fisons Chemicals, Loughborough, UK) and the amount of radiation measured using a liquid scintillation counter (Wallac 1410; Pharmacia Biotech, Uppsala, Sweden).

2.4.2. Metatarsal [³H]Thymidine Proliferation Assay

On day 4 of culture 3 μ Ci/ml [³H]-thymidine was added to each metatarsal for the last 4hrs of culture (Mushtaq *et al.*, 2004). The bones were then washed 3 times in PBS (15mins) and unbound thymidine extracted using two incubations with 5% TCA (30mins), in individual glass

vials. They were then washed twice in PBS and solubilised in a 5:1 mixture of dH₂O and tissue solubiliser (NCS-II, 0.5N; Amersham) at 60°C for 1 hour. The solubilised mixture was added to 3ml scintillation fluid (OptiPhase HiSafe 2) in scintillation vials and the levels of radiation measured using a liquid scintillation counter (Wallac 1410).

2.5. Processing Tissue

2.5.1. Paraffin Embedding Tissue

Femurs and tibias dissected from mice for histological analysis were fixed for 24hrs at room temperature in 10% NBF (tibias; neutral buffered formaldehyde) or 75% ethanol/5% acetic acid (femurs). Bones for histological analysis were then decalcified in 10% EDTA (pH 7.4) on rollers at 4°C for ≥ 21 days, with regular EDTA changes. Metatarsals (post culture) were fixed in 4% paraformaldehyde (PFA) at 4°C for 24hrs, and then put into 70% ethanol (not decalcified). All tissue was then dehydrated through a series of alcohol steps on rollers at room temperature as follows: two washes in PBS; two 1hr incubations in 70% ethanol; two 1hr incubations in 80% ethanol; two 1hr incubations in 95% ethanol; 1hr incubation in 100% ethanol; overnight incubation in 100% ethanol. The bones were then put into embedding cassettes in glass jars (metatarsals into glass vials) and incubated with xylene for 1hr (twice) on rollers/shaker at room temperature. They were then placed into pre-melted paraffin wax at 60°C for 1hr, then into fresh wax overnight.

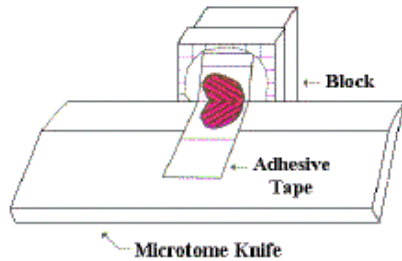
The bones were then embedded at 60°C in appropriate sized plastic or metal moulds and left to cool. Excess wax was trimmed on a microtome (Ernst Leitz AG, Germany; blades used were MX35 Premier+ Microtome Blades, Thermo Scientific, Cheshire, UK) at 10-15 μ m until the growth plate was visible. The samples were then cooled on ice before sections were cut at 5 μ m (tibias/femurs) or 2 μ m (metatarsals). Ribbons of sections were separated in water bath (45-50°C) and mounted onto poly-l-lysine coated slides (VWR International Ltd, Lutterworth, Leicestershire, UK), with

typically 2-3 sections per slide. The slides were then placed in a 60°C oven overnight to adhere, and stored at room temperature until use.

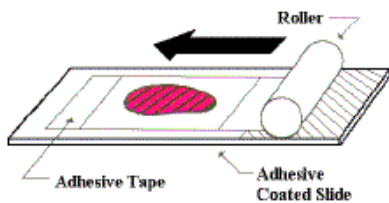
2.5.2. Frozen Tissue

To analyse calcein labelling of the mineralisation front at the chondro-osseous junction sections were cut from frozen tissue. Tibias were dissected from mice and cut in half, then coated in 4% aqueous (wt./vol.) polyvinyl alcohol (PVA; Grade GO4/140, Wacker Chemicals, Walton-on-Thames, UK) and snap frozen in a hexane bath (approximately -80°C) (Altman and Barnett, 1975). The hexane bath was prepared approximately 30mins in advance, and consisted of a large glass jar containing a mix of dry ice and 100% ethanol, within which was a small beaker filled with *n*-hexane (BDH, Poole, UK; grade low in aromatic hydrocarbons). The tissue was then stored at -80°C until use.

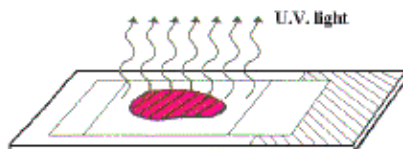
CryoJane® Tape-Transfer Process

**Cutting**

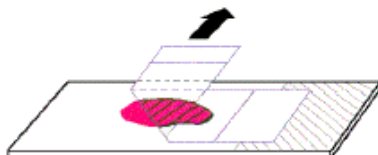
After the block is trimmed, a cold adhesive tape is adhered to the block face. The tape supports and captures the section as it is being cut, eliminating the need for a brush or anti-roll device.

**Transfer to Slide**

A cold adhesive-coated slide is placed on a temperature-controlled pad. The adhesive tape is placed section-side-down on the adhesive-coated slide, and is laminated to the adhesive layer using a cold roller.

**Curing the Adhesive Coating**

A flash of ultraviolet light passes through the slide to polymerize the adhesive layer on the slide into a hard, solvent-resistant plastic, tightly anchoring the section to the slide.

**Removal of Tape**

The tape is peeled away leaving the still frozen section tightly bonded to the plastic layer.

The slide is then air-dried and fixed with the fixative of your choice.

Figure 2.4. The CryoJane tape transfer system. Pictures depicting the steps of the CryoJane system, used to cut frozen section of calcified bone.

Adapted from: www.instrumedics.com/cryojanetapetransferprocess.htm

Sections were cut from frozen tissue using a cryostat (OTF500/HS-001, Brights, Huntington, UK) and the CryoJane tape-transfer system (Instrumedics Inc, Richmond, IL, US). The CryoJane tape-transfer system was used as calcified bone is very difficult to cut without sections losing their morphology and/or shredding. A tungsten carbon knife (Brights) was used, with the blade angle set to 25°. Firstly, frozen tissue was embedded in OCT (optimal cutting temperature compound; Brights) and attached to a metal chuck using the cryostat quick-freeze plate (typically -40°C). Excess OCT was trimmed from the samples at 15µm until the growth plate was visible. Sections were then cut at 10µm using the CryoJane system, as follows. A piece of transfer tape was carefully attached to the surface of the tissue using a small hand roller, and as the section was cut tweezers were used to carefully pull the tape-attached section away. The tape was then placed section-down onto an adhesive slide (4X; Leica Microsystems, Milton Keynes, UK) and again the hand roller was used to attach the section flat and securely to the slide. This was repeated so a second section was placed on the slide, which was then zapped under a UV light. This activates the adhesive on the slide to harden and attach the section firmly. The back of the slide was then rubbed gently with a thumb to warm as the tape was peeled off, leaving the section on the slide. The slides were air dried and mounted with fluoromount (BDH Chemicals Ltd, Poole, UK). The steps of the CryoJane tape-transfer system detailed above are depicted in Figure 2.4.

2.5.3. Immunohistochemistry of BrdU

Paraffin embedded sections from tibias that had been fixed in 10% NBF and decalcified as described in Section 2.5.1 were used to measure proliferation by analysing BrdU uptake. Slides were dewaxed and rehydrated as follows: 2x5mins Histo-Clear II (National Diagnostics, Hessle, East Riding of Yorkshire, UK); 2x5mins 100% ethanol; 2x5mins 90% ethanol; 2x5mins 70% ethanol; 5mins 50% ethanol; 2x5mins tap water. The number of cells with BrdU incorporated in their nuclei was detected using a streptavidin-biotin BrdU staining kit (Zymed laboratories, Invitrogen). Sections were quenched in peroxidase quenching solution consisting of a 9:1 mix of absolute

methanol and 30% H₂O₂ (10mins), and rinsed in PBS (3x2mins). Tissue antigen unmasking was achieved by digestion in a trypsin solution (25%) in a 37°C humidified chamber for 4mins, and rinsed in dH₂O (3x2mins). The sections were then denatured to uncoil the DNA and allow antibody access to the incorporated BrdU in a denaturing solution for 20mins, rinsed in PBS (3x2mins) and blocked for 10mins at room temperature in blocking solution. Biotinylated mouse anti-BrdU was then added and incubated for 30mins, following 3 rinses in PBS (2mins), 10mins incubation with streptavidin-peroxidase and further PBS rinses (3x2mins). DAB (3,3'-diaminobenzidine) substrate was then added for 3mins, and slides rinsed well in dH₂O. The sections were finally counterstained with haematoxylin for 4mins, followed by a wash in tap water and then submerged in PBS until the blue counter stain was visible (approx. 30secs), and rinsed in dH₂O.

The sections were then dehydrated as follows: 5mins 50% ethanol; 2x5mins 70% ethanol; 2x5mins 90% ethanol; 2x5mins 100% ethanol; 2x5mins xylene. The slides were then mounted with histomount (Invitrogen). Quantification of proliferating cells was performed as previously described by Chagin and colleagues, where the number of BrdU positive cells in the whole growth plate (stained brown) were counted and normalised to the length of the growth plate (Chagin *et al.*, 2004). Two sections were analysed per mouse.

2.5.4. Toluidine Blue Staining

Toluidine blue is a metachromatic dye that stains the nucleus blue and the cytoplasm light blue/purple, thus will stain the different zones of the growth plate (proliferating and hypertrophic) different shades of blue/purple making them more clearly defined. Paraffin embedded decalcified tibia sections (that had been fixed in 10% NBF) were dewaxed and rehydrated as described in Section 2.5.3. They were then placed into a 1% solution of toluidine blue in 50% isopropanol/50% dH₂O for 2mins (room temperature). The slides were rinsed thoroughly in fresh isopropanol, then cleared in xylene (2x5mins) and mounted with histomount (Invitrogen). The zone widths were measured at 10 points along the whole growth plate at X10

magnification, using a Nikon eclipse TE300 microscope with a digital camera attached, using Image Tool (Image Tool Version 3.00). Two sections were analysed per mouse.

2.5.5. Von Kossa and H&E Staining

Paraffin embedded metatarsal sections that had been fixed and processed as described in Section 2.5.1 were stained for Von Kossa (stains mineral dark brown/black), followed by haematoxylin and eosin (H&E; stains nuclei blue and cytoplasm pink), to allow measurement of growth plate zone widths and the mineralisation centre. The slides were dewaxed and rehydrated as described in Section 2.5.3. They were then incubated with 5% silver nitrate (BDH; in dH₂O) for 30mins under a strong light, washed in dH₂O (3x2mins) and fixed in 2.5% sodium thiosulphate (in dH₂O). The slides were then immersed in Harris haematoxylin (freshly filtered) for 10mins; rinsed for 10mins in running tap water; put into 1% acid alcohol (HCl in 70% ethanol) for 5secs; dunked 10x in tap water; put into Scott's tap water for 10mins (alkaline); immersed in 1% eosin for 10mins (in dH₂O with 0.5µl/ml glacial acetic acid (Fisher Scientific, Loughborough, UK)). Slides were then dehydrated by 2 dunks (very quick as eosin leeches in water) in 90% ethanol; 2x1min in 100% ethanol; 2x1min xylene. They were then mounted in histomount (Invitrogen). The zone widths were measured at X4 magnification using a Nikon eclipse TE300 microscope with a digital camera attached, using Image Tool (Image Tool Version 3.00).

2.5.6. Immunohistochemistry of Phosphorylated STAT5

Paraffin embedded sections from femurs that had been fixed in 75% ethanol/5% acetic acid and decalcified as described in Section 2.5.1 were used to measure phosphorylated STAT5 by immunohistochemistry. The method described by Gevers *et al.* was followed, using a Tyramide Signal Amplification kit (TSA kit, Perkin Elmer, Cambridge, UK) that has been shown to enhance immunostaining (Gevers *et al.*, 2002; Gevers *et al.*, 2009)

Slides were dewaxed and rehydrated as described in Section 2.5.3. The sections were quenched in peroxidase quenching solution (3% H₂O₂ in methanol) for 12mins and washed in wash buffer. The slides were then unmasked of tissue antigens in 1mg/ml trypsin/PBS (12mins), washed and blocked in blocking buffer for 30mins in a humidified chamber at room temperature, with agitation. The blocking buffer was drained off the slides and primary antibody applied. Primary antibody used was rabbit anti-phosphorylated STAT5 (Zymed Laboratories, Invitrogen), which was diluted from 0.25mg/ml to 5µg/ml in blocking buffer. As a negative control rabbit IgG (Cell Signalling Technologies, New England Biolabs) was used in place of phosphorylated STAT5, to detect any non-specific binding. Slides were incubated with primary antibody overnight at 4°C.

Following the overnight incubation, slides were washed in wash buffer (3x5mins). They were then incubated with secondary antibody, HRP-linked goat anti-rabbit (Dako, Cambridgeshire, UK) diluted 1:100 in blocking buffer, for 30mins at room temperature (in humidified chamber). Sections were washed in wash buffer (3x5mins), and then incubated with 200µl Biotynyl Tyramide (Amplification Reagent) working solution for 10mins (at room temperature with agitation). Slides were washed 5x3mins in wash buffer, then incubated for 30mins (room temperature in humidified chamber) with Streptavidin-HRP (supplied with TSA Kit, Perkin-Elmer) that had been diluted 1:100 in blocking buffer. They were washed in wash buffer (3x5mins), and incubated with DAB solution for 5mins (in the dark) to allow visualisation, and rinsed well in dH₂O. The slides were counterstained in Harris haematoxylin for 3.5mins and rinsed in running tap water for 10mins, then put into Scott's tap water for 10mins and dehydrated through alcohols as described in Section 2.5.3. The slides were then mounted with histomount (Invitrogen). The number of cells stained positive for phosphorylated STAT5 (brown) was quantified as a percentage of total cells in an area.

2.6. Transfecting ATDC5 Cells

2.6.1. SOCS2 Over-expression and Control Plasmids

pEF-FLAG-I/mSOCS2 (SOCS2 over-expression) and pEF-FLAG-I (control) plasmids were kindly obtained from Prof D. Hilton (The Walter and Eliza Hall Institute for Medical Research, Parkville, Victoria, Australia). The plasmids have been used previously by Hilton *et al.* to investigate the role of SOCS proteins in the differentiation of murine monocytic leukemic M1 cells to macrophages (Nicholson *et al.*, 1999). The pEF-FLAG-I plasmid was made by digesting the pEF-BOS plasmid (plasmid map in Appendix 10.3.1.; (Mizushima and Nagata, 1990)) with Xba I and annealing to oligonucleotides encoding an ATG (with upstream Kozac sequences) and the FLAG epitope tag. This created an expression cassette that leads to the expression of intracellular proteins with a FLAG tag under the control of the Elongation Factor 1 alpha promoter. The plasmid map, expression cassette and sequencing primers for the pEF-FLAG-I plasmid are shown in Appendix 10.3.2. The pEF-FLAG-I/mSOCS2 plasmid was made by cloning a SOCS2 coding region (minus ATG) that was Mlu I amplified into the Mlu I site of pEF-FLAG-I. The plasmid map and expression cassette for pEF-FLAG-I/mSOCS2 are in Appendix 10.3.3.

The pEF-FLAG-I and pEF-FLAG-I/mSOCS2 plasmids confer resistance to ampicillin, which can be used for transformation into bacteria, but do not have resistance to any antibiotics suitable for selection when transfection into eukaryotic cells (ampicillin is not effective in eukaryotic cells). Thus the plasmids were co-transfected with the commercially available plasmid pcDNA3.1⁽⁺⁾ (Invitrogen; derived from pcDNA3), which contains the neomycin gene which confers resistance to Geneticin (G418). The plasmid map and sequencing primers for pcDNA3.1⁽⁺⁾ are in Appendix 10.3.4.

2.6.2. Transformation of *E. coli*

The three plasmids described in Section 2.6.1 were transformed into *Escherichia coli* (*E. coli*) to enable DNA amplification. JM109 competent cells (Stratagene, Agilent Technologies, Cheshire, UK) were used, which are endonuclease and recombination deficient thus improving the quality of DNA and stability. JM109 cells were thawed on ice (from -80°C) and aliquoted (100µl) in pre-chilled Falcon polypropylene round-bottom tubes. The cells were incubated for 10mins with 0.8µl β-mercaptoethanol, on ice with regular swirling (to increase transformation efficiency). 5µl (10ng/µl in H₂O) of experimental DNA or 1µl pUC18 control plasmid (0.1ng/µl in TE buffer; provided with JM109 cells to indicate transformation efficiency) was added to each aliquot and incubated for 30mins on ice. The tubes were then heat-pulsed for 45secs at 42°C and incubated on ice for 2mins. 0.9ml of pre-heated (42°C) S.O.C. medium (Super Optimal broth with Catobolite repression; Invitrogen) was added and the tubes were incubated at 37°C for 1hr with shaking at 225-250rpm (loose caps). 200µl of the transformation mixture (5µl in 200µl SOC medium for pUC18 control) was spread on LB agar (Luria-Bertani Broth) plates and incubated at 37°C overnight.

Individual colonies for each plasmid were streaked onto LB-agar ampicillin plates (100µg/ml) with a sterilised wire loop, and incubated at 37°C overnight for glycerol stocks and minipreps. The pattern used for streaking colonies is shown in Figure 2.5.

2.6.3. Preparing Glycerol Stocks

Single colonies of transformed *E. coli*, from plates streaked as described in Section 2.6.2, were incubated in 5ml liquid LB-broth containing 100µg/ml ampicillin at 37°C overnight with shaking (250rpm). 10µl of the overnight culture was added to 4ml LB-broth and incubated at 37°C with shaking (250rpm) for 7hrs, then mixed with 2ml 50% glycerol (molecular grade glycerol in H₂O) and aliquoted (2ml in 15ml falcon tubes). The glycerol stocks were stored at -80°C.

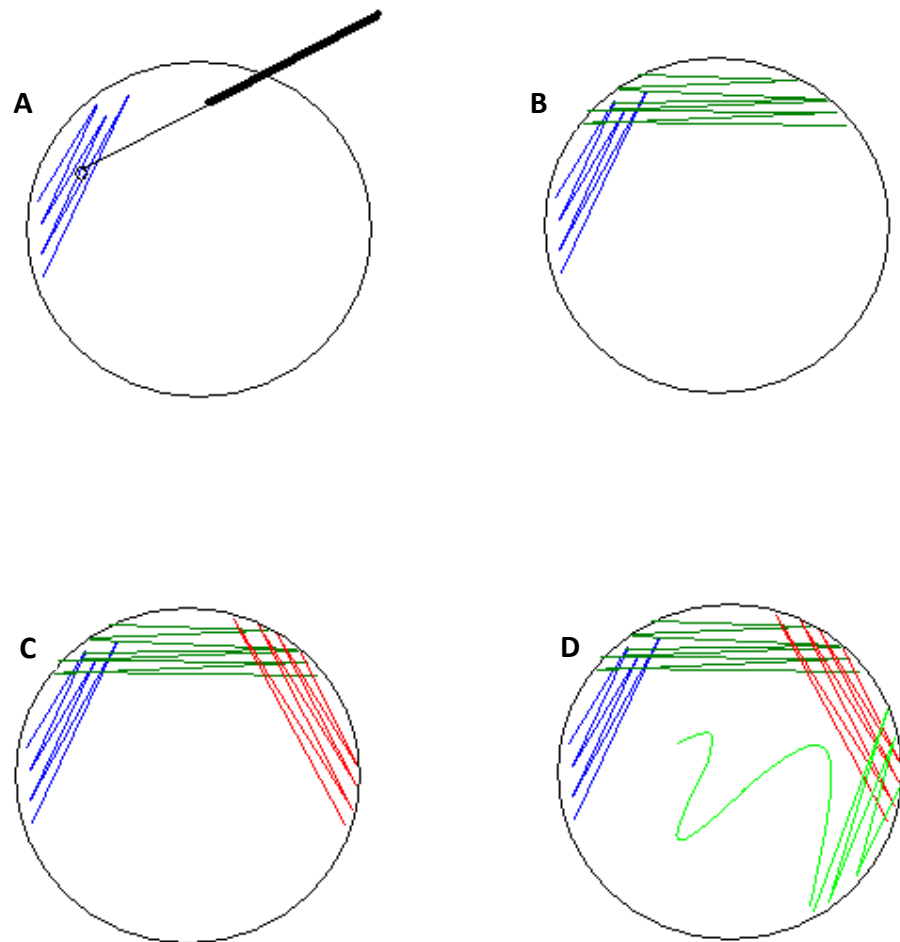


Figure 2.5. Streaking agar plates. A sterile wire loop (A) was used to streak single colonies onto agar plates. The bacteria are diluted by streaking along different sides of the plate (A, B and C) then finally into the middle of the plate (D) where individual colonies will grow.

2.6.4. Minipreparation of Plasmid DNA

The remaining overnight liquid cultures from Section 2.6.3 were used for isolating the plasmid DNA using a PureLink Quick plasmid miniprep kit (Invitrogen). The cultures were centrifuged at 11,000rpm for 15mins to pellet, all medium was removed and the cell pellets were resuspended in 250µl resuspension buffer, mixed gently by inverting 5 times, and incubated for 5mins at room temperature. The mixture was then precipitated by adding 350µl precipitation buffer and inverting to mix until a homogenous solution was achieved, then centrifuged at 13,500rpm to remove the lysis debris. The supernatant was loaded onto a spin column that contains silica membranes that selectively bind plasmid DNA. The column was centrifuged at 13,500rpm for 1min, and the flow-through discarded. Contaminants were washed by adding 500µl wash buffer W10, incubating for 1min and centrifuging at 13,500rpm (flow-through discarded), then adding 700µl wash buffer W9 and centrifuging at 13,500rpm for 2x1min (flow-through discarded). The DNA was then eluted by adding 75µl TE buffer (preheated to 67°C; 10mM Tris-HCl, pH 8.0; 0.1mM EDTA) to the centre of the column and incubating for 1min (room temperature) then centrifuging at 13,500rpm for 2mins. DNA concentration and quality was read on a Nanodrop spectrophotometer (ND-1000). Quality was assessed by the A_{260}/A_{280} ratio, where 1.8 was considered optimum.

2.6.5. Restriction Digest

DNA purified by miniprep as described in Section 2.6.4 was assessed by restriction digest to ensure the plasmids were complete and the correct size. For the pEF-FLAG-I plasmid restriction enzymes Asc I (cuts within FLAG to produce a 5353bp band) and EcoR1 were used (cuts twice to produce 4614bp and 739bp bands). The pEF-FLAG-I/mSOCS2 plasmid was cut with Nde I (Nuclear disruption E protein-1; cuts within the FLAG/mSOCS2 to produce a 5953bp band) and EcoR1 (cuts twice to produce 1339bp and 4614bp bands). The pcDNA3.1⁽⁺⁾ plasmid was cut with Nhe I (cuts once producing a 5428bp band) and Pst I (cuts twice producing 1356bp and 4072bp bands)

enzymes. To linearise DNA for transfection, all three plasmids were cut with Sca I (cuts once within the ampicillin gene). For Nde I and Asc I enzymes, 1 μ l DNA (1 μ g/ μ l) was added to 0.05 μ l enzyme (20U; New England Biolabs), 5 μ l NEB buffer 4 and 43.95 μ l H₂O. For EcoR1, Nhe I, Pst I, and Sca I enzymes 1 μ l DNA (1 μ g/ μ l) was added to 0.25 μ l enzyme (10U/ μ l; Roche, West Sussex, UK), 2.5 μ l SuRE/Cut buffer H and 21.25 μ l H₂O. The reactions were incubated at 37°C for 1hr and 65°C for 25mins. The products were diluted 5:1 with 5X blue loading buffer (Bioline). 12 μ l was loaded per sample in separate wells in 1.2% Agarose/1XTAE gels containing 0.25 μ g/ml Ethidium Bromide. Gels were run in TAE buffer in an electrophoresis tank at 120V. HyperLadder I (Bioline) was used as molecular weight markers. Gels were imaged under UV light using a Gel Logic 200 Imaging System and software (Kodak).

2.6.6. EndoFree Maxipreparation of Plasmid DNA

For transfection into mammalian cells, plasmid DNA needs to be free of endotoxins found in *E. coli* to improve the transfection efficiency. Therefore an EndoFree Plasmid Maxiprep kit (Qiagen, Crawley, UK) was used to purify DNA for transfection. The pEF-FLAG-I and pEF-FLAG-I/mSOCS2 plasmids are classed as low copy, whereas the pcDNA3.1⁽⁺⁾ plasmid is high copy, therefore they were treated slightly differently according to the kit instructions. Single colonies of transformed *E. coli*, from plates streaked as described in Section 2.6.2, were incubated in 5ml liquid LB-broth containing 100 μ g/ml ampicillin at 37°C for 7hrs (250rpm). For low copy plasmids, 500 μ l of the liquid culture was added to 250ml LB-broth containing 100 μ g/ml ampicillin and incubated at 37°C with shaking (250rpm) overnight. For high copy plasmid, 200 μ l of the liquid culture was added to 100ml LB-broth containing 100 μ g/ml ampicillin (incubated at 37°C overnight, 250rpm). The cells were pelleted by centrifugation at 5,000rpm for 15mins at 4°C. The medium was removed and pellets resuspended in 10ml buffer P1 and 10ml lysis buffer P2 with thorough mixing, and incubated for 5mins (room temperature). 10ml chilled neutralization buffer P3 was added to the lysate and mixed, causing precipitation of genomic DNA, proteins, cell debris and SDS. The lysate

was poured into a QIAfilter cartridge and incubated for 10mins (room temperature), allowing the precipitate to separate to the top of the mixture thus ensuring efficient filtration. The plunger was then inserted and the lysate filtered through the QIAfilter cartridge into a sterile tube, removing SDS precipitates and bacterial lysates. 2.5ml endotoxin removal buffer (ER) was added to the filtered lysate, mixed by inversion and incubated on ice for 30mins. The lysate was then added to an equilibrated QIAGEN-tip 500 and allowed to enter the anion-exchange resin by gravity flow, which selectively bind plasmid DNA under low-salt and pH conditions. Contaminants (RNA, proteins, metabolites, and other impurities) were removed by washing the QIAGEN-tip twice with 30ml medium-salt wash buffer QC. The DNA was then eluted with 15ml high-salt buffer QN, precipitated by addition of 10.5ml isopropanol and pelleted by 30mins centrifugation at 11,200rpm (4°C). The supernatant was discarded and the DNA pellet washed in 70% ethanol (10mins, 11,200rpm), pellet air dried and resuspended in 50µl TE buffer. DNA concentration and quality was read on a Nanodrop spectrophotometer (ND-1000). Quality was assessed by the A_{260}/A_{280} ratio, where 1.8 was considered optimum.

2.6.7. Transfection of ATDC5 Cells

For transfection into ATDC5 cells, endotoxin free DNA obtained as described in Section 2.6.7 was linearised using Sca I enzyme as described in Section 2.6.5. Linear DNA will incorporate into the genomic DNA more efficiently upon transfection, and the plasmids were linearised at the ampicillin gene site ensuring the genes of interest for transfection were intact. The cells were transfected using the transfection reagent FuGene 6 (Roche), which consists of a blend of lipids and other components in 80% ethanol, and has very low cytotoxicity. During lipid-based transfection the transfection complex (FuGENE 6 bound DNA) transports the cell membrane through endocytosis, as a result of the positive charge of the lipid fusing with the negatively charged cell membrane. ATDC5 cells were plated in 10cm culture dishes (Costar) in maintenance medium as described in Section 2.2.1. The cells were transfected when 50% confluent, in

maintenance medium without gentamicin (antibiotics can adversely affect the transfection efficiency). For transfection, 18µl FuGene 6 was incubated with 582µl DMEM/F-12 (1:1) with GlutaMAX I (Invitrogen) for 5mins (room temperature). DNA was then added to the mixture. As the pEF-FLAG-I and pEF-FLAG-I/mSOCS2 plasmids were being co-transfected with the pcDNA3.1⁽⁺⁾ to give antibiotic resistance, they were co-transfected at a ratio of 5:1 to try and ensure that when pcDNA3.1⁽⁺⁾ was successfully transfected, pEF-FLAG-I or pEF-FLAG-I/mSOCS2 would be also. Therefore, 5µg linearised pEF-FLAG-I or pEF-FLAG-I/mSOCS2 was mixed with 1µg linearised pcDNA3.1⁽⁺⁾ and added to the DMEM/FuGENE 6 mixture, vortexed and incubated for 15mins (room temperature). The transfection reagent: DNA complex was then added to the ATDC5 cells in a drop-wise manner. Control cells were incubated with FuGENE 6/DMEM alone. The cells were incubated in a humidified atmosphere (37°C, 5% CO₂). 48hrs after the transfection the medium was changed to maintenance medium containing Geneticin (500µg/ml; Gibco, Invitrogen) to select the successfully transfected cells.

2.6.8. Growing Single Colonies of Transfected Cells

Because the pEF-FLAG-I and pEF-FLAG-I/mSOCS2 plasmids were co-transfected with the pcDNA3.1⁽⁺⁾, it was necessary to isolate colonies of cells that had a single transfected cell origin, grow them up and examine for SOCS2 over-expression. Cells that had been transfected as described in Section 2.6.7 and selected with Geneticin were seeded at low density in 10cm culture dishes (Costar), in maintenance medium containing Geneticin (500µg/ml; Gibco, Invitrogen). Single cells were marked and their growth monitored. When a large colony of cells had grown, they were isolated using cloning rings (8mm x 8mm). This was done by removing the culture medium, sticking the cloning ring over the colony and filling it with 100µl trypsin which was gently pipetted to encourage cells to detach. The cells were then pelleted in an Eppendorf, resuspended in 1ml maintenance medium (containing 500µg/ml geneticin) and put in 1 well of a 24-well plate (Costar). The cells were then grown up, seeded to larger plates: 6-well plate, T25 flask, T75 flask,

and finally 2xT175 flasks (all Costar). The cells were then frozen as described in Section 2.2.2. Examples of cell colonies are shown in Figure 2.6.

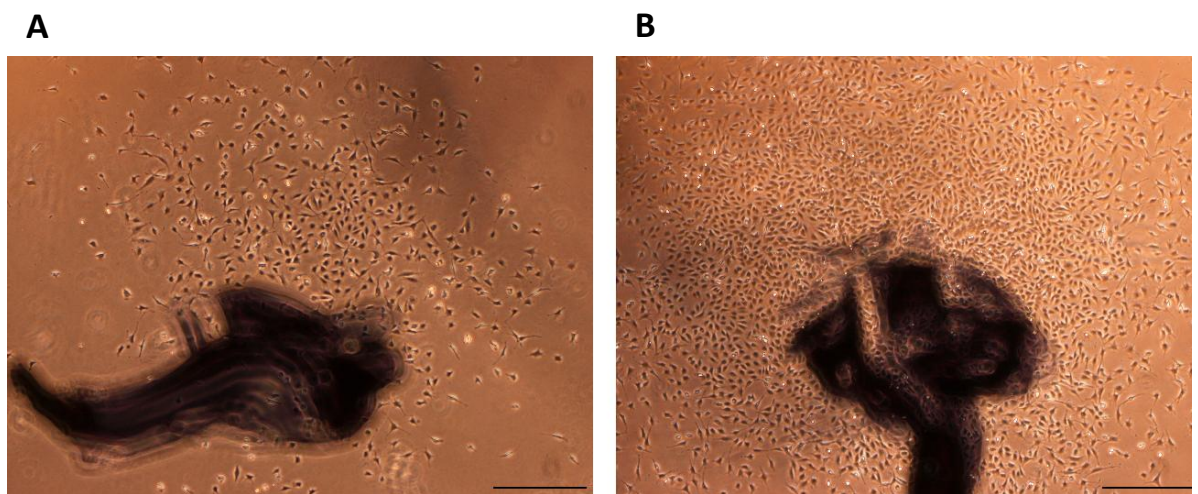


Figure 2.6. Individual cell clones. Pictures taken at X4 magnification of transfected ATDC5 single cell clones that are early in development (A) and late, just before being picked (B). The large black marks are pen marks to locate the colonies on the plate. Scale bars show 500 μ m.

2.7. PCR

2.7.1. RNA Isolation

Cells that had been cultured in 6-well plates were scraped in PBS, centrifuged at 13,000rpm for 5mins and pellets stored at -80°C until use. RNA was isolated from the pelleted cells using an RNeasy Mini Kit (Qiagen). The cells were homogenized in highly denaturing guanidine-thiocyanate-containing RLT buffer (10µl/ml β-mercaptoethanol) using a handheld homogenizer (IKA-Werke, D-79219 Staufen, Germany), in 10secs bursts. The buffer immediately inactivates RNAses so that the RNA purified is intact. 1 volume of 70% ethanol was added to the homogenized lysate and pipetted to mix. The sample was then placed in an RNeasy spin column in a 2ml collection tube and centrifuged for 15secs at 10,000rpm, allowing the RNA to bind to the silica membrane within the column. The flow through was discarded. The spin column was washed of contaminants once in 700µl buffer RW1 (15secs 10,000rpm; flow through discarded) and twice in 500µl buffer RPE (15secs 10,000rpm; flow through discarded). The RNeasy column was then placed in a fresh collection tube and RNA eluted by adding 50µl nuclease free H₂O (10,000rpm 1min). RNA concentration and quality was read on a Nanodrop spectrophotometer. Quality was assessed by the A_{260}/A_{280} ratio, where 2.0 was considered optimum. Samples were then diluted to the same concentration (that of the lowest sample) in RNase free water. The RNA was stored at -80°C.

2.7.2. Reverse Transcription

Reverse transcriptase is a RNA-dependant DNA polymerase that is used by viruses to copy their RNA into DNA for integration into host genomic DNA. It can be used in a reverse transcription PCR reaction to transcribe RNA to single stranded cDNA, which can then be used for PCR. 10µl diluted RNA sample was denatured by incubating with 2µl random hexamers (random primers; 50ng/µl; Invitrogen) at 70°C for 10mins in a Hybaid PCR Express Thermal cycler (Thermo Scientific). Blanks were included as negative controls, containing 10µl nuclease free H₂O instead of RNA. 8µl master

mix was then added to each sample, which contained 4µl First Strand Buffer (5X; Invitrogen), 2µl DTT (Dithiothreitol; 0.1M; Invitrogen), 1µl dNTP mix (10mM; Invitrogen) and 1µl Superscript II RNase H enzyme (200U/µl; Invitrogen). For RT-PCR, negative controls were set up with no Superscript enzyme in the master mix. The samples were then run on the following programme in the Hybaid PCR machine: 25°C for 10mins (annealing); 42°C for 50mins (elongation); 70°C for 10mins (termination). The cDNA samples were stored at -20°C.

2.7.3. Polymerase Chain Reaction (PCR)

Reverse transcription polymerase chain reaction (RT-PCR) was performed on samples prepared as described in Sections 2.7.1 and 2.7.2 to amplify the gene of interest. cDNA samples were diluted to 100ng/µl in nuclease free H₂O. Reaction tubes were set up containing 4µl cDNA (100ng/µl), 4µl primer pairs (1pmol forward and 1pmol reverse primers), 11.4µl master mix and 0.6µl 1:1 mix of Taq Polymerase (Invitrogen) and Taq Start (Clontech, Saint-Germain-en-Laye, France). PCR reactions were performed on a DNA Engine Dyad machine (Peltier Thermal Cycler, Bio-Rad Laboratories) under the following conditions: 2mins denaturing at 92°C; 30 or 35 thermocycles consisting of 1min at 92°C (denaturing), 1min at 55°C (annealing), and 1min at 72°C (extension); 10mins extension at 72°C. Number of cycles was altered for different primers to optimize conditions. Primers used for collagen type-II, GH receptor (GHR), IGF-1 receptor (IGF-1R), and IL-1β receptor 1 (IL-1βRI) are shown in Table 2.2, along with the number of cycles used. 18S primers (Ambion) were used as a loading control.

Gene	Forward Primer (5' to 3')	Reverse Primer (5' to 3')	No. of PCR Cycles
Collagen II	CACACTGGTAAGTGGGGCAAGACCG	GGATTGTGTTGTTTCAGGGTTCGGG	30
GHR	CATTGGCCTCAACTGGACTT	GACTTCGCTGAACTCGCTGT	30
IGF-1R	CACCGAGAACAACGACTGCT	CTGACCGAATCGATGGTTT	35
IL-1βRI	ACCCCATATCAGCGGACCG	TTGCTTCCCCGCAACGTAT	35

Table 2.2. PCR primer pairs. Details of primers used for RT-PCR and the number of thermocycles for each.

The PCR products were diluted 5:1 with 5X Blue DNA Loading Buffer (Bioline). 12µl was loaded per sample in separate wells in 1.5% Agarose/1XTAE gels containing 0.25µg/ml Ethidium Bromide. Gels were run in TAE buffer in an electrophoresis tank at 150V. A protein standard, Hyperladder I (Bioline), was run with the samples. Gels were imaged under UV light using a Gel Logic 200 Imaging System and software (Kodak).

2.7.4. Quantitative PCR (qPCR)

qPCR was performed on samples prepared as described in Section 2.7.1 and 2.7.2. Primers for qPCR were selected within the gene of interest (genomic sequence obtained from Ensembl; www.ensembl.org) using the online resource Primer 3 (frodo.wi.mit.edu) ensuring that: the primers spanned two introns; the product size was 100-150bp; there were no repeats >3 nucleotides; melting temperatures of each primer close to 60°C and close to that of the other primer; GC content of 40-60%. qPCR was performed using FastStart Universal SYBR Green Master Mix (ROX) (Roche), which allows real-time qPCR amplification and quantification of DNA with a ROX reference dye for normalisation of fluorescent signals. The fluorescent dye SYBR Green I intercalates with double stranded DNA, generating a measurable fluorescent signal that is directly proportional to the DNA concentration, and thus the amount of double stranded DNA generated during the PCR reaction. This master mix also contains dUTP, which ensure the prevention of UDG carryover. FastStart Taq DNA Polymerase is also included to ensure a “hot-start” (75°C) of the Taq activity.

Primers were optimised by producing a standard curve, to ensure they worked and primer dimerisation wasn't present. For this, undiluted cDNA produced from a sample predicted to contain a high level of the gene of interest was used to create a 1:10 dilution series from 10^{-10} to 10^{-5} , ensuring it spanned 10ng/µl (the concentration used for the experiment). Nuclease free water (NFW) was used as a no template control. Each sample was analysed in duplicate. 96-well plates (AbGene, Thermo Scientific) were used with MicroAmp Optical caps (8-strip; Applied

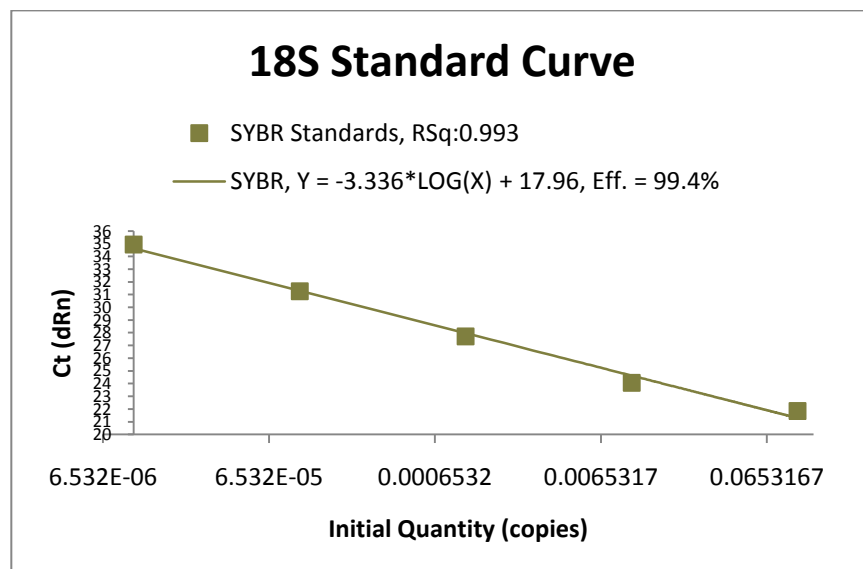
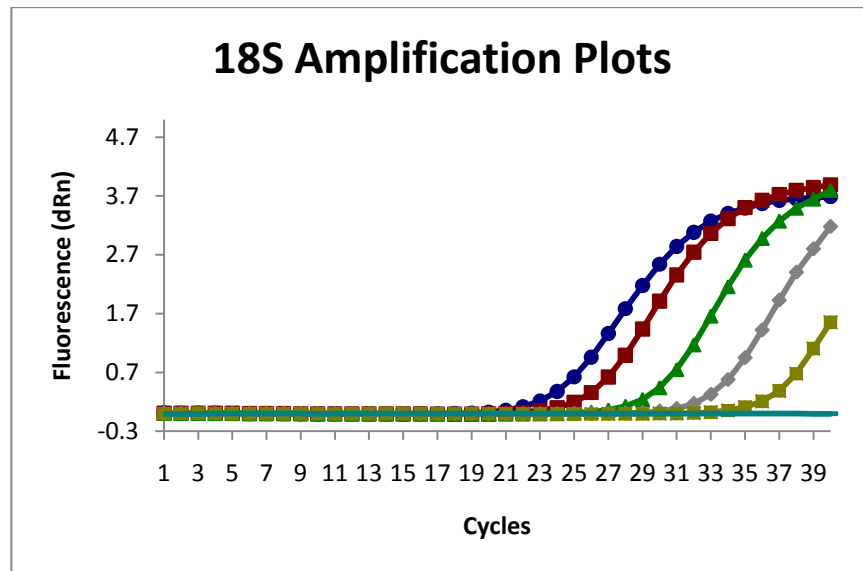
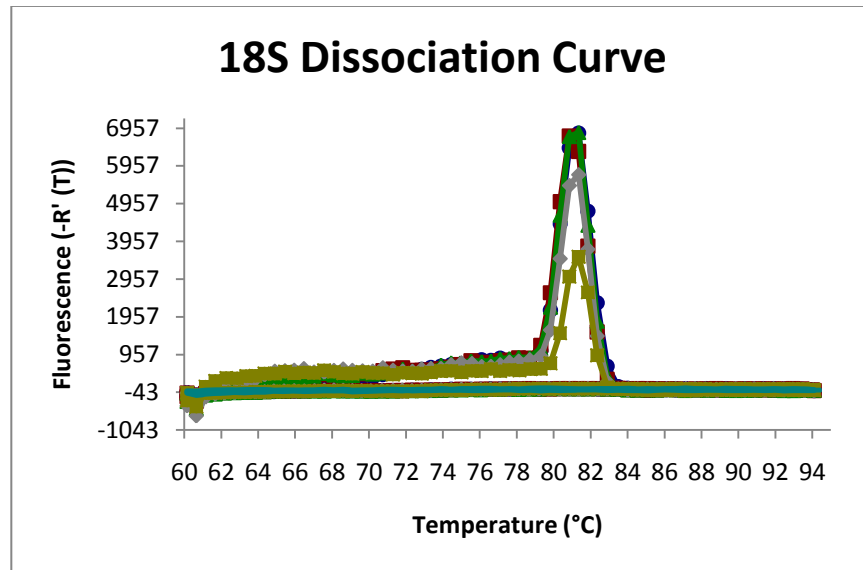
Biosystems, Cheshire, UK). Each well contained one reaction consisting of: 5µl cDNA/NFW; 0.5µl forward primer (10mM); 0.5µl reverse primer (10pmol/µl); 6.5µl NFW; 12.5µl FastStart Universal SYBR Green Master Mix (ROX) (Roche). The qPCR reaction was completed using a Stratagene Mx3000P qPCR machine and MxPro software, as follows: 1 cycle of 2mins at 50°C, 2mins at 95°C (UDG incubation); 40 cycles of 15secs at 95°C (denaturing), 30secs at 60°C (annealing and elongation); 1 cycle of 1min at 95°C (disassociation), 30secs at 60°C (reanneal), 15secs at 95°C (records temperature fluorescence drops off) and 30secs at 25°C. Results were analysed using MxPro software. Primers were considered acceptable if they met the following criteria: a standard curve with an R^2 value of 0.9-1.0; amplification efficiency of 90-100%; a dissociation curve showing one clear peak and no other, smaller peaks (*i.e.* one product); an amplification curve with sigmoid curves at regular intervals along the dilution series. The optimisation results for primers used are shown in Figure 2.7.

Following satisfactory standard curves, the qPCR reaction was carried out as above using 10ng/µl cDNA, with each sample analysed in triplicate and NFW used as no template control. 18S was used as a housekeeping gene upon which results were normalised. Primers used are shown in Table 2.3. The expression of genes was analysed by comparing Ct values between samples (following normalisation to housekeeping gene Ct Values).

Gene	Forward Primer (5' to 3')	Reverse Primer (5' to 3')
18S (Housekeeping)	GTA ACC CGT TGA ACC CCA TT	CCA TCC AAT CGG TAG TAG CG
IGF-1	CAC ACT GAC ATG CCC AAG AC	TGG GAG GCT CCT CCT ACA TT

Table 2.3. qPCR primer pairs. Details of primers used for real time qPCR.

A



B

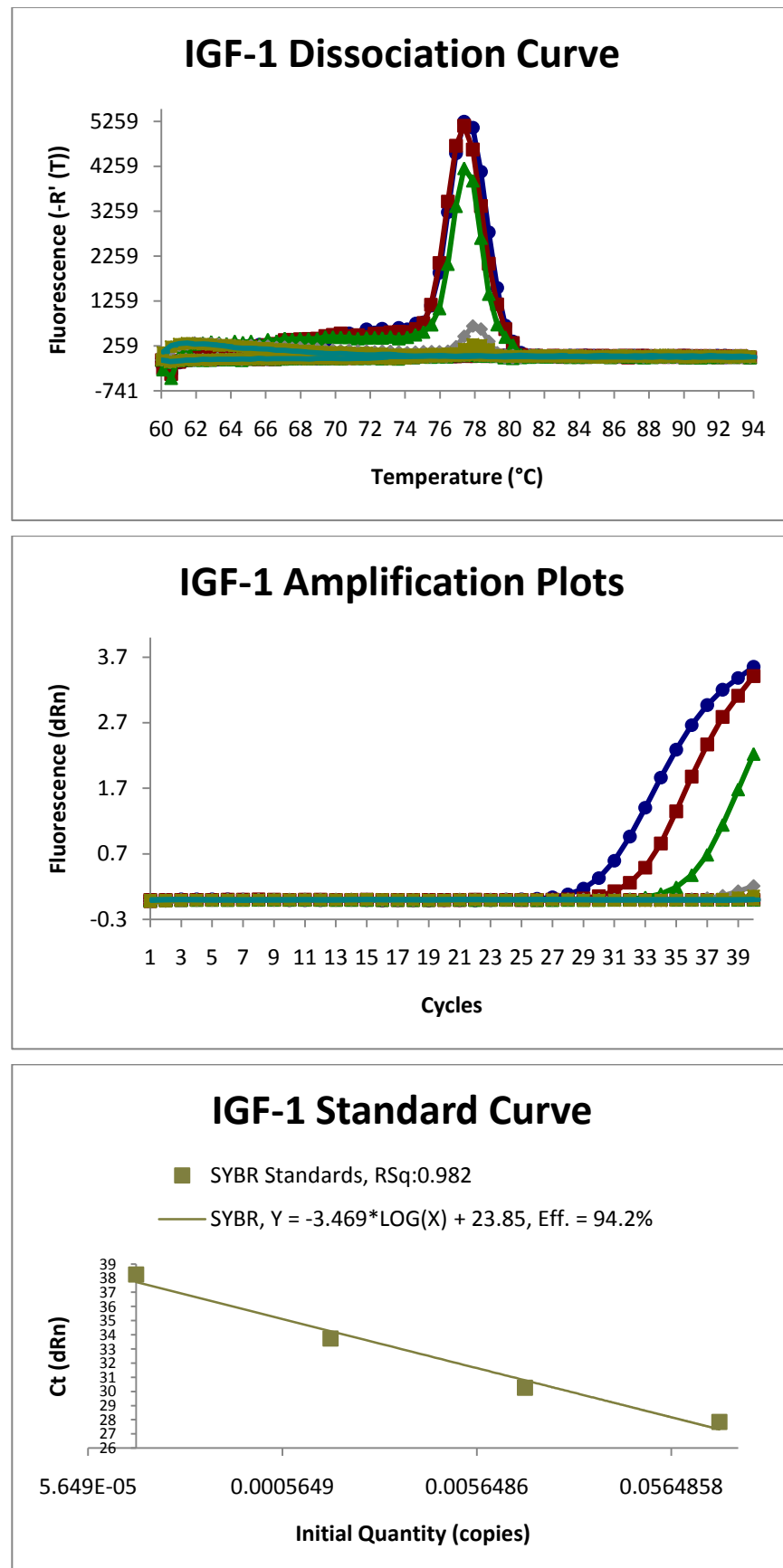


Figure 2.7. Primer optimisation. Dissociation curves, amplification plots and standard curves for (A) 18S and (B) IGF-1 qPCR primers.

2.8. Western Blotting

2.8.1. Extracting Protein

Primary chondrocytes and ATDC5 cells were washed in PBS to remove excess medium. For experiments looking at phosphorylated protein (STATs), cells were scraped in Phospho-Safe Extraction Reagent (Novagen, Merck Biosciences, Nottingham, UK) containing 143µl/ml protease inhibitor cocktail mix (Roche, *Burgess Hill*, West Sussex, UK). Otherwise, cells were scraped in RIPA buffer, again containing protease inhibitors. Each well was scraped in 125µl buffer, and wells treated the same (typically 2 or 3 wells) were scraped into the same Eppendorf. Excess cell structure proteins were removed by centrifuging and the pellet discarded. Samples were then stored at -20°C.

Protein content was determined using a DC (detergent compatible) protein assay (Bio-Rad Laboratories), which is a colorimetric assay for protein concentration based on the Lowry assay (Lowry *et al.*, 1951). Standards were made using lyophilized bovine plasma gamma globulin protein (2mg/ml; Bio-Rad Laboratories) by doing serial dilutions ranging from 2mg/ml to 0.125mg/ml, plus a blank (0mg/ml), using the same buffer that the cells were scraped in. For the assay, 96-well plates were used, and each well contained 5µl sample/standard, 25µl Reagent A' (containing 20µl Reagent S per ml Reagent A) and 200µl Reagent B. The plate was incubated at room temperature for 15mins, then protein levels were measured by absorbance at 690nm using a Multiskan Ascent plate reader (Thermo Electron Corporation, Thermo Scientific). The protein concentration in each sample was calculated from the standard curve gained from the protein standards.

2.8.2. Western Blot

The same quantity of protein was added for each sample, depending on the lowest yield achieved (typically 15µg of protein was loaded). Protein lysates were mixed with sample buffer (3:1;

Invitrogen) and reducing agent (10:1; Invitrogen), then denatured at 70°C for 10mins and cooled on ice. Pre-cast 3-8% Tris-Acetate or 10% Bis-tris gels (Invitrogen) were used with Tris Acetate or MOPS running buffer (1X; Invitrogen), respectively. The type of gel used depended on the size of the protein of interest. The gels were placed in a Novex Gel Tank (Invitrogen) and the denatured protein samples were loaded into the wells, with an All Blue Precision Plus Protein Standard (Bio-Rad Laboratories) loaded as a weight marker. The gel tank was filled with running buffer, and the centre of the tank also contained an anti-oxidant (2.5µl/ml; Invitrogen; to preserve the reduced proteins). The gels were to run at 200V for 50mins.

Following electrophoresis, the protein was transferred onto a membrane. This was done by placing a Hybond-ECL Nitrocellulose membrane (GE Healthcare, Amersham) on top of the gel and then sandwiching it in filter paper and foam pads that had been soaked in transfer buffer. This sandwich was then placed in an X-blot transfer module (Invitrogen) which was clamped into the electrophoresis tank. The module was filled with ice cold transfer buffer, and the rest of the tank filled with ice cold H₂O. The proteins were transferred at 30V for 90mins (overnight for weak or small proteins) on ice.

Following transfer, the nitrocellulose was washed 4x15mins in TBS/T. For weakly expressed proteins, a Pierce signal enhancer was used (Thermo Scientific) with the following steps: the nitrocellulose was washed in dH₂O; incubated with reagent 1 for 2mins; rinsed 5x in dH₂O; incubated with reagent 2 for 10mins; rinsed in H₂O. The nitrocellulose was then blocked in 5% BSA (Albumin, Bovine Serum, Fraction V) in TBS/T for 1hr at room temperature or overnight at 4°C, and washed in TBS/T (4x15mins). Primary antibody was diluted according to manufacturer's recommendations (typically 1:1000) in 5% BSA (Fraction V). The nitrocellulose was incubated with primary antibody at 4°C overnight or at room temperature for 1hr, according to manufacturer's instructions. Diluted primary antibodies were reserved and re-used by adding a couple of Sodium Azide crystals and storing at 4°C. The nitrocellulose was washed in TBS/T (4x15mins) and then

incubated for 90mins with secondary antibody diluted 1:5000 in 5% non-fat milk (Marvel; Chivers Ireland Ltd, Dublin, Ireland). Table 2.4 shows all primary antibodies used, and the relevant secondary antibodies. The nitrocellulose was washed again in TBS/T.

Primary Antibody	Dilution	Secondary Antibody
SOCS1 (ab)	1:666 in 5% BSA	HRP-linked rabbit anti-goat (d)
SOCS2 (cs)	1:1000 in 5% BSA	HRP-linked goat anti-rabbit (cs)
SOCS3 (ab)	1:369 in 5% BSA	HRP-linked goat anti-rabbit (cs)
HRP-linked β -Actin (s)	1:25,000 in 5% n/f milk	n/a
Phospho-STAT1 (cs)	1:1000 in 5% BSA	HRP-linked goat anti-rabbit (cs)
STAT1 (cs)	1:1000 in 5% BSA	HRP-linked goat anti-rabbit (cs)
Phospho-STAT3 (cs)	1:1000 in 5% BSA	HRP-linked goat anti-rabbit (cs)
STAT3 (cs)	1:1000 in 5% BSA	HRP-linked goat anti-rabbit (cs)
Phospho-STAT5 (cs)	1:1000 in 5% BSA	HRP-linked goat anti-rabbit (cs)
STAT5 (cs)	1:1000 in 5% BSA	HRP-linked goat anti-rabbit (cs)
Phospho-Akt (cs)	1:1000 in 5% BSA	HRP-linked goat anti-rabbit (cs)
Akt (cs)	1:1000 in 5% BSA	HRP-linked goat anti-rabbit (cs)
Phospho-p44/42 MAPK (Erk1/2) (cs)	1:1000 in 5% BSA	HRP-linked goat anti-rabbit (cs)
p44/42 MAPK (Erk1/2) (cs)	1:1000 in 5% BSA	HRP-linked goat anti-rabbit (cs)

Table 2.4. Western blot antibodies. Primary and secondary antibodies used for western blotting and their dilutions used. BSA = Bovine serum albumin, Fraction V; n/f = non fat; HRP = horseradish peroxidase; cs = Cell Signalling Technology (New England Biolabs); s = Sigma; ab = Abcam (Cambridge, UK); d=Dako.

Bound antibody was detected using Amersham ECL Western blotting detection reagents A and B (GE Healthcare) which were added to the nitrocellulose at a 1:1 ratio, incubated for 1min, poured off and the nitrocellulose sandwiched between transparent sheets in a film cassette. To visualise very faint bands, Amersham ECL Plus reagents were used (GE Healthcare), with 25 μ l reagent A added to 1ml reagent B, and incubated for 10mins on the nitrocellulose. Chemiluminescence was detected with Amersham ECL Hyperfilm (GE Healthcare), which was developed using a Medical Film Processor (SRX-101A; Konica Minolta, Bloxham, Banbury, UK). Band intensities were measured using Quantity One software (Bio-Rad Laboratories).

2.8.3. Stripping Nitrocellulose

Nitrocellulose membranes were stripped of antibody by incubating in 20ml Restore Plus Stripping buffer (Thermo Scientific) at room temperature for 2-4hrs. Stubborn antibodies were removed by incubating at 37°C for 15-30mins. The nitrocellulose membranes were then washed in TBS/T. The membranes were probed again with the appropriate HRP-labelled secondary antibody, washed in TBS/T and detected with ECL reagents and Hyperfilm (as in Section 2.8.2) to test for complete removal of primary antibody. The nitrocellulose could then be re-probed with different antibodies.

2.9. Statistical Analysis

For most experiments data were analysed for statistical significance by analysis of variance (ANOVA), using Minitab 15 (USA). Groups were compared using a general linear model incorporating pair wise comparisons.

For growth curve analysis, data was analysed by linear mixed-effect models, using R (version 2.13.1, <http://www.r-project.org/>). These models had mouse identification nested within each litter as the random effects, measuring variance in weight gain taking into account mouse genotype and sex. In addition, a series of fixed effects were added to the model (week, genotype and sex) and the interactions between them investigated. For all models the residuals were checked for normality prior to examination of statistical significance. This examination revealed that the growth curve (body weight and lengths) data change with week was not linear, and was in fact curvilinear. Therefore the change with week was fitted as $y = x + x^2$. The full model with all interactions was fitted first and non-significant interaction terms were then excluded sequentially until a final model of just those interactions and associated main effects remained.

Data are presented as mean plus standard error of the mean (SEM). In all cases P values <0.05 were taken to indicate statistical significance, and are represented as follows: * P<0.05; ** P<0.01; *** P<0.001.

CHAPTER 3

ESTABLISHING GH, IGF-1 AND SOCS SIGNALLING IN THE GROWTH PLATE

3. Establishing GH, IGF-1 and SOCS Signalling in the Growth Plate

3.1. Introduction

Postnatal endochondral bone growth is regulated by GH whose mode of action is thought to be direct via interactions with growth plate chondrocyte GH-receptors (GHR) and/or indirect through enhanced levels of systemically derived liver IGF-1 (Salmon and Daughaday, 1957; Isaksson *et al.*, 1982; Nilsson *et al.*, 1986). GH signalling occurs through several signalling pathways, including the JAK/STAT, MAPK, and phosphatidylinositol-3 kinase (PI-3K) pathways. The most established pathway is the JAK/STAT pathway, which is required for the GH induction of IGF-1 production (Herrington *et al.*, 2000). STAT1, STAT3 and STAT5 are known to be activated by GH through JAK2 and it is well recognised that the JAK2/STAT5b pathway is pivotal for growth promotion, where inactivating mutations or elimination in mice of STAT5b result in reduced growth (Udy *et al.*, 1997; Teglund *et al.*, 1998; Davey *et al.*, 1999; Sims *et al.*, 2000). To date, the specific STAT family member(s) activated for mediating GH signalling in growth plate chondrocytes has focussed on STAT5b and a role for STAT1 and STAT3 is, as yet, unclear (Gevers *et al.*, 2009).

SOCS proteins are generated in response to cytokines including GH and can inhibit JAK signalling and downstream STAT activation (Hilton, 1999; Rico-Bautista *et al.*, 2006; Pass *et al.*, 2009). It is recognised that the GH/IGF-1 signalling cascade is inhibited by SOCS1-3. Whilst SOCS1^{-/-} and SOCS3^{-/-} mice are perinatal and embryonic lethal, respectively, mice missing the SOCS2 gene have increased linear bone growth and body mass due to increased signalling through the GHR (Marine *et al.*, 1999a; Marine *et al.*, 1999b; Metcalf *et al.*, 2000; Roberts *et al.*, 2001; Lorentzon *et al.*, 2005; MacRae *et al.*, 2009). As SOCS2^{-/-} mice do not have increased circulating IGF-1 levels it is likely that the increased bone growth and observed structural differences within SOCS2^{-/-} growth plates are a direct consequence of altered SOCS2 mediated GH/IGF-1 signalling within the growth plate, which warrants investigation (Alexander *et al.*, 1999; Turnley, 2005; MacRae *et al.*, 2009). It

has been shown that SOCS2 localises to growth plate chondrocytes in all zones, with strong expression observed in the resting and proliferating zones (Figure 3.1), indicating a role in regulating GH signalling at the growth plate level (MacRae *et al.*, 2009).

The increased body mass and bone growth of SOCS2 null mice is not observed when mutants are mated with mice lacking the STAT5b gene (Greenhalgh *et al.*, 2002a). This suggests that the SOCS2^{-/-} overgrowth phenotype is dependent on STAT5b downstream signalling events and that uninhibited GH signalling through STAT1 and STAT3 does not contribute to the SOCS2^{-/-} overgrowth phenotype. However, currently, there is no evidence that the increased growth of the SOCS2 null mice is due to increased STAT5 mediated GH signalling, specifically at the level of the growth plate.

Many chronic paediatric inflammatory diseases, such as Crohn's disease, are often associated with growth retardation and elevated inflammatory cytokines such as IL-1 β and TNF α (Davies *et al.*, 1997; MacRae *et al.*, 2006c). Raised levels of such cytokines have been shown to inhibit chondrocyte proliferation and promote apoptosis leading to narrowing of growth plate zones and reduced endochondral growth (MacRae *et al.*, 2006c). MacRae *et al.* (2009) found that SOCS2 is up-regulated by TNF α in chondrocytes, indicating that SOCS2 may play a role in inflammation induced growth retardation which requires further clarification and investigation (MacRae *et al.*, 2009).

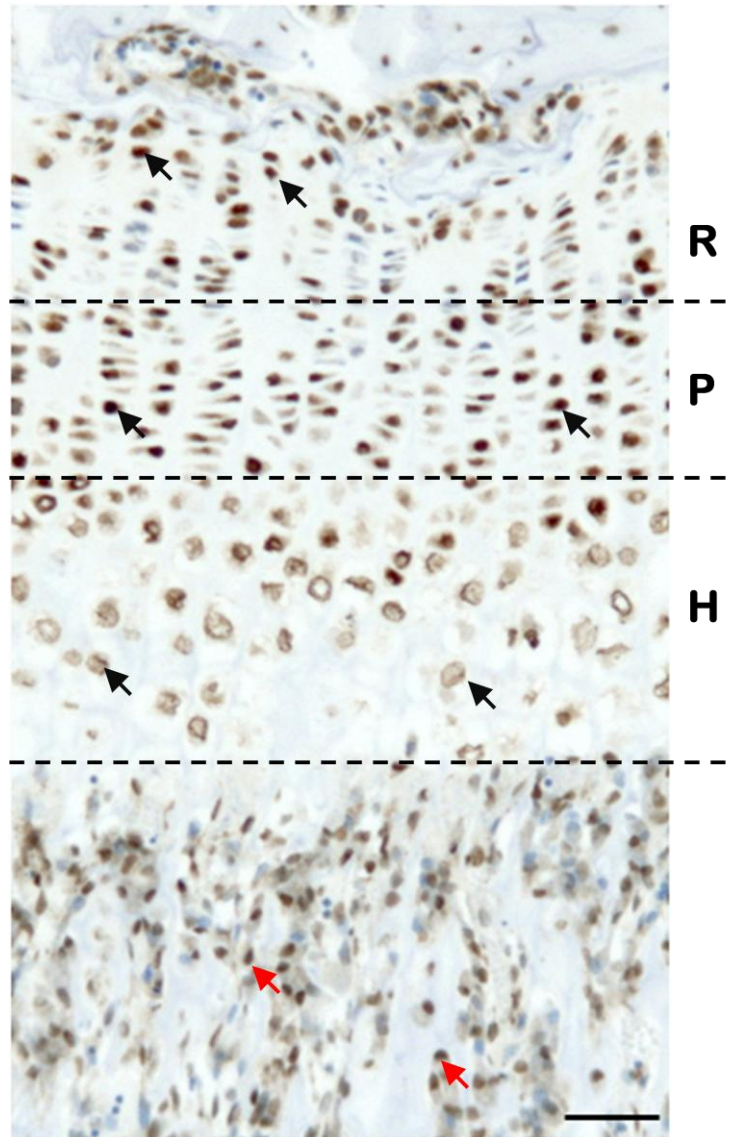


Figure 3.1. Immunohistochemistry of SOCS2 expression. Image showing localization of SOCS2 in a 3 week old mouse tibia (X10 magnification). Strong staining can be seen in the resting (R) and proliferating (P) zones of the growth plate, with weaker staining in the hypertrophic zone (H); as indicated by the black arrows. SOCS2 staining was also observed in osteoblasts (red arrows). Scale bar shows 50 μ m. Image adapted from MacRae *et al.* (2009).

3.2. Aims and Hypothesis

3.2.1. Hypothesis

SOCS2 is the primary SOCS protein to regulate endochondral growth by inhibiting chondrocyte GH signalling through the JAK/STAT pathway. Inflammatory cytokines, such as IL-1 β , act to inhibit growth by stimulating SOCS2.

3.2.2. Aims

- Establish by RT-PCR that receptors for GH, IGF-1 and IL-1 β are present in chondrocytes
- Determine which STAT proteins are activated in chondrocytes by GH and the effects of IL-1 β on this
- Investigate which SOCS proteins are involved in regulating chondrocyte GH signalling
- Analyse SOCS2 expression in response to inflammatory cytokines

3.3. Materials and Methods

3.3.1. Cell culture

ATDC5 cells were culture as described in Section 2.2.1. Primary chondrocytes were isolated from 1- to 3-day old Swiss mice as described in Section 2.3.7. Primary osteoblasts were isolated from 4-day old C57/Bl6 (WT) mice as described in Section 2.3.8. Cells were cultured in 6-well (for RT-PCR or western blot) plates in differentiation medium (ATDC5 cells), primary chondrocyte medium (primary cells) or osteoblast medium (osteoblasts) as described in Sections 2.2.1, 2.3.7 and 2.3.8 respectively. Temporal expression of SOCS proteins was investigated by challenging cells with 500ng/ml GH (Bachem), 50ng/ml IGF-1 (Bachem), 10ng/ml IL-1 β (Autogen Bioclear, Calne, Wiltshire, UK), or 10ng/ml TNF α (Autogen Bioclear) at intervals from 8hrs to 72hrs. To investigate STAT signalling, cells were cultured in serum free medium (containing no FBS or ITS) 24hrs prior to stimulation with growth factors or cytokines (24hrs IL-1 β ; 15mins 500ng/ml GH; 15mins 50ng/ml IGF-1).

3.3.2. RT-PCR

RNA was extracted from ATDC5 cells and primary cells that had not been serum deprived or exposed to any cytokines as described in Section 2.7.1. RT-PCR was performed using primers for GH, IGF-1 and IL-1 β receptors; 18S (loading control); collagen II (chondrocyte marker) as described in Sections 2.7.2 and 2.7.3. Details of the primers used are in Table 2.2.

3.3.3. Western Blotting

Cells were cultured as described in Section 3.3.1 and scraped for protein as described in Section 2.8.1. Western blotting was performed as described in Sections 2.8.2 and 2.8.3. Antibodies used are detailed in Table 2.4.

3.4. Results

3.4.1. Expression of GH, IGF-1 and IL-1 β Receptors in Chondrocytes

As the signalling pathways examined in this chapter are poorly studied in chondrocytes, it was first necessary to confirm the expression of specific ligand receptors. Accordingly, RT-PCR analysis was performed on ATDC5 cells and primary chondrocytes to confirm the expression of receptors for GH, IGF-1 and IL-1 β (Figure 3.2). IL-1 β has two receptors: receptor 1 (IL-1RI) and receptor 2 (IL-1RII). IL-1RI was analysed here as it is capable of activating cells through its long cytoplasmic domain, unlike IL-1RII which has a short intracellular domain and no biological activity (Arend *et al.*, 2008). Collagen type-II was analysed as a chondrocyte marker to confirm the cells had maintained their chondrogenic phenotype. Both primary chondrocytes and ATDC5 cells expressed collagen type-II indicating that the chondrocyte phenotype was maintained (Figure 3.2).

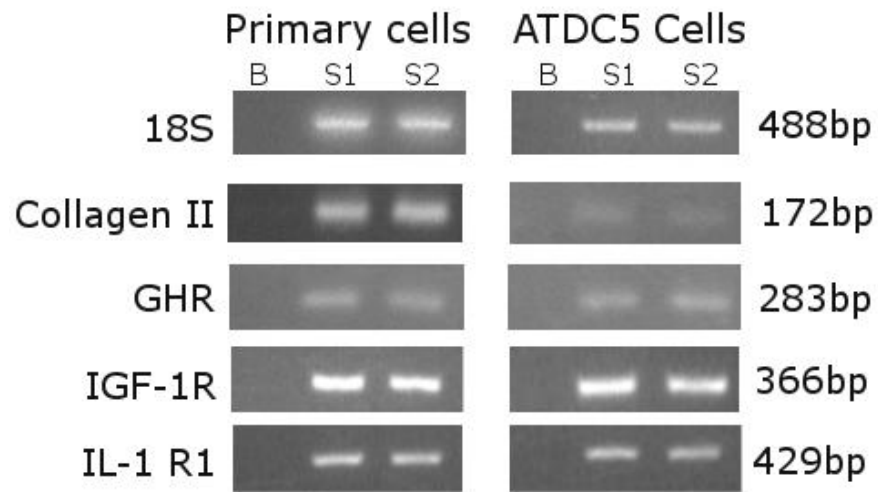


Figure 3.2. Receptor expression. PCR results showing expression of GH receptor (GHR), IGF-1 receptor (IGF-1R) and IL-1 β receptor 1 (IL-1 R1). 18S shows equal loading and collagen type-II (collagen II) is a chondrocyte marker. Results are shown for a blank control (no cDNA; B) and two individual samples (S1 and S2).

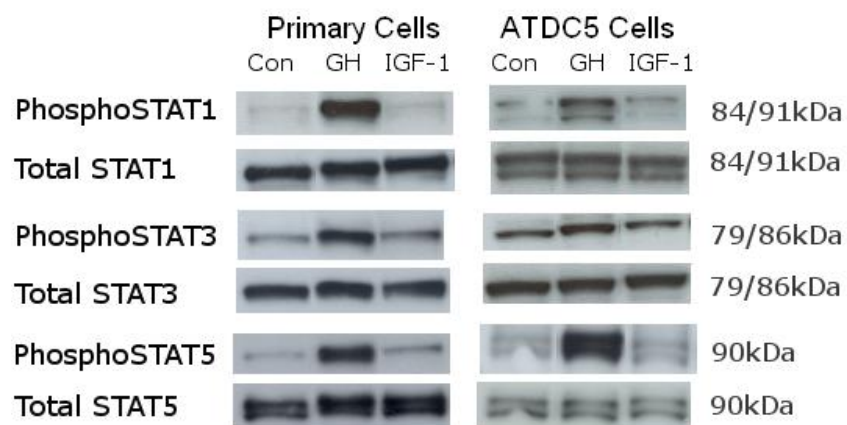


Figure 3.3. STAT signalling. Western blot results showing expression of phosphorylated (Phospho) STAT1, STAT3 and STAT5 in response to GH (500ng/ml) and IGF-1 (50ng/ml) in primary chondrocytes and ATDC5 cells, with total STAT proteins as loading controls. Where two bands are present, these represent the two subunits of the STAT protein.

3.4.2. STAT Phosphorylation in Response to GH and IGF-1

Although it is well recognised that GH signalling is mediated by STAT activation in many cell types, the identity of the STATs involved in propagating GH intracellular signalling in growth plate chondrocytes is largely unknown (Smit *et al.*, 1996; Han *et al.*, 1996; Herrington *et al.*, 2000; Waters *et al.*, 2006; Brooks *et al.*, 2008). Therefore, both primary chondrocytes and ATDC5 cells were stimulated by GH and IGF-1 for 15mins and the phosphorylation of STAT1, STAT3, and STAT5 determined (Figure 3.3). Concentrations of GH (500ng/ml) and IGF-1 (50ng/ml) used are based on similar studies in 3T3 F442A cells (a murine adipocyte cell line) by Han *et al.* and in 293T cells (a human renal epithelial cell line) by Zong *et al.* (Han *et al.*, 1996; Zong *et al.*, 2000).

In both ATDC5 cells and primary chondrocytes, GH increased the phosphorylation of STAT1, STAT3, and STAT5 (Figure 3.3). Exposure of primary chondrocytes or ATDC5 cells to IGF-1 had no effect on STAT phosphorylation. Total STAT1, STAT3, and STAT5 expression were unchanged by any treatment in both primary cells and ATDC5 cells.

3.4.3. The Effects of Inflammatory Cytokines on STAT Signalling

During chronic inflammatory conditions, such as Crohn's disease, growth retardation is observed in association with raised levels of inflammatory cytokines. The raised levels of these cytokines, for example IL-1 β and TNF α , are associated with inhibition of chondrocyte proliferation but the mechanisms behind this inhibition are poorly understood (MacRae *et al.*, 2006b). Therefore STAT signalling in chondrocytes was further investigated by extending the previous experiment (Figure 3.3) to include the inflammatory cytokine IL-1 β , to determine its effects of GH stimulation of STAT phosphorylation (Figure 3.4). IL-1 β was added to the culture medium 24hrs before the addition of GH or IGF-1 (15mins) at a concentration of 10ng/ml. The concentration of IL-1 β used was based on previous publications in which proliferation and chondrocyte marker gene expression were shown to be down regulated in the same cells types (MacRae *et al.*, 2006b). The experiment was repeated in three independent experiments.

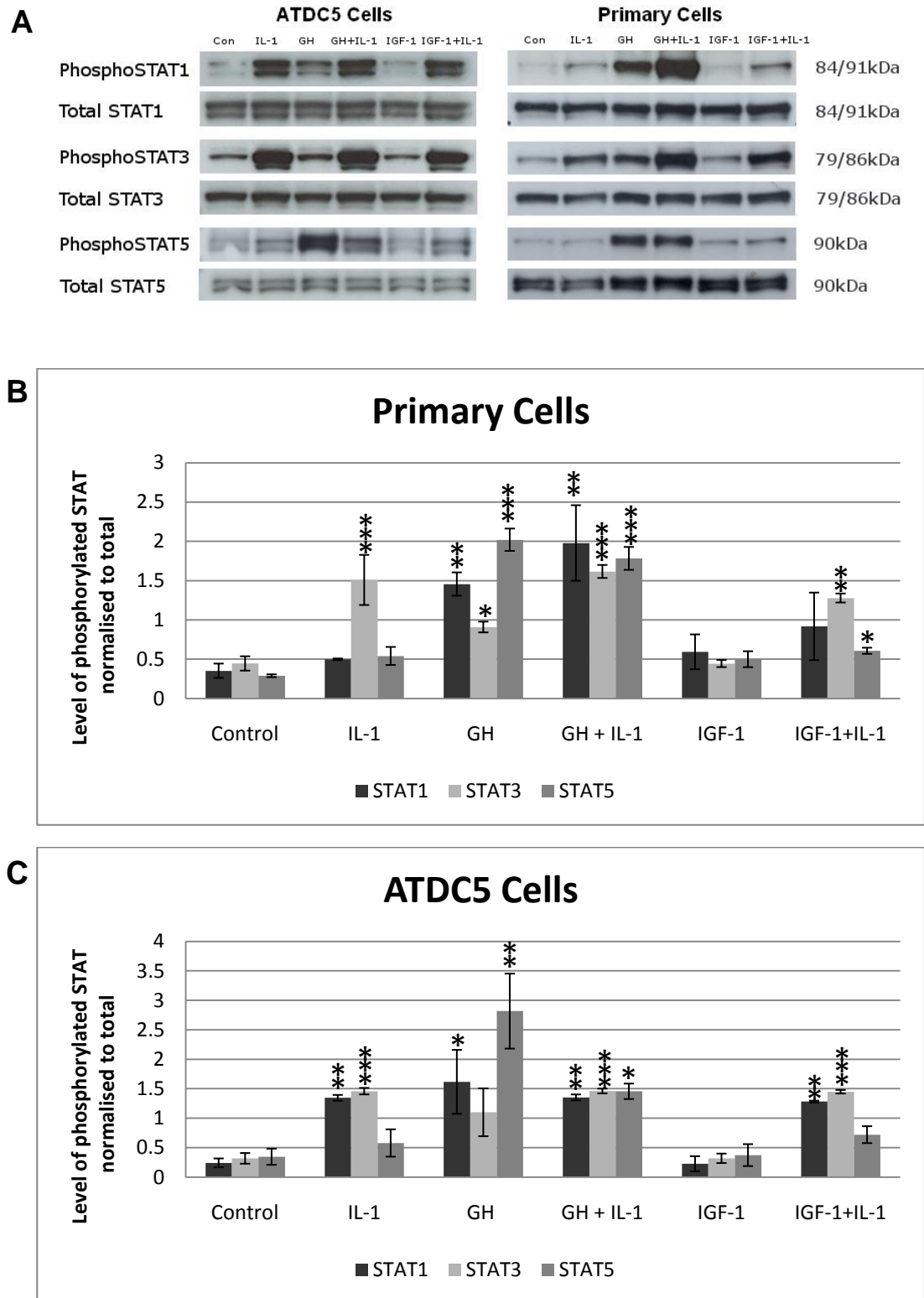


Figure 3.4. STAT signalling with IL-1 β . Western blot results showing activation of STAT1, STAT3 and STAT5 in response to GH (500ng/ml), IGF-1 (50ng/ml) and/or IL-1 β (10ng/ml) in chondrocytes. (A) Typical results gained for primary and ATDC5 cells of phosphorylated (Phospho) STAT proteins, with total STAT proteins as loading controls. Results from 3 independent experiments were quantified by densitometry and normalised against total STAT protein, giving (B) and (C) for primary and ATDC5 cells, respectively. Results were analysed statistically by ANOVA. Data are shown as mean \pm SEM; *P<0.05; **P<0.01; ***P<0.001 compared to Control.

The results in Figure 3.3 were repeated with GH stimulating a significant increase in phosphorylation of STAT1, STAT3, and STAT5 ($P < 0.01$, $P < 0.05$ and $P < 0.001$ respectively) in primary cells (Figure 3.4a & b). ATDC5 cells showed increased activation of STAT1 and STAT5 in response to GH ($P < 0.05$ and $P < 0.001$ respectively), with a non-significant increase observed for STAT3 (Figure 3.4a & c). Again IGF-1 had no effect on STAT phosphorylation. IL-1 β stimulated phosphorylation of STAT1 and STAT3 in ATDC5 cells ($P < 0.01$ and $P < 0.001$ respectively), but only of STAT3 in primary cells ($P < 0.001$; Figure 3.4). There was a trend of increased STAT1 and STAT3 phosphorylation in ATDC5 and primary cells in the presence of GH and IL-1 β compared with GH alone (significant only for STAT3; $P < 0.05$ in ATDC5 cells, $P < 0.01$ in primary chondrocytes), suggesting an additive effect of IL-1 β stimulation. In contrast, there was an indication of decreased STAT5 phosphorylation in response to GH+IL-1 β compared with GH treatment alone, however this did not reach significance.

3.4.4. IGF-1 Signalling in Chondrocytes

To confirm the lack of STAT signalling in response to IGF-1 it was necessary to establish that the IGF-1 recombinant protein being added to the cells was biologically active in this system. Hence, phosphorylation of Akt and P44/42 MAPK, two recognised downstream signalling molecules of IGF-1, were determined by western blot (Figure 3.5) in samples used and described Section 3.3.

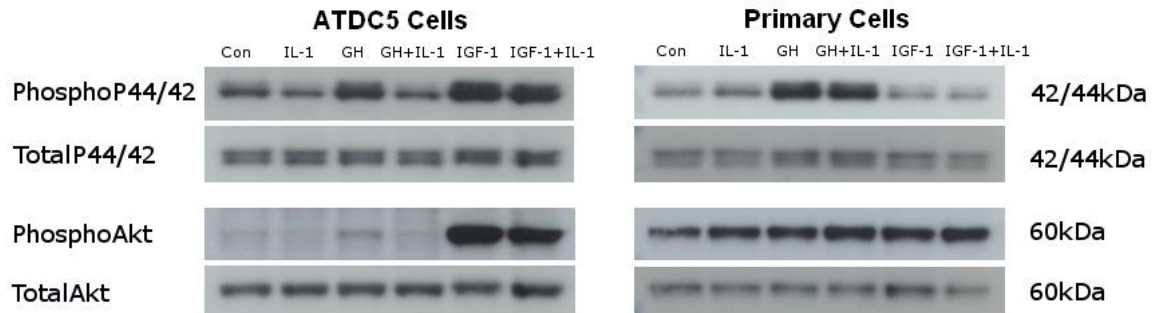


Figure 3.5. IGF-1 Signalling. Western blot showing phosphorylation of P44/42 MAPK (P44/42) and Akt in response to GH (500ng/ml), IGF-1 (50ng/ml) and/or IL-1 β (10ng/ml) in ATDC5 and primary cells.

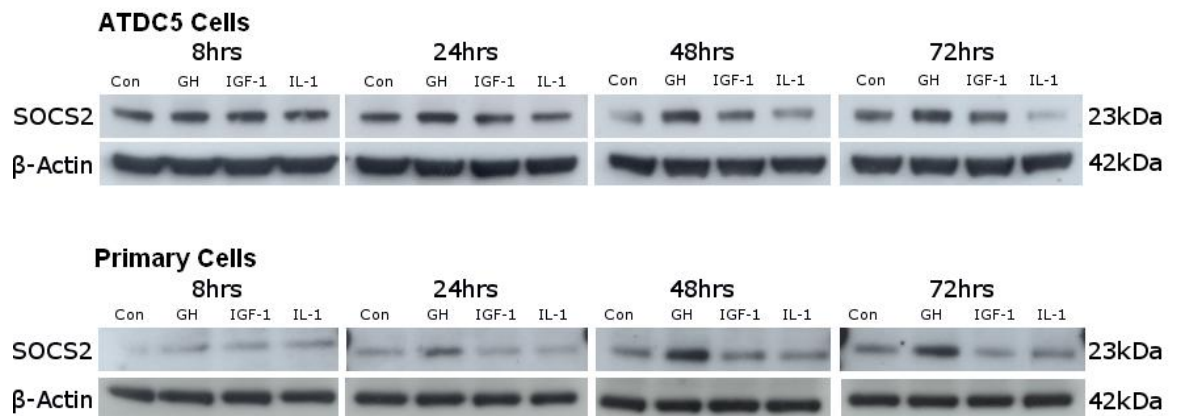


Figure 3.6. SOCS2 expression. Western blots showing temporal expression of SOCS2 in response to GH (500ng/ml), IGF-1 (50ng/ml) and IL-1 β (10ng/ml) in ATDC5 cells and primary chondrocytes. β -actin is shown as a loading control.

Activation of P44/42 MAPK and Akt by the various ligands differed in the two cell types (Figure 3.5). In ATDC5 cells, phosphorylation of both P44/42 and Akt was increased in response to GH and IGF-1. In primary cells, P44/42 MAPK was phosphorylated in response to GH, but not IGF-1. In contrast, Akt phosphorylation remained high in the unstimulated control cells and was not altered in response to any treatments. Of interest, IL-1 β appeared to inhibit phosphorylation of P44/42 MAPK and Akt in ATDC5 cells and this was also noted in cells cultured in the presence of GH and IL-1 β where phosphorylation of P44/42 MAPK and Akt was lower than in cells challenged by GH alone. Although the lack of P44/42 MAPK and Akt phosphorylation by IGF-1 in primary cells was unexpected, the IGF-1 induced phosphorylation in ATDC5 confirms the IGF-1 used in the experiments was biologically active, which was the main aim of this experiment. It can therefore be concluded that the lack of STAT activation with IGF-1 noted in Figures 5, 6 and 7 is likely to be a true biological result.

3.4.5. The Expression of SOCS Proteins in Chondrocytes

Previous studies have shown that SOCS2 expression is up-regulated in response to TNF α in chondrocytes (MacRae *et al.*, 2009). The results in Section 3.3 indicate that GH activation of STAT5 is inhibited by the addition of inflammatory cytokine IL-1 β . This effect could be mediated by SOCS2, so the studies by MacRae and colleagues were repeated and extended by examining the expression of SOCS2 in response to IL-1 β over an 8 – 72 hrs incubation period (Figure 3.6). SOCS2 is thought to negatively regulate GH signalling as part of a negative feedback loop, whereby it is produced downstream of GH signalling (Tollet-Egnell *et al.*, 1999). There is also evidence that SOCS2 can act to regulate IGF-1 signalling (Dey *et al.*, 1998; Michaylira *et al.*, 2006b), so this study also looked at chondrocyte SOCS2 expression in response to GH and IGF-1 over the time period (Figure 3.6).

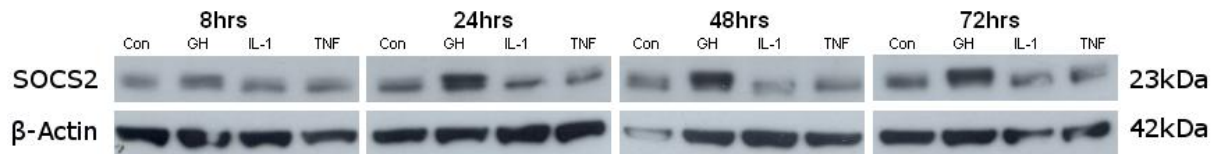


Figure 3.7. SOCS2 expression with inflammatory cytokines. Western blot results for SOCS2 expression over time in primary chondrocytes in response to GH (500ng/ml), IL-1 β (10ng/ml) and TNF α (10ng/ml). β -actin is shown as a loading control

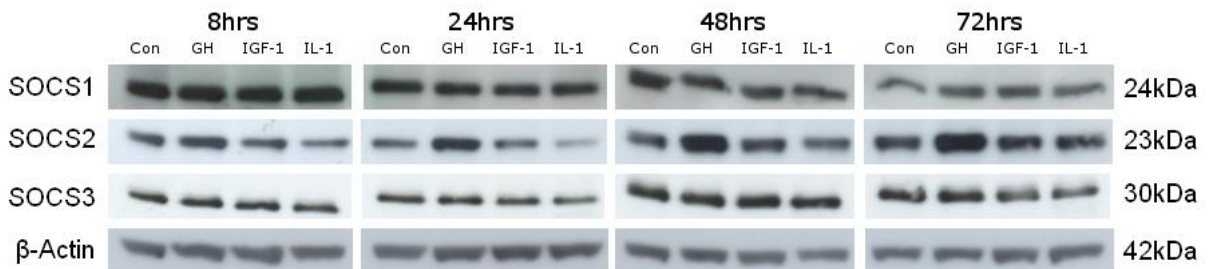


Figure 3.8. SOCS proteins in chondrocytes. Western blot showing expression of SOCS1, SOCS2 and SOCS3 in primary chondrocytes in response to GH (500ng/ml), IGF-1 (50ng/ml) and IL-1 β (10ng/ml) over time, with β -actin as a loading control.



Figure 3.9. SOCS2 in osteoblasts. Western blot showing SOCS2 expression in response to GH (500ng/ml) over time in primary osteoblasts, with β -actin as a loading control.

In both ATDC5 cells and primary chondrocytes GH increased SOCS2 expression after 24 hrs and this stimulation was maintained for the duration of the experiment. Neither IGF-1 nor IL-1 β affected expression of SOCS2. In fact, in ATDC5 cells, IL-1 β appears to inhibit the expression of SOCS2 at the later time points. This latter result was inconsistent with the published data by MacRae *et al.* (2009) who reported that chondrocyte SOCS2 expression was stimulated by TNF α . Therefore to determine if this stimulation of SOCS2 expression was specific to TNF α the experiment was repeated but this time primary chondrocytes were challenged with TNF α or IL-1 β (both 10ng/ml) (Figure 3.7). Again SOCS2 expression was increased in the presence of GH, but there was no increase in SOCS2 expression in response to IL-1 β or TNF- α .

Finally it was necessary to establish which of the other SOCS proteins known to inhibit GH signalling are activated in chondrocytes. Therefore the expression of SOCS1 and SOCS3 was examined in primary chondrocytes challenged with GH, IGF-1 and IL-1 β (Figure 3.8).

In contrast to SOCS2, whose expression was increased by GH confirming the data in Figures 3.6 and 3.7, neither SOCS1 nor SOCS3 expression levels were altered by GH challenge at any of the time points studied. Similarly, the expression of SOCS1, SOCS2 and SOCS3 was not altered in response to IGF-1 or IL-1 β at any time points studied. These data indicate that SOCS2 is the predominant GH regulated SOCS protein in growth plate chondrocyte.

3.4.6. The Expression of SOCS2 in Osteoblasts

SOCS2^{-/-} mice have increased bone mass and this is consistent with the known anabolic effects of GH on the skeleton (MacRae *et al.*, 2009). To determine if SOCS2 expression is increased in response to GH in osteoblasts in a similar manner to that observed in chondrocytes the temporal expression of SOCS2 was analysed in calvarial primary osteoblasts cultured with GH (500ng/ml) or IGF-1 (50ng/ml) (Figure 3.9). The data clearly indicated that SOCS2 was increased in response to GH in primary osteoblasts, an effect that peaked after 48hrs.

3.5. Discussion

This study confirmed recent findings by Gevers *et al.* that STAT5 phosphorylation is activated in both primary chondrocytes and ATDC5 cells in response to GH (Gevers *et al.*, 2009), and also found that STAT1 and STAT3 are activated in response to GH. According to the recognised GH signalling mechanisms it is likely that this STAT activation leads to increased IGF-1 expression, which acts via different signalling cascades to increase chondrocyte proliferation and thus endochondral growth (Hoshi *et al.*, 2004; MacRae *et al.*, 2007a; Klammt *et al.*, 2008). Zong *et al.* have demonstrated previously that IGF-1 is capable of signalling via STAT3 in 293T cells (a human renal epithelial cell line) and in C2C12 cells (a mouse myoblast cell line) (Zong *et al.*, 2000). It is possible that this is a cell type specific effect as this study has demonstrated *in vitro* that IGF-1 does not stimulate STAT activation in chondrocytes. This result was expected as the IGF-1 receptor does not contain the specific tyrosine motifs recognised by STAT proteins (Stahl *et al.*, 1995; Decker and Kovarik, 2000)

IGF-1 signalling occurs through two primary signalling pathways: Shc/Ras/Raf/MAPK and IRS-1/PI3K/Akt/PKB (LeRoith, 2000). In particular the latter pathway, involving IRS-1 mediated PI3K signalling, has been shown to be important in the regulation of endochondral bone growth (Hoshi *et al.*, 2004; MacRae *et al.*, 2007a). Therefore the phosphorylation of key downstream IGF-1 signalling proteins, namely Akt and P44/42 MAPK (also known as Erk1/2), were investigated to confirm that the IGF-1 used was biologically active in the experimental system. Interestingly Akt and P44/42 MAPK showed different activation patterns in ATDC5 cells compared to primary chondrocytes. In ATDC5 cells, phosphorylation of both Akt and P44/42 MAPK was activated by GH and IGF-1, and inhibited by IL-1 β . In primary chondrocytes only GH stimulated phosphorylation of P44/42 MAPK, whereas Akt was not activated by GH or IGF-1. Furthermore, IL-1 β did not show inhibition or activation of either signalling molecule. The aim of the experiment was to demonstrate that the IGF-1 used in the system was biologically active, which is confirmed by the

signalling in ATDC5 cells, but such large differences between the two cell types are unexpected. IGF-1 stimulation of Akt and P44/42 MAPK was expected in primary chondrocytes. Other authors have shown IGF-1 to stimulate phosphorylation of P44/42 MAPK and Akt in ATDC5 cells and primary chick chondrocytes, but little work has been done using murine chondrocytes (Koike *et al.*, 2003; Phornphutkul *et al.*, 2004; Kiepe *et al.*, 2005; MacRae *et al.*, 2007a). Phornphutkul and colleagues (2004) investigated primary chick chondrocytes in distinct stages of differentiation, demonstrating that proliferating chondrocytes show increased P44/42 MAPK activation in response to IGF-1 but that hypertrophic chondrocytes did not. It is therefore possible to propose that the lack of response found in these studies is a result of the primary murine chondrocytes being a mixed population of cells at various stages of differentiation, from resting to hypertrophic.

The gigantism phenotype of the SOCS2^{-/-} mice, and the observed increased length of longitudinal bones (Metcalf *et al.*, 2000; MacRae *et al.*, 2009), indicate that SOCS2 may have a predominant role in regulating growth plate GH signalling. GH signalling is thought to be inhibited completely by SOCS1 and SOCS3, and partially by CIS and SOCS2 (Adams *et al.*, 1998; Starr *et al.*, 1998; Hansen *et al.*, 1999; Alexander *et al.*, 1999; Roberts *et al.*, 2001; Inaba *et al.*, 2005). This study has shown that in chondrocytes, GH stimulates the expression of SOCS2 but not that of SOCS1 or SOCS3. Thus from this data it can be argued that, at the growth plate level, SOCS2 is the primary SOCS protein acting to regulate GH signalling. SOCS1 is predominantly expressed in the thymus and SOCS1^{-/-} exhibit IFN γ dependant premature lethality due to lymphocyte deficiencies, monocyte infiltration and liver fat deposition (Starr *et al.*, 1998; Naka *et al.*, 1998; Alexander *et al.*, 1999; Marine *et al.*, 1999b). In contrast, SOCS3 is required for liver haematopoiesis, and SOCS3^{-/-} mice die embryonically due to erythropoiesis and placental defects (Marine *et al.*, 1999a; Roberts *et al.*, 2001). These findings support the above hypothesis as it appears that SOCS1 and SOCS3 do not act to inhibit GH signalling in the growth plate, but are involved in signal regulation in other tissues. It would be very interesting and informative to generate mice in which SOCS1 and SOCS3 genes are knocked-out only in the epiphyseal cartilage (tissue specific knock-outs). This would be

possible through exploitation of Cre-Lox system and would permit the study of viable growing mice. To date these mice have not yet been generated. Conflicting reports exist on the phenotype of the CIS knockout mice. The mice have been reported to exhibit no remarkable phenotype or that they have a phenotype consistent with a role for CIS in the regulation of haemopoietic growth factors (Hilton, 1999; Yoshimura *et al.*, 2005).

MacRae and colleagues (2009) recently showed increased expression of SOCS2 in response to TNF α in chondrocytes, leading to the hypothesis that SOCS2 may mediate the negative effects of pro-inflammatory cytokines on endochondral bone growth. Therefore the effect of the pro-inflammatory cytokine IL-1 β on chondrocyte GH signalling through STAT proteins was investigated. On its own, IL-1 β significantly increased the phosphorylation of STAT1 and STAT3 in ATDC5 cells and STAT3 in primary chondrocytes. When added in combination with GH, IL-1 β suppressed the level of STAT5 phosphorylation compared to GH alone, an effect that may be mediated by the stimulation of SOCS2 expression. However, in contrast to the findings by MacRae *et al.* (2009), SOCS2 was not stimulated in response to IL-1 β nor TNF α in ATDC5 cells or primary chondrocytes. This result was repeated several times (not all replicate data shown), indicating that the findings by MacRae and colleagues must be treated with some caution. Taken together the results of this part of the work provide no evidence to support the suggestion that pro-inflammatory cytokines inhibit bone growth by reducing GH signalling through SOCS2 mediated mechanisms.

SOCS2 expression was increased in osteoblasts in response to GH challenge, indicating it may also play a role in regulating bone formation in response to GH. This is consistent with findings by MacRae *et al.* (2009), where SOCS2 expression was observed in osteoblasts by immunohistochemistry (Figure 3.1). Furthermore, these authors found increased cortical bone area and increased levels of osteoblast and osteoclast markers, namely osteocalcin and TRAP5b respectively, indicating increased levels of bone turnover (MacRae *et al.*, 2009). These combined

results indicate a role for SOCS2 in appositional bone growth, something that clearly warrants further investigation. Unfortunately this was not a priority of this studentship which was focussed on investigating the role of SOCS2 in the regulation of endochondral bone growth.

3.6. Conclusion

This study has demonstrated that in growth plate chondrocytes GH signals via STAT1, STAT3 and STAT5, with predominant signalling through STAT5. SOCS2 is the main SOCS protein to act in the growth plate, where it is stimulated by GH. The role of SOCS2 in inflammatory induced growth retardation is not clear, with conflicting results from this study and others requiring further investigation.

CHAPTER 4

ANALYSING THE SOCS2^{-/-} GROWTH PHENOTYPE

4. Analysing the SOCS2^{-/-} Growth Phenotype

4.1. Introduction

Metcalf and colleagues first described the overgrowth phenotype of SOCS2^{-/-} mice in 2000. They observed that the gigantism didn't occur until weaning (about 3-weeks of age), and that male SOCS2 null mice grew to be 40% larger than their WT litter mates (Figure 4.1), while female SOCS2 null mice demonstrated a more modest increase reaching a comparable size to WT males (Metcalf *et al.*, 2000). This increase in body weight was not associated with more fatty tissue but rather an increase in organ size, muscle and bone (Metcalf *et al.*, 2000). The increased size of organs has been reported as a result of increased cell number as opposed to an increase in cell size, and SOCS2^{-/-} mice were found to have increased body length with longer bones (Metcalf *et al.*, 2000).



Figure 4.1. SOCS2^{-/-} phenotype. Picture of a 2 month old male SOCS2^{-/-} mouse (left) with a 2 month old male WT mouse (right). Image taken from Metcalf *et al.* (2000).

It was later confirmed that SOCS2 acts to negatively regulate GH signalling through the JAK/STAT pathway, in particular STAT5, by demonstrating that the SOCS2^{-/-} overgrowth phenotype can be attenuated by crossing SOCS2^{-/-} mice with STAT5b^{-/-} mice (Greenhalgh *et al.*, 2002a). These authors also reported that removal of GH from SOCS2^{-/-} mice (by crossing with Ghrhr^{lit/lit} mice which have no circulating GH) prevents the overgrowth phenotype, an effect that can be rescued by GH treatment (Greenhalgh *et al.*, 2005). These experiments eloquently show that SOCS2 plays an important role in negatively regulating body growth through its inhibitory effects on GH signalling. It has also been shown that circulating levels of GH and IGF-1 are unchanged in SOCS2^{-/-} mice and it is therefore likely that the overgrowth phenotype is the result of changes at local tissue levels (Metcalf *et al.*, 2000; Greenhalgh *et al.*, 2002a). Indeed, increased levels of IGF-1 have been found in many tissues in SOCS2^{-/-} mice, and STAT5 activation was found to be prolonged in SOCS2^{-/-} hepatocytes (Metcalf *et al.*, 2000; Greenhalgh *et al.*, 2002a).

It is known that IGF-1 acts to regulate pre- and post-natal growth whereas GH acts to regulate postnatal growth only, with GH receptor null mice exhibiting impaired growth from approximately 2-weeks of age (Lupu *et al.*, 2001). The occurrence of the SOCS2^{-/-} overgrowth from 3-weeks of age is consistent with the knowledge that GH activity occurs between postnatal days 20–40 (Wang *et al.*, 2004). Although no alterations to the growth plate were noted in the first description of SOCS2^{-/-} mice (Metcalf *et al.*, 2000), MacRae and colleagues found increased widths of growth plate zones in 7-week old SOCS2^{-/-} mice compared to WT and this was associated with an increased long bone length (MacRae *et al.*, 2009). They also found by μ CT analysis at 7-weeks of age that SOCS2^{-/-} mice had increased bone mass, demonstrated by increased bone volume, trabecular number and trabecular thickness but these authors reported no differences in bone mineral density between WT and SOCS2^{-/-} mice (MacRae *et al.*, 2009). This was contrary to previous findings by Lorentzon and colleagues, who found lower trabecular and cortical bone mineral density in SOCS2^{-/-} mice (at 4- and 15-weeks of age) as well as reduced cortical cross-sectional area and cortical thickness (at 4-weeks of age) (Lorentzon *et al.*, 2005). Both studies

found raised levels of osteocalcin (a marker of bone formation) in serum from SOCS2^{-/-} mice, with MacRae *et al.* also reporting elevated levels of TRAP5 (a marker of osteoclast number) (Lorentzon *et al.*, 2005; MacRae *et al.*, 2009). These results indicate an increase in bone turnover in SOCS2^{-/-} mice.

From previous studies it is clear that bones from SOCS2^{-/-} mice are longer than their WT counterparts but the cellular basis at the growth plate level have not been identified. It is also unclear what the effect of increased GH signalling has on the cortical and trabecular compartment of SOCS2^{-/-} mice. Therefore the aim of this chapter was to determine the bone phenotype and the underlying cellular basis for the increased endochondral bone growth in SOCS2^{-/-} mice. Furthermore, as the overgrowth phenotype is not obvious until 3- to 4-weeks of post-natal age it was assumed that changes in growth plate indices, bone growth rate and bone structure and geometry would not be evident until the overgrowth phenotype had occurred. This hypothesis was also examined.

4.2. Aims and Hypothesis

4.2.1. Hypothesis

Indices of bone accretion and increased linear growth will be evident within the cortical and trabecular bone compartments and the growth plate respectively of overgrowth SOCS2^{-/-} mice but not in younger SOCS2^{-/-} mice showing normal growth.

4.2.2. Aims

- Confirm the overgrowth phenotype and in particular the increased longitudinal bone growth in the colony of SOCS2^{-/-} mice used for these studies.
- Determine the cellular basis within the growth plate for the overgrowth SOCS2^{-/-} phenotype by investigating growth plate zone widths, chondrocyte proliferation and longitudinal bone growth rate at 3-weeks (pre-overgrowth) and 6-weeks of age (post-

overgrowth). Use male mice for this as they have been reported to have a more prominent overgrowth phenotype.

- Investigate trabecular and cortical bone parameters at 3- and 6-weeks of age in WT and SOCS2^{-/-} mice by μ CT analysis, again using male mice.

4.3. Materials and Methods

4.3.1. Growth Analysis

Body weights and lengths (crown to rump) were established in 5 SOCS2^{-/-} and 5 WT litters (33 WT and 40 SOCS2^{-/-} mice in total) from 2- until 7-weeks of age, as described in Section 2.3.6.

4.3.2. Analysis of Growth Plate Dynamics

6 male SOCS2^{-/-} and 6 male WT mice were used to analyse growth plate dynamics at 3- and 6-weeks of age. The mice received an i.p. injection of 10mg/ml calcein at days 18 or 39 as described in Section 2.3.9. They also received an i.p. injection of BrdU at days 22 or 43 as described in Section 2.3.10. The mice were then sacrificed on days 23 or 44 (3- and 6-weeks respectively). Both tibiae and both femurs were dissected.

One tibia was snap frozen in a hexane freezing bath and cryostat sections were cut for calcein labelling analysis, as described in Section 2.5.2. The distance between the chondro-osseous junction and the mineralising front was measured at 10 points along the whole growth plate on two sections per mouse under UV light using a Nikon Eclipse TE300 microscope.

The other tibia was fixed in 10% NBF for 24hrs then decalcified in 10% EDTA, paraffin embedded and cut as described in Section 2.5.1. Sections were analysed for BrdU labelling as described in Section 2.5.3. Sections were also analysed for zone widths by toluidine blue staining, as described in Section 5.4.2. One femur was fixed in 70% ethanol and used for μ CT analysis.

4.3.3. μ CT Analysis

One femur from each mouse used in Section 4.3.2 was fixed in 70% ethanol for micro computer tomography (μ CT) analysis. The analysis was carried out in collaboration with Dr. Rob Van't Hof at the Rheumatic Diseases Unit, The University of Edinburgh. μ CT analysis was performed using a SkyScan 1172 instrument (SkyScan, Asrtselaar, Belgium). The bones were wrapped in parafilm to retain moisture and mounted in the machines sample holder (3 bones at a time). The instrument was set at 60kV/167 μ A with a resolution of 4.9 μ m, using an Alum 0.5mm filter and rotation step of 0.6°. The camera was set to 1000x524 pixels (medium).

The images were reconstructed using the SkyScan NRecon program. Once reconstructed, a reference slice at the bottom of the growth plate was selected. This was recognised as the point where the last “bridges” of the primary spongiosa (fine bony structures) are broken. Trabecular analysis was done in the metaphysis, a section of 200 slices that was taken 50 slices down from reference slice. Cortical analysis was performed on a region of 100 slices taken 300 or 500 slices from the reference slice (for 3- or 6-week old mice respectively). Different areas were selected for cortical bone analysis as the bones were shorter at 3-weeks of age, and had been cut in half so it was not possible to take 500 slices down from the growth plate for 3-week old mice. The trabecular and cortical sections were analyzed using SkyScan CTAn software.

4.4. Results

4.4.1. SOCS2^{-/-} Growth Curves

Although the growth curves have previously been established in the line of SOCS2^{-/-} mice used for the study by MacRae *et al.* (2009), there have been genotyping problems with the line in the past and a different generation of mice is now being used. Therefore, to ensure the SOCS2^{-/-} overgrowth phenotype was maintained, it was necessary to repeat growth curves of body weight and length in WT and SOCS2^{-/-} mice. This was performed in male and female mice from 5 litters

per genotype from 2-weeks until 7-weeks of age, representing a period where the majority of growth occurs (Figure 4.2).

From 3- to 7-weeks of age there was increased weight and length change in male mice compared to female ($P < 0.001$), and in SOCS2^{-/-} mice compared to WT ($P < 0.001$). During this time period male WT mice grew on average 3.40g and 0.66cm per week compared to male SOCS2^{-/-} mice, which grew 5.24g and 0.79cm per week. Female WT mice grew on average 2.20g and 0.51cm per week, compared to female SOCS2^{-/-} mice which grew 3.03g and 0.63cm per week.

Furthermore, the relationship between weight change and sex was dependant upon genotype, with additional weight gain observed in male SOCS2^{-/-} mice compared to WT than in female mice ($P < 0.001$). These results are consistent with the knowledge that GH is the major regulator of post-natal growth in mice, where peak GH activity occurs between postnatal days 20–40 (Wang *et al.*, 2004).

4.4.2. Growth Plate Zone Widths in SOCS2^{-/-} Mice

MacRae and colleagues found that the SOCS2^{-/-} mice displayed increased widths of maturational growth plate zone at 7-weeks of age. This was extended to analyse the growth plate widths, using toluidine blue staining, in tibiae from male mice at 3-weeks and 6-weeks of age, allowing a comparison of mice before and after the overgrowth phenotype (Figure 4.3A & B).

There were no differences in zone widths between SOCS2^{-/-} and WT mice at 3-weeks of age. At 6-weeks of age, SOCS2^{-/-} mice had wider growth plates (23%; $P < 0.05$) with significantly wider proliferative and hypertrophic zones (20.7% ($P < 0.05$) and 26.4% ($P < 0.05$) respectively).

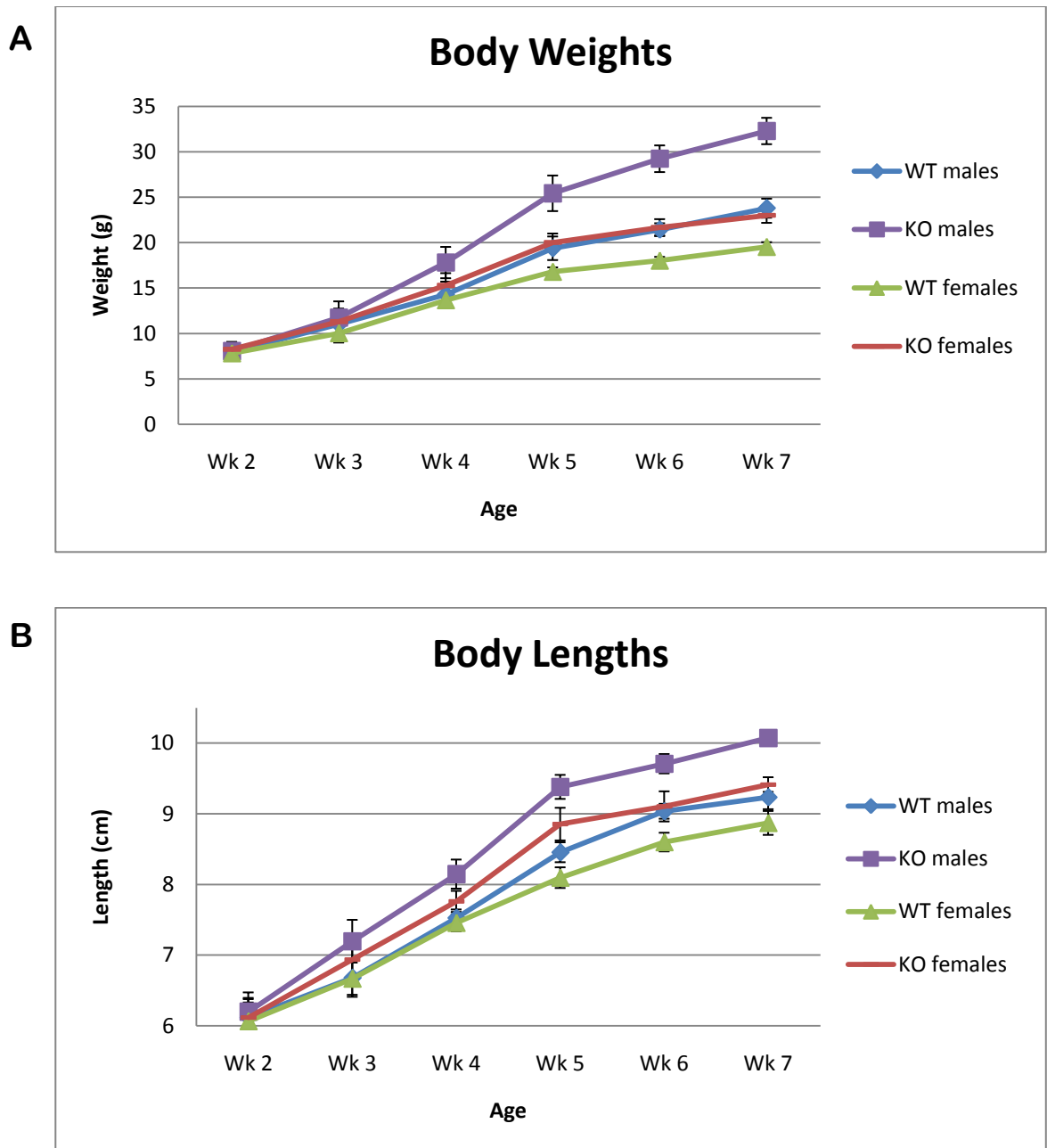


Figure 4.2. Growth curves. Growth curves of WT and $SOCS2^{-/-}$ (KO) mice from 2- until 7-weeks (Wk) of age. (A) Increased weight change in male compared to female mice ($P < 0.001$) and in $SOCS2^{-/-}$ compared to WT mice ($P < 0.001$), with the relationship between weight and sex dependant on genotype ($P < 0.001$). (B) Increased body length in male mice compared to female ($P < 0.001$) and in $SOCS2^{-/-}$ mice compared to WT mice ($P < 0.001$), but with no additive effect of sex and genotype ($P = 0.9$). Results are from 5 litters per group, expressed as mean \pm SEM. Data was analysed by linear mixed-effect model (see Section 2.9).

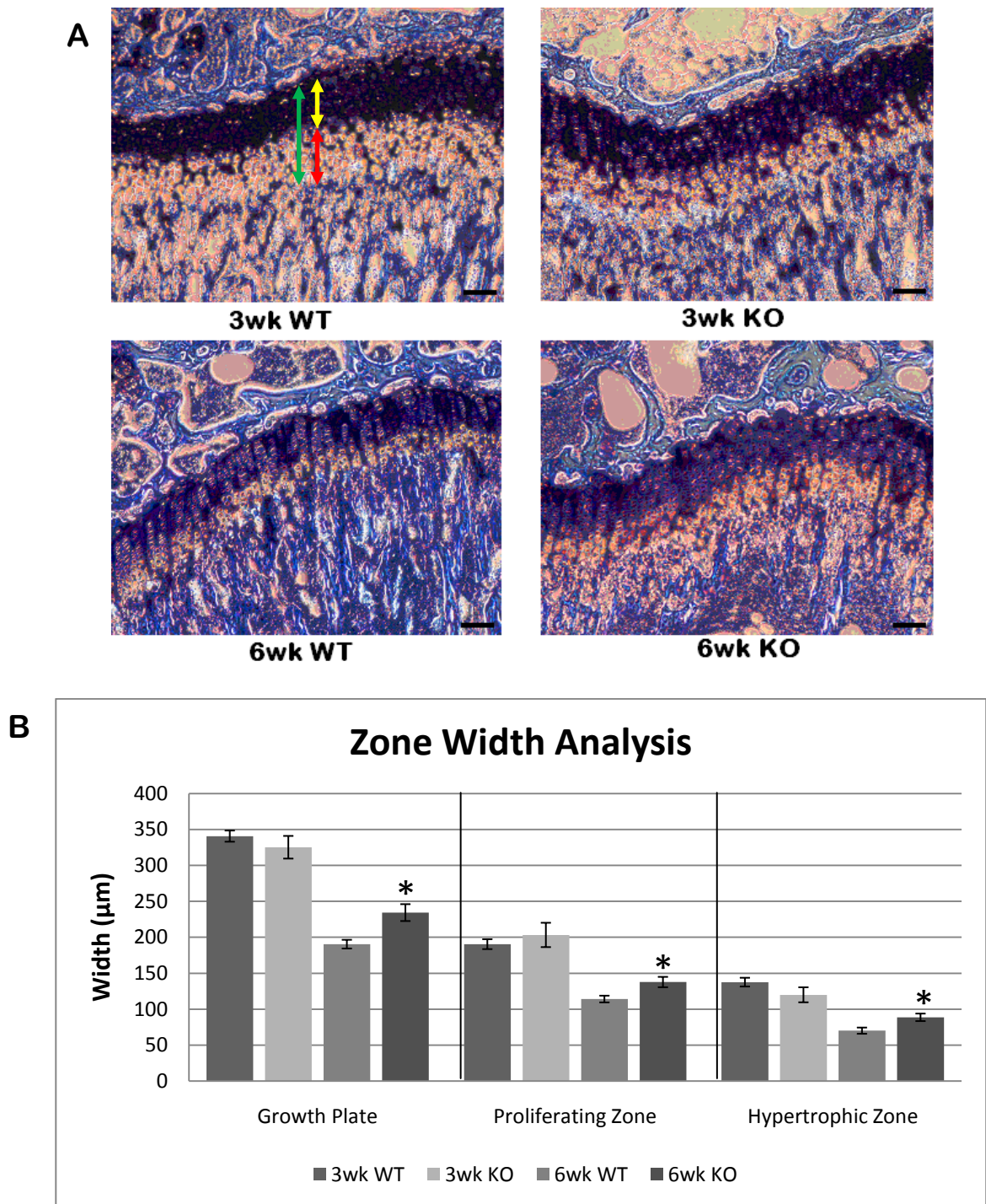


Figure 4.3. Toluidine blue stained growth plate sections from 3wk and 6wk old mice. Analysis of growth plate zone widths in tibiae from 3-week (3wk) and 6-week (6wk) old male WT and SOCS2^{-/-} (KO) mice. (A) Paraffin embedded sections were stained with toluidine blue to allow measurement of zone widths. Arrows show examples of total growth plate width (green), proliferating zone width (yellow) and hypertrophic zone width (red). Scale bars = 100 μm . (B) Graph of results of growth plate zone widths, expressed as mean \pm SEM for 2 sections per mouse (n=6); * P<0.05 compared to 6-week WT.

4.4.3. Chondrocyte Proliferation in SOCS2^{-/-} Mice

It is likely that the increased zone widths observed at 6-weeks in Figure 4.3 are as a result of increased chondrocyte proliferation in the SOCS2^{-/-} growth plates. Given the role of SOCS2 in inhibiting GH signalling it is expected that the SOCS2^{-/-} mice exhibit increased STAT signalling, leading to increased chondrocyte proliferation. This would contribute to the overgrowth phenotype observed in the SOCS2^{-/-} mice. Cell proliferation within the growth plate was assessed by analysing BrdU labelling of proliferating chondrocytes in the male 3-week and 6-week old mice used previously for Section 4.4.2 (Figure 4.4).

At 3-weeks the number of proliferating chondrocytes in the growth plate was the same in WT and SOCS2^{-/-} mice. Chondrocyte proliferation decreased with age but was significantly higher (26.9%; P=0.001) in the 6-week old SOCS2^{-/-} mice compared to the similarly aged WT mice (Figure 4.4).

4.4.4. SOCS2^{-/-} Endochondral Growth Rate

The observed increased length in SOCS2^{-/-} mice from 3-weeks of age is likely to be the result of increased endochondral growth rate, as a result of increased cell proliferation as shown in 4.4.3. To confirm this, mineral apposition rate of endochondral growth was measured by analysing calcein labelling in tibiae from the 3-week and 6-week old male mice (Figure 4.5).

At 3-weeks of age there was no difference in the mineral apposition rate between WT and SOCS2^{-/-} mice, whereas by 6-weeks SOCS2^{-/-} mice displayed a significant increase in growth rate (26.98%; P<0.05) (Figure 4.5B).

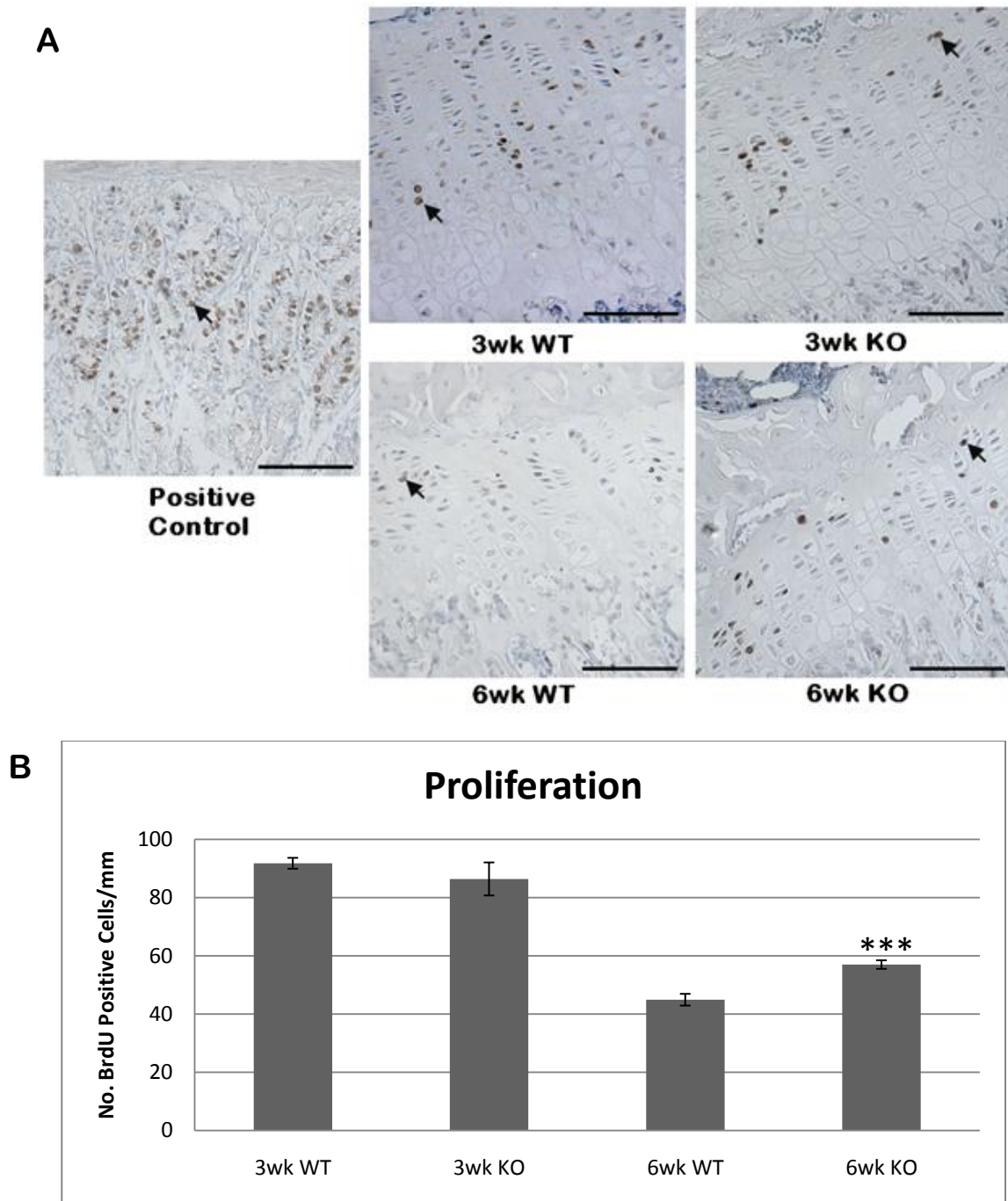


Figure 4.4. BrdU labelling in 3- and 6-week old mice Measurement of chondrocyte proliferation in tibiae from 3-week (3wk) and 6-week (6wk) old WT and SOCS2^{-/-} (KO) male mice by BrdU uptake. (A) Decalcified paraffin embedded sections showing proliferating cells labelled brown for BrdU and counterstained with haematoxylin. Examples are shown for WT and SOCS2^{-/-} mice at 3- and 6-weeks of age, and a positive control section from mouse small intestine. Positive staining is indicated by black arrows. Scale bars = 100µm. (B) Quantification of proliferating cells expressed as number of BrdU positive cells per mm of the growth plate length. Analysis was performed on 2 sections per mouse (n=6). Data are expressed as mean±SEM; ***P<0.001 compared to 6-week old WT.

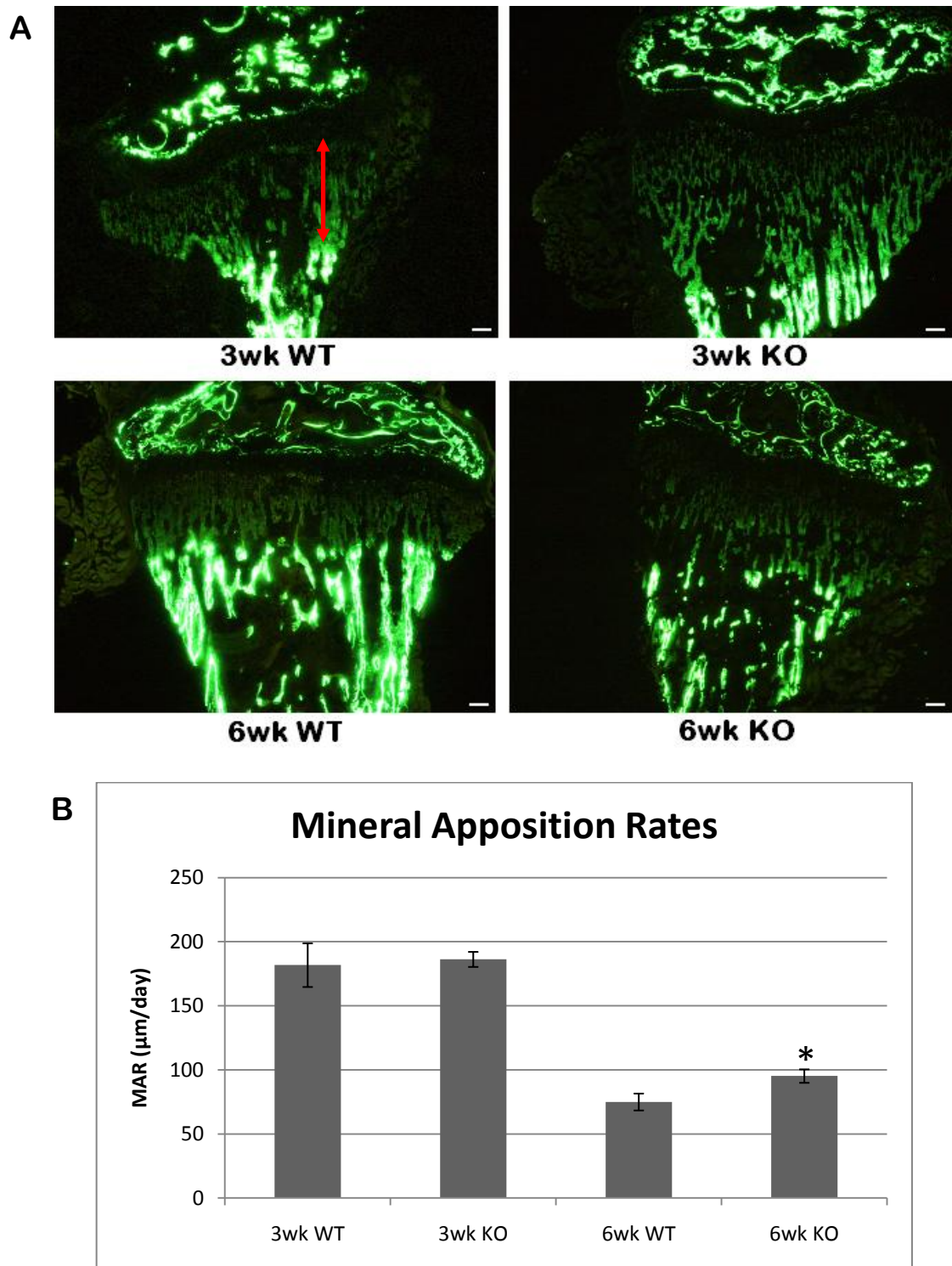


Figure 4.5. Calcein labelling in 3- and 6-week old mice. Measurement of endochondral mineral apposition rate in tibiae from 3-week (3wk) and 6-week (6wk) old male WT and SOCS2^{-/-} (KO) mice by calcein labelling. (A) Sections showing calcein labelling of mineralised trabecular bone in frozen tibia sections. Examples are shown for WT and SOCS2^{-/-} mice at 3- and 6-weeks of age. Daily mineral apposition rate was calculated by measuring the distance from the chondro-osseous junction to the calcein labelled mineralisation front, as indicated by the red arrow, and dividing by the number of days from calcein injection to cull (4 days). Scale bars = 100μm. (B) Graph of results of mineral apposition rates (MAR), expressed as mean±SEM for 2 sections per mouse (n=6); * P<0.05 compared to 6-week old WT.

4.4.5. μ CT Analysis of SOCS2^{-/-} Mice

Femurs from the 3-week and 6-week old male WT and SOCS2^{-/-} mice were analysed by μ CT. Previously the SOCS2^{-/-} mice have been shown to have increased trabecular bone volume, number, and thickness at 7-weeks of age, with an increase in structural model index indicating a more 'plate-like' structure to the trabeculae and no change in BMD (MacRae *et al.*, 2009). This was coupled with increased cortical bone area, again with no change in cortical BMD and no change in cortical thickness (MacRae *et al.*, 2009). These results are consistent with higher bone mass and increased resistance to bending, consistent with increased GH signalling on the skeleton (MacRae *et al.*, 2009). However, though consistent with the SOCS2^{-/-} phenotype, these results contradicted those of Lorentzon *et al.* (2005) who found a decrease in cortical and trabecular BMD, cortical thickness and cortical bone area (these latter two results were found at 4-weeks but not at 15-weeks of age).

Therefore it was necessary to firstly confirm the findings by MacRae *et al.*, and also to compare 3-week old and 6-week old mice, again expecting no changes in bone architecture and geometry at 3-weeks of age with significant increase in bone volume by 6-weeks of age. μ CT analysis was performed on femurs and the results obtained are shown in Table 4.1 and Figure 4.6.

At 3-weeks of age there was no difference in any of the parameters measured for trabecular or cortical bone. In 6-week old mice, there was an increase in trabecular tissue volume and trabecular tissue surface ($P < 0.05$), with no differences observed in the cortical parameters.

Parameter	3wk WT Mice	3wk KO Mice	6wk WT Mice	6wk KO Mice
Trabecular Analysis				
Tissue Volume (x10 ⁵ μm ³)	11600 ± 451	13200 ± 813	284 ± 7.19	351 ± 1.50 *
Bone Volume (x10 ⁵ μm ³)	1210 ± 158	1230 ± 105	27.6 ± 2.75	27.9 ± 3.90
Percent Bone Volume (% BV/TV)	10.4 ± 1.20	9.31 ± 0.464	9.66 ± 0.881	7.88 ± 0.873
Tissue Surface (x10 ⁴ μm ²)	772 ± 21.6	835 ± 43.2	59.0 ± 1.13	68.7 ± 2.32 *
Bone Surface (x10 ⁵ μm ²)	138 ± 16.4	135 ± 95.2	12.3 ± 1.17	12.6 ± 1.32
Intersection Surface (x10 ³ μm ²)	660 ± 80.3	657 ± 65.3	19.8 ± 1.94	17.0 ± 1.66
Bone Surface/Volume Ratio (x10 ⁻³ 1/μm)	115 ± 1.36	112 ± 5.53	448 ± 14.1	461 ± 26.3
Bone Surface Density (x10 ⁻⁴ 1/μm)	119 ± 12.6	104 ± 6.75	431 ± 36.0	356 ± 26.1
Trabecular Thickness (μm)	34.2 ± 0.238	36.1 ± 1.86	7.74 ± 0.192	7.55 ± 0.345
Trabecular Separation (μm)	230 ± 14.8	274 ± 14.2	65.6 ± 3.75	76.2 ± 3.90
Trabecular Number (x10 ⁻⁴ 1/μm)	30.3 ± 3.32	26.2 ± 1.84	125 ± 11.59	104 ± 8.18
Trabecular Pattern Factor (x10 ⁻³ 1/μm)	27.6 ± 1.84	27.9 ± 1.92	199 ± 9.68	32.9 ± 24.0
Structure Model Index (x10 ⁻²)	182 ± 5.45	188 ± 5.80	63.5 ± 11.4	66.3 ± 26.3
Degree of Anisotropy (x10 ⁻²)			168 ± 7.32	171 ± 9.53
Cortical Analysis				
Tissue Volume (x10 ⁷ μm ³)	53.9 ± 3.21	54.1 ± 4.87	79.1 ± 3.19	82.3 ± 7.46
Bone Volume (x10 ⁷ μm ³)	19.3 ± 1.35	20.5 ± 1.52	38.2 ± 1.51	41.2 ± 3.75
Percent Bone Volume (% BV/TV)	35.8 ± 0.546	38.3 ± 1.11	48.4 ± 1.46	50.7 ± 3.76
Tissue Surface (x10 ⁵ μm ²)	68.9 ± 2.37	70.9 ± 3.43	87.2 ± 2.06	90.4 ± 3.67
Bone Surface (x10 ⁵ μm ²)	58.2 ± 2.92	60.6 ± 1.90	75.6 ± 2.33	78.1 ± 2.94
Intersection Surface (x10 ⁴ μm ²)	72.6 ± 5.69	78.5 ± 6.03	152 ± 5.95	166 ± 15.9
Bone Surface/Volume Ratio (x10 ⁻³ 1/μm)	30.4 ± 1.39	30.1 ± 1.51	20.0 ± 1.05	19.4 ± 1.28
Bone Surface Density (x10 ⁻⁴ 1/μm)	109 ± 3.88	115 ± 7.07	96.1 ± 3.56	97.4 ± 7.50

Table 4.1. μCT analysis of 3- and 6-week old mice. μCT analysis of trabecular and cortical bone parameters in femurs from 3-week (3wk) and 6-week (6wk) old male WT and SOCS2^{-/-} (KO) mice. Data are expressed as mean ± SEM (n=6 for 3-week KO and WT; n=6 for 6-week WT, n=5 for 6-week KO). * = P<0.05 compared to 6-week old WT.

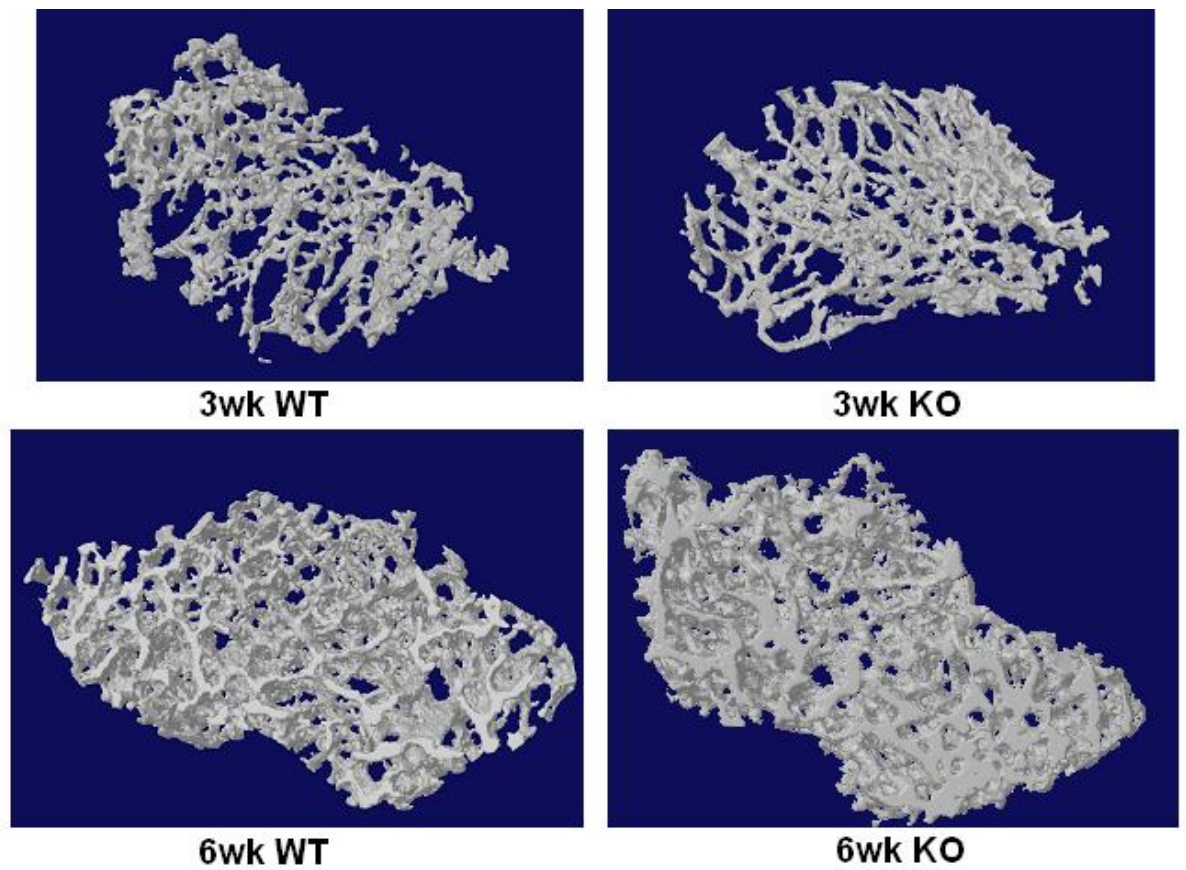


Figure 4.6. μ CT analysis of 3- and 6-week old mice. Examples of 3D reconstruction images gained for trabecular bone in 3-week (3wk) and 6-week (6wk) old male WT and SOCS2^{-/-} (KO) mice.

4.5. Discussion

The SOCS2^{-/-} overgrowth phenotype was confirmed in this study, with SOCS2^{-/-} mice displaying increased growth from 3-weeks of age as demonstrated by increased body weight and body length compared to WT. By the end of the study period (7-weeks of age), SOCS2^{-/-} male mice were 35% larger than WT males while SOCS2^{-/-} females were 18% larger than WT females (a similar size to WT males), consistent with previous findings (Metcalf *et al.*, 2000; MacRae *et al.*, 2009). This confirmed that the mice used in this study and throughout the work of this thesis were exhibiting the SOCS2^{-/-} phenotype as expected.

The increased growth of SOCS2^{-/-} mice from 3-weeks of age is demonstrated by increased body length, with longer longitudinal bones (Metcalf *et al.*, 2000; MacRae *et al.*, 2009). It has previously been shown that the growth plates of SOCS2^{-/-} mice have increased maturational zone widths compared to WT mice at 7-weeks of age (MacRae *et al.*, 2007a). This has been confirmed and extended in this study by investigating growth plate phenotypes of male mice at 3-weeks and 6-weeks of age, therefore looking for changes before and after the start of the increased growth rate in SOCS2^{-/-} mice. The widths of the tibia growth plate maturational zones (total growth plate width, proliferating zone and hypertrophic zone) were found to be the same in WT and SOCS2^{-/-} mice at 3-weeks of age. By 6-weeks of age, all maturational zones were significantly wider in SOCS2^{-/-} mice compared with those from WT mice which is consistent with findings by MacRae *et al.* (2005). Growth plates become narrower with increasing age in association with decreased chondrocyte proliferation, with the growth plate closing in many species, but not rodents, once adult size has been reached (Kember and Sissons, 1976; Nilsson *et al.*, 2005). The wider growth plate zones observed in SOCS2^{-/-} mice are therefore indicative of a higher rate of endochondral bone growth and greater levels of proliferation.

To investigate this further, growth plate proliferation levels were analysed in tibiae from 3- and 6-week old male WT and SOCS2^{-/-} mice by BrdU uptake and chondrocyte labelling. Again no

difference was observed between the two genotypes at 3-weeks of age, but SOCS2^{-/-} 6-week old mice had higher levels of proliferating chondrocytes than WT. This is consistent with the zone widths, and is likely to lead to the increased growth of long bones from 3-weeks of age. Previous studies have shown a positive correlation between growth rate and chondrocyte proliferation, with increased proliferative cell cycle time and cell number associated with higher growth rate (Kember, 1985; Farnum and Wilsman, 1993; Wilsman *et al.*, 1996a). Growth rate is, however, not only determined by proliferation but also by matrix synthesis and hypertrophic cell size (Hunziker *et al.*, 1987; Breur *et al.*, 1991; Wilsman *et al.*, 1996b). To investigate if growth rate was altered in SOCS2^{-/-} mice, the rate of endochondral growth (the mineral apposition rate) was measured in tibiae using calcein labelling. At 3-weeks of age, male WT and SOCS2^{-/-} mice showed the same growth rate, but by 6-weeks of age male SOCS2^{-/-} mice had a significantly higher mineral apposition rate than male WT mice. This is consistent with the increased levels of chondrocyte proliferation and increased growth plate zone widths at this age, and will result in the observed high growth of SOCS2^{-/-} mice from weaning. Previous studies have found mineral apposition rate is reduced during conditions that inhibit bone growth (Altman *et al.*, 1992; Owen *et al.*, 2009), consistent with the increased bone growth in SOCS2^{-/-} mice causing raised mineral apposition rate.

SOCS2 is known to act by inhibiting GH signalling, particularly through STAT5 (Greenhalgh *et al.*, 2002a). GH signalling through the JAK/STAT pathway leads to downstream IGF-1 signalling, and in chondrocytes IGF-1 acts to stimulate proliferation (Isaksson *et al.*, 1982; Wang *et al.*, 1999). It therefore seems likely that in SOCS2^{-/-} mice there is increased local GH signalling through STAT proteins from around 3-weeks of age, leading to increased production of IGF-1 and raised levels of proliferation. This hypothesis is consistent with the findings above, and is further investigated in subsequent chapters of this thesis.

GH is known to be anabolic for bone (Ohlsson *et al.*, 1998; Andreassen and Oxlund, 2001) and therefore the increased GH signalling in SOCS2^{-/-} mice would be expected to alter cancellous bone architecture (trabecular bone) and cortical bone geometry. Previous studies by Lorentzon *et al.* used DXA (Dual-emission X-ray absorptiometry) and pQCT (peripheral quantitative computed tomography) to analyse bone mineral density, and found a decrease in SOCS2^{-/-} mice compared to WT at 4- and 15-weeks of age (Lorentzon *et al.*, 2005). They also showed decreased cortical bone area and thickness in 4-weeks old, but not 15-weeks old, SOCS2^{-/-} mice (Lorentzon *et al.*, 2005). However MacRae *et al.* have recently used μ CT analysis to show an increase in bone volume, trabecular number, trabecular thickness and trabecular separation in trabecular bone in 7-week old SOCS2^{-/-} mice, coupled with increased cortical bone volume, tissue area and mean polar moment of inertias (MacRae *et al.*, 2009). They saw no difference in bone mineral density, and their findings are more consistent with increased GH/IGF-1 signalling in the absence of SOCS2. In this study, μ CT analysis was performed on male 3- and 6-week old mice to analyse bone parameters before and after the SOCS2^{-/-} gigantism. At 3-weeks of age, there was no difference in any parameters of trabecular or cortical bone analysis, as expected. SOCS2^{-/-} mice exhibited increased trabecular tissue volume and tissue surface at 6-weeks of age compared to WT. Increased tissue volume is consistent with the findings by MacRae *et al.* and with increased GH/IGF-1 signalling, however this study did not find the increased bone volume, trabecular number, trabecular thickness or trabecular separation. Nor were there any differences in cortical bone parameters. The reasons for the discrepancy in results between the results of this study and that of MacRae *et al.* (2009) are not immediately clear. There we're however a number of differences between the studies that could have contributed to the different results obtained. Firstly, there was a lot of variation between samples observed in this study, which probably masked the strength of some results. Secondly, the mice used in this study were a week younger than in the study by MacRae and colleagues and they used female mice whereas male mice were used here due to their more significant overgrowth phenotype (and by Lorentzon *et al.* 2005).

Thirdly, analysis was done on femurs in this study as opposed to tibiae in the MacRae study, and the loading in these two bones is likely to be different which may cause different results (MacRae *et al.*, 2009; Huesa *et al.*, 2011). It is possible that by 6-weeks of age the trabecular and cortical bone have not changed as dramatically as by 7-weeks in the SOCS2^{-/-} mice. The increased tissue volume and tissue surface are consistent with increased trabecular bone but these parameter changes would be expected to be coupled with increased bone volume. Unfortunately, it was not possible to measure bone mineral density in this study as density phantoms were not available for use. Clearly it would be worthwhile performing a larger study of μ CT analysis with both tibiae and femurs from adult WT and SOCS2^{-/-} mice, both female and male, to fully establish the bone parameters.

4.6. Conclusion

SOCS2^{-/-} mice display an overgrowth phenotype that occurs from 3- to 4-weeks of age and is coupled with increased size of longitudinal bones. The increased longitudinal growth of SOCS2^{-/-} mice is the result of raised levels of chondrocyte proliferation, wider growth plate zone and subsequent higher rates of endochondral growth. The signalling pathways responsible for these altered growth plate parameters are likely to involve the GH/IGF-1 signalling cascade and this is investigated in Chapter 5.

CHAPTER 5

THE EFFECTS OF SOCS2 ON GH SIGNALLING THROUGH STAT PROTEINS IN CHONDROCYTES

5. The Effects of SOCS2 on GH Signalling through STAT Proteins in Chondrocytes

5.1. Introduction

GH signalling is known to be important for regulating post-natal endochondral bone growth, with GH deficiency resulting in growth retardation and excessive GH resulting in gigantism (Cuttler *et al.*, 1989; Lupu *et al.*, 2001). GH is thought to promote longitudinal growth through GHR signalling via the JAK/STAT pathway, which can lead to direct growth promoting actions or indirect production of IGF-1, with its consequential signalling cascades promoting chondrocyte proliferation and hypertrophy (Nilsson *et al.*, 2005). While the liver is recognised as a key target organ of GH signalling, leading to increased circulating IGF-1 and subsequent growth promotion, GH is known to also act locally on other tissues, including bone (Isaksson *et al.*, 1982; Green *et al.*, 1985; Spencer *et al.*, 1991). Upon binding its receptor GH can signal through a variety of pathways (Figure 3.5, Chapter 3), however the most recognised is JAK/STAT signalling whereby JAK2 activation leads to STAT phosphorylation, resulting in downstream transcription of target genes, including IGF-1 (Herrington *et al.*, 2000). GH is capable of signalling through STAT1, STAT5 and STAT3 proteins (Waters *et al.*, 2006; Brooks *et al.*, 2008). Gevers *et al.* have demonstrated both *in vitro* and *in vivo* that GH signals through STAT5 in the growth plate (Gevers *et al.*, 2009). In Chapter 3, GH was found to activate STAT1 and STAT3, in addition to STAT5, in both ATDC5 cells and primary chondrocytes.

SOCS2 is known to negatively regulate growth by inhibiting GH signalling through the JAK/STAT pathway, with the SOCS2^{-/-} mouse exhibiting an overgrowth phenotype from 3-weeks of age that is coupled with increased longitudinal growth (Metcalf *et al.*, 2000; Rico-Bautista *et al.*, 2006). In Chapter 4 the growth plate phenotype of SOCS2^{-/-} mice was investigated, determining that the increased longitudinal growth observed in SOCS2^{-/-} mice is associated with increased chondrocyte

proliferation and wider growth plate zone widths, resulting in a greater endochondral growth rate. Postnatal IGF-1 signalling is considered to be largely GH dependant, and as IGF-1 is known to increase chondrocyte proliferation it seems likely that the observed increased chondrocyte proliferation in the absence of SOCS2 could be the result of raised GH signalling through the JAK/STAT pathway leading to increased levels of local IGF-1 (Hoshi *et al.*, 2004; Klammt *et al.*, 2008). This would suggest that physiologically SOCS2 acts to negatively regulate growth plate GH signalling, and that SOCS2 may be implicated in growth disorders that result in short stature.

Of interest, it has been found that mice over-expressing SOCS2 do not exhibit stunted growth but in fact have an overgrowth phenotype also, with males growing to be 13-15% larger than WT (Greenhalgh *et al.*, 2002b; Turnley, 2005). It seems that the effects of SOCS2 on GH signalling are dose dependant, and it has been proposed that SOCS2 normally acts to inhibit GH signalling but at higher doses can inhibit signalling of other SOCS proteins; SOCS3 and SOCS1, that are more potent GH inhibitors (Favre *et al.*, 1999; Greenhalgh *et al.*, 2002b; Turnley, 2005). Given the findings in Chapter 3 that neither SOCS1 nor SOCS3 are expressed by chondrocytes in response to GH, increased levels of SOCS2 in chondrocytes may act to inhibit GH signalling and STAT phosphorylation.

5.2. Aims and Hypothesis

5.2.1. Hypothesis

SOCS2 acts to negatively regulate GH signalling through the JAK/STAT pathway, and the overgrowth phenotype in the SOCS2^{-/-} mice is the result of increased chondrocyte GH signalling through STAT proteins leading to raised levels of IGF-1. Increased levels of SOCS2 in chondrocytes will result in diminished STAT phosphorylation in response to GH.

5.2.2. Aims

- Compare temporal STAT phosphorylation in response to GH in primary chondrocytes isolated from WT and SOCS2^{-/-} mice
- Generate a line of ATDC5 cells over-expressing SOCS2 and use these chondrocytes to compare temporal STAT phosphorylation in response to GH in chondrocytes over-expressing SOCS2 with normal ATDC5 cells
- Investigate *in vivo* STAT phosphorylation in growth plates from SOCS2^{-/-} mice compared to WT mice at 6-weeks of age (post-overgrowth)
- Analyse and compare expression levels of IGF-1 in primary chondrocytes from WT and SOCS2^{-/-} mice

5.3. Materials and Methods

5.3.1. Cell Culture

Primary chondrocytes were isolated from 1- to 3-day old WT or SOCS2^{-/-} mice as described in Section 2.3.7. SOCS2^{-/-} were previously generated as described in Section 2.3.2. All parents of litters used were genotyped as described in Sections 2.3.3, 2.3.4 and 2.3.5 to ensure litters used were the correct genotype. ATDC5 cells were cultured as described in Section 2.2.1. ATDC5 cells over-expressing SOCS2 were generated as described in Section 2.6. Cells were cultured in 6-well plates in differentiation medium (ATDC5 cells) or primary chondrocyte medium (primary cells). Temporal expression of STAT and SOCS proteins was investigated by challenging cells with GH (500ng/ml) at intervals from 15mins to 240mins. Cells were serum deprived for 24hrs prior to challenge with GH.

5.3.2. Western Blotting

Cells were cultured as described in Section 5.3.1 and scraped for protein analysis as described in Section 2.8.1. Western blotting was performed as described in Sections 2.8.2 and 2.8.3. Antibodies used are detailed in Table 2.4.

5.3.3. PhosphoSTAT5 Immunohistochemistry

Femurs from 5 male SOCS2^{-/-} and 5 WT mice at 6-weeks of age were used to analyse phosphorylated STAT5 in the growth plate. The femurs were fixed in 75% ethanol/5% acetic acid for 24hrs, then decalcified in 10% EDTA, paraffin embedded and sections cut as described in Section 2.5.1. Sections were analysed for phosphorylated STAT5 expression by immunohistochemistry as described in Section 2.5.6.

5.3.4. qPCR

RNA was extracted as described in Section 2.7.1 from freshly isolated primary chondrocytes from 1- to 3-day old WT or SOCS2^{-/-} mice as described in Section 2.3.2. For 6-week old mice, the growth plate and surrounding perichondrium were dissected from tibias and stored in RNA later (Qiagen). They were then homogenised using a hand homogenizer (IKA-Werke) and RNA extracted as described in Section 2.7.1. Samples were reverse transcribed as described in Section 2.7.2. qPCR was performed using primers for 18S (housekeeping gene) and IGF-1 as described in Section 2.7.4. Details of primers used are in Table 2.3.

5.4. Results

5.4.1. Temporal STAT Phosphorylation in SOCS2^{-/-} Chondrocytes in Response to GH

Prolonged STAT5 signalling in response to GH has been reported in SOCS2^{-/-} hepatocytes (Greenhalgh *et al.*, 2002a), confirming that SOCS2 acts to negatively regulate GH signalling. The increased longitudinal growth observed in SOCS2^{-/-} and greater chondrocyte proliferation

(Chapter 4) is likely to be due to increased or prolonged STAT activation by GH in chondrocytes. To test this hypothesis, the effects of GH on phosphorylation of STAT1, STAT3 and STAT5 in primary chondrocytes from WT and SOCS2^{-/-} mice was analysed over a 15mins to 240mins time course (Figure 5.1). This extended the studies in Chapter 3, which showed activation of STAT1, STAT3 and STAT5 in chondrocytes from Swiss mice after 15mins stimulation.

In chondrocytes from WT mice the activation of STAT1, STAT3, and STAT5 were increased after 15mins GH treatment, with an effect still observed after 60mins GH exposure. No activation of STAT signalling was noted after 2 and 4hrs GH incubation. A similar temporal response was also observed in chondrocytes from SOCS2^{-/-} mice. However, the phosphorylation status of all 3 STAT proteins, in comparison to WT cells, was both increased and in the case of STAT5 also prolonged where STAT5 activation was still evident after 4hrs GH treatment.

5.4.2. Temporal Expression of SOCS1 and SOCS3 in SOCS2^{-/-} Chondrocytes in Response to GH

While chondrocytes from SOCS2^{-/-} mice displayed enhance STAT activation by GH in comparison to WT mice there was still an obvious decrease with prolonged GH stimulation (Figure 5.1). Although it was found that neither SOCS1 nor SOCS3 were activated by GH in chondrocytes (Figure 3.8), it is possible that in the absence of SOCS2 one or both of these other GH inhibiting SOCS proteins may be responsible for this eventual decrease in STAT activation. Therefore the expression of both SOCS1 and SOCS3 were examined in primary chondrocytes stimulated with GH over a 15mins to 240mins time course, as in Section 5.4.1 (Figure 5.2).

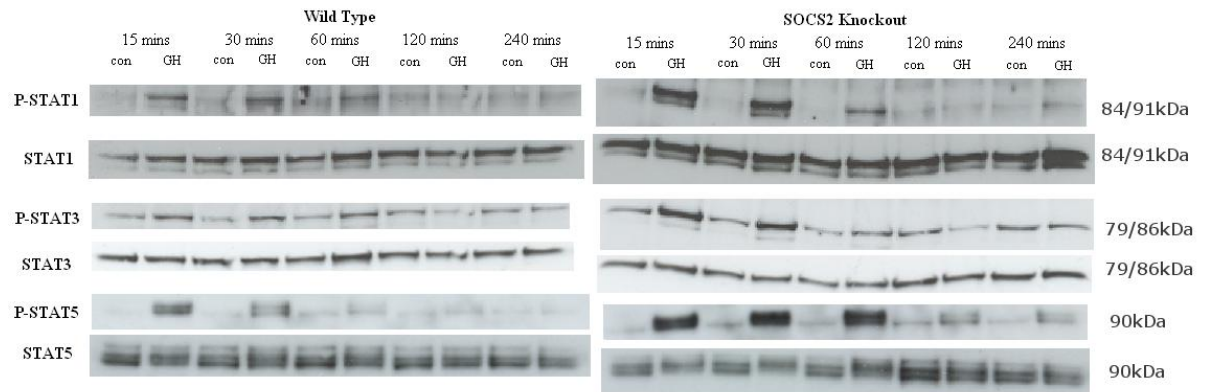


Figure 5.1. Temporal STAT signalling. Western blot analysis of phosphorylated (P-) STAT1, STAT3 and STAT5 in WT and SOCS2^{-/-} chondrocytes challenged with GH (500ng/ml) for up to 240mins. Total STAT proteins are also shown as loading controls. Where two bands are present, these represent the two subunits of the STAT protein.

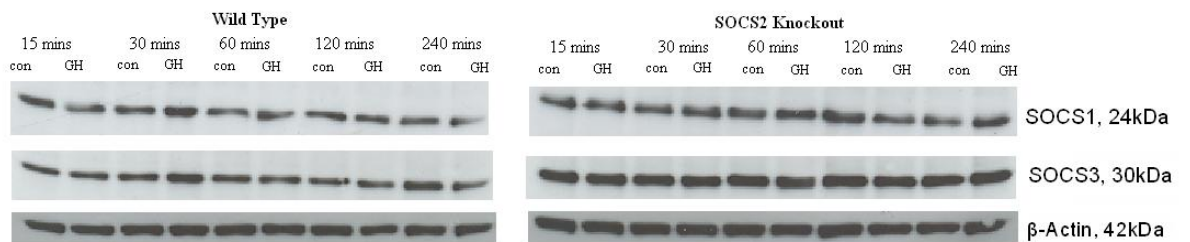


Figure 5.2. Temporal SOCS1 and SOCS3 expression. Western blot analysis of SOCS1 and SOCS3 in WT and SOCS2^{-/-} chondrocytes challenged with GH (500ng/ml) for up to 240mins. β-Actin is shown as a loading control.

The expression of both SOCS1 and 3 by SOCS2^{-/-} cells did not change over the time course that showed a significant decrease in STAT activation with prolonged GH stimulation. Although, SOCS3 expression appeared to be increased in SOCS2 null cells, this expression was not altered by GH stimulation. This shows that the reduction in STAT activation in chondrocytes from SOCS2^{-/-} mice following prolonged GH stimulation decrease was not due to a temporal increase in expression of SOCS1 or SOCS3.

5.4.3. The Effect of SOCS2 Over-Expression on STAT Signalling in Response to GH

To further confirm the negative role of SOCS2 on GH signalling in chondrocytes, ATDC5 cells over-expressing SOCS2 were produced. A western blot was completed to confirm the increased SOCS2 expression in cells containing the SOCS2 over-expression plasmid compared to cells transfected with the control plasmid (Figure 5.3). The cells were then analysed for expression of phosphorylated STAT1, STAT3 and STAT5 in response to GH over a 15mins to 120mins period (Figure 5.4), encompassing the peak and decline of STAT signalling observed in WT chondrocytes in Figure 5.1.

Cells expressing the control plasmid showed an increase in phosphorylation of STAT1, STAT3 and STAT5 over a 15mins to 60mins period of GH exposure, similar to the response seen in primary WT growth plate chondrocytes. Phosphorylation of STAT1, STAT3 and STAT5 did not respond to GH treatment at any time point in cells over-expressing SOCS2. This confirms that in growth plate chondrocytes SOCS2 acts to negatively regulate GH signalling through STAT proteins.



Figure 5.3. SOCS2 over-expression cells. Western blot showing increased expression of SOCS2 protein in ATDC5 cells containing the SOCS2 over-expression plasmid (SOCS2+) compared to cells containing the control plasmid (con). The extra SOCS2 produced in over-expression cells is a higher weight than physiological SOCS2 as it is attached to a FLAG epitope.

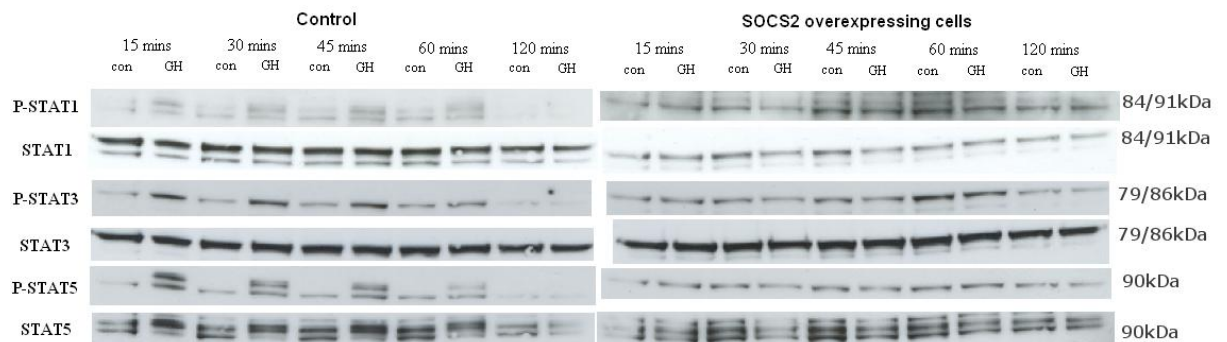


Figure 5.4. STAT expression in SOCS2 over-expressing cells. Western blot analysis of expression of phosphorylated (P-) STAT1, STAT3 and STAT5 in control and SOCS2 over-expressing ATDC5 cells in response to GH (500ng/ml) for up to 120mins. Total STAT proteins are also shown as loading controls. Where two bands are present, these represent the two subunits of the STAT protein.

5.4.4. Immunohistochemistry of Phosphorylated STAT5 in the Growth Plate

In Section 5.4.1 chondrocytes from SOCS2^{-/-} mice when maintained *in vitro* exhibited enhanced STAT signalling in response to GH, with increased and prolonged activation observed for STAT5. To extend these findings, growth plate chondrocyte STAT5 activation *in vivo* was analysed by immunohistochemistry in femurs from 6-week old WT and SOCS2^{-/-} mice (Figure 5.5). By this age the gigantism phenotype of SOCS2^{-/-} mice is established.

Detectable phosphorylated STAT5 staining (brown) was seen in all zones of the growth plate, with stronger staining in resting and proliferating chondrocytes. Although these zones contained the highest number of positively stained cells, there was no difference in the number of STAT5 positively stained cells in the proliferating zone of WT and SOCS2^{-/-} growth plates. In contrast, quantification of the number of positively stained cells (taken as a percentage of total cells) revealed that more hypertrophic cells expressed phosphorylated STAT5 in SOCS2^{-/-} mice compared to WT (P<0.001).

5.4.5. IGF-1 Expression in Primary Chondrocytes

GH signalling through STAT proteins is known to lead to IGF-1 transcription and chondrocyte proliferation (Nilsson *et al.*, 1986; Nilsson *et al.*, 2005). Therefore the increased STAT signalling observed in SOCS2^{-/-} chondrocytes is likely to lead to increased IGF-1 expression in chondrocytes and explain the greater growth rate noted in SOCS2^{-/-} bones (Figure 4.5; Chapter 4). In an attempt to directly determine if IGF-1 expression was increased in growth plate chondrocyte of SOCS2^{-/-} mice, growth plates dissected from tibiae of 6-week old WT and SOCS2^{-/-} were used to analyse IGF-1 mRNA expression by chondrocytes. Unfortunately, inadequate amount of chondrocyte specific RNA could be extracted from the thinning growth plates in the 6-week old animals. Therefore, IGF-1 mRNA expression was analysed in chondrocytes isolated from 1- to 3-day old WT and SOCS2^{-/-} mice (Figure 5.6).

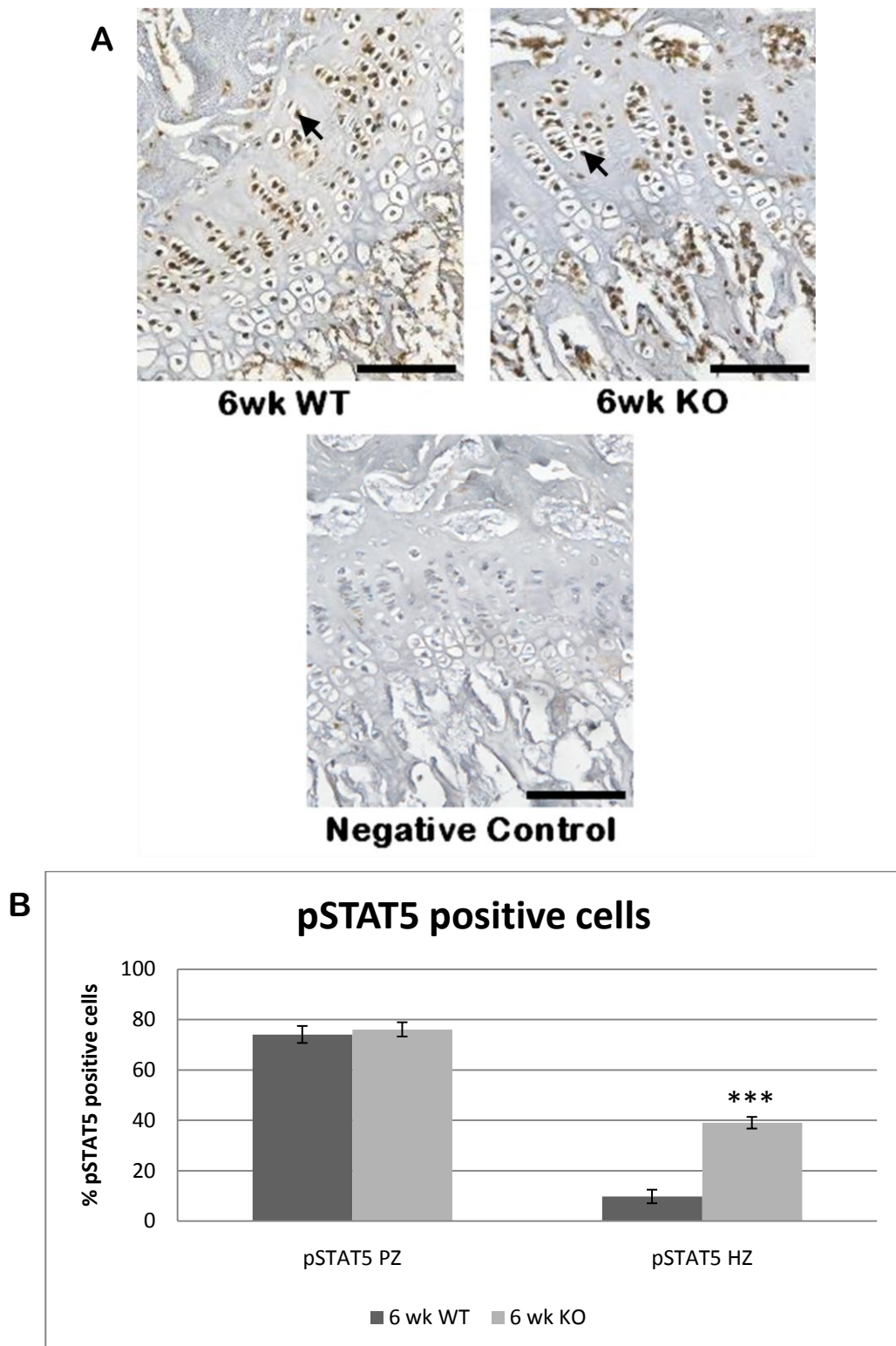


Figure 5.5. Phosphorylated STAT5 immunohistochemistry. Analysis of phosphorylated STAT5 in growth plates of femurs from 6-week (6wk) old WT and $SOCS2^{-/-}$ (KO) mice. (A) Decalcified paraffin embedded sections showing phosphorylated STAT5 staining (brown) and counterstained with haematoxylin. Examples are shown for WT and $SOCS2^{-/-}$ mice and a negative control. Black arrows indicate some positive stained cells. Scale bars = 100 μ m. (B) Quantification of STAT5 phosphorylation in the proliferating (PZ) and hypertrophic (HZ) zones expressed as a percentage of total cells. Analysis was done on two different areas in two sections per mouse (n=5). Data are expressed as mean \pm SEM; ***P<0.001.

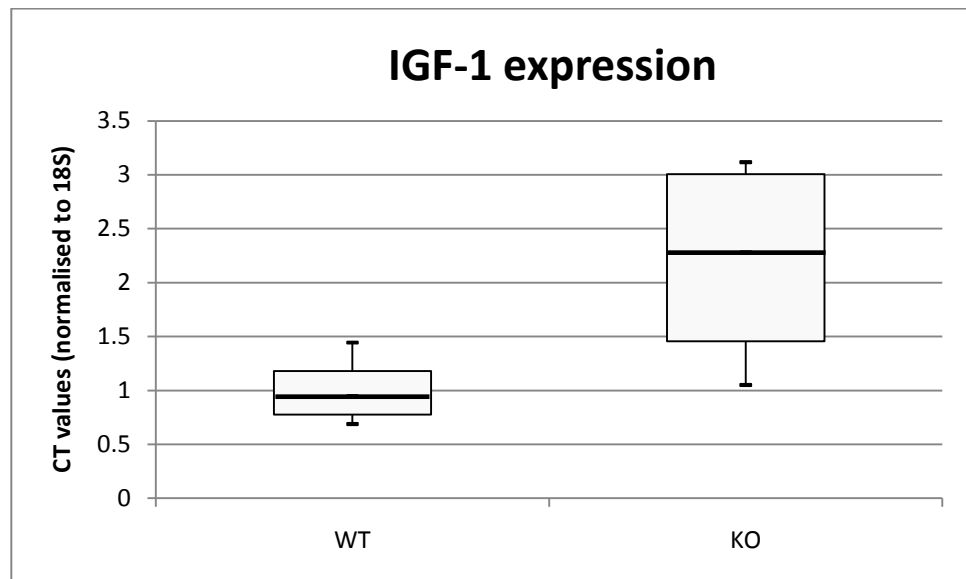


Figure 5.6. IGF-1 qPCR. Graph showing IGF-1 expression in *SOCS2*^{-/-} (KO) and WT mice, represented by relative change in IGF-1 expression ($2^{\Delta CT}$) normalised against 18S (housekeeping gene). Data are represented by a box plot displaying the median with upper and lower quartiles, and whiskers from minimum to maximum. RNA was isolated from chondrocytes taken from 1-day old mice; n=5 litters.

IGF-1 was greater in chondrocytes from costochondral cartilage of 1-day old SOCS2^{-/-} mice compared to WT mice but the difference was not statistically significant (Figure.5.6). These data are consistent with the observation that the overgrowth phenotype is not clearly observed in the whole animal until after 3-weeks of age.

5.5. Discussion

The overgrowth phenotype observed in SOCS2^{-/-} mice and associated increased growth rate (Chapter 4) is likely to be the result of increased chondrocyte GH signalling through STAT proteins leading to raised levels of IGF-1. To investigate this, the findings in Chapter 3 were extended to show that in chondrocytes isolated from SOCS2^{-/-} mice phosphorylation of STAT proteins was increased and, in the case of STAT5, prolonged compared to WT. This is consistent with findings by Greenhalgh *et al.*, who found prolonged STAT5 phosphorylation in hepatocytes from SOCS2^{-/-} mice (Greenhalgh *et al.*, 2002a). Increased GH signalling through STAT proteins will likely lead to raised IGF-1 levels, which will stimulate chondrocyte proliferation and the subsequent increased endochondral growth observed in SOCS2^{-/-} mice (Isgaard *et al.*, 1988).

Although enhanced and prolonged STAT phosphorylation was observed in SOCS2^{-/-} chondrocytes, the activation still decreased towards the end of the study period as in WT cells. The reasons for this decreased STAT activation are unclear. SOCS1 and SOCS3 are known to be potent inhibitors of GH signalling through the JAK/STAT pathway, and while we found in WT chondrocytes that their expression was not stimulated by GH, it is plausible that they have a redundancy role whereby in the absence of SOCS2 they do become active inhibitors of GH signalling in the growth plate. To test this hypothesis, the temporal expression of SOCS1 and SOCS3 was analysed in response to GH. Neither SOCS1 nor SOCS3 was stimulated by GH in WT or SOCS2^{-/-} chondrocytes, indicating that they are not responsible for the decline in STAT signalling. It is possible the level of STAT phosphorylation decreased with time because all the available STAT protein has been activated or because of other signalling events deregulating GH signalling, for example the protein tyrosine

phosphatase SHP-1 (SH2 domain-containing protein tyrosine phosphatase) which can dephosphorylate JAK2 (Klingmüller *et al.*, 1995).

Consistent with the raised levels of STAT activation observed in the absence of SOCS2, chondrocytes over-expressing SOCS2 showed reduced STAT phosphorylation in response to GH. Previous studies have shown that SOCS2 has dual functions, acting to inhibit up to 50% GH signalling at low and physiological concentrations, but to enhance signalling up to 200% at high concentrations (Adams *et al.*, 1998; Favre *et al.*, 1999). Furthermore, transgenic mice that over-express SOCS2 do not exhibit repressed growth, but in fact also exhibit an overgrowth phenotype similar to SOCS2^{-/-} mice (Greenhalgh *et al.*, 2002b). In these mice, SOCS2 was found to bind the GH receptor. One theory for the positive effect of SOCS2 on GH signalling is that at high concentrations SOCS2 can inhibit binding sites of the more potent GH inhibitors SOCS1 and SOCS3 (Greenhalgh *et al.*, 2002b). This hypothesis has been confirmed by studies showing that *in vitro* SOCS2 can block and restore the negative effects of SOCS1 and SOCS3 on GH signalling (Favre *et al.*, 1999; Dif *et al.*, 2001). In Chapter 3, and Figure 5.2, it was found that neither SOCS1 nor SOCS3 responded to GH in chondrocytes. Consistent with this, Kiu and colleagues found that SOCS2 does not regulate SOCS3 signalling in hematopoietic cells (Kiu *et al.*, 2009). These results indicate that high levels of SOCS2 can only act to influence other SOCS proteins in certain tissues, and that the overgrowth phenotype observed in mice with high levels of SOCS2 may be mediated by the systemic effects of GH signalling only.

In vivo analysis of phosphoSTAT5 expression in growth plates from 6-week old WT and SOCS2^{-/-} mice by immunohistochemistry showed an increase in the number of hypertrophic chondrocytes expressing phosphorylated STAT5 in SOCS2^{-/-} compared to WT. There was no difference in the number of cells stained in the proliferating zones suggesting that STAT5 activation in these cells of WT and SOCS2^{-/-} cells was similar. However, as immunohistochemistry is a poorly quantifiable technique, whilst allowing quantification of the number of cells stained for phosphorylated STAT5

it is not sensitive enough to establish the quantity of STAT5 activated by each cell. The increased number of hypertrophic cells stained for activated STAT5 confirms that the SOCS2^{-/-} overgrowth phenotype is associated with altered STAT5 phosphorylation, consistent with the *in vitro* findings in Figure 5.1 where increased and prolonged STAT5 signalling in primary chondrocytes isolated from SOCS2^{-/-} mice was noted. Gevers *et al.* reported parallel distributions of GHR and total STAT5 protein in growth plates of normal mice, with staining observed mainly in resting chondrocytes, some proliferating cells and prehypertrophic chondrocytes (Gevers *et al.*, 2009). Previous studies by the same group in rats found GHR protein expression in all zones of the growth plate, predominantly proliferating and early hypertrophic chondrocytes, which is more consistent with the localisation of phosphorylated STAT5 found here (Gevers *et al.*, 2002). Studies by Parker and colleagues also found GHR mRNA expression by analysis of RNA from the different zones of the growth plate (resting, proliferative, prehypertrophic and hypertrophic), although the levels of GHR found were low (Parker *et al.*, 2007). Gevers *et al.* reported greatly reduced GHR and total STAT5 expression in GH deficient mice, which have narrower growth plates and reduced growth (Gevers *et al.*, 2009). After injection of murine GH, phosphorylated STAT5 expression was observed in resting and prehypertrophic chondrocytes in growth plates from GH deficient mice (Gevers *et al.*, 2009). This distribution of phosphorylated STAT5 in the growth plate (Gevers *et al.*, 2009) had a more restricted distribution than observed in the WT and SOCS2^{-/-} mice of this study. The reasons for this are unclear but were not due to the immunohistochemical procedure used which was identical in both studies. A possible explanation could be that Gevers and colleagues (2009) studied GH deficient mice which have lower levels of GHR and narrower growth plate zones. However, they also reported no detectable phosphorylated STAT5 staining in normal mice (4- to 5-week old Albino Swiss mice) that were GH-sufficient (Gevers *et al.*, 2009). This is contradictory to our finding in WT mice, where phosphorylated STAT5 was found in all zones of the growth plate, particularly the resting and proliferating. This difference in results could partially be due to strain and age differences, but such stark differences are hard to reconcile. The

increased STAT5 activation in hypertrophic chondrocytes of SOCS2^{-/-} mice indicates that SOCS2 acts to mediate GH effects on hypertrophic chondrocytes, acting to regulate their size. This is consistent with the increased growth of SOCS2^{-/-} mice as the size of hypertrophic chondrocytes is known to be a major determinant of growth rate (Hunziker and Shenk, 1989; Breur *et al.*, 1991; Wilsman *et al.*, 1996b). Increased GH signalling through STAT5 will lead to raised IGF-1 signalling, and studies by Mushtaq *et al.* have shown that IGF-I increases hypertrophic cells which is likely to contribute to increased growth rates (Mushtaq *et al.*, 2004). Furthermore, IGF-I null mice have reduced growth that is associated with smaller hypertrophic chondrocytes (Wang *et al.*, 1999).

The observed increased STAT phosphorylation in chondrocytes from SOCS2^{-/-} mice both *in vitro* and *in vivo* demonstrates that increased GH signalling in these mice occurs through the JAK/STAT pathway, which is likely to lead to IGF-1 production. RT-qPCR analysis did not find a significant change in IGF-1 levels in chondrocytes isolated from 1-day old mice. It seems likely that this is due to a lack of GH signalling at that age, consistent with the gigantism phenotype of SOCS2^{-/-} occurring only from 3-to 4-weeks of age. Studies on microdissected growth plates found that IGF-1 mRNA in the rat growth plate increased with age, with a 25 fold increase observed from 1- to 9-weeks of age (Parker *et al.*, 2007). However, this study found that IGF-1 was expressed at much lower levels in the growth plate than in surrounding tissue, so that growth plate IGF-1 may in fact largely originate from the surrounding perichondrium, plasma and bone (Parker *et al.*, 2007). These findings may explain the lack of increase of IGF-1 in SOCS2^{-/-} chondrocytes found here. This data is also consistent with a similar analysis of SOCS2^{-/-} bone tissue where no change in IGF-1 mRNA expression was noted (Metcalf *et al.*, 2000). This analysis, however, was done on whole bone samples and did not separate cortical bone, trabecular bone, and epiphyseal cartilage (Metcalf *et al.*, 2000). They also reported normal systemic levels of GH and IGF-1 indicating that the SOCS2^{-/-} overgrowth phenotype is the result of tissue changes in GH signalling pathways, consistent with the findings in this study in chondrocytes (Metcalf *et al.*, 2000; Greenhalgh *et al.*, 2002a). However, an increase in local levels of IGF-1 in the absence of SOCS2 has yet to be

demonstrated, with the analysis performed here incomplete as IGF-1 mRNA levels were not measured in growth plates from SOCS2^{-/-} mice displaying the overgrowth phenotype. Such analysis could be performed in the future using the method of growth plate microdissection described by Parker *et al*, which would allow a more comprehensive analysis of the growth plate while retaining better RNA quality by using frozen tissue.

5.6. Conclusion

SOCS2^{-/-} growth plate chondrocytes display increased phosphorylation of STAT proteins in response to GH *in vitro*. Also, chondrocytes over-expressing SOCS2 show decreased STAT signalling in response to GH, confirming the negative role of SOCS2 on GH signalling in the growth plate. Altered STAT5 phosphorylation was also observed in the hypertrophic chondrocytes of SOCS2^{-/-} mice *in vivo*. This increased STAT phosphorylation may lead to increased local IGF-1 signalling and explain the altered growth plate phenotype and increased tibial growth rates (observed in Chapter 4) of the SOCS2^{-/-} mice. Several studies have demonstrated that serum levels of IGF-1 remain unchanged in SOCS2^{-/-} mice (Metcalf *et al.*, 2000; MacRae *et al.*, 2009), highlighting the importance of local GH/IGF-1 signalling. Whilst a role for locally increased chondrocyte IGF-I levels in mediating the increased growth rates of SOCS2^{-/-} mice has yet to be confirmed the studies in this chapter clearly show that SOCS2 is capable of modulating chondrocyte STAT activation in response to GH. This confirms the importance of local (autocrine/paracrine) GH/IGF-I signalling events in the control of bone growth.

CHAPTER 6

DIRECT EFFECTS OF INCREASED GH SIGNALLING IN SOCS2^{-/-} METATARSALS

6. Direct Effects of Increased GH Signalling in SOCS2^{-/-} Metatarsals

6.1. Introduction

The overgrowth phenotype of SOCS2^{-/-} has led to studies confirming that SOCS2 acts to negatively regulate GH signalling through the JAK/STAT pathway, in particular STAT5 (Metcalf *et al.*, 2000; Greenhalgh *et al.*, 2002a). In Chapter 4 the growth plate phenotype of SOCS2^{-/-} mice was analysed, and the increased bone length from 3-weeks of age was associated with wider growth plate zones, increased chondrocyte proliferation and a higher rate of bone growth. These studies were extended in Chapter 5, where in comparison to cells from WT mice chondrocytes isolated from SOCS2^{-/-} mice displayed increased activation of STAT1, STAT3 and STAT5 in response to GH, and immunohistochemistry of STAT5 disclosed increased numbers of hypertrophic cells expressing phosphorylated STAT5 in SOCS2^{-/-} mice compared to WT mice. From the available evidence it seems probable that in SOCS2^{-/-} growth plates raised levels of STAT phosphorylation in response to GH leads to increased bone growth and this is mediated by direct or indirect (via IGF-1) stimulation of chondrocyte proliferation.

Several authors have demonstrated the direct proliferative effect of IGF-1 on chondrocytes *in vitro* (Phornphutkul *et al.*, 2004; MacRae *et al.*, 2006a; Hutchison *et al.*, 2007). However, similar studies investigating a proliferative response to GH have reported conflicting results. Hutchison and colleagues noted no chondrocyte proliferative response to GH, although interestingly they also reported that STAT5 was not phosphorylated in response to GH in chondrocytes which is contrary to studies by Gevers and colleagues and the results in Chapters 3 and 5 of this thesis (Hutchison *et al.*, 2007; Gevers *et al.*, 2009). In contrast Madsen and colleagues showed a concentration dependant increase in chondrocyte proliferation in response to GH, consistent with other studies showing that GH can induce proliferation (Madsen *et al.*, 1983; Livne *et al.*, 1997).

Due to the different results gained in these studies, it was felt necessary to establish ATDC5 and primary chondrocyte proliferation responses to GH and IGF-1 under the conditions of this model.

Several investigators have used the foetal mouse metatarsal culture method to investigate the effects of IGF-1 on bone growth (Scheven and Hamilton, 1991; Coxam *et al.*, 1996; Mushtaq *et al.*, 2004; Martensson *et al.*, 2004; MacRae *et al.*, 2006a; MacRae *et al.*, 2007a). This culture system provides an *ex vivo* method of analysing endochondral bone growth that is more physiological, as the chondrocyte interactions with each other and with the surrounding matrix are preserved. Mushtaq and colleagues found increased metatarsal growth in response to IGF-1 which was coupled with increased proliferation (Mushtaq *et al.*, 2004). These findings were extended by MacRae and colleagues who demonstrated that the IGF-1 stimulated increase in metatarsal growth and associated proliferation was through PI3K signalling via Akt and not Erk1/2 signalling (MacRae *et al.*, 2007a).

Growth retardation is frequently observed during chronic inflammatory conditions and although glucocorticoid use, disease associated malnutrition, and altered GH/IGF-1 signalling will all contribute to the growth retardation (Mushtaq and Ahmed, 2002; MacRae *et al.*, 2007a), it is likely that increased levels of inflammatory cytokines such as IL-6, IL-1 β and TNF α play a crucial role in mediating poor growth. These pro-inflammatory cytokines have been shown to inhibit chondrocyte proliferation, increase apoptosis, and reduce chondrocyte expression of important matrix proteins (Davies *et al.*, 1997; Martensson *et al.*, 2004; MacRae *et al.*, 2006b; MacRae *et al.*, 2006c). The mechanisms by which these effects are mediated are poorly understood and while MacRae and colleagues found that TNF α increased chondrocyte expression of SOCS2, this result could not be replicated in this thesis (Chapter 3) (MacRae *et al.*, 2009). These authors also investigated the growth of SOCS2^{-/-} metatarsals challenged with TNF α and found their growth was inhibited to the same degree as WT metatarsals (MacRae *et al.*, 2009). However, given the lack of GH induced growth in mice at this age (pre-weaning; 19-day old foetal and 1-day old neonatal) it

seems unlikely that SOCS2 would influence chondrocyte dynamics at that age, particularly given that the SOCS2 overgrowth phenotype only occurs from 3-weeks of age. As a direct link between STAT phosphorylation, chondrocyte proliferation and bone growth has yet to be confirmed, the aims of this study were to investigate this further.

6.2. Aims and Hypothesis

6.2.1. Hypothesis

The increase in GH mediated STAT activation observed in chondrocytes of SOCS2^{-/-} mice leads to increased chondrocyte proliferation and endochondral growth.

6.2.2. Aims

- Establish chondrocyte proliferation in response to GH and IGF-1 using primary chondrocytes and ATDC5 cells. Extend these studies to investigate proliferation in chondrocytes from SOCS2^{-/-} mice and in cells over-expressing SOCS2.
- Exploit the embryonic metatarsal culture model to investigate the growth response of WT and SOCS2^{-/-} bones to GH and IGF-1.
- Exploit the embryonic metatarsal culture model to investigate chondrocyte intracellular signalling in WT and SOCS2^{-/-} bones in response to GH and IGF-1.
- Establish the effects of the pro-inflammatory cytokine IL-1 β in combination with IGF-1 or GH on WT and SOCS2^{-/-} metatarsal growth.

6.3. Materials and Methods

6.3.1. Cell Culture

ATDC5 cells were culture as described in Section 2.2.1. Primary chondrocytes were isolated from 1- to 3-day old Swiss mice as described in Section 2.3.7. Cells were cultured in 48-well plates in differentiation medium (ATDC5 cells) or primary chondrocyte medium (primary cells) as described

in Sections 2.2.1 and 2.3.7 respectively. For the proliferation assay, cells were cultured in serum free medium for 24hrs prior to incubation with GH or IGF-1 (24hrs).

6.3.2. Embryonic Metatarsal Culture

Metatarsals were isolated from 17-day old embryos and cultured as described in Section 2.3.11. All parents of embryos used were genotyped as described in Sections 2.3.3, 2.3.4 and 2.3.5 to ensure embryos used were the correct genotype. Metatarsals were cultured with the addition of 100ng/ml GH (Bachem); 100ng/ml IGF-1 (Bachem); 10 μ M LY-294002 (Sigma); 10ng/ml IL-1 β (Autogen Bioclear). The diluent for LY-294002 was DMSO, which was added to cultures at a final concentration of 0.07% to all metatarsals (including controls) in experiments using LY-294002.

6.3.3. [³H]Thymidine Proliferation Assay

Cell proliferation was measured using a thymidine proliferation assay as described in Section 2.4.1. Proliferation levels in metatarsals were analysed as described in Section 2.4.2.

6.3.4. Metatarsal Von Kossa and H&E Staining

Metatarsals were cultured for 4 days and then paraffin embedded and cut as described in Section 2.5.1. Sections were stained for Von Kossa and H&E as described in Section 2.5.5.

6.4. Results

6.4.1. Chondrocyte Proliferation in Response to GH and IGF-1

One of the downstream effects of GH binding to its receptor is IGF-1 signalling, which can lead to increased cell proliferation. This was investigated using tritiated thymidine uptake in ATDC5 cells and primary chondrocytes in response to GH (500ng/ml) and IGF-1 (50ng/ml) (Figure 6.1.). Proliferation was increased in response to IGF-1 ($P < 0.001$), but not GH, in ATDC5 cells. Primary cells showed no increase in proliferation with either GH or IGF-I, and had greater variation in values between individual samples. As various investigators (Madsen *et al.*, 1983; Ohlsson *et al.*,

1992b; Hutchison *et al.*, 2007) reported on the ability of different concentrations of GH and IGF-1 to stimulate chondrocyte proliferation, a concentration curve was also carried out in primary chondrocytes to determine if GH and IGF-1 induced proliferation was concentration dependent. Again neither GH nor IGF-1 increased proliferation in primary chondrocytes at any of the concentrations analysed (Figure 6.2). In fact, IGF-1 caused a decrease in proliferation at all concentrations examined ($P < 0.001$); a result that was both unexpected and inconsistent with the literature (Ohlsson *et al.*, 1992b; Kiepe *et al.*, 2005; MacRae *et al.*, 2006a; Hutchison *et al.*, 2007). As there was no proliferation response to GH or IGF-1, these studies with primary cells were not extended into SOCS2^{-/-} mice.

6.4.2. Growth of WT and SOCS2^{-/-} Metatarsals in Response to GH and IGF-1

It has been well established that embryonic metatarsals grow in length in response to IGF-1 but the response to GH is more equivocal (Scheven and Hamilton, 1991; Mushtaq *et al.*, 2004). It is possible that metatarsal growth is altered in SOCS2^{-/-} mice, in particular in response to GH as SOCS2 acts to inhibit GH signalling. To investigate this, 17-day old embryonic metatarsals were cultured with GH or IGF-1 over a 13-day period and their growth measured (Figure 6.3). Concentrations of GH and IGF-1 used (both 100ng/ml) were based on similar studies in murine metatarsals (Mushtaq *et al.*, 2004; MacRae *et al.*, 2006a).

In WT metatarsals, increased growth was seen in response to IGF-1 ($P < 0.05$ from day 5, Figure 6.3A), with no response to GH compared to controls over the duration of the experiment. In SOCS2^{-/-} metatarsals increased growth was again observed in response to IGF-1 and also in response to GH, from day 5 of culture ($P < 0.01$). In addition, in the SOCS2^{-/-} metatarsals there was no difference in the growth of metatarsals in response to IGF-1 and GH (Figure 6.3B). This indicates that in WT metatarsals, SOCS2 is acting to inhibit growth in response to GH. The growth of WT and SOCS2^{-/-} metatarsals in response to IGF-1 was similar indicating that SOCS2 does not regulate IGF-1 functional effects on growth.

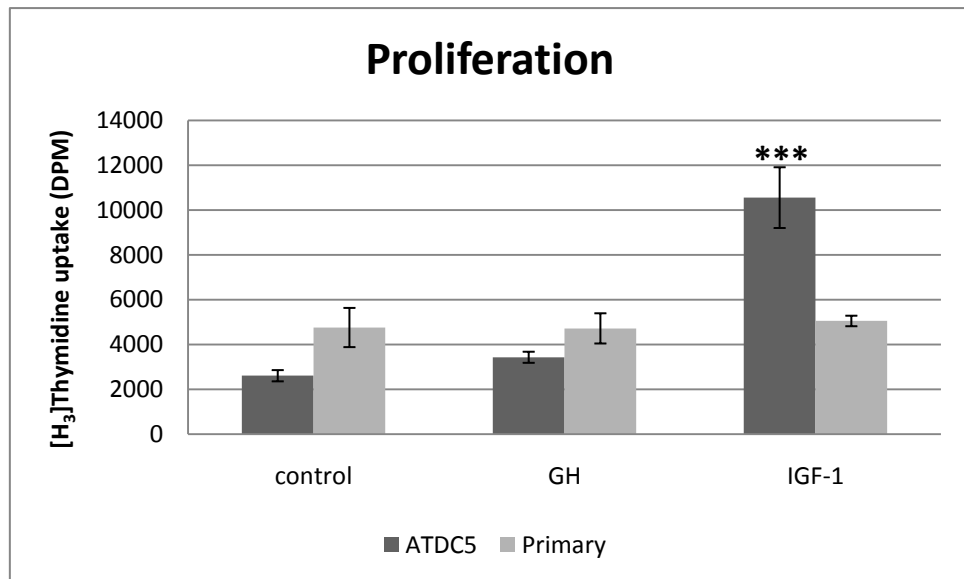


Figure 6.1. Proliferation assay. Uptake of tritiated thymidine was measured as depreciations per minute (DPM; Y-axis) in ATDC5 cells and primary chondrocytes in response to 24hrs exposure of GH (500ng/ml) and IGF-1 (50ng/ml). Results were analysed statistically by ANOVA (n≥6). Data are shown as mean ± SEM; ***P<0.001 compared to ATDC5 control.

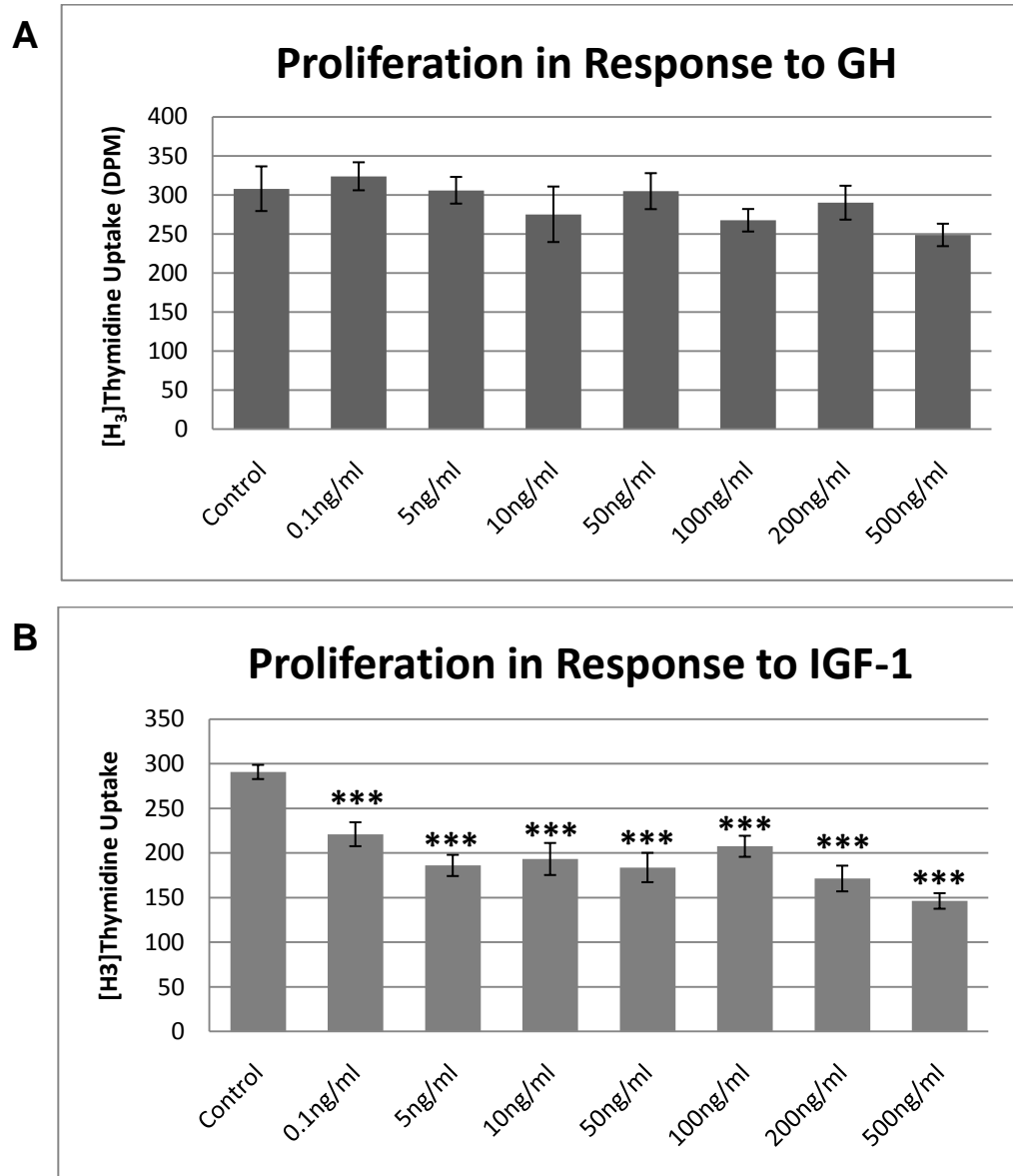


Figure 6.2. Proliferation assay concentration curves. Results for tritiated thymidine uptake in primary chondrocytes measured by deprecations per minute (DPM; y-axis) in response to 24hrs exposure with different concentrations of GH (A) and IGF-1 (B). Results were analysed statistically by ANOVA. Data are shown as mean \pm SEM; ***P<0.001 compared to control; n \geq 6.

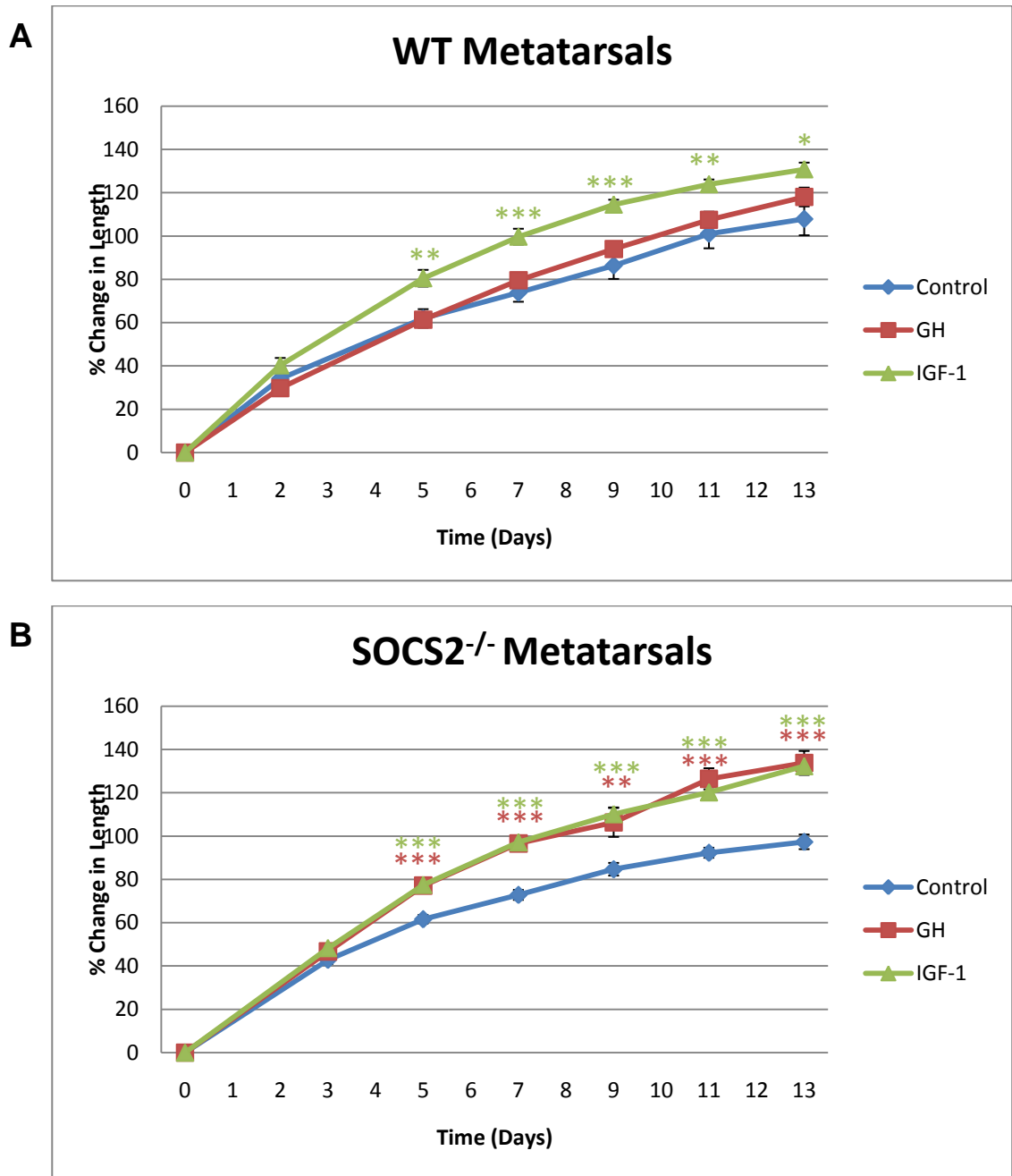


Figure 6.3. Analysis of WT and $SOCS2^{-/-}$ metatarsals growth. Embryonic metatarsals were cultured with GH (100ng/ml) and IGF-1 (100ng/ml). (A) Growth of wild-type (WT) metatarsals in response to GH and IGF-1. Data are expressed as mean percentage change in length from day 0, \pm SEM. Results were analysed statistically by ANOVA ($n \geq 6$). * $P < 0.05$, ** $P < 0.01$, *** $P < 0.001$ compared to control at the same time point (colour used matches that of treatment analysed statistically). (B) Growth of $SOCS2^{-/-}$ metatarsals in response to GH and IGF-1. Data are expressed as mean percentage change in length from day 0, \pm SEM. Results were analysed statistically by ANOVA ($n \geq 6$). ** $P < 0.01$, *** $P < 0.001$ compared to control at the same time point (colour used matches that of treatment analysed statistically).

6.4.3. SOCS2^{-/-} and WT Metatarsal Proliferation in Response to GH and IGF-1

A thymidine proliferation assay was used to investigate if the increased growth of WT metatarsals in response to IGF-1, and of SOCS2^{-/-} metatarsals in response to GH and IGF-1 was due to increased chondrocyte proliferation. 17-day old WT and SOCS2^{-/-} embryonic metatarsals were cultured for 4 days in the presence of GH or IGF-1 before analysis for proliferation by [³H]-thymidine uptake (Figure 6.4.). This culture time was chosen as it falls within the period of maximum growth in both WT and SOCS2^{-/-} metatarsals in response to GH and/or IGF-1 (Figure 6.3).

In WT metatarsals proliferation levels were increased in response to IGF-1 (P<0.05), but not GH. Proliferation levels in SOCS2^{-/-} metatarsals increased in response to both IGF-1 and GH (P<0.05). This confirms that the increased growth of WT and SOCS2^{-/-} metatarsals in Figure 6.3 is associated with increased chondrocyte proliferation.

6.4.4. Zone Widths in SOCS2^{-/-} and WT Metatarsals

Von Kossa and H&E staining were used to measure zone widths in WT and SOCS2^{-/-} metatarsals. 17-day old WT and SOCS2^{-/-} metatarsals were cultured with GH or IGF-1 for 4 days before being fixed, embedded and cut. Sections were then stained and zone widths analysed (Figure 6.5). Again this culture time was chosen as it falls within the period of maximum growth in both WT and SOCS2^{-/-} metatarsals in response to GH and/or IGF-1. No significant changes were observed in zone widths of WT metatarsals, which was inconsistent with their increased length in response to IGF-1. In SOCS2^{-/-} chondrocytes, IGF-1 caused an increase in width of the hypertrophic zone (P<0.01), with no significant changes observed for GH. Again, this latter finding is inconsistent with the observed increased metatarsal growth. It is possible that non-significant increases in zone widths contributed to the observed increase in metatarsal length for WT metatarsals challenged with IGF-1, and for SOCS2^{-/-} metatarsals challenged with GH.

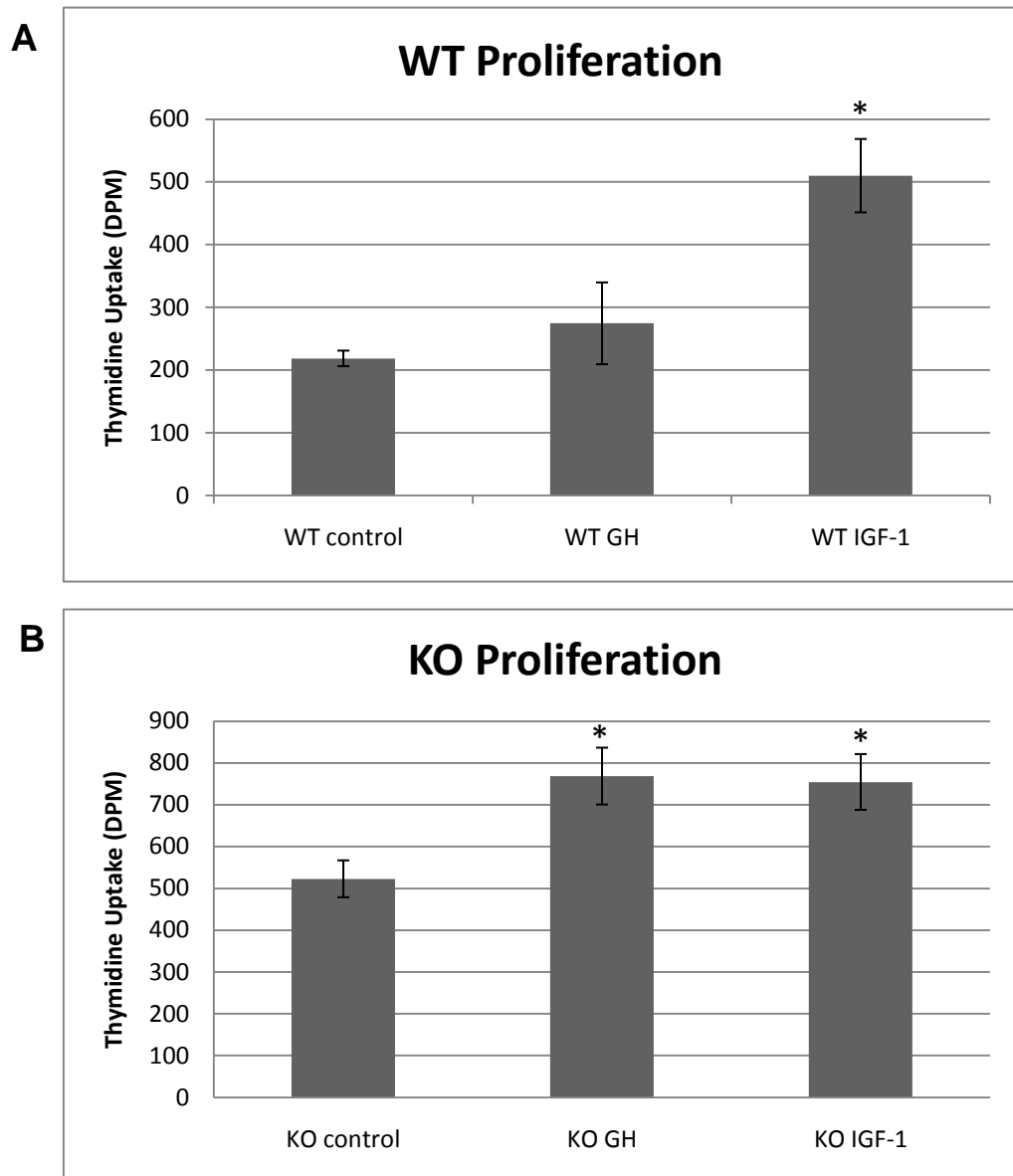


Figure 6.4. Chondrocyte proliferation in metatarsals. Embryonic metatarsals were cultured for 4 days with GH (100ng/ml) or IGF-1 (100ng/ml) then measured for levels of [³H]thymidine uptake as a measure of cell proliferation. (A) Proliferation levels in wild-type (WT) metatarsals measured by depreciations per minute (DPM). Data are expressed as mean±SEM and was analysed by ANOVA (n=4). *P<0.05 compared to control. (B) Proliferation levels in *SOCS2*^{-/-} (KO) metatarsals measured by depreciations per minute (DPM). Data are expressed as mean±SEM and was analysed by ANOVA (n=4). *P<0.05 compared to control.

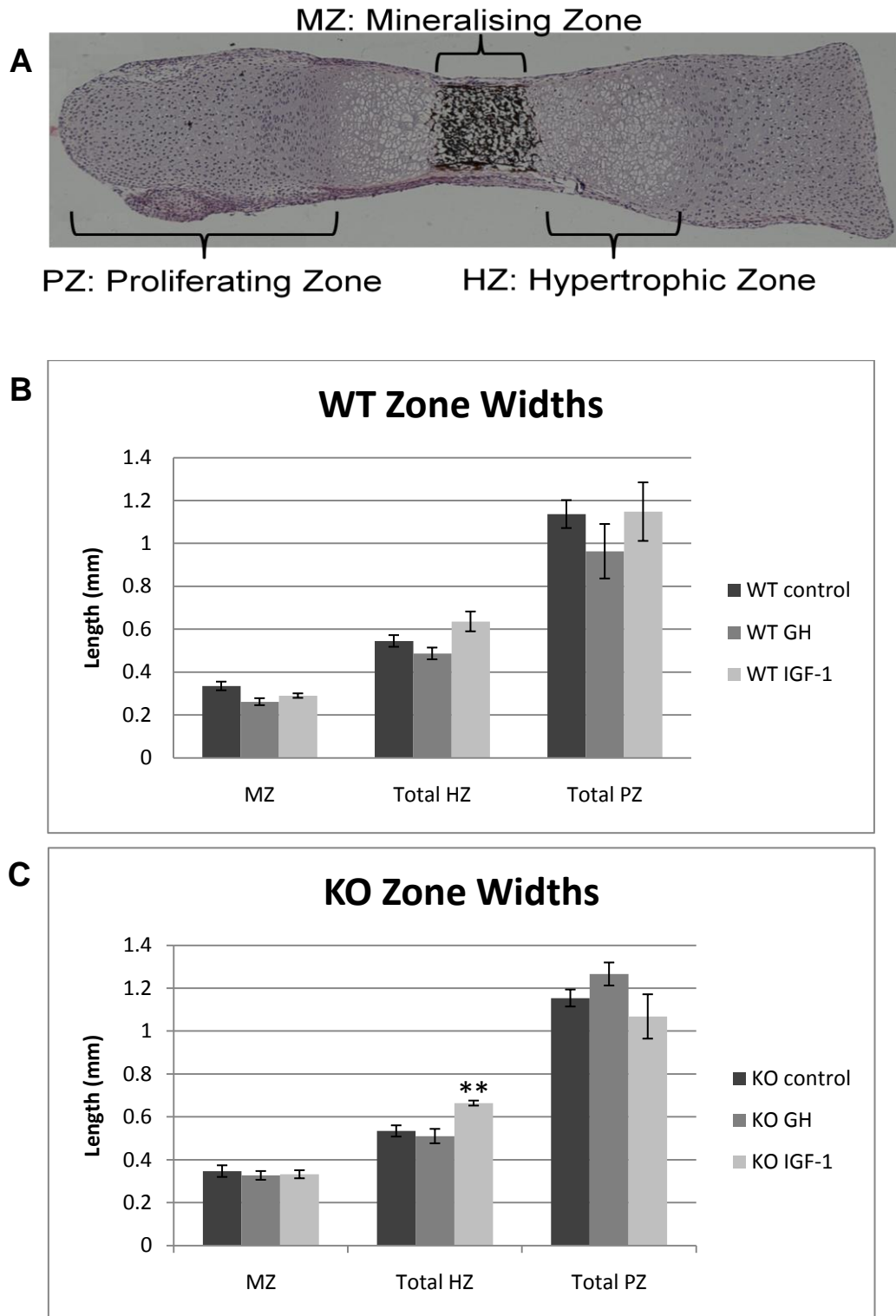


Figure 6.5. Metatarsals zone widths. Metatarsal sections were stained with Von Kossa, and H&E to allow zone width analysis. (A) An example of a stained section showing the areas measured - mineralising zone (MZ), hypertrophic zones (HZ) and proliferating zones (PZ). For HZ and PZ, measurements were taken from both sides of the MZ to give the total measurements. Results for total measurements for the three zones are shown for (B) wild-type (WT) metatarsals and (C) *SOCS2*^{-/-} (KO) metatarsals cultured with GH or IGF-1 for 4 days. Results are mean±SEM and were analysed by ANOVA (n=6). **P<0.01 compared to control hypertrophic zone.

6.4.5. Investigating if GH Signals through IGF-1 in SOCS2^{-/-} Metatarsals

The GH induced growth observed in SOCS2^{-/-} metatarsals (Figure 6.3) was associated with increased proliferation. To test whether this effect of GH was mediated through IGF-1, an inhibitor of IGF-1 signalling was used. MacRae *et al.* found that IGF-1 induced metatarsal growth was inhibited by the PI3K inhibitor LY-294002 (MacRae *et al.*, 2007a). Their studies showed that an Erk1/2 inhibitor did not affect IGF-1 stimulated growth, therefore demonstrating that the primary pathway used by IGF-1 in chondrocytes is the IRS-1/PI3K/Akt pathway, as opposed to SHC/RAS/RAF/MEK/MAPK (Erk 1/2) (MacRae *et al.*, 2007a). A concentration curve for LY-294002 was carried out by MacRae and colleagues to establish the lowest concentration required to inhibit chondrocyte proliferation by IGF-1 and this was found to be 10 μ M (MacRae *et al.*, 2007a). In this study WT and SOCS2^{-/-} metatarsals were cultured with GH (100ng/ml), IGF-1 (100ng/ml), LY-294002 (10 μ M), LY-294002 (10 μ M) plus IGF-1 (100ng/ml) or LY-294002 (10 μ M) plus GH (100ng/ml) and growth measured (Figure 6.6).

The results in Figure 6.3 were confirmed with increased growth in response to IGF-1 in WT and SOCS2^{-/-} metatarsals, with SOCS2^{-/-} metatarsals also responding to GH. LY-294002 inhibited growth compared to control metatarsals for both WT and SOCS2^{-/-} (P<0.001 from day 4). The addition of GH or IGF-1 did not increase metatarsal growth in the presence of LY-294002, indicating that the IGF-1 stimulated growth in both WT and SOCS2^{-/-} metatarsals is through signalling by PI3K, consistent with previous studies (MacRae *et al.*, 2007a). This also indicates that increased growth of SOCS2^{-/-} bones in direct response to GH is mediated by the actions of PI3K.

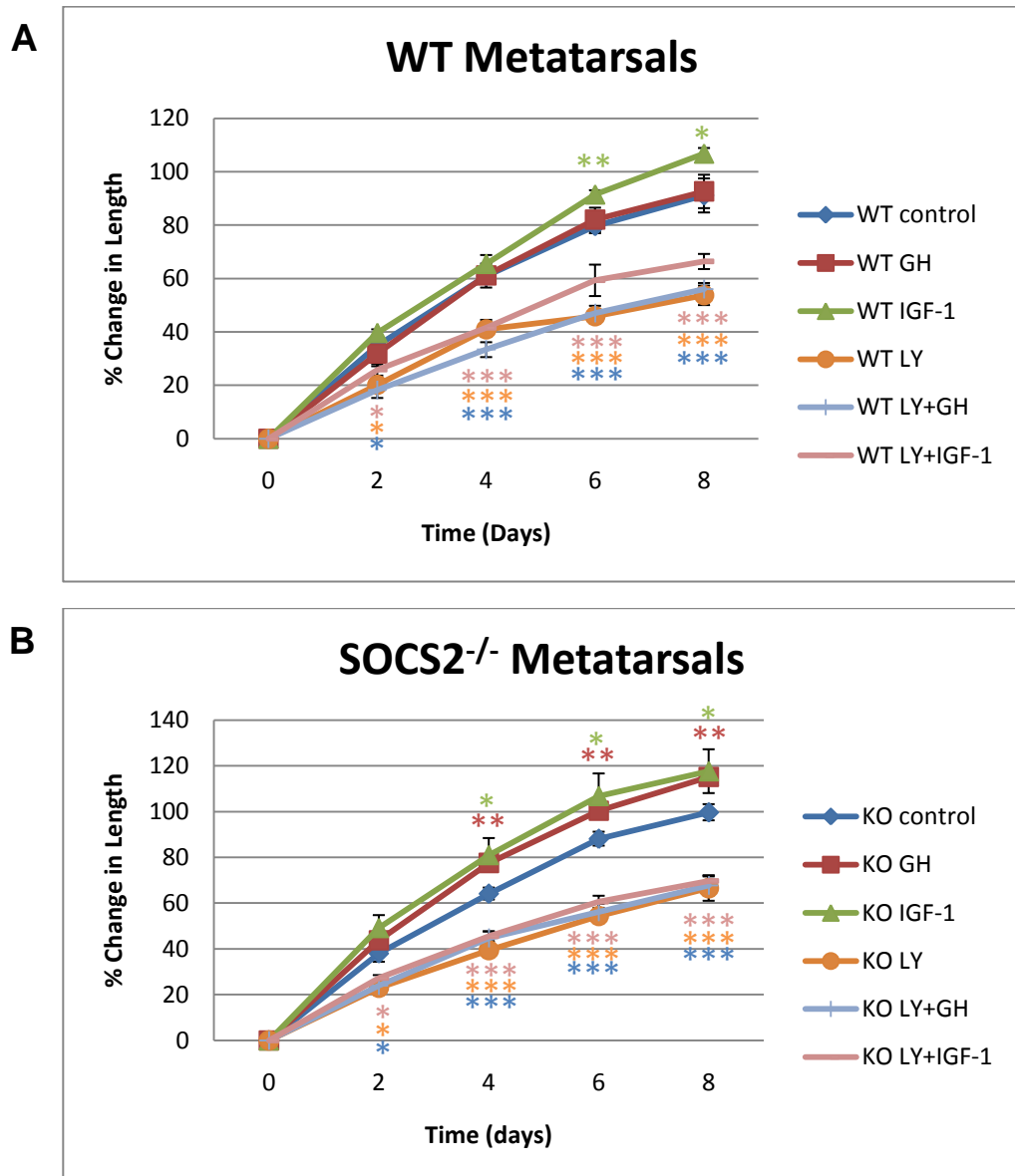


Figure 6.6. Metatarsal growth curves with IGF-1 signalling inhibitor. Embryonic metatarsals were cultured with GH (100ng/ml), IGF-1 (100ng/ml), LY-294002 (LY) (10 μ M), LY-294002+IGF-1 (LY+IGF-1) or LY-294002+GH (LY+GH). (A) Growth of wild-type (WT) metatarsals. Data are expressed as mean percentage change in length from day 0, \pm SEM. Results were analysed statistically by ANOVA ($n \geq 5$). * $P < 0.05$, ** $P < 0.01$, *** $P < 0.001$ compared to control at each time point (colour used matches that of treatment analysed statistically). (B) Growth of *SOCS2*^{-/-} metatarsals (KO). Data are expressed as mean percentage change in length from day 0, \pm SEM. Results were analysed statistically by ANOVA ($n \geq 6$). * $P < 0.05$, ** $P < 0.01$, *** $P < 0.001$ compared to control at each time point (colour used matches that of treatment analysed statistically).

6.4.6. The Effects of IL-1 β on Metatarsal Growth

MacRae and colleagues reported that the inflammatory cytokine TNF α caused a similar amount of growth inhibition in SOCS2^{-/-} and WT metatarsals. However, this was in the absence of growth factors, in particular GH or IGF-1. It was interesting to speculate that the positive effect of GH on SOCS2^{-/-} metatarsal growth observed in this study (Figure 6.3) may act to prevent the growth inhibition induced by inflammatory cytokines and offer therapeutic opportunities. To test this hypothesis, WT and SOCS2^{-/-} metatarsals were cultured with GH (100ng/ml), IGF-1 (100ng/ml), IL-1 β (10ng/ml), IL-1 β (10ng/ml) plus GH (100ng/ml), IL-1 β (100ng/ml) plus IGF-1 (100ng/ml) (Figure 6.7). The concentration of IL-1 β used (10ng/ml) was based on similar studies using IL-1 β in metatarsal cultures (Martensson *et al.*, 2004; MacRae *et al.*, 2006b; MacRae *et al.*, 2007a).

In WT metatarsals IL-1 β significantly inhibited metatarsal growth, an effect that was seen from day 4 of culture and was not altered by the addition of GH or IGF-1. The growth of SOCS2^{-/-} metatarsals was also significantly inhibited by IL-1 β , by a comparable amount to WT metatarsals ($P < 0.001$ from day 8). SOCS2^{-/-} metatarsals exposed to both IL-1 β and IGF-1 showed less growth reduction than those challenged with IL-1 β alone, with significantly increased growth at day 6 ($P < 0.05$), day 8 ($P < 0.01$) and day 10 ($P < 0.01$) of culture compared to IL-1 β alone; although their growth was still less than untreated SOCS2^{-/-} metatarsals. A similar effect was observed in SOCS2^{-/-} metatarsals cultured with IL-1 β and GH, with no growth reduction from control, untreated, bones observed until day 10 of culture, resulting in a significant increase in growth at days 4, 6, 8 (all $P < 0.05$) and day 10 ($P < 0.01$) of culture when compared to IL-1 β alone.

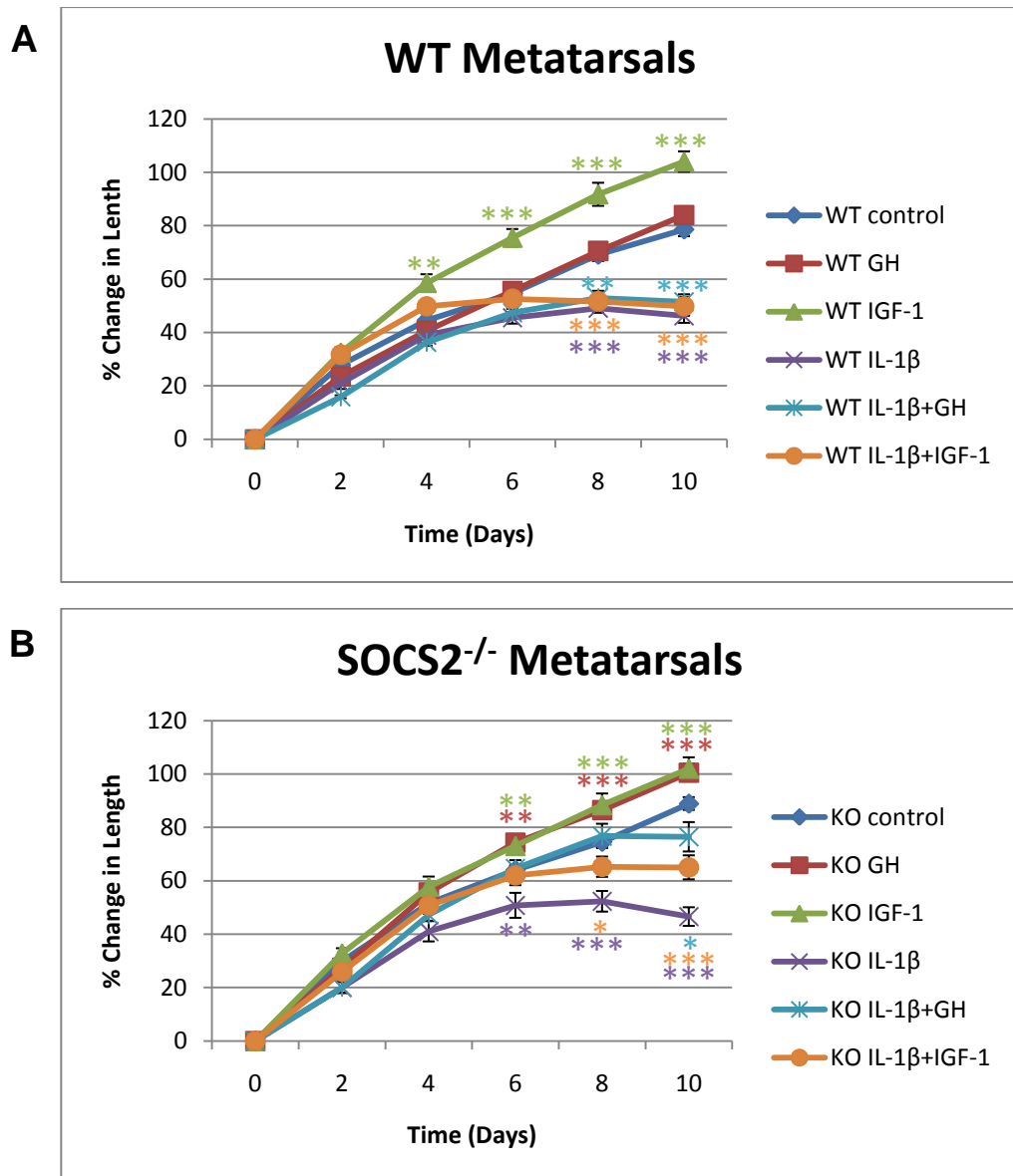


Figure 6.7. Metatarsal growth curves in response to IL-1 β . Embryonic metatarsals were cultured with GH (100ng/ml), IGF-1 (100ng/ml), IL-1 β (10ng/ml), IL-1 β +GH or IL-1 β +IGF-1. (A) Growth of wild-type (WT) metatarsals. Data are expressed as mean percentage change in length from day 0, \pm SEM. Results were analysed statistically by ANOVA ($n \geq 5$). ** $P < 0.01$, *** $P < 0.001$ compared to control at each time point (colour used matches that of treatment analysed statistically). (B) Growth of *SOCS2*^{-/-} metatarsals (KO). Data are expressed as mean percentage change in length from day 0, \pm SEM. Results were analysed statistically by ANOVA ($n \geq 5$). * $P < 0.05$, ** $P < 0.01$, *** $P < 0.001$ compared to control at each time point (colour used matches that of treatment analysed statistically).

6.5. Discussion

GH stimulation of the JAK/STAT pathway is known to lead to downstream IGF-1 signalling, which in turn stimulates proliferation. This was investigated by examining the proliferation of chondrocytes in response to GH and IGF-1. ATDC5 cells showed increased proliferation in response to IGF-1, consistent with previous studies (Phornphutkul *et al.*, 2004; MacRae *et al.*, 2006a). GH did not stimulate proliferation of ATDC5 cells. Previous studies investigating the effects of GH on chondrocyte proliferation have reported inconsistent results. Hutchison *et al.* have shown that GH does not stimulate proliferation, however other studies have found a proliferative response to GH (Madsen *et al.*, 1983; Ohlsson *et al.*, 1992b; Hutchison *et al.*, 2007). Importantly, none of these studies used ATDC5 cells and different culturing conditions are likely to be crucial to the proliferative response, as demonstrated by Ohlsson *et al.* (1992). In primary chondrocytes, neither GH nor IGF-1 increased proliferation. The levels of proliferation in different samples within the replicates of each individual experiment varied greatly in primary cells and this is likely to have masked any GH mediated increases in cell proliferation. This is probably due to the fact that they are a mixed population of chondrocytes in different stages of differentiation, unlike ATDC5 cells which are a transformed cell line that show distinct stages of differentiation as they are cultured. However, as primary chondrocytes also did not show increased IGF-1 signalling it is possible the cells are not responsive to IGF-1 in this system. Other authors who have shown primary chondrocytes proliferating in response to IGF-1 have used chondrocytes isolated from 3- to 6-week old rats or rabbits (Madsen *et al.*, 1983; Ohlsson *et al.*, 1992b). An interesting study by Eden *et al.* (1983) showed that chondrocytes isolated from different locations demonstrate different binding affinities to GH, with rib cage chondrocytes showing very little specific binding compared to ear and epiphyseal chondrocytes (Eden *et al.*, 1983). There are therefore several possible explanations for the lack of IGF-1 and GH responses seen in primary chondrocytes in this study: mixed chondrocyte population; age of mice; lack of GH binding activity; previous exposure to FBS containing growth factors that even upon removal mask results. The latter explanation

seems likely in this experimental model as recent experiments performed by a master student, Lorna Halley, has found that when cultured without FBS primary chondrocytes do proliferate in response to IGF-1 ($P < 0.001$), but not GH.

As the proliferation assay could not be used to measure the downstream effects of GH and IGF-1 stimulation of WT and SOCS2^{-/-} chondrocytes, the metatarsal culture model was exploited as a possible physiological alternative measure of bone growth. Both WT and SOCS2^{-/-} metatarsals responded similarly to IGF-1 with increased growth, consistent with previous studies in murine metatarsals (Mushtaq *et al.*, 2004; MacRae *et al.*, 2007a). Increased bone growth was also demonstrated by SOCS2^{-/-} metatarsals challenged with GH which is likely to be mediated through increased JAK/STAT signalling, taking into account the previous findings of increased GH stimulated STAT activation in chondrocytes of SOCS2^{-/-} mice (Chapter 5). The IGF-1 response of SOCS2^{-/-} metatarsals was coupled with increased hypertrophic zone width, but no zone width changes were seen in WT metatarsals stimulated with IGF-1 nor SOCS2^{-/-} metatarsals with GH. These results are inconsistent with the increased growth observed in these metatarsals. This was, however, a rather crude method of measuring zone widths as due to their small size it was difficult to orientate the metatarsals accurately for sectioning along the same plane, and so slight differences resulting from this may account for the lack of significance noted. There was also significant variation between individual bones. Non-significant increases in hypertrophic zone width of WT metatarsals were noted in response to IGF-1, and in proliferating zone width of SOCS2^{-/-} metatarsals in response to GH. Studies by Mushtaq and colleagues found increased hypertrophic zone widths in embryonic metatarsals challenged with IGF-1 for 4-days and 10-days, indicating that IGF-1 acts to stimulate endochondral bone growth by altering the dynamics of the hypertrophic zone, including increasing hypertrophic cell height (Mushtaq *et al.*, 2004). This is consistent with findings in IGF-1^{-/-} mice, which have short stature associated with decreased hypertrophic, but not proliferative, zone width and reduced hypertrophic cell size coupled with reduced expression of collagen type-X (Wang *et al.*, 1999). These results indicate that IGF-1

primarily acts on the hypertrophic, not proliferative, zone of the growth plate. The GH response of *SOCS2*^{-/-} metatarsals was associated with increased chondrocyte proliferation as was the IGF-1 response in WT and *SOCS2*^{-/-} metatarsals. This latter result is consistent with previous studies (Mushtaq *et al.*, 2004). Furthermore, the addition of the PI3K inhibitor LY-294002 to *SOCS2*^{-/-} metatarsals suppressed GH and IGF-1 promoted bone growth in a similar manner to that seen with WT metatarsals in response to IGF-1 (MacRae *et al.*, 2007a). These results indicate that GH acts to stimulate bone growth by signalling through PI3K, which is likely to be stimulated by IGF-1 or to act directly downstream of GH to increase IGF-1 production (Argetsinger and Carter-Su, 1996; LeRoith, 2000; MacRae *et al.*, 2007a).

Increased levels of inflammatory cytokines such as IL-1 β and TNF α are known to inhibit chondrocyte actions in the epiphyseal growth plate, contributing to the reduced endochondral growth associated with chronic inflammatory diseases such as juvenile idiopathic arthritis and inflammatory bowel disease (Martensson *et al.*, 2004; MacRae *et al.*, 2006b; MacRae *et al.*, 2006c). Given the increased growth observed in *SOCS2* deficient mice, inhibition of *SOCS2* expression may have a positive effect on longitudinal growth in such patients and therefore offer potential as a therapeutic target. MacRae and colleagues (2009) found that the response of *SOCS2*^{-/-} and WT metatarsals to TNF α were similar, with bone growth significantly inhibited in both genotypes. These findings were confirmed and extended in this study with reduced bone growth observed in WT and *SOCS2*^{-/-} embryonic metatarsals exposed to the pro-inflammatory cytokine, IL-1 β . The addition of GH or IGF-1 did not alter this negative effect on growth in WT metatarsals and this is contrary to findings by Martensson *et al.* (2004) who showed that the addition of IGF-1 to rat metatarsals did partially prevent IL- β induced growth retardation (Martensson *et al.*, 2004). In these present studies however IGF-1 did act to reduce IL-1 β induced growth retardation in *SOCS2*^{-/-} metatarsals, although it did not completely rescue growth of *SOCS2*^{-/-} metatarsals to the same level as control bones. In contrast, the addition of GH did completely prevent the IL-1 β effect on *SOCS2*^{-/-} metatarsals for the first 8 days of culture, with

comparable longitudinal growth achieved to control SOCS2^{-/-} metatarsals. These results imply that the inhibitory actions of pro-inflammatory cytokines on growth plate chondrocyte actions can be partially rescued in the absence of SOCS2, where increased GH signalling can compensate for the inflammatory induced growth retardation. The observation that IGF-1 also partially rescued growth of SOCS2^{-/-} metatarsals in the presence of IL-1 β indicates that while SOCS2 primarily acts on the GH signalling cascade, it may also regulate IGF-1 signalling. This is consistent with studies showing that SOCS2 can bind the IGF-1 receptor, thus may be capable of regulating IGF-1 signalling also (Dey *et al.*, 1998; Michaylira *et al.*, 2006b). This regulation, however, is not via STAT activation as in Chapter 3 it was clearly shown that IGF-1 does not stimulate STAT phosphorylation in chondrocytes.

6.6. Conclusion

Although a proliferative response in primary chondrocytes was not achieved, IGF-1, but not GH, did stimulate the growth of WT embryonic metatarsals. In contrast, SOCS2^{-/-} metatarsals responded to stimulation by both GH and IGF-1, with both responses suppressed by the addition of the PI3K inhibitor LY-294002. The increased growth of metatarsals in response to GH or IGF-1 was associated with increased chondrocyte proliferation. These data confirm that SOCS2 acts to negatively regulate GH stimulation of endochondral bone growth, and indicates that GH has the potential to directly increase bone growth when the SOCS2 inhibitory actions on chondrocyte STAT signalling are removed. This GH promotion of bone growth is, in part, regulated by increased chondrocyte proliferation via the PI3K pathway. The inflammatory cytokine IL-1 β inhibited bone growth, an effect that could be partially overcome by addition of GH or IGF-1 in SOCS2^{-/-}, but not WT, metatarsals. This suggests that the removal or inhibition of SOCS2 expression/activity may offer the potential for clinical intervention to suppress the inhibited endochondral growth observed during chronic inflammatory conditions. Indeed, potential target sites in the SOCS2 C

terminus for low-molecular-weight protein interaction inhibitors have been identified and could be used to develop SOCS2 antagonists (Bullock *et al.*, 2006).

CHAPTER 7

INDUCING INFLAMMATION IN SOCS2^{-/-} MICE

7. Inducing Inflammation in SOCS2^{-/-} Mice

7.1. Introduction

Paediatric inflammatory diseases are known to have adverse effects on the skeleton, with growth retardation and osteoporosis observed in chronic inflammatory conditions such as inflammatory bowel disease (IBD) and systemic juvenile idiopathic arthritis (JIA) (Simon *et al.*, 2002b; MacRae *et al.*, 2006c; Tilg *et al.*, 2008). Studies investigating the use of GH to treat short stature in these patients have reported mixed results, with more recent data indicating that normal height can be achieved if therapy is started early (Simon *et al.*, 2002b; Bechtold *et al.*, 2007; Simon *et al.*, 2007). Whilst it is very likely that there are disease specific issues that contribute to the impaired longitudinal growth in these conditions, inflammation remains a common factor. These diseases are often accompanied by elevated levels of pro-inflammatory cytokines, in particular IL-1 β , TNF α and IL-6 (Hildebrand *et al.*, 1994; Simon *et al.*, 2002a). It is likely that pro-inflammatory cytokines compromise bone growth and bone mass by a number of different mechanisms, including interference with the systemic as well as the tissue-level GH/IGF-1 axis which has recognised anabolic actions on skeletal development (de Hooge *et al.*, 2003; Martensson *et al.*, 2004; MacRae *et al.*, 2006b; MacRae *et al.*, 2007b). Studies using a murine model of colitis have found that inhibited growth is associated with decreased IGF-1, and recovery is enhanced in the presence of elevated GH (Ballinger *et al.*, 2000; Williams *et al.*, 2001). Consistent with these findings, patients with inflammatory conditions have lowered levels of systemic IGF-1, but not GH (Davies *et al.*, 1997; De Benedetti *et al.*, 2001a). Transgenic mice that over-express systemic IL-6 also have lowered levels of systemic IGF-1, and exhibit growth retardation that is rescued by the administration of an IL-6 receptor antibody (De Benedetti *et al.*, 1997). Inflammatory cytokines IL-1 β and TNF α have been found to inhibit chondrocyte proliferation and differentiation, increase apoptosis and decrease chondrocyte production of matrix proteins aggrecan, collagen type-II and

-X; leading to decreased growth plate zone widths and impaired longitudinal growth (Goldring *et al.*, 1988; Horiguchi *et al.*, 2000; Aizawa *et al.*, 2001; Martensson *et al.*, 2004; MacRae *et al.*, 2006b; MacRae *et al.*, 2006c). The mechanisms by which inflammatory cytokines exert these negative effects on chondrocytes are unknown, and it is possible that alteration of GH/IGF-1 signalling is involved.

It has been shown that pro-inflammatory cytokines can induce tissue-specific expression of SOCS proteins, with up-regulation of SOCS3 by IL-1 β , TNF α and IL-6 in certain cell types (Denson *et al.*, 2003; Shi *et al.*, 2004). The embryonic lethality of SOCS3^{-/-} mice is partially caused by IL-6 hypersensitivity, also demonstrating its important role in regulating inflammatory cytokine signalling. Studies in the SOCS1^{-/-} have shown that it is important in IFN- γ signalling and T-cell function (Alexander *et al.*, 1999; Marine *et al.*, 1999b). However, the role of these SOCS proteins in mediating inflammatory cytokine signalling in the growth plate has not been investigated. In particular, the overgrowth phenotype of the SOCS2^{-/-} mice, coupled with the altered growth plate dynamics observed in Chapters 4 and 5, make it a prime target when investigating the growth retardation observed in conditions such as IBD and JIA. The results by MacRae and colleagues showing that TNF α increased chondrocyte expression of SOCS2 could not be replicated in this thesis (Chapter 3) (MacRae *et al.*, 2009). These authors also found that the addition of TNF α to primary chondrocytes from 1-day old mice inhibited the production of important matrix proteins aggrecan, collagen type-II and collagen type-X; an effect that was not altered in the absence of SOCS2 (MacRae *et al.*, 2009). MacRae and colleagues extended their studies into the metatarsal mode of bone growth to confirm previous studies that the addition of the inflammatory cytokine TNF α inhibited metatarsal growth, again finding that this effect was also noted in the SOCS2^{-/-} mice (MacRae *et al.*, 2009). In Chapter 6 these latter findings were repeated using IL-1 β and extended to show that the addition of GH or IGF-1 rescued the IL-1 β mediated growth inhibition in SOCS2^{-/-}, but not WT, metatarsals. These *in vitro* results indicate that in the absence of SOCS2, the negative effects of inflammatory cytokines on longitudinal bone growth are somewhat

diminished possibly through compensatory effects of enhanced GH signalling. The aim of this study was to extend these observations to an *in vivo* model of inflammation.

7.2. Aims and Hypothesis

7.2.1. Hypothesis

SOCS2 plays a significant role in mediating the growth retardation observed during chronic inflammatory diseases and therefore the removal or inhibition of SOCS2 in inflammatory situations will help restore physiological endochondral growth.

7.2.2. Aims

- Conduct a pilot study using LPS to induce inflammation in 4-week old WT and SOCS2^{-/-} mice and measure changes in body weight, body length and tibia length over a 7-day period.
- Extend this study to the dextran sodium sulphate (DSS) experimental colitis model in 4-week old WT and SOCS2^{-/-} mice, using pair-fed genotype matched control mice.
- Investigate the effect of colitis on the following parameters in WT mice compared to SOCS2^{-/-} mice: growth (change in body weight, body length and bone lengths); bone phenotype (longitudinal mineral apposition rate, growth plate analysis); disease severity (health of mice scored daily and distal colon studied); speed of recovery upon DSS removal; serum analysis of inflammatory cytokines (TNF α , IL-1 β and IL-6), bone turnover markers (alkaline phosphatase and N-terminal procollagen peptides), and IGF-1.

7.3. Materials and Methods

7.3.1. LPS Model of Inflammation

LPS was used in a pilot study investigating the effects of inflammation on growth in SOCS2^{-/-} mice. 4 female WT and 4 female SOCS2^{-/-} mice were challenged with LPS to induce inflammation as described in Section 2.3.12. 4-week old mice were injected with 50 μ g/kg LPS daily for 7 days, with

saline administered to age, genotype and sex matched control mice. To allow growth analysis mice were weighed, measured crown to rump and whole body x-rayed at days 0 and day 7. Scanned x-ray films were used to measure tibiae lengths using Image J.

7.3.2. DSS Model of Colitis

For the dose concentration pilot study 2 male WT mice were given 3% DSS, 2 male WT mice were given 4% DSS and 2 male WT mice were given 5% DSS. The mice were 8-weeks old and were housed individually. The mice were challenged with DSS in their drinking water for 5 days followed by a 10 day recovery. The mice were weighed, measured crown to rump and their health scored throughout the 14 day period.

For the main DSS study 4-week old WT and SOCS2^{-/-} mice were challenged with 4% DSS in their drinking water for 5 days, followed by a 10 day recovery period as described in Section 2.3.13. The amount of food consumed by each DSS treated mouse was weighed daily, and then given to a pair fed, genotype and sex matched control mouse, which received un-supplemented drinking water. The mice were then culled, blood collected and dissected. The distal colon was isolated and snap frozen in a hexane bath as described in Section 2.5.2. One tibia was also snap frozen, and the second tibia and two femurs were fixed in 10% NBF. The mice were x-rayed at days 1, 8 and 15 to allow measurement of long bone lengths. Daily measurements were taken for weight, crown to rump lengths and health scores. They were injected with calcein at day 10 and with BrdU at day 14. The study design is shown in Table 7.1.

Day 1	Day 2	Day 3	Day 4	Day 5	Day 6	Day 7	Day 8	Day 9	Day 10	Day 11	Day 12	Day 13	Day 14	Day 15
X-ray 4% DSS in water	4% DSS in water			X-ray		Calcein Injection				BrdU Injection	Cull, X-ray Blood collected Dissected			

Table 7.1. Main DSS study experimental design.

7.3.3. Analysis of Growth Plate Dynamics

5 days prior to cull, mice received a calcein injection as described in Section 2.3.9. Upon sacrifice, tibias were dissected. One tibia was snap frozen in a hexane freezing bath and cryostat sections cut for calcein analysis, as described in Section 2.5.2. The distance between the chondro-osseous junction and the mineralising front was measured at 10 points along the growth plate on two sections per mouse under UV light using a Nikon Eclipse TE300 microscope.

The other tibia was fixed in 10% NBF for 24hrs then decalcified in 10% EDTA, paraffin embedded and cut as described in Section 2.5.1. Sections were analysed for BrdU labelling as described in Section 2.5.3. Sections were also analysed for zone widths by toluidine blue staining, as described in Section 5.4.2.

7.4. Results

7.4.1. The Effects of LPS Challenge on Growth in WT and SOCS2^{-/-} Mice

Lipopolysaccharide (LPS) challenge has been widely used as a reproducible model of systemic inflammation. LPS is a bacterial endotoxin that causes a phagocyte mediated widespread increase in inflammatory cytokines such as IL-6, IL-1 β and TNF α which have toxic effects including sickness, malaise, weight reduction and, at high doses, mortality (Rivera *et al.*, 1998; Fortier *et al.*, 2004; Ashdown *et al.*, 2006).

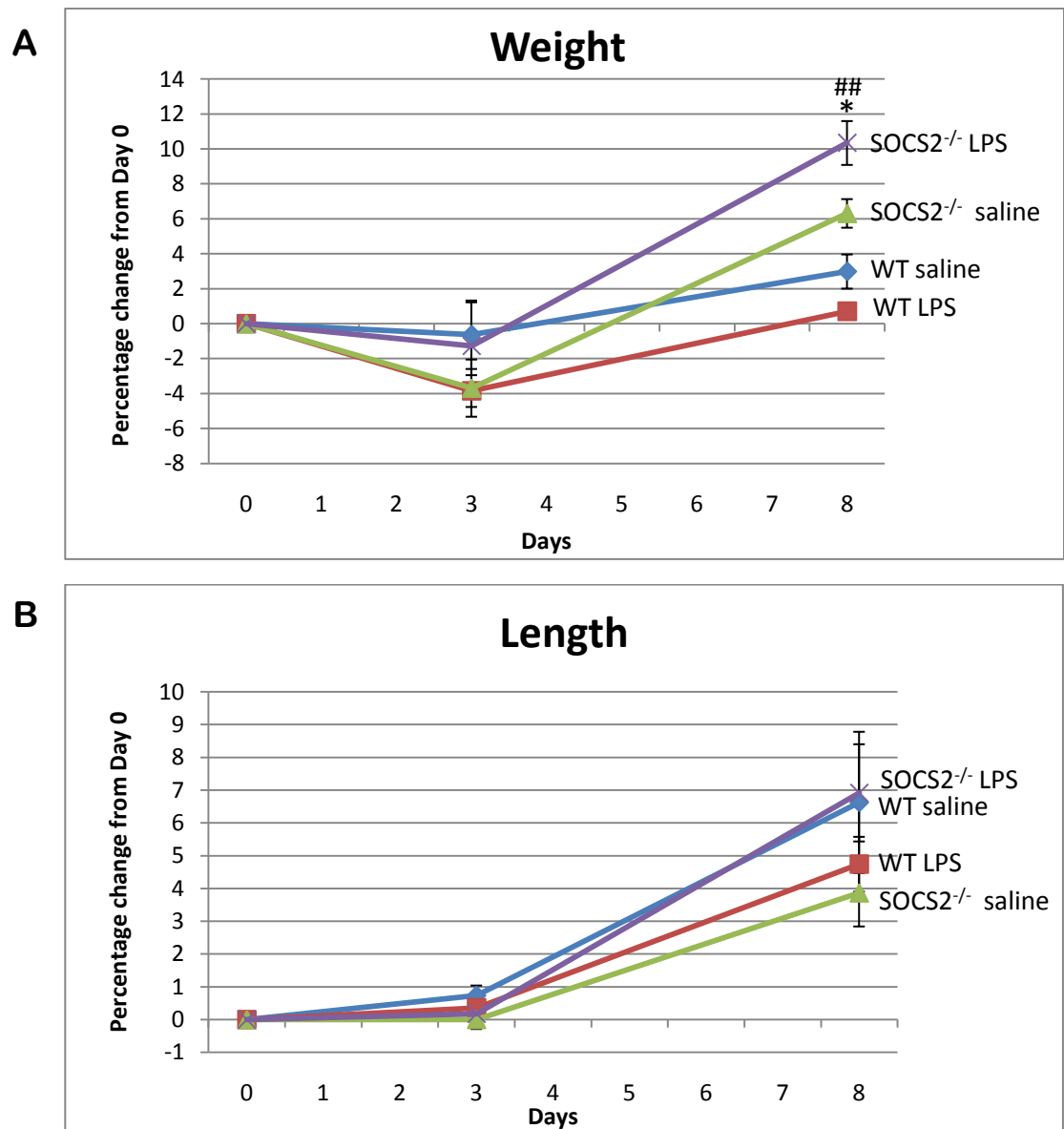


Figure 7.1. Growth of mice treated with LPS. 4-week old WT and SOCS2^{-/-} mice were injected with 50µg/kg LPS for 7 days, with saline controls (Days 1-7). (A) Weight measurements were taken at days 0, 3 and 8. Results are expressed as mean±SEM (n=4). *P<0.05 for SOCS2^{-/-} LPS treated mice vs SOCS2^{-/-} saline controls; ##P<0.01 for SOCS2^{-/-} LPS treated mice vs WT LPS treated mice. (B) Crown to rump length measurements were also taken at days 0, 3 and 8. Results are expressed as mean±SEM (n=4).

As a pilot study investigating the effects of inflammation on growth in the absence of SOCS2, 4 week-old WT and SOCS2^{-/-} mice (n=4) were injected with 50µg/kg LPS daily for a 7 day period, with saline controls. This dose of LPS was used as it is consistent with the dose used by Fortier *et al.*, and is lower than that used by many other authors thus unlikely to cause mortality (Fortier *et al.*, 2004). 4-week old mice were used as this is after the overgrowth phenotype appears in SOCS2^{-/-} mice, and is an age before adult height is reached so the mice are still growing, allowing any growth retardation to be observed. Body lengths and weights were measured at day 0 (24hrs before first LPS injection), day 3 and day 8 (24hrs after LPS injection) (Figure 7.1).

WT mice treated with LPS showed a non-significant trend of reduced body weight and length over the 8-day period compared to WT controls. An opposite effect was observed in SOCS2^{-/-} mice treated with LPS which grew more than SOCS2^{-/-} mice treated with saline, with a significant increase in body weight by day 8 (P<0.05). SOCS2^{-/-} mice treated with LPS showed much greater growth than WT mice treated with LPS, with significant increased body weight at day 8 (P<0.01). There was not a significant difference between SOCS2^{-/-} mice treated with saline and WT mice treated with saline. These results indicate that the removal of SOCS2 may act to protect from LPS induced growth retardation. None of the groups exhibited significant changes in body lengths throughout the study, which is probably due to the small study size (4 mice per group) and because the crown to rump measurement is hard to take accurately.

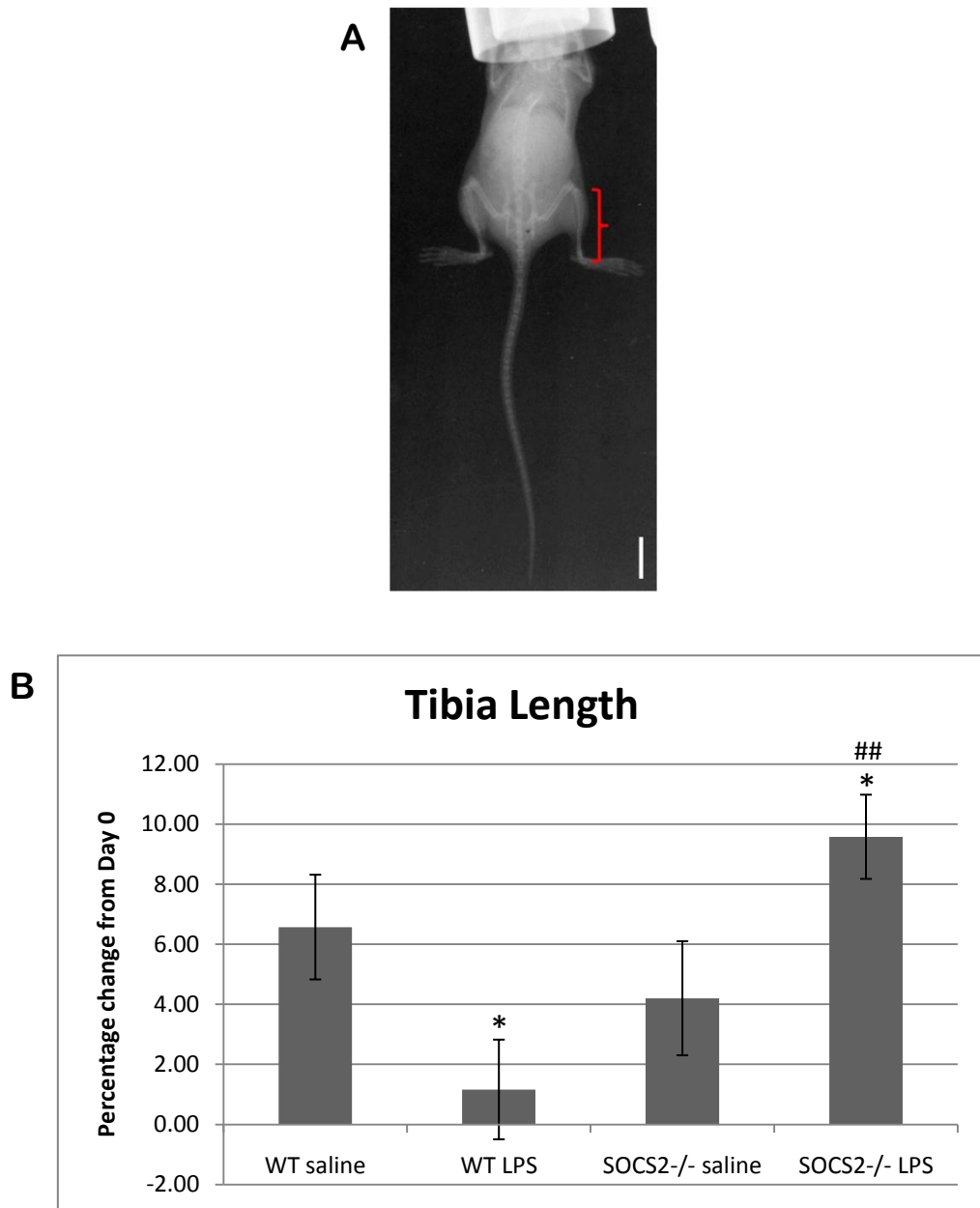


Figure 7.2. Bone growth in mice treated with LPS. 4-week old WT and SOCS2^{-/-} mice were injected with 50 μ g/kg LPS for 7 days, with saline controls. The mice were x-rayed at the start (day 0) and end (day 8) of the study to allow measurement of tibiae lengths. (A) An example of an x-ray. The red bracket indicates the distance measured for each tibia. Scale bar = 1cm. (B) Percentage change in tibiae lengths from day 0 to day 8 for SOCS2^{-/-} and WT mice treated with LPS or saline. Data are expressed as mean \pm SEM for 2 tibiae per mouse (n=4); * P<0.05 compared to saline control for the same genotype; ## P<0.01 for SOCS2^{-/-} LPS treated mice vs WT LPS treated mice.

Tibia lengths were measured using x-ray analysis at day 0 and day 8 (Figure 7.2), to measure bone growth following LPS treatment period. In WT mice, LPS caused a significant reduction in tibia growth ($P < 0.05$). An opposite effect was observed in SOCS2^{-/-} mice, with increased tibia growth observed in response to LPS ($P < 0.05$). Consistent with the weight data, LPS treated SOCS2^{-/-} mice showed significantly higher tibia growth than WT mice treated with LPS ($P < 0.01$). There was no difference between the saline controls for the two genotypes, which is consistent with the results for weight gain and again indicates that inflammatory induced growth retardation may be prevented by the removal of SOCS2.

7.4.2. The Effect of LPS Challenge on Growth Plate Morphology and Endochondral Growth Rate

At the end of the LPS study described in Section 7.4.1, both tibiae were dissected from each mouse to analyse the effects of LPS treatment on growth plate dynamics. One tibia was used to analyse growth plate zone widths in WT and SOCS2^{-/-} mice treated with LPS or saline (control), using toluidine blue staining (Figure 7.3). The second tibia was used to measure the mineral apposition rate of endochondral growth in LPS treated WT and SOCS2^{-/-} mice, by analysing calcein labelling (Figure 7.4).

WT mice treated with LPS had wider growth plates than WT control mice ($P < 0.05$), associated with increased hypertrophic zone size ($P < 0.05$) and no difference in the proliferative zone. There were no significant changes in zone widths of SOCS2^{-/-} mice treated with LPS compared to control SOCS2^{-/-} mice. Control SOCS2^{-/-} mice exhibited wider growth plates than WT control mice ($P < 0.05$), which was coupled with a significant increase in SOCS2^{-/-} hypertrophic zones ($P < 0.01$). Similarly, increased growth plate and hypertrophic zone widths were found for SOCS2^{-/-} mice treated with LPS compared to LPS challenged WT mice ($P < 0.05$).

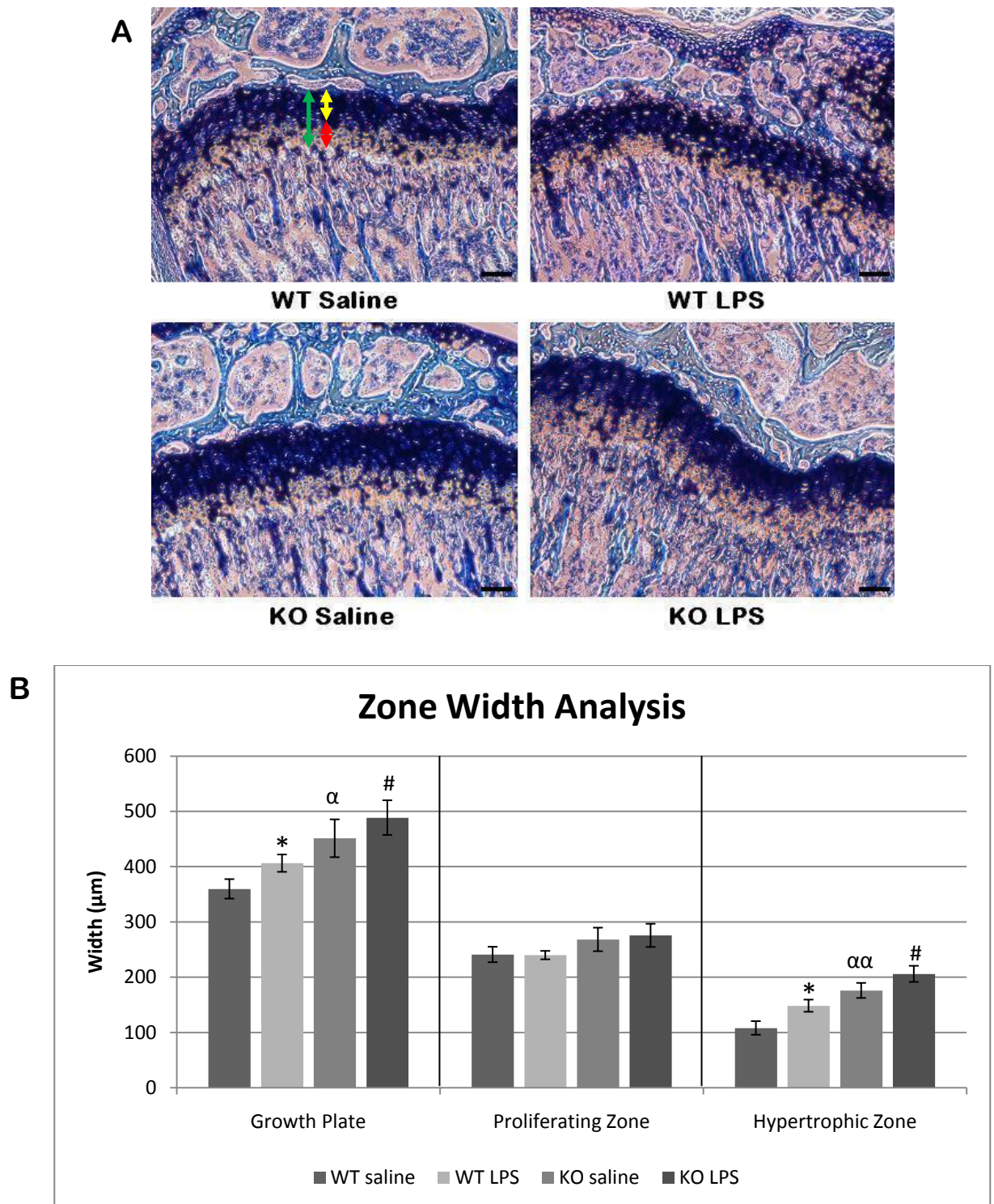


Figure 7.3. Toluidine blue staining in growth plates from mice treated with LPS. Analysis of growth plate zone widths in tibiae from LPS treated WT and SOCS2^{-/-} (KO) mice, with saline controls. (A) Paraffin embedded sections were stained with toluidine blue to allow measurement of zone widths. Arrows show examples of total growth plate width (green), proliferating zone width (yellow) and hypertrophic zone width (red). Scale bars = 100μm. (B) Graph of results of growth plate zone widths, expressed as mean±SEM for 2 sections per mouse (n≥3); *P<0.05 for WT LPS compared to WT saline; α P<0.05, ααP<0.01 for SOCS2^{-/-} saline compared to WT saline; # P<0.05 for SOCS2^{-/-} LPS compared to WT LPS.

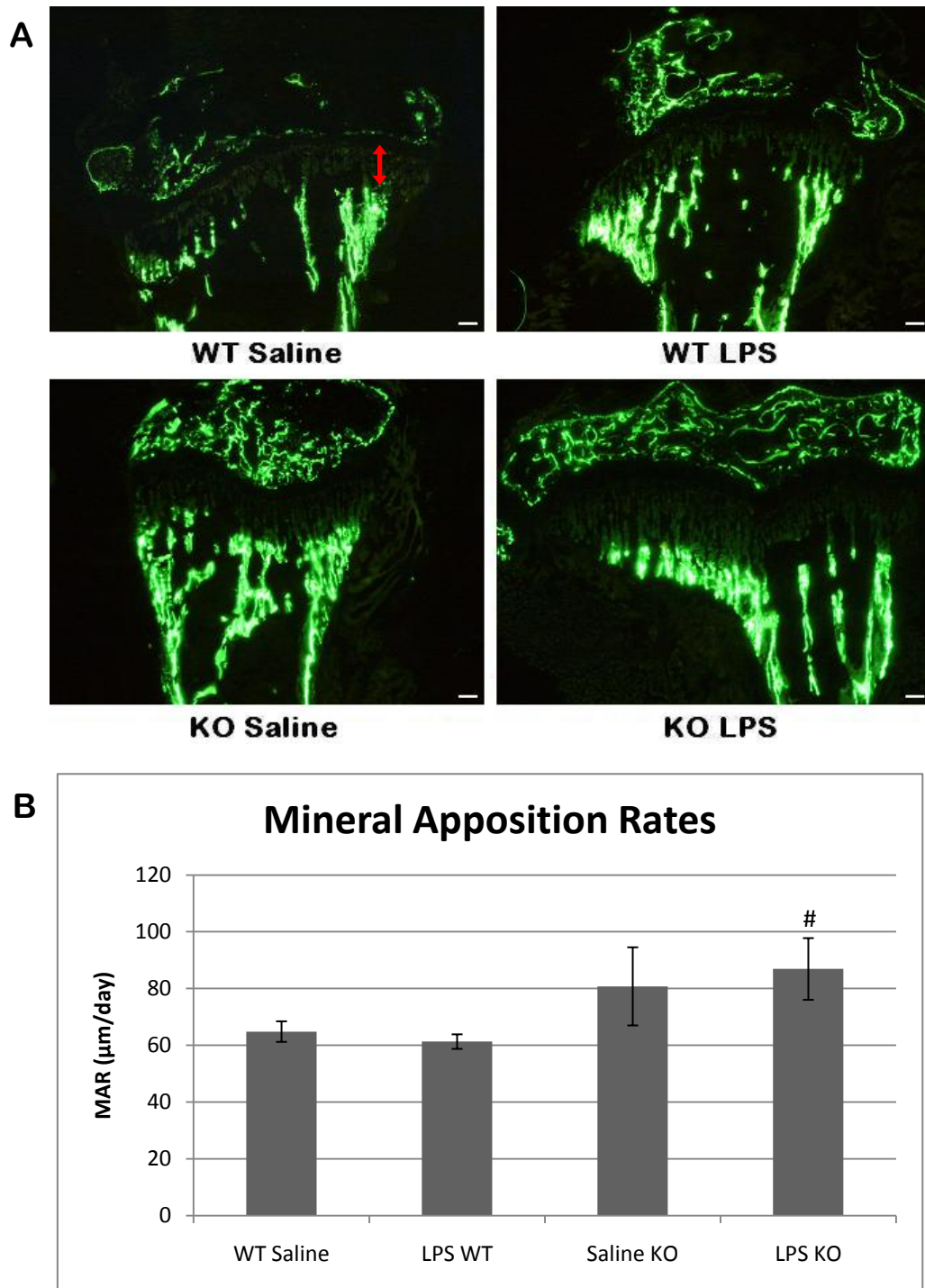


Figure 7.4. Calcein labelling in mice treated with LPS. Measurement of endochondral mineral apposition rate in tibiae from LPS treated WT and SOCS2^{-/-} (KO) mice, with saline controls, using calcein labelling. (A) Sections showing calcein labelling of mineralised trabecular bone in frozen tibia sections. Examples are shown for LPS and saline treated WT and SOCS2^{-/-} mice. Daily mineral apposition rate was calculated by measuring the distance from the chondro-osseous junction to the calcein labelled mineralisation front, as indicated by the red arrow, and dividing by the number of days from calcein injection to cull (5 days). Scale bars = 100μm. (B) Graph of results of mineral apposition rates (MAR), expressed as mean±SEM for 2 sections per mouse (n≥3); # P<0.05 for SOCS2^{-/-} LPS compared to WT LPS.

There was no significant difference in mineral apposition rate of WT mice treated with LPS compared to WT control mice, nor in LPS challenged SOCS2^{-/-} mice compared to SOCS2^{-/-} controls. SOCS2^{-/-} mice treated with LPS did show significantly increase in growth rate compared to LPS treated WT mice (P<0.05).

7.4.3. DSS Induced Colitis Concentration Curve

One of the most widely used murine models of experimental colitis is the use of DSS to induce colitis. DSS can be administered orally via the drinking water, and is toxic to intestinal epithelial cells causing the release of antigens and subsequent inflammation and damage to the intestinal crypts of the distal colon (Dieleman *et al.*, 1998; Hamdani *et al.*, 2008; Harris *et al.*, 2009). This leads to the up-regulation of pro-inflammatory cytokines and subsequent negative effects on health, including inflammation of the intestine and associated bloody stools, impaired growth with decreased bone length and reduced bone volume (Cooper *et al.*, 1993; Williams *et al.*, 2001; Hamdani *et al.*, 2008; Harris *et al.*, 2009; DeBoer *et al.*, 2010). DSS can be used to cause acute colitis (DSS administered in water for up to 14 days) or chronic colitis (DSS administered for up to 14 days followed by a 1-5 week recovery period) (Cooper *et al.*, 1993; Dieleman *et al.*, 1998; Williams *et al.*, 2001; Melgar *et al.*, 2007). Williams and colleagues reported that transgenic mice over-expressing GH exhibited enhanced survival and better intestinal repair following DSS-induced colitis (Williams *et al.*, 2001). The LPS pilot study indicated that SOCS2^{-/-} mice are less susceptible to inflammatory induced growth retardation. The DSS model of colitis is a more physiological method of measuring the effects of inflammation than LPS, and the results by Williams and colleagues support the hypothesis that SOCS2^{-/-} mice are protected from the growth retardation, and associated impaired bone growth, that occurs following increased inflammatory cytokines.

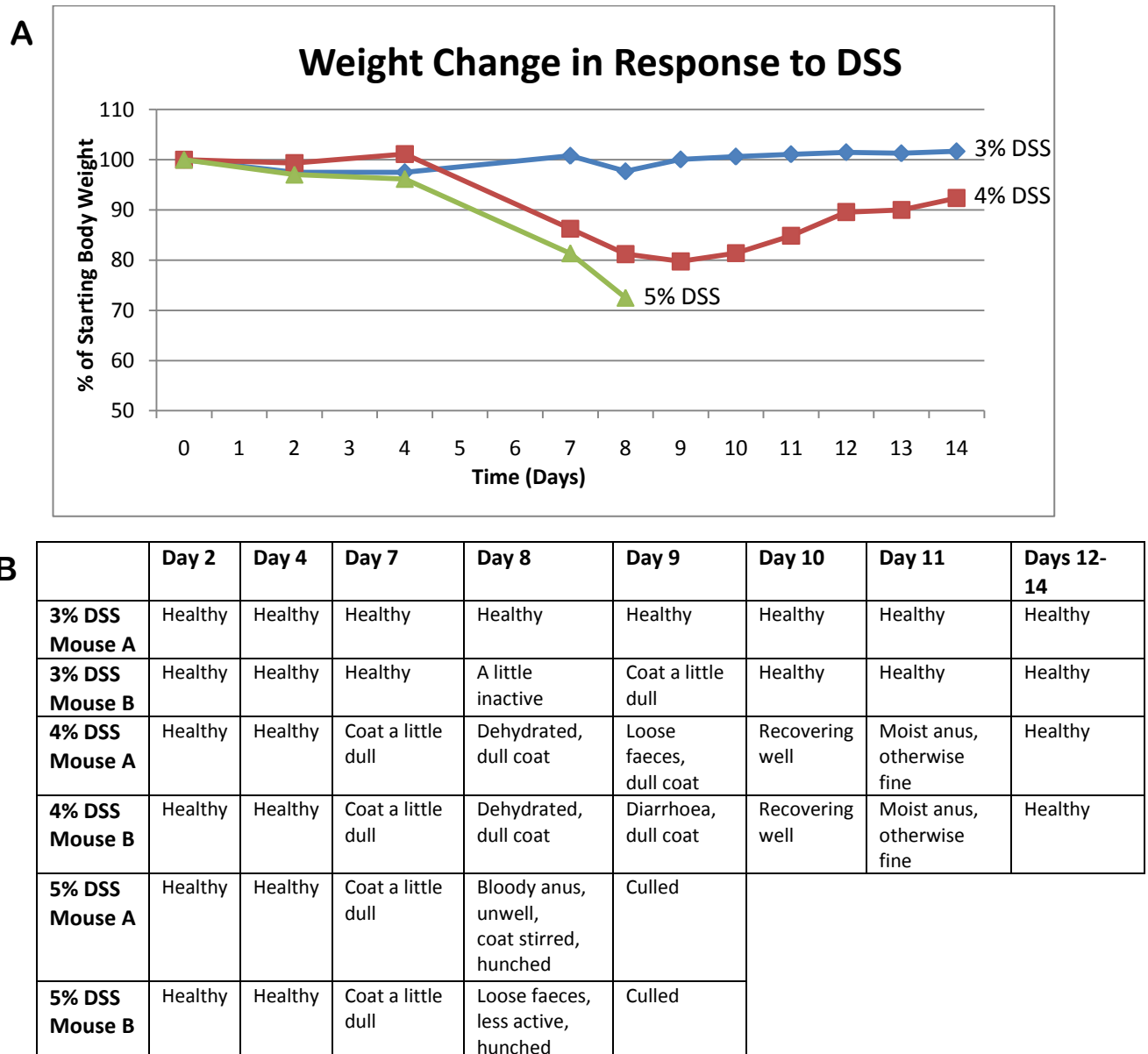


Figure 7.5. DSS concentration curve. 8-week old WT mice were treated with 3%, 4% or 5% DSS for 5 days, followed by a 10 day recovery period. (A) The mice were weighed regularly throughout the study to monitor their health and disease status. Results are expressed as mean (n=2). Any mice whose weight dropped more than 25% were culled in accordance with the home office licence. (B) The health of the mice was also monitored throughout the study and noted. This again allowed the disease status to be monitored, and any mice whose health deteriorated drastically were culled.

Previous authors have used different concentrations of DSS depending on the mouse strain, and it has also been reported that water intake varies between mouse strains (Tordoff *et al.*, 2007). Therefore it was necessary to conduct a small pilot study investigating which concentration of DSS was appropriate in the SOCS2^{-/-} line. For this, WT mice were given 3%, 4% or 5% DSS in their drinking water for a 5 day period, followed by a 10 day recovery. Their weights were measured throughout, and their health was scored (Figure 7.5). Any mice that lost more than 25% of their body weight were culled in accordance with the projects Home Office animal license regulations.

Mice given 3% DSS showed very little signs of illness and minimal weight loss. 4% DSS induced a drop of weight between days 5 and 9 to approximately 80% of the starting weight, which was coupled with loose faeces and dull coats. This was followed by a recovery with weight increasing from day 9 onwards, and associated improved health. Mice receiving 5% DSS also lost weight from days 5 to 9 but this was a more severe weight loss, and was associated with ill health including hunched posture, inactivity and bloody anus. These mice were culled at day 9 as their weight had dropped by over 25%, and they were extremely unwell.

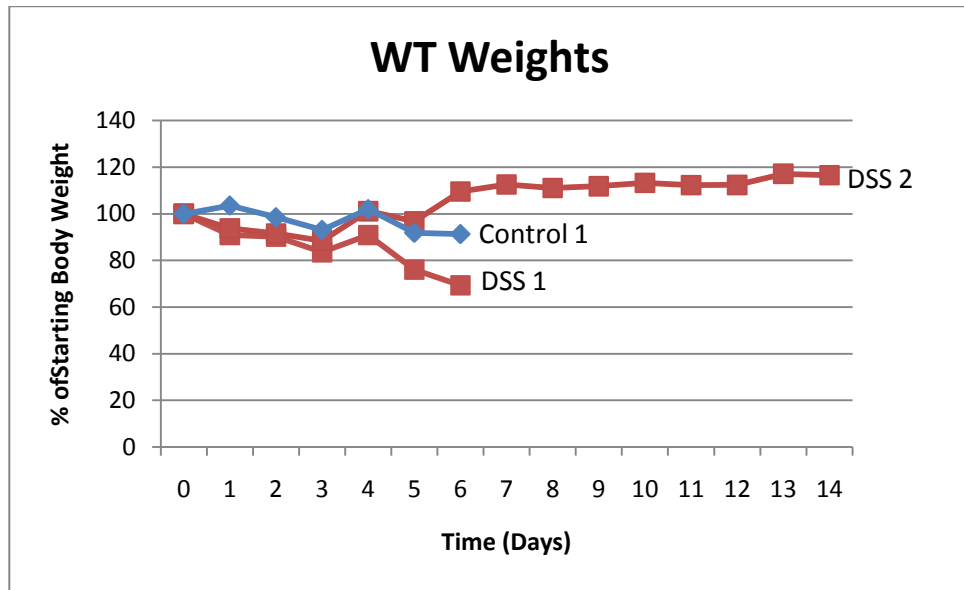
7.4.4. Main DSS Study

The results from the pilot studies detailed in Section 7.4.3 indicate that 4% DSS is the best dose to use, as 5% caused severe illness and extreme body weight loss while 3% DSS had little effect. 4% DSS resulted in weight loss from day 5, associated with some illness including loose stools and dull coat, followed by a recovery phase where the mice gained weight again and their health recovered. This is similar to studies by other authors (Williams *et al.*, 2001; Melgar *et al.*, 2007), and was considered to be a good protocol for investigating the effects of inflammatory disease on growth in SOCS2^{-/-} mice. The weight loss observed in DSS treated mice may be attributed to a reduction in food intake (Harris *et al.*, 2009; DeBoer *et al.*, 2010). In order to separate weight loss as a result of reduced food intake from inflammation-induced weight loss it is necessary to pair feed control mice with DSS treated mice. This method has been previously described by Ballinger *et al.*, who

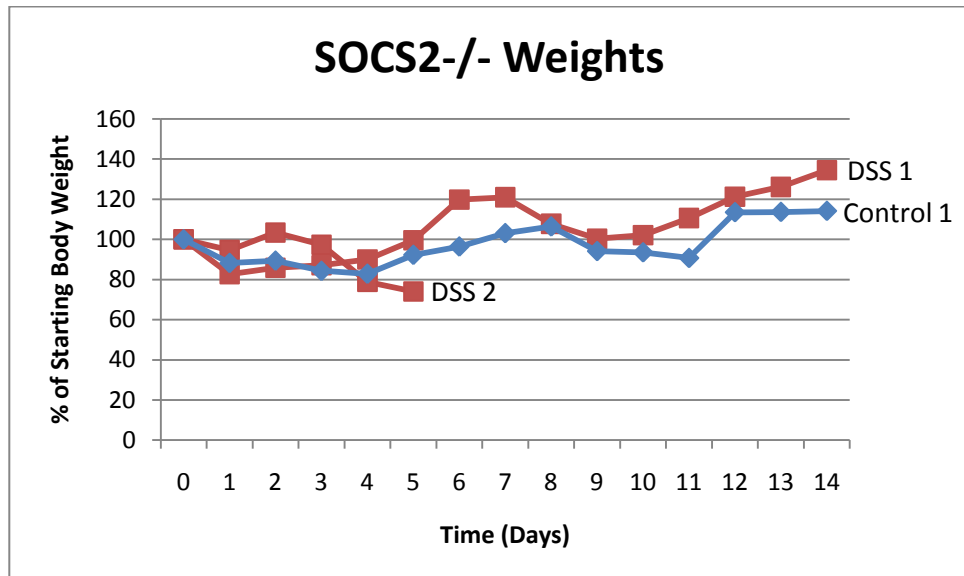
used a different model of colitis (trinitrobenzenesulphonic acid (TNBS) induced) to demonstrate that mice whose food intake was paired with that of the TNBS treated mice grew less than control mice that had access to unlimited food, but still grew more than the colitic mice (Ballinger *et al.*, 2000).

In order to investigate the effects of DSS induced colitis on growth SOCS2^{-/-} mice, 4-week old male SOCS2^{-/-} and WT mice were treated with 4% DSS for 5 days followed by a 10 day recovery. Their daily food intake was weighed every 24hrs and administered to genotype matched control mice. All mice were weighed, measured crown to rump and scored for health daily (Figure 7.6). The experiment started with 3 male SOCS2^{-/-} and 3 male WT mice, as these were the mice available at the desired age, with the intention to continue with more mice when available to achieve 6 mice within each control and experimental group. Within each genotype, two mice were challenged with DSS and the third mouse was used as a pair fed control to one of the DSS treated mice. The weight of food consumed daily for the other DSS treated mouse in each genotype was recorded so that it could be administered to a pair fed control at a later date.

A i



ii



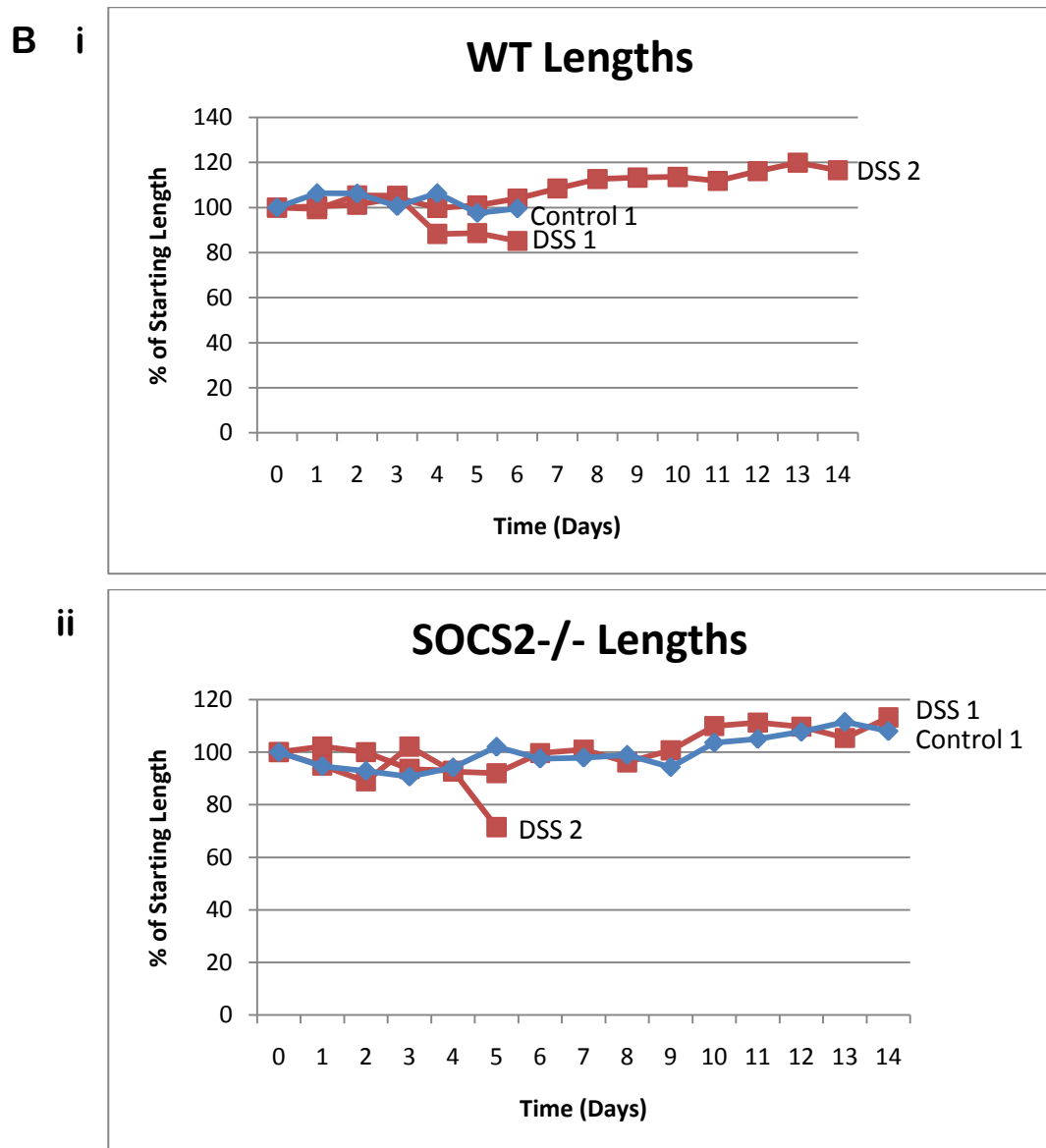


Figure 7.6. Main DSS study. 4-week old male mice were treated with 4% DSS for 5 days, followed by a 10 day recovery period. Control mice were pair fed to a DSS treated, genotype-matched mouse. (A) The mice were weighed daily throughout the study to monitor their health and disease status. Results are shown for (i) WT and (ii) SOCS2^{-/-} mice. Any mice whose weight dropped more than 25% were culled in accordance with the home office licence. (B) The mice were also measured from crown to rump daily as another indication of their health and growth. Results are shown for (i) WT and (ii) SOCS2^{-/-} mice

The results from this first group of mice were unexpected. One of the DSS treated WT mice remained healthy throughout the study and had minimal weight loss, while the other had much more significant weight loss that breached the 25% loss threshold and had to be culled. It showed signs of illness, including a bloody anus and hunched body. The control mouse was pair fed to this latter DSS treated mouse, and lost some weight but not as much as the DSS treated mouse. SOCS2^{-/-} mice treated with DSS gave very similar results, with one mouse losing a small amount of weight before gaining weight while the other lost a significant amount of weight and died. This latter mouse was extremely ill from day 4 with a lot of blood loss from the anus, dehydration and a hunched body, shown by the body weight measurements. To try and aid recovery its food was soaked in water, but its health deteriorated very rapidly and it died on day 6. The SOCS2^{-/-} control mouse was pair fed with the first DSS treated mouse, and it showed a similar pattern of weight fluctuations over the study, and gained slightly less weight than the DSS treated mouse.

Such dramatic changes in response to DSS in different mice of the same genotype were unexpected. To confirm the result was not an anomaly, the study was repeated using 3 SOCS2^{-/-} and 8 WT mice (each genotype consisting of littermates). All mice were treated with 4% DSS, so that if there was still a 50% cull/death rate pair fed control mice would not be wasted. The mice were again 4-weeks old, and this time were a mix of males and females as limited numbers of male mice were available. The mice received 4% DSS for 5 days followed by a 10 day recovery. All mice were weighed, measured crown to rump and scored for health daily (Figure 7.7). The daily weight of food consumed for each mouse was recorded so that it could be administered to a pair fed control (genotype, age and sex-matched) at a later date.

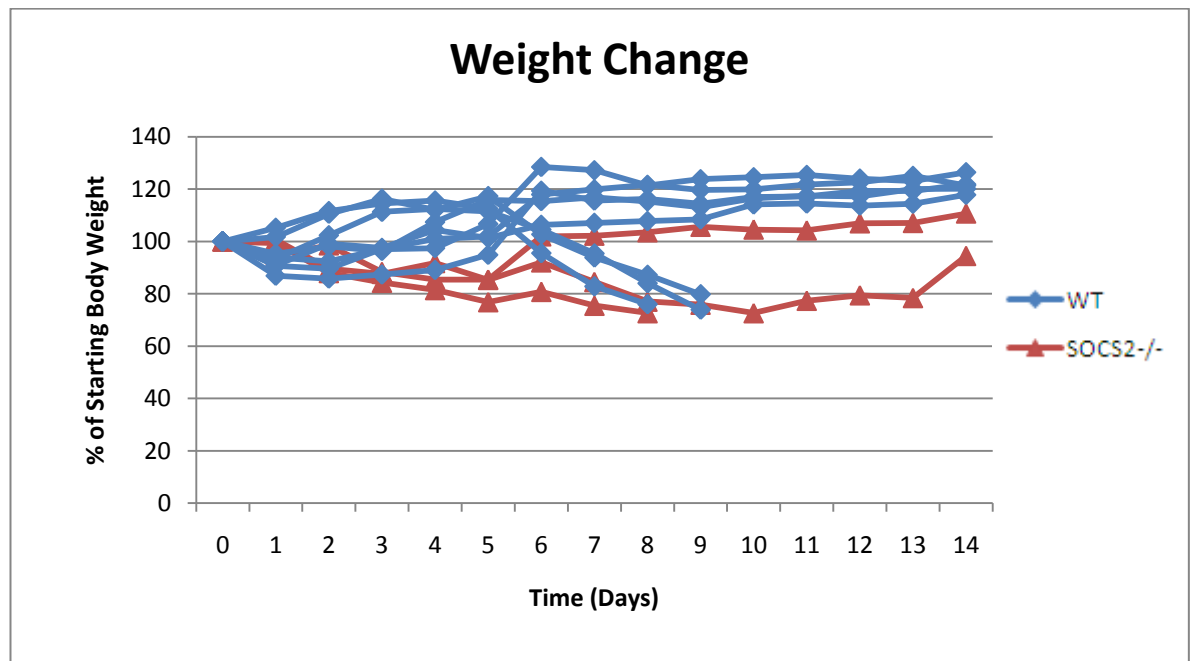


Figure 7.7. SOCS2^{-/-} and WT mice treated with DSS. 4-week old mice were treated with 4% DSS for 5 days, followed by a 10 day recovery period. The mice were weighed daily throughout the study to monitor their health and disease status. Results are shown for WT and SOCS2^{-/-} mice. Any mice whose weight dropped more than 25% were culled in accordance with the home office licence.

Again there were large mouse to mouse differences, with some mice showing very little ill health and weight loss in response to DSS while others became very ill and were culled due to large weight loss and/or ill health. This was seen in both genotypes, with both genders showing the same results. Because of these vast differences the colitis model was considered unreliable, and the study was stopped. The planned additional analysis was therefore not carried out, *i.e.* bone lengths, bone phenotype (mineral apposition rate and growth plate analysis), and serum analysis (inflammatory cytokines, bone turnover markers and IGF-1).

7.5. Discussion

Growth retardation is frequently observed during chronic inflammatory IBD and JIA (Simon *et al.*, 2002b; MacRae *et al.*, 2006c; Tilg *et al.*, 2008). In Chapter 6, it was found that the addition of GH or IGF-1 to SOCS2^{-/-} metatarsals reduced their growth inhibition in response to the inflammatory cytokine IL-1 β . This suggests that the removal or inhibition of SOCS2 and the consequent increase in GH signalling can help restore physiological endochondral growth in inflammatory situations, offering an alternative to GH therapy which can have undesired side effects such as insulin resistance. To test this hypothesis further, the growth of SOCS2^{-/-} and WT mice was analysed in a small pilot study using LPS to induce systemic inflammation.

Analysis of weight as an indication of growth showed that SOCS2^{-/-} mice challenged with LPS grew significantly more than WT mice challenged with LPS over a 7 day period, and also grew more than saline control SOCS2^{-/-} mice. The same changes were seen for tibia lengths. In contrast, WT mice treated with LPS grew less than WT saline controls, a difference that was not significant for weight but was significant for tibia length. The fact that SOCS2^{-/-} mice treated with LPS grew more than LPS treated WT mice, but that there was not a significant difference between WT and SOCS2^{-/-} saline controls, indicates that the removal of SOCS2 does appear to offer protection from growth retardation during chronic inflammation. The increased growth of SOCS2^{-/-} mice treated with LPS compared to saline control SOCS2^{-/-} mice indicates that in the absence of SOCS2, inflammatory

cytokines may actually stimulate growth. Martensson and colleagues found that the inflammatory cytokine IL-1 β can stimulate metatarsal growth at low concentrations, indicating that the effects of inflammatory cytokines are dose dependant (Martensson *et al.*, 2004). Inflammatory cytokines have been shown to stimulate STAT signalling, as demonstrated using IL-1 β in Chapter 3, so it is possible that in the absence of SOCS2 inflammatory cytokines act to stimulate growth through activation of the JAK/STAT pathway. However, closer analysis of the growth plate and of endochondral growth rate did not find a difference between SOCS2^{-/-} mice treated with saline and LPS. Consistent with increased endochondral growth rate, SOCS2^{-/-} mice treated with LPS had wider growth plates than WT mice treated with LPS, with increased hypertrophic zones. Hypertrophic cell height has been positively correlated with endochondral bone growth in previous studies. The same was seen for SOCS2^{-/-} saline controls compared to WT saline controls, which is consistent with the fact that the overgrowth phenotype occurs in SOCS2^{-/-} mice from 3-weeks of age and is associated with wider growth plates, as shown by MacRae and colleagues and in Chapter 4 (MacRae *et al.*, 2009). However these groups of mice didn't show significant changes in weight or tibia length, probably because it is soon after the start of the overgrowth phenotype and weight is very variable between individuals so small changes are hard to detect with a small number of mice. WT mice treated with LPS also had wider growth plates than WT saline control mice as the result of increased hypertrophic, but not proliferative, zone width. This could be the result of an inflammatory induced arrest in chondrocyte differentiation and apoptosis and therefore not indicative of increased bone growth. There was no difference in mineral apposition rates between LPS treated mice and their saline controls, indicating the increased growth plate widths did not lead to increased endochondral growth. There was an increase in mineral apposition rate in SOCS2^{-/-} mice challenged with LPS compared to LPS treated WT mice. This is consistent with the increased tibia length and wider growth plate widths observed and suggests that SOCS2^{-/-} mice are protected from inflammatory cytokine induced growth retardation.

To extend the LPS pilot data into a more physiological disease setting, a DSS-induced model of colitis was used. This is a widely used and well studied disease model that leads to the up-regulation of pro-inflammatory cytokines which have negative effects on health, including growth retardation (Cooper *et al.*, 1993; Williams *et al.*, 2001; Hamdani *et al.*, 2008; Harris *et al.*, 2009; DeBoer *et al.*, 2010). It was necessary to carry out a concentration curve with DSS in the mice to establish which concentration should be used in the SOCS2^{-/-} mouse line. The results for this were promising; with 3% DSS causing very minimal signs of illness, while 4% DSS induced a period of weight loss and ill health followed by a recovery and 5% DSS caused more severe illness and weight loss that resulted in the mice being culled in accordance with the home office regulations. These results were consistent with similar studies by other authors (Williams *et al.*, 2001; Harris *et al.*, 2009), and indicated that for this mouse line 4% DSS was the optimum concentration required to induce colitis. Therefore a study was carried out to investigate the effects of colitis on growth in SOCS2^{-/-} mice compared to WT. Unfortunately this study was not completed as the results in the pilot study were not reproduced, with individual mice reacting very differently to the DSS treatment. Some mice showed very little signs of illness, with minimal weight loss, similar to those treated with 3% DSS in the pilot study. Other mice became very ill and died or had to be culled due to severe weight loss, similar to those treated with 5% DSS in the pilot study. These mixed results were very confusing, and were not influenced by genotype, sex or the starting weight of the mice. Unfortunately, due to the time and financial constraints of this studentship the study could not be continued. It is possible the different results between the mice was due to their age as the pilot study was conducted in 8-week old mice that were available and not required for other studies, whereas the main study used 4-week old mice so that they were at an age of rapid growth so that the effects on growth could be monitored. These mice had therefore only recently been weaned and separated from their mother and littermates; so that it is possible the change in environment had a negative effect on some mice. The majority of other studies using DSS have been performed in 7- to 9-week old mice (Sävendahl *et al.*, 1997; Dieleman *et al.*, 1998; Melgar *et*

al., 2007; Hamdani *et al.*, 2008), however Harris and colleagues used 4-week old C57BL/6 mice (the same strain as SOCS2^{-/-} mice) to induce colitis using 5% DSS (Harris *et al.*, 2009). They were able to induce colitis characterised by inflammatory bowel disease, decreased body weight and reduced bone mass (Harris *et al.*, 2009). However, in accordance with American animal ethical approval, their mice were allowed to drop their body weight to approximately 66% of their starting weight, which is almost 10% more than permitted for this study (Harris *et al.*, 2009). A study by Williams and colleagues showed that mice over-expressing GH enhanced the survival of mice treated with DSS, and that this occurred despite the GH transgenic mice consuming more DSS treated water than WT mice (Williams *et al.*, 2001). The quantity of water consumed by each mouse was not measured in this study, but it is likely that the amount consumed will affect disease severity.

7.6. Conclusion

A pilot study using LPS to induce inflammation in WT and SOCS2^{-/-} mice found that SOCS2^{-/-} mice treated with LPS grew more than LPS treated WT mice, demonstrated by increased body weight, tibia length, growth plate width, hypertrophic zone width and mineral apposition rate. WT mice treated with LPS grew less than WT saline controls, although this was only significant for tibia length. These findings indicate that the removal of SOCS2 may help to protect from inflammation induced growth retardation. To further test this hypothesis, the DSS model was used to induce colitis in SOCS2^{-/-} and WT mice. However, the results from this study were inconclusive as there was a large mouse to mouse variation for WT and SOCS2^{-/-} mice. The reasons for this are unclear and further investigations are required.

CHAPTER 8

GENERAL DISCUSSION AND FUTURE WORK

8. General Discussion and Future Work

8.1. General Discussion

It is well recognised that GH/IGF-I signalling is negatively regulated by SOCS proteins, in particular CIS and SOCS1-3, but little information exists on the effects of SOCS proteins in regulating endochondral bone growth. Greenhalgh and colleagues have confirmed that the GH/IGF-1 axis is the key signalling pathway regulated by SOCS2 and that increased linear bone growth occurs in SOCS2^{-/-} mice despite normal systemic IGF-I levels (Metcalf *et al.*, 2000; Rico-Bautista *et al.*, 2005). Studies by MacRae and colleagues have demonstrated that SOCS2 plays an important role in negatively regulating longitudinal bone growth (MacRae *et al.*, 2009). These data emphasise the importance of local GH signalling in endochondral growth and confirms the value of the SOCS2 null mouse for studying the autocrine/paracrine effects of GH on chondrocyte dynamics and bone growth. The aim of this study was to determine the role of SOCS2 in mediating chondrocyte GH signalling, proliferation and linear bone growth.

It is recognised that local GH infusion into the growth plate stimulates growth by inducing proliferation of the growth plate germinal cells (Ohlsson *et al.*, 1992a), however it is unclear if these effects are direct or independent of local IGF-I production (Govoni *et al.*, 2007). The precise STAT family member(s) activated during GH signalling in growth plate chondrocytes is largely unknown, although studies by Gevers and colleagues have suggested a role for STAT5 activation (Gevers *et al.*, 2009). This present study has shown that in addition to STAT5 activation GH also phosphorylates STAT1 and STAT3 in chondrocytes. Although IGF-I independent effects cannot be ruled out, it is likely that this STAT activation leads to increased IGF-1 expression, which serves to initiate multiple signalling pathways to cause increased chondrocyte proliferation and linear bone

growth (Hoshi *et al.*, 2004; MacRae *et al.*, 2007a; Klammt *et al.*, 2008). No evidence was obtained to suggest that IGF-1 is capable of signalling via STATs in chondrocytes and despite the observations by Zong and colleagues this was expected as the IGF-1 receptor does not contain specific tyrosine motifs recognised by STAT proteins (Stahl *et al.*, 1995; Zong *et al.*, 2000; Decker and Kovarik, 2000).

The *in vitro* experiments clearly showed that SOCS2 expression influenced the ability of GH to activate STAT1, STAT3 and STAT5 in chondrocytes. This was particularly noticeable with STAT5, whose activation in SOCS2^{-/-} cells was greatly increased and prolonged in response to GH challenge, suggesting that STAT5 is the major STAT responsible for regulating the pace of endochondral bone growth. The importance of STAT5 in this process is also suggested by the observation that the SOCS2^{-/-} overgrowth phenotype is dependent on STAT5b downstream signalling events (Greenhalgh *et al.*, 2002a). Consistent with the raised levels of STAT signalling found in SOCS2^{-/-} mice, chondrocytes over-expressing SOCS2 show reduced STAT activation in response to GH. Of interest, mice that over-express SOCS2 do not show limited growth as may be expected, but in fact, also exhibit an overgrowth phenotype (Greenhalgh *et al.*, 2002b). It seems likely, therefore, that SOCS2 exhibits dual effects on GH signalling that are dose dependant (Greenhalgh *et al.*, 2002b; Flores-Morales *et al.*, 2006). One hypothesis is that at physiological levels, SOCS2 inhibits GH signalling by preventing STAT activation at the GHR, but at higher levels SOCS2 can inhibit the actions of other SOCS proteins (such as SOCS1 and 3) which are more effective at inhibiting GH signalling (Favre *et al.*, 1999; Greenhalgh *et al.*, 2002b). It was found that neither SOCS1 nor SOCS3 respond to GH in growth plate chondrocytes, thus at the growth plate level increased levels of SOCS2 may only act to inhibit STAT signalling and not influence other SOCS proteins. This is consistent with recent findings by Kiu and colleagues who reported that SOCS2 does not regulate SOCS3 signalling in hematopoietic cells (Kiu *et al.*, 2009). Therefore, in

transgenic mice over-expressing SOCS2, the overgrowth phenotype may be mediated by the systemic effects of GH signalling (Greenhalgh *et al.*, 2002b).

The increased STAT signalling in SOCS2^{-/-} chondrocytes is likely to be responsible for the increased chondrocyte proliferation and linear growth observed in SOCS2^{-/-} metatarsals in response to GH. The observation that WT and SOCS2^{-/-} metatarsals responded similarly to IGF-1 in culture is consistent with the observed lack of IGF-1 induced STAT phosphorylation in SOCS2^{-/-} chondrocyte and raises doubts as to the physiological significance of the reported SOCS2 binding to the IGF-1 receptor (Dey *et al.*, 1998; Michaylira *et al.*, 2006b). Stimulation of metatarsal growth by IGF-1 has been previously reported, with some investigators also reporting a lack of GH effect on metatarsal growth (Coxam *et al.*, 1996; Mushtaq *et al.*, 2004; Martensson *et al.*, 2004; MacRae *et al.*, 2006a; MacRae *et al.*, 2007a). However, Scheven and Hamilton did report GH stimulatory effects on metatarsal length, which is in contrast to the data of this present study (Scheven and Hamilton, 1991). These studies did show that SOCS2^{-/-} metatarsals increased in growth in response to GH, suggesting that modulation of SOCS2 expression may be a critical method of altering GH insensitivity and raising local IGF-1 concentration. The stimulation of growth of SOCS2^{-/-} metatarsals by GH, which was associated with increased chondrocyte proliferation, was suppressed by the PI3K inhibitor LY-294002. Whilst not clarifying if the direct effects of GH on bone growth are IGF-1 dependent or not, these studies do show that the positive effects of GH on bone growth are mediated by PI3K either through the downstream signalling actions of IGF-1 or by directly increasing steady state IGF-1 mRNA levels (Shoba *et al.*, 2001).

If the increased linear bone growth observed in the SOCS2^{-/-} mice is an IGF-1 dependent mechanism operating at the level of the growth plate then IGF-1 mRNA expression should be increased in the chondrocytes of SOCS2^{-/-} mice. Attempts to analyse IGF-1 expression in 6-week old growth plates were unsuccessful but there were no changes in IGF-1 levels in chondrocytes isolated from 1-day old mice. This may be due to a lack of increased GH signalling at this age,

consistent with the overgrowth phenotype of $SOCS2^{-/-}$ occurring only from 3-weeks of age. Alternatively, the growth plate chondrocyte may not be the primary source of IGF-I. Recently a combination of growth plate microdissection and quantitative PCR has revealed that IGF-I mRNA levels are very low in growth plate chondrocytes suggesting that the biological importance of this source of IGF-I may be negligible (Parker *et al.*, 2007). Interestingly, these authors suggest that the source of IGF-I interacting with its chondrocyte receptor maybe derived from the surrounding perichondrium and/or bone (Parker *et al.*, 2007).

The divergence in body length and weight in $SOCS2^{-/-}$ mice was noted to occur at about 3-weeks of age and this is consistent with the knowledge that GH is the major regulator of post-natal growth in mice, where peak GH activity occurs between postnatal days 20–40 (Wang *et al.*, 2004). This divergence in body length between WT and $SOCS2^{-/-}$ mice from approximately 3-weeks of age was associated with increased rate of bone growth in which mineral apposition rate was similar in 3-week old WT and $SOCS2^{-/-}$ mice but was significantly greater in the $SOCS2^{-/-}$ mice at 6-weeks of age. This was consistent with the *in vivo* analysis of growth plate structural composition and chondrocyte proliferation measured by BrdU incorporation. The alteration in growth rate was reflected in growth plate architecture; the 6-week old $SOCS2^{-/-}$ mice had wider growth plates with significantly wider proliferative and hypertrophic zones whereas no differences were noted at 3-weeks of age. Increased STAT activation within the $SOCS2^{-/-}$ growth plate is likely to lead to increased chondrocyte proliferation which, in part, may explain the enhanced growth of the $SOCS2^{-/-}$ mice.

These findings confirm and extend previous data and raise the possibility that the changes, suggested by the *in vitro* studies, are a consequence of altered chondrocyte STAT activation (MacRae *et al.*, 2009). Whilst there were no difference in the number of proliferating cells stained positively for phosphorylated STAT5 in the $SOCS2^{-/-}$ growth plates it was not possible, due to the non-quantitative nature of immunohistochemistry, to estimate levels of activated STAT5

expression. The presence of STAT5 phosphorylation in hypertrophic chondrocytes is consistent with GHR expression in these cells (Gevers *et al.*, 2002), and the increased number of positively stained hypertrophic cells in the SOCS2^{-/-} growth plates suggests that SOCS2 can regulate longitudinal growth through the modulation of hypertrophic cell size. This notion would be consistent with the known positive effects of IGF-I on hypertrophic chondrocyte size and the recognised relationship between hypertrophic cell size and rate of bone growth (Kember, 1985; Breur *et al.*, 1991; Wang *et al.*, 1999; Mushtaq *et al.*, 2004).

Contrary to studies by MacRae and colleagues (MacRae *et al.*, 2009), chondrocyte expression of SOCS2 was not altered by inflammatory cytokines, indicating that inflammatory cytokines do not cause growth retardation by up regulating SOCS2. However, in SOCS2^{-/-} metatarsals the addition of GH and IGF-1 acted to reduce the negative effects of inflammatory cytokines on bone growth. This indicates that in the absence of SOCS2, increased GH signalling can help combat the inhibitory actions of inflammatory cytokines on longitudinal growth. To further investigate this hypothesis, chronic inflammation was induced in SOCS2^{-/-} mice. SOCS2^{-/-} mice were protected from LPS induced growth retardation, shown by increased body weight, tibia length and mineral apposition rate compared to LPS treated WT mice. These studies were extended using DSS induced colitis as a more physiological model of inflammation, but unfortunately the results were inconclusive as there was considerable variation in response to the inflammation by both genotypes.

The crucial importance of SOCS2 in mediating the local effects of GH on chondrocyte STAT activation, chondrocyte proliferation and bone growth has been demonstrated. The SOCS2^{-/-} mouse model represents an important model for studying the effects of GH through local IGF-1 production. Modulating SOCS2 may represent an effective method for improving growth, particularly during inflammation, and warrants further investigation. While recombinant human GH therapy has had promising results in treating inflammatory induced growth retardation

(Bechtold *et al.*, 2007; Simon *et al.*, 2007), its use has been associated with unpleasant side effects such as altered carbohydrate metabolism so that the development of SOCS2 antagonists may provide an alternative treatment (Bullock *et al.*, 2006). Very recent findings by Suda and colleagues, which were presented at the conference Endo 2011 in Boston, reported a patient presenting with increased height and weight as the result of a heterozygous mutation in the SOCS2 gene (Suda *et al.*, 2011). These data represent the first documentation of a human SOCS2 mutation, confirming that SOCS2 has a role in regulating GH signalling in humans and further highlights the potential clinical importance of SOCS2.

8.2. Future Work

The results found in this studentship have confirmed that SOCS2 is a critical regulator of endochondral bone growth. However there are many more questions regarding the role of SOCS2 in bone growth yet to be investigated. It has not been confirmed if the actions of SOCS2 on systemic levels of GH influence bone growth, or if the overgrowth phenotype of SOCS2^{-/-} mice is the result of increased local signalling in chondrocytes. A way of investigating this would be to generate tissue specific knockout mice with a targeted deletion of SOCS2 in growth plate chondrocytes. This could be done using the Cre recombinase-LoxP system. Similarly, while the results here suggest that neither SOCS1 nor SOCS3 regulate chondrocytes GH signalling, this could be investigated further using mice generated with SOCS1 or SOCS3 knocked-out in the growth plate. To date none of these mice have been generated.

The cellular pathways responsible for poor growth in patients with chronic inflammatory diseases such as IBD and JIA are poorly understood, and a role for SOCS2 is yet to be fully established. This study found that although SOCS2 expression was not altered in chondrocytes in response to inflammatory cytokines, the growth of SOCS2^{-/-} metatarsals was improved with the addition of GH and SOCS2^{-/-} mice appear to be protected from LPS induced inflammation. However, the use of DSS to induce colitis and associated inflammation gave mixed results with large mouse to mouse

variation in response, in both SOCS2^{-/-} and WT mice. It is possible that systemic signalling pathways are influencing the response, so that it would be interesting to use the conditional SOCS2 knockout mice described above in the DSS model of inflammation. However, a different model of inflammation may be necessary to induce a more consistent inflammatory disease model. There are other models of colitis available, for example through administration of 2,4,6-trinitrobenzenesulphonic acid (Ballinger *et al.*, 2000), in addition to models of arthritis such as collagen type-II induced or glucosephosphate-isomerase induced arthritis (Courtenay *et al.*, 1980; Kamradt and Schubert, 2005).

Osteoblast expression of SOCS2 increased in response to GH, indicating a role for SOCS2 in regulating signalling during bone formation. It would therefore be interesting to know if other bone cells, namely osteoclasts and osteocytes, express SOCS2 also, and the role of SOCS2 in signalling events controlling bone turnover in diseases such as osteoporosis. Studies by MacRae and colleagues found an increase in circulating osteocalcin and TRAP5b, indicating a role of SOCS2 in bone turnover. Changes in osteoblast and osteoclast number in SOCS2^{-/-} mice could be examined in sections from methyl methacrylate embedded bones. Further μ CT analysis of bone architecture at different ages using femurs and tibiae from both sexes is required in the SOCS2^{-/-} mice given the different results gained by me, MacRae *et al.* and Lorentzon *et al.* (Lorentzon *et al.*, 2005; MacRae *et al.*, 2009). These techniques could also be used to examine changes in bone cells during inflammation in the absence of SOCS2 using models of arthritis or colitis as described previously.

The increased GH signalling through STAT proteins observed in SOCS2^{-/-} mice is likely to lead to raised local levels of IGF-1 in chondrocytes, which acts to stimulate proliferation and therefore growth. Local levels of IGF-1 in the growth plate in the absence of SOCS2 have not been determined. This analysis should be performed in the future to determine if the SOCS2 regulated effects of GH on chondrocytes acts via IGF-1 or through independent signalling pathways. This

could be performed using a cryostat to cut sections of frozen bones, allowing microdissection of the tissue as described by other authors while retaining the quality of the RNA (Parker *et al.*, 2007). Furthermore, the IGF-1R inhibitor picropodophyllin could be used in metatarsal cultures and/or injected into SOCS2^{-/-} mice to determine if the increased growth is dependent on IGF-1 signalling (Duan *et al.*, 2009; Tomizawa *et al.*, 2010).

There are other signalling pathways that SOCS2 is thought to regulate, which could also be involved in chondrocyte function. Investigation into this could commence with a microarray analysis of chondrocyte genes from SOCS2^{-/-} mice compared to WT mice, highlighting possible signalling pathways for further study. Others have shown that SOCS2 is involved in regulating signalling by IL-6, LIF and prolactin in other cell types (Minamoto *et al.*, 1997; Nicholson *et al.*, 1999; Pezet *et al.*, 1999), the latter of which have also been shown to influence chondrocyte function (Suntornsaratoon *et al.*, 2010).

CHAPTER 9

REFERENCE LIST

9. Reference List

- Adams,T.E., Hansen,J.A., Starr,R., Nicola,N.A., Hilton,D.J. and Billestrup,N. (1998). Growth hormone preferentially induces the rapid, transient expression of SOCS-3, a novel inhibitor of cytokine receptor signaling. *The Journal of Biological Chemistry* 273, 1285-1287.
- Ahmed,S.F. and Sävendahl,L. (2009). Promoting growth in chronic inflammatory disease: lessons from studies of the growth plate. *Hormone Research* 72, 42-47.
- Ahmed,S.F., Tucker,P., Mushtaq,T., Wallace,A.M., Williams,D.M. and Hughes,I.A. (2002). Short-term effects on linear growth and bone turnover in children randomized to receive prednisolone or dexamethasone. *Clinical Endocrinology* 57, 185-191.
- Aizawa,T., Kon,T., Einhorn,T.A. and Gerstenfeld,L.C. (2001). Induction of apoptosis in chondrocytes by tumor necrosis factor-alpha. *Journal of Orthopaedic Research* 19, 785-796.
- Akiyama,H., Chaboissier,M.C., Martin,J.F., Schedl,A. and de Crombrughe,B. (2002). The transcription factor Sox9 has essential roles in successive steps of the chondrocyte differentiation pathway and is required for expression of Sox5 and Sox6. *Genes & Development* 16, 2813-2828.
- Alexander,W.S., Starr,R., Fenner,J.E., Scott,C.L., Handman,E., Sprigg,N.S., Corbin,J.E., Cornish,A.L., Darwiche,R., Owczarek,C.M., Kay,T.W.H., Nicola,N.A., Hertzog,P.J., Metcalf,D. and Hilton,D.J. (1999). SOCS1 is a critical inhibitor of interferon [gamma] signaling and prevents the potentially fatal neonatal actions of this cytokine. *Cell* 98, 597-608.
- Altman,A., Hochberg,Z. and Silberman,M. (1992). Interactions between growth hormone and dexamethasone in skeletal growth and bone structure of the young mouse. *Calcified Tissue International* 51, 298-304.
- Altman,F.P. and Barnett,R.J. (1975). The ultra-structural localisation of enzyme activity in unfixed sections. *Histochemistry* 44, 179-183.
- Anderson,H.C. (1969). Vesicles associated with calcification in the matrix of epiphyseal cartilage. *The Journal of Cell Biology* 41, 59-72.
- Andreassen,T.T. and Oxlund,H. (2001). The effects of growth hormone on cortical and cancellous bone. *Journal of musculoskeletal & neuronal interactions* 2, 49-58.
- Arend,W.P., Palmer,G. and Gabay,C. (2008). IL-1, IL-18, and IL-33 families of cytokines. *Immunological Reviews* 223, 20-38.
- Argetsinger,L.S. and Carter-Su,C. (1996). Mechanism of signaling by growth hormone receptor. *Physiological Review* 76, 1089-1107.
- Ashdown,H., Dumont,Y., Poole,S., Boksa,P. and Luheshi,G.N. (2006). The role of cytokines in mediating effects of prenatal infection on the fetus: implications for schizophrenia. *Molecular Psychiatry* 11, 47-55.
- Atsumi,T., Miwa,Y., Kimata,K. and Ikawa,Y. (1990). A chondrogenic cell line derived from a differentiating culture of AT805 teratocarcinoma cells. *Cell Differentiation and Development* 30, 109-116.

- Baker,J., Liu,J.P., Robertson,E.J. and Efstratiadis,A. (1993). Role of insulin-like growth factors in embryonic and postnatal growth. *Cell* 75, 73-82.
- Ballinger,A.B., Azooz,O., El-Haj,T., Poole,S. and Farthing,M.J. (2000). Growth failure occurs through a decrease in insulin-like growth factor 1 which is independent of undernutrition in a rat model of colitis. *Gut* 46, 694-700.
- Ballock,R.T. and O'Keefe,R.J. (2003). The biology of the growth plate. *Journal of Bone and Joint Surgery* 85, 715-726.
- Ballock,R.T. and Reddi,A.H. (1994). Thyroxine is the serum factor that regulates morphogenesis of columnar cartilage from isolated chondrocytes in chemically defined medium. *The Journal of Cell Biology* 126, 1311-1318.
- Barreca,A., Ketelslegers,J.M., Arvigo,M., Minuto,F. and Thissen,J.P. (1998). Decreased acid-labile subunit (ALS) levels by endotoxin in vivo and by interleukin-1[beta] in vitro. *Growth Hormone & IGF Research* 8, 217-223.
- Baxter,R.C. and Martin,J.L. (1989). Structure of the Mr 140,000 growth hormone-dependent insulin-like growth factor binding protein complex: determination by reconstitution and affinity-labeling. *Proceedings of the National Academy of Sciences of the United States of America* 86, 6898-6902.
- Bechtold,S., Ripperger,P., Muhlbayer,D., Truckenbrodt,H., Hafner,R., Butenandt,O. and Schwarz,H.P. (2001). GH therapy in juvenile chronic arthritis: Results of a two-year controlled study on growth and bone. *The Journal of Clinical Endocrinology and Metabolism* 86, 5737-5744.
- Bechtold,S., Ripperger,P., Dalla Pozza,R., Bonfig,W., Häfner,R., Michels,H. and Schwarz,H.P. (2007). Growth hormone increases final height in patients with juvenile idiopathic arthritis: data from a randomized controlled study. *The Journal of Clinical Endocrinology and Metabolism* 92,3013-3018.
- Bi,W., Deng,J.M., Zhang,Z., Behringer,R.R. and de Crombrughe,B. (1999). Sox9 is required for cartilage formation. *Nature Genetics* 22, 85-89.
- Böhme,K., Conscience-Eqli,M., Tschan,T., Winterhalter,K.H. and Bruchner,P. (1992). Induction of proliferation or hypertrophy of chondrocytes in serum-free culture: the role of insulin-like growth factor-I, insulin, or thyroxine. *The Journal of Cell Biology* 116, 1035-1042.
- Boisclair,Y.R., Wang,J., Shi,J., Hurst,K.R. and Ooi,G.T. (2000). Role of the suppressor of cytokine signaling-3 in mediating the inhibitory effects of interleukin-1beta on the growth hormone-dependent transcription of the acid-labile subunit gene in liver cells. *The Journal of Biological Chemistry* 275, 3841-3847.
- Bonewald,L.F. (2007a). Osteocyte messages from a bony tomb. *Cell Metabolism* 5, 410-411.
- Bonewald,L.F. (2007b). Osteocytes as dynamic multifunctional cells. *Annals of the New York Academy of Sciences* 1116, 281-290.
- Börjesson,A.E., Lagerquist,M.K., Liu,C., Shao,R., Windahl,S.H., Karlsson,C., Movérare-Skrtic,S., Antal,M.C., Krust,A., Mohan,S., Chambon,P., Sävendahl,L. and Ohlsson,C. (2010). The role of

estrogen receptor α in growth plate cartilage for longitudinal bone growth. *Journal of Bone and Mineral Research* 25, 2690-2700.

Boyan, B.D., Sylvia, V.L., Dean, D.D., Del Toro, F. and Schwartz, Z. (2002). Differential regulation of growth plate chondrocytes by $1\alpha,25-(OH)_2D_3$ and $24R,25-(OH)_2D_3$ involves cell-maturation-specific membrane-receptor-activated phospholipid metabolism. *Critical Reviews in Oral Biology & Medicine* 13, 143-154.

Breur, G.J., Farnum, C.E., Padgett, G.A. and Wilsman, N.J. (1992). Cellular basis of decreased rate of longitudinal growth of bone in pseudoachondroplastic dogs. *Journal of Bone and Joint Surgery. American Volume* 74, 516-528.

Breur, G.J., Turgai, J., Vanenkevort, B.A., Farnum, C.E. and Wilsman, N.J. (1994). Stereological and serial section analysis of chondrocytic enlargement in the proximal tibial growth plate of the rat. *The Anatomical Record* 239, 255-268.

Breur, G.J., VanEnkevort, A., Farnum, C.E. and Wilsman, N.J. (1991). Linear relationship between the volume of hypertrophic chondrocytes and the rate of longitudinal bone growth in growth plates. *Journal of Orthopaedic Research* 9, 348-359.

Brooks, A.J., Wooh, J.W., Tunny, K.A. and Waters, M.J. (2008). Growth hormone receptor; mechanism of action. *The International Journal of Biochemistry & Cell Biology* 40, 1984-1989.

Broussard, S.R., McCusker, R.H., Novakofski, J.E., Strle, K., Shen, W.H., Johnson, R.W., Dantzer, R. and Kelley, K.W. (2004). IL-1 β impairs insulin-like growth factor I-induced differentiation and downstream activation signals of the insulin-like growth factor I receptor in myoblasts. *The Journal of Immunology* 172, 7713-7720.

Buckwalter, J.A., Mower, D., Ungar, R., Schaeffer, J. and Ginsberg, B. (1986). Morphometric analysis of chondrocyte hypertrophy. *Journal of Bone and Joint Surgery. American Volume* 68, 243-255.

Bullock, A.N., Debreczeni, J.E., Edwards, A.M., Sundström, M. and Knapp, S. (2006). Crystal structure of the SOCS2-elongin C-elongin B complex defines a prototypical SOCS box ubiquitin ligase. *Proceedings of the National Academy of Sciences of the United States of America* 103, 7637-7642.

Burch, W.M. and Lebovitz, H.E. (1982). Triiodothyronine stimulates maturation of porcine growth-plate cartilage in vitro. *Journal of Clinical Investigation* 70, 496-504.

Cancedda, R., Cancedda, F.D. and Castagnola, P. (1995). Chondrocyte differentiation. *International Review of Cytology* 159, 265-358.

Carlevero, M.F., Cermelli, S., Cancedda, R. and Descalzi Cancedda, F. (2000). Vascular endothelial growth factor (VEGF) in cartilage neovascularization and chondrocyte differentiation: auto-paracrine role during endochondral bone formation. *Journal of Cell Science* 113, 59-69.

Carrascosa, A., Audi, L., Ferrandez, M.A. and Ballabriga, A. (1990). Biological effects of androgens and identification of specific dihydrotestosterone-binding sites in cultured human fetal epiphyseal chondrocytes. *The Journal of Clinical Endocrinology and Metabolism* 70, 134-140.

Chagin, A.S., Lindberg, M.K., Andersson, N., Moverare, S., Gustafsson, J.A., Sävendahl, L. and Ohlsson, C. (2004). Estrogen receptor-beta inhibits skeletal growth and has the capacity to mediate growth plate fusion in female mice. *Journal of Bone and Mineral Research* 19, 72-77.

- Cooper,H.S., Murthy,S.N., Shah,R.S. and Sedergran,D.J. (1993). Clinicopathologic study of dextran sulfate sodium experimental murine colitis. *Laboratory Investigation* 69, 238-249.
- Courtenay,J.S., Dallman,M.J., Dayan,A.D., Martin,A. and Mosedale,B. (1980). Immunisation against heterologous type II collagen induces arthritis in mice. *Nature* 283, 666-668.
- Coxam,V., Miller,M.A., Bowman,M.B. and Miller,S.C. (1996). Ontogenesis of IGF regulation of longitudinal bone growth in rat metatarsal rudiments cultured in serum-free medium. *Archives of Physiology and Biochemistry* 104, 173-179.
- Cuttler,L., Jackson,J.A., Saeed uz-Zafar,M., Levitsky,L.L., Mellinger,R.C. and Frohman,L.A. (1989). Hypersecretion of growth hormone and prolactin in McCune-Albright syndrome. *The Journal of Clinical Endocrinology & Metabolism* 68, 1148-1154.
- Dallas,S.L. and Bonewald,L.F. (2010). Dynamics of the transition from osteoblast to osteocyte. *Annals of the New York Academy of Sciences* 1192, 437-443.
- Daughaday,W.H. (1989). A personal history of the origin of the somatomedin hypothesis and recent challenges to its validity. *Perspectives in Biology and Medicine* 32, 194-211.
- Daughaday,W.H., Hall,K., Raben,M.S., Salmon,W.D., Van den Brande,J.L. and Van Wyk,J.J. (1972). Somatomedin: Proposed designation for sulphation factor. *Nature* 235, 107.
- Davey,H.W., McLachlan,M.J., Wilkins,R.J., Hilton,D.J. and Adams,T.E. (1999). STAT5b mediates the GH-induced expression of SOCS-2 and SOCS-3 mRNA in the liver. *Molecular and Cellular Endocrinology* 158, 111-116.
- Davies,U.M., Jones,J., Reeve,J., Camacho-Hubner,C., Charlett,A., Ansell,B.M., Preece,M.A. and Woo,P.M.M. (1997). Juvenile rheumatoid arthritis. Effects of disease activity and recombinant human growth hormone on insulin-like growth factor 1, insulin-like growth factor binding proteins 1 and 3, and osteocalcin. *Arthritis and Rheumatism* 40, 332-340.
- De Benedetti,F., Alonzi,T., Moretta,A., Lazzaro,D., Costa,P., Poli,V., Martini,A., Ciliberto,G. and Fattori,E. (1997). Interleukin 6 causes growth impairment in transgenic mice through a decrease in insulin-like growth factor-I. A model for stunted growth in children with chronic inflammation. *Journal of Clinical Investigation* 99, 643-650.
- De Benedetti,F., Meazza,C., Oliveri,M., Pignatti,P., Vivarelli,M., Alonzi,T., Fattori,E., Garrone,S., Barreca,A. and Martini,A. (2001a). Effect of IL-6 on IGF binding protein-3: A study in IL-6 transgenic mice and in patients with systemic juvenile idiopathic arthritis. *Endocrinology* 142, 4818-4826.
- De Benedetti,F., Pignatti,P., Vivarelli,M., Meazza,C., Ciliberto,G., Savino,R. and Martini,A. (2001b). In vivo neutralization of human IL-6 (hIL-6) achieved by immunization of hIL-6-transgenic mice with a hIL-6 receptor antagonist. *The Journal of Immunology* 166, 4334-4340.
- de Hooge,A.S.K., van de Loo,F.A.G., Bennink,M.B., Arntz,O.J., Fiselier,T.J.W., Franssen,M.J.A.M., Joosten,L.A.B., van Lent,P.L.E.M., Richards,C.D. and van den Berg,W.B. (2003). Growth plate damage, a feature of juvenile idiopathic arthritis, can be induced by adenoviral gene transfer of oncostatin M: A comparative study in gene-deficient mice. *Arthritis and Rheumatism* 48, 1750-1761.

- Dean,D.D., Boyan,B.D., Schwart,Z., Muniz,O.E., Carreno,M.R., Maeda,S. and Howell,D.S. (2001). Effect of 1 α ,25-dihydroxyvitamin D3 and 24R,25-dihydroxyvitamin D3 on metalloproteinase activity and cell maturation in growth plate cartilage in vivo. *Endocrine* 14, 311-323.
- DeBoer,M.D., Li,Y. and Cohn,S. (2010). Colitis causes delay in puberty in female mice out of proportion to changes in leptin and corticosterone. *Journal of Gastroenterology* 45, 277-284.
- Decker,T. and Kovarik,P. (2000). Serine phosphorylation of STATs. *Oncogene* 19, 2628-2637.
- Delhanty,P.J.D. (1998). Interleukin-1[β] suppresses growth hormone-induced acid-labile subunit mRNA levels and secretion in primary hepatocytes. *Biochemical and Biophysical Research Communications* 243, 269-272.
- Denson,L.A., Held,M.A., Menon,R.K., Frank,S.J., Parlow,A.F. and Arnold,D.L. (2003). Interleukin-6 inhibits hepatic growth hormone signaling via upregulation of Cis and Socs-3. *American Journal of Physiology-Gastrointestinal and Liver Physiology* 284, G646-G654.
- Dessau,W., von der Mark,H., von der Mark,K. and Fischer,S. (1980). Changes in the patterns of collagens and fibronectin during limb-bud chondrogenesis. *Journal of Embryology and Experimental Morphology* 57, 51-60.
- Dey,B.R., Spence,S.L., Nissley,P. and Furlanetto,R.W. (1998). Interaction of human suppressor of cytokine signaling (SOCS)-2 with the insulin-like growth factor-I receptor. *The Journal of Biological Chemistry* 273, 24095-24101.
- Dieleman,L.A., Palmem,M.J.H.J., Akol,H., Bloemena,E., Pena,A.S. and Meuwissen,S.G.M. (1998). Chronic experimental colitis induced by dextran sulphate sodium (DSS) is characterized by Th1 and Th2 cytokines. *Clinical and Experimental Immunology* 114, 385-391.
- Dif,F., Saunier,E., Demeneix,B., Kelly,P.A. and Edery,M. (2001). Cytokine-inducible SH2-containing protein suppresses PRL signaling by binding the PRL receptor. *Endocrinology* 142, 5286-5293.
- Dogusan,Z., Hooghe-Peters,E.L., Berus,D., Velkeniers,B. and Hooghe,R. (2000). Expression of SOCS genes in normal and leukemic human leukocytes stimulated by prolactin, growth hormone and cytokines. *Journal of Neuroimmunology* 109, 34-39.
- Donohue,M.M. and Demay,M.B. (2002). Rickets in VDR null mice is secondary to decreased apoptosis of hypertrophic chondrocytes. *Endocrinology* 143, 3691-3694.
- Duan,Z., Choy,E., Harmon,D., Yang,C., Ryu,K., Schwab,J., Mankin,H. and Hornicek,F.J. (2009). Insulin-like growth factor-I receptor tyrosine kinase inhibitor cyclolignan picropodophyllin inhibits proliferation and induces apoptosis in multidrug resistant osteosarcoma cell lines. *Molecular Cancer Therapeutics* 8, 2122-2130
- Ducy,P., Schinke,T., Karsenty,G. and The osteoblast: A sophisticated f (2000). The osteoblast: A sophisticated fibroblast under central surveillance. *Science* 289, 1501-1504.
- Durbin,J.E., Hackenmiller,R., Simon,M.C. and Levy,D.E. (1996). Targeted disruption of the mouse Stat1 gene results in compromised innate immunity to viral disease. *Cell* 84, 443-450.
- Eden,S., Isaksson,O.G.P., Madsen,K. and Friberg,U. (1983). Specific binding of growth hormone to isolated chondrocytes from rabbit ear and epiphyseal plate. *Endocrinology* 112, 1127-1129.

- Ehlen,H.W., Buelens,L.A. and Vortkamp,A. (2006). Hedgehog signaling in skeletal development. *Birth Defects Research Part C: Embryo Today: Reviews* 78, 267-279.
- Farnum,C.E. and Wilsman,N.J. (1987). Morphologic stages of the terminal hypertrophic chondrocyte of growth plate cartilage. *The Anatomical Record* 219, 221-232.
- Farnum,C.E. and Wilsman,N.J. (1993). Determination of proliferative characteristics of growth plate chondrocytes by labeling with bromodeoxyuridine. *Calcified Tissue International* 52, 110-119.
- Farquharson,C. (2003). Bone growth. In *Biology of Growth of Domestic Animals*, C.G.Scanes, ed. (Iowa State Press), pp. 170-185.
- Farquharson,C., Jefferies,D., Seawright,E. and Houston,B. (2001). Regulation of chondrocyte terminal differentiation in the postembryonic growth plate: the role of the PTHrP-Indian hedgehog axis. *Endocrinology* 142, 4131-4140.
- Farquharson,C. and Loveridge,N. (1990). Cell proliferation within the growth plate of long bones assessed by bromodeoxyuridine uptake and its relationship to glucose 6-phosphate dehydrogenase activity. *Bone and Mineral* 10, 121-130.
- Favre,H., Benhamou,A., Finidori,J., Kelly,P.A. and Edery,M. (1999). Dual effects of suppressor of cytokine signaling (SOCS-2) on growth hormone signal transduction. *FEBS Letters* 453, 63-66.
- Fernandez-Cancio,M., Esteban,C., Carrascosa,A., Toran,N., Andaluz,P. and Audi,L. (2008). IGF-I and not IGF-II expression is regulated by glucocorticoids in human fetal epiphyseal chondrocytes. *Growth Hormone & IGF Research* 18, 497-505.
- Ferrara,N. (1999). Role of vascular endothelial growth factor in the regulation of angiogenesis. *Kidney International* 56, 794-814.
- Firth,S.M. and Baxter,R.C. (2002). Cellular actions of the insulin-like growth factor binding proteins. *Endocrine Reviews* 23, 824-854.
- Flores-Morales,A., Greenhalgh,C.J., Norstedt,G. and Rico-Bautista,E. (2006). Negative regulation of growth hormone receptor signaling. *Molecular Endocrinology* 20, 241-253.
- Fortier,M., Joobar,R., Luheshi,G.N. and Boksa,P. (2004). Maternal exposure to bacterial endotoxin during pregnancy enhances amphetamine-induced locomotion and startle responses in adult rat offspring. *Journal of Psychiatric Research* 38, 335-345.
- Frost,R.A., Nystrom,G.J. and Lang,C.H. (2000). Stimulation of insulin-like growth factor binding protein-1 synthesis by interleukin-1{beta}: requirement of the mitogen-activated protein kinase pathway. *Endocrinology* 141, 3156-3164.
- Gerber,H.P., Vu,T.H., Ryan,A.M., Kowalski,J., Werb,Z. and Ferrara,N. (1999). VEGF couples hypertrophic cartilage remodeling, ossification and angiogenesis during endochondral bone formation. *Nature Medicine* 5, 623-628.
- Gevers,E.F., Hannah,M.J., Waters,M.J. and Robinson,I.C.A.F. (2009). Regulation of rapid signal transducer and activator of transcription-5 phosphorylation in the resting cells of the growth plate and in the liver by growth hormone and feeding. *Endocrinology* 150, 3627-3636.

- Gevers,E.F., van der Eerden,B.C., Karperien,M., Raap,A.K., Robinson,I.C. and Wit,J.M. (2002). Localization and regulation of the growth hormone receptor and growth hormone-binding protein in the rat growth plate. *Journal of Bone and Mineral Research* 17, 1408-1419.
- Giustina,A., Mazziotti,G. and Canalis,E. (2008). Growth hormone, insulin-like growth factors, and the skeleton. *Endocrine Reviews* 29, 535-559.
- Goldring,M.B., Birkhead,J., Sandell,L.J., Kimura,T. and Krane,S.M. (1988). Interleukin 1 suppresses expression of cartilage-specific types II and IX collagens and increases types I and III collagens in human chondrocytes. *Journal of Clinical Investigation* 82, 2026-2037.
- Govoni,K.E., Lee,S.K., Chung,Y.S., Behringer,R.R., Wergedal,J.E., Baylink,D.J. and Mohan,S. (2007). Disruption of insulin-like growth factor-I expression in type II α collagen-expressing cells reduces bone length and width in mice. *Physiological Genomics* 30, 354-362.
- Green,H., Morikawa,M. and Nixon,T. (1985). A dual effector theory of growth-hormone action. *Differentiation* 29, 195-198.
- Greenhalgh,C.J. and Alexander,W.S. (2004). Suppressors of cytokine signalling and regulation of growth hormone action. *Growth Hormone & IGF Research* 14, 200-206.
- Greenhalgh,C.J., Bertolino,P., Asa,S.L., Metcalf,D., Corbin,J.E., Adams,T.E., Davey,H.W., Nicola,N.A., Hilton,D.J. and Alexander,W.S. (2002a). Growth enhancement in suppressor of cytokine signaling 2 (SOCS-2)-deficient mice is dependent on signal transducer and activator of transcription 5b (STAT5b). *Molecular Endocrinology* 16, 1394-1406.
- Greenhalgh,C.J., Metcalf,D., Thaus,A.L., Corbin,J.E., Uren,R., Morgan,P.O., Fabri,L.J., Zhang,J.G., Martin,H.M., Willson,T.A., Billestrup,N., Nicola,N.A., Baca,M., Alexander,W.S. and Hilton,D.J. (2002b). Biological evidence that SOCS-2 can act either as an enhancer or suppressor of growth hormone signaling. *The Journal of Biological Chemistry* 277, 40181-40184.
- Greenhalgh,C.J., Rico-Bautista,E., Lorentzon,M., Thaus,A.L., Morgan,P.O., Willson,T.A., Zervoudakis,P., Metcalf,D., Street,I., Nicola,N.A., Nash,A.D., Fabri,L.J., Norstedt,G., Ohlsson,C., Flores-Morales,A., Alexander,W.S. and Hilton,D.J. (2005). SOCS2 negatively regulates growth hormone action in vitro and in vivo. *Journal of Clinical Investigation* 115, 397-406.
- Grimsrud,C.D., Romano,P.R., D'Souza,M., Puzas,J.E., Reynolds,P.R., Rosier,R.N. and O'Keefe,R.J. (1999). BMP-6 is an autocrine stimulator of chondrocyte differentiation. *Journal of Bone and Mineral Research* 14, 475-482.
- Guo,J., Chung,U.I., Yang,D., Karsenty,G., Bringhurst,F.R. and Kronenberg,H.M. (2006). PTH/PTHrP receptor delays chondrocyte hypertrophy via both Runx2-dependent and -independent pathways. *Developmental Biology* 292, 116-128.
- Hamdani,G., Gabet,Y., Rachmilewitz,D., Karmeli,F., Bab,I. and Dresner-Pollak,R. (2008). Dextran sodium sulfate-induced colitis causes rapid bone loss in mice. *Bone* 43, 945-950.
- Han,Y.L., Leaman,D.W., Watling,D., Rogers,N.C., Groner,B., Kerr,I.M., Wood,W.I. and Stark,G.R. (1996). Participation of JAK and STAT proteins in growth hormone-induced signaling. *The Journal of Biological Chemistry* 271, 5947-5952.

- Hansen, J.A., Lindberg, K., Hilton, D.J., Nielsen, J.H. and Billestrup, N. (1999). Mechanism of inhibition of growth hormone receptor signaling by suppressor of cytokine signaling proteins. *Molecular Endocrinology* *13*, 1832-1843.
- Harris, L., Senagore, P., Young, V.B. and McCabe, L.R. (2009). Inflammatory bowel disease causes reversible suppression of osteoblast and chondrocyte function in mice. *American Journal of Physiology-Gastrointestinal and Liver Physiology* *296*, G1020-G1029.
- Heino, T.J., Chagin, A.S., Takigawa, M. and Sävendahl, L. (2008). Effects of alendronate and pamidronate on cultured rat metatarsal bones: Failure to prevent dexamethasone-induced growth retardation. *Bone* *42*, 702-709.
- Herrington, J., Smit, L.S., Schwartz, J. and Carter-Su, C. (2000). The role of STAT proteins in growth hormone signaling. *Oncogene* *19*, 2585-2597.
- Hildebrand, H., Karlberg, J. and Kristiansson, B. (1994). Longitudinal growth in children and adolescents with inflammatory bowel disease. *Journal of Pediatric Gastroenterology and Nutrition* *18*, 165-173.
- Hilton, D.J. (1999). Negative regulators of cytokine signal transduction. *Cellular and Molecular Life Sciences* *55*, 1568-1577.
- Hindmarsh, P.C. and Dattani, M.T. (2006). Use of growth hormone in children. *Nature Clinical Practice Endocrinology & Metabolism* *2*, 260-268.
- Hirao, M., Tamai, N., Tsumaki, N., Yoshikawa, H. and Myoui, A. (2006). Oxygen tension regulates chondrocyte differentiation and function during endochondral ossification. *The Journal of Biological Chemistry* *281*, 31079-31092.
- Horiguchi, M., Akiyama, H., Ito, H., Shigeno, C. and Nakamura, T. (2000). Tumour necrosis factor- α up-regulates the expression of BMP-4 mRNA but inhibits chondrogenesis in mouse clonal chondrogenic EC cells, ATDC5. *Cytokine* *12*, 526-530.
- Horner, A., Bishop, N.J., Bord, S., Beeton, C., Kelsall, A.W., Coleman, N. and Compston, J.E. (1999). Immunolocalisation of vascular endothelial growth factor (VEGF) in human neonatal growth plate cartilage. *Journal of Anatomy* *194*, 519-524.
- Horvat, S. and Medrano, J.F. (1995). Interval mapping of high growth (hg), a major locus that increases weight gain in mice. *Genetics* *139*, 1737-1748.
- Horvat, S. and Medrano, J.F. (1998). A 500-kb YAC and BAC contig encompassing the high-growth deletion in mouse chromosome 10 and identification of the murine Raidd/Cradd gene in the candidate region. *Genomics* *54*, 159-164.
- Horvat, S. and Medrano, J.F. (2001). Lack of Socs2 expression causes the high-growth phenotype in mice. *Genomics* *72*, 209-212.
- Hoshi, K., Ogata, N., Shimoaka, T., Terauchi, Y., Kadowaki, T., Kenmotsu, S., Chung, U.I., Ozawa, H., Nakamura, K. and Kawaguchi, H. (2004). Deficiency of insulin receptor substrate-1 impairs skeletal growth through early closure of epiphyseal cartilage. *Journal of Bone and Mineral Research* *19*, 214-223.

- Huang,W., Chung,U.I., Kronenberg,H.M. and de Crombrugge,B. (2001). The chondrogenic transcription factor Sox9 is a target of signaling by the parathyroid hormone-related peptide in the growth plate of endochondral bones. *Proceedings of the National Academy of Sciences of the United States of America* 98, 160-165.
- Huesa,C., Yadav,M.C., Finnilä,M.A.J., Goodyear,S.R., Robins,S.P., Tanner,K.E., Aspden,R.M., Millán,J.L. and Farquharon,C. 2011 PHOSPHO1 is essential for mechanically competent mineralization and the avoidance of spontaneous fractures. *Bone* 48:1066-1074
- Hunziker,E.B., Schenk,R.K. and Cruz-Orive,L.M. (1987). Quantitation of chondrocyte performance in growth-plate cartilage during longitudinal bone growth. *Journal of Bone and Joint Surgery. American Volume* 69, 162-173.
- Hunziker,E.B. and Shenk,R.K. (1989). Physiological mechanisms adopted by chondrocytes in regulating longitudinal bone growth in rats. *Journal of Physiology* 414, 55-71.
- Hurley,M.M., Marie,P.J. and Florkiewicz,R.Z. (1996). Fibroblast Growth Factors (FGF) and FGF Receptor Families in Bone. In *Principles of Bone Biology*, J.P.Bilezikian, L.G.Raisz, and G.A.Rodan, eds. (San Diego: Academic Press), pp. 825-851.
- Hutchison,M.R., Bassett,M.H. and White,P.C. (2007). Insulin-like growth factor-I and fibroblast growth factor, but not growth hormone, affect growth plate chondrocyte proliferation. *Endocrinology* 148, 3122-3130.
- Inaba,M., Saito,H., Fujimoto,M., Sumitani,S., Ohkawara,T., Tanaka,T., Kouhara,H., Kasayama,S., Kawase,I., Kishimoto,T. and Naka,T. (2005). Suppressor of cytokine signaling 1 suppresses muscle differentiation through modulation of IGF-I receptor signal transduction. *Biochemical and Biophysical Research Communications* 328, 953-961.
- Isaksson,O.G.P., Jansson,J.O. and Gause,I.A.M. (1982). Growth hormone stimulates longitudinal bone growth directly. *Science* 216, 1237-1239.
- Isgaard,J., Möller,C., Isaksson,O.G., Nilsson,A., Mathews,L.S. and Norstedt,G. (1988). Regulation of insulin-like growth factor messenger ribonucleic acid in rat growth plate by growth hormone. *Endocrinology* 122, 1515-1520.
- Jilka,R.L., Weinstein,R.S., Bellido,T., Parfitt,A.M. and Manolagas,S.C. (1998). Osteoblast programmed cell death (apoptosis): modulation by growth factors and cytokines. *Journal of Bone and Mineral Research* 13, 793-802.
- Jones,J.I., D'Ercole,A.J., Camacho-Hubner,C. and Clemmons,D.R. (1991). Phosphorylation of insulin-like growth factor (IGF)-binding protein 1 in cell culture in vivo: Effects on affinity for IGF-I. *Proceedings of the National Academy of Sciences of the United States of America* 88, 7481-7485.
- Juul,A. (2001). The effects of oestrogens on linear bone growth. *Human Reproduction Update* 7, 303-313.
- Kamradt,T. and Schubert,D. (2005). The role and clinical implications of G6PI in experimental models of rheumatoid arthritis. *Arthritis Research & Therapy* 7, 20-28.
- Kember,N.F. (1972). Comparative patterns of cell division in epiphyseal cartilage plates in the rat. *Journal of Anatomy* 111, 137-172.

- Kember,N.F. (1985). Comparative patterns of cell division in epiphyseal cartilage plates in the rabbit. *Journal of Anatomy* 142, 185-190.
- Kember,N.F. and Sissons,H.A. (1976). Quantitative histology of the human growth plate. *Journal of Bone and Joint Surgery. British Volume* 58-B, 426-435.
- Kenchappa,P., Yadav,A., Singh,G., Nandana,S. and Banerjee,K. (2004). Rescue of TNF-alpha--inhibited neuronal cells by IGF-1 involves Akt and c-Jun N-terminal kinases. *Journal of Neuroscience Research* 76, 466-474.
- Kiepe,D., Ciarmatori,S., Hoeflich,A., Wolf,E. and Tönshoff,B. (2005). Insulin-like growth factor (IGF)-I stimulates cell proliferation and induces IGF binding protein (IGFBP)-3 and IGFBP-5 gene expression in cultured growth plate chondrocytes via distinct signaling pathways. *Endocrinology* 146, 3096-3104.
- Kirkwood,J.K., Spratt,D.M. and Duignan,P.J. (1989). Patterns of cell proliferation and growth rate in limb bones of the domestic fowl (*Gallus domesticus*). *Research in Veterinary Science* 47, 139-147.
- Kirsch,T. (2006). Determinants of pathological mineralization. *Current Opinion in Rheumatology* 18, 174-180.
- Kirsch,T., Nah,H.D., Shapiro,I.M. and Pacifici,M. (1997). Regulated production of mineralization-competent matrix vesicles in hypertrophic chondrocytes. *The Journal of Cell Biology* 137, 1149-1160.
- Kiu,H., Greenhalgh,C.J., Thaus,A., Hilton,D.J., Nicola,N.A., Alexander,W.S. and Roberts,A.W. (2009). Regulation of multiple cytokine signalling pathways by SOCS3 is independent of SOCS2. *Growth Factors* 27, 384-393.
- Klammt,J., Pfäffle,R., Werner,H. and Kiess,W. (2008). IGF signaling defects as causes of growth failure and IUGR. *Trends in Endocrinology & Metabolism* 19, 197-205.
- Klingmüller,U., Lorenz,U., Cantley,L.C., Neel,B.G. and Lodish,H.F. (1995). Specific recruitment of SH-PTP1 to the erythropoietin receptor causes inactivation of JAK2 and termination of proliferative signals. *Cell* 80, 729-738.
- Kofoed,E.M., Hwa,V., Little,B., Woods,K.A., Buckway,C.K., Tsubaki,J., Pratt,K.L., Bezrodnik,L., Jasper,H., Tepper,A., Heinrich,J.J. and Rosenfeld,R.G. (2003). Growth hormone insensitivity associated with a STAT5b mutation. *The New England Journal of Medicine* 349, 1139-1147.
- Koike,M., Yamanaka,Y., Inoue,M., Tanaka,H., Nishimura,R. and Seino,Y. (2003). Insulin-like growth factor-1 rescues the mutated FGF receptor 3 (G380R) expressing ATDC5 cells from apoptosis through phosphatidylinositol 3-kinase and MAPK. *Journal of Bone and Mineral Research* 18, 2043-2051.
- Krebs,D.L. and Hilton,D.J. (2001). SOCS proteins: Negative regulators of cytokine signaling. *Stem Cells* 19, 378-387.
- Kronenberg,H.M. (2003). Developmental regulation of the growth plate. *Nature* 423, 332-336.

- Kronenberg,H.M., Lee,K., Lanske,B. and Segre,G.V. (1997). Parathyroid hormone-related protein and Indian hedgehog control the pace of cartilage differentiation. *Journal of Endocrinology* *154*, S39-S45.
- Lang,C.H., Fan,J., Cooney,R. and Vary,T.C. (1996). IL-1 receptor antagonist attenuates sepsis-induced alterations in the IGF system and protein synthesis. *American Journal of Physiology - Endocrinology and Metabolism* *270*, E430-E437.
- Lang,C.H., Nystrom,G.J. and Frost,R.A. (1999). Regulation of IGF binding protein-1 in Hep G2 cells by cytokines and reactive oxygen species. *American Journal of Physiology - Gastrointestinal and Liver Physiology* *276*, G719-G727.
- Lefebvre,V., Garofalo,S., Zhou,G., Metsäranta,M., Vuorio,E. and de Crombrughe,B. (1994). Characterization of primary cultures of chondrocytes from type II collagen/[beta]-galactosidase transgenic mice. *Matrix Biology* *14*, 329-335.
- Legendre,F., Dudhia,J., Pujol,J.P. and Bogdanowicz,P. (2003). JAK/STAT but not ERK1/ERK2 pathway mediates interleukin (IL)-6/soluble IL-6R down-regulation of type II collagen, aggrecan core, and link protein transcription in articular chondrocytes. *The Journal of Biological Chemistry* *278*, 2903-2912.
- LeRoith,D. (2000). Insulin-like growth factor I receptor signaling-overlapping or redundant pathways? *Endocrinology* *141*, 1287-1288.
- LeRoith,D., Bondy,C., Yakar,S., Liu,J.L. and Butler,A. (2001). The somatomedin hypothesis: 2001. *Endocrine Reviews* *22*, 53-74.
- LeRoith,D. and Nissley,P. (2005). Knock your SOCS off! *Journal of Clinical Investigation* *115*, 233-236.
- Leung,K.C., Doyle,N., Ballesteros,M., Sjogren,K., Watts,C.K.W., Low,T.H., Leong,G.M., Ross,R.J.M. and Ho,K.K.Y. (2003). Estrogen inhibits GH signaling by suppressing GH-induced JAK2 phosphorylation, an effect mediated by SOCS-2. *Proceedings of the National Academy of Sciences of the United States of America* *100*, 1016-1021.
- Li,P. and Schwartz,E.M. (2003). The TNF-alpha transgenic mouse model of inflammatory arthritis. *Springer Seminars in Immunopathology* *25*, 19-33.
- Li,S., Xu,X., Sundstedt,A., Paulsson,K.M., Anderson,P., Karlsson,S., Sjögren,H.O. and Wang,P. (2000). Cytokine-induced Src homology 2 protein (CIS) promotes T cell receptor-mediated proliferation and prolongs survival of activated T cells. *Journal of Experimental Medicine* *191*, 985-994.
- Li,W.Q., Dehnade,F. and Zafarullah,M. (2001). Oncostatin M-induced matrix metalloproteinase and tissue inhibitor of metalloproteinase-3 genes expression in chondrocytes requires janus kinase/STAT signaling pathway. *The Journal of Immunology* *166*, 3491-3498.
- Liu,J.L., Yakar,S. and LeRoith,D. (2000). Conditional knockout of mouse insulin-like growth factor-1 gene using the Cre/loxP system. *Proceedings of the Society for Experimental Biology and Medicine* *223*, 344-351.
- Liu,X.B., Shi,Q. and Sigmund,C.D. (2006). Interleukin-1 beta attenuates renin gene expression via a mitogen-activated protein kinase kinase-extracellular signal-regulated kinase and signal

transducer and activator of transcription 3-dependent mechanism in As4.1 cells. *Endocrinology* **147**, 6011-6018.

Livne,E., Laufer,D. and Blumenfeld,I. (1997). Comparison of in vitro response to growth hormone by chondrocytes from mandibular condyle cartilage of young and old mice. *Calcified Tissue International* **61**, 62-67.

Lorentzon,M., Greenhalgh,C.J., Mohan,S., Alexander,W.S. and Ohlsson,C. (2005). Reduced bone mineral density in SOCS-2-deficient mice. *Pediatric Research* **57**, 223-226.

Lowry,O.H., Rosebrough,N.J., Farr,A.L. and Randall,R.J. (1951). Protein measurement with the folin phenol reagent. *The Journal of Biological Chemistry* **193**, 265-275.

Lupu,F., Terwilliger,J.D., Lee,K., Segre,G.V. and Efstratiadis,A. (2001). Roles of growth hormone and insulin-like growth factor 1 in mouse postnatal growth. *Developmental Biology* **229**, 141-162.

Mackie,E.J., Ahmed,Y.A., Tatarczuch,L., Chen,K.S. and Mirams,M. (2008). Endochondral ossification: How cartilage is converted into bone in the developing skeleton. *The International Journal of Biochemistry & Cell Biology* **40**, 46-62.

Mackie,E.J., Thesleff,I. and Chiquet-Ehrismann,R. (1987). Tenascin is associated with chondrogenic and osteogenic differentiation in vivo and promotes chondrogenesis in vitro. *The Journal of Cell Biology* **105**, 2569-2579.

MacRae,V.E., Ahmed,S.F., Mushtaq,T. and Farquharson,C. (2007a). IGF-I signalling in bone growth: Inhibitory actions of dexamethasone and IL-1[beta]. *Growth Hormone & IGF Research* **17**, 435-439.

MacRae,V.E., Burdon,T., Ahmed,S.F. and Farquharson,C. (2006a). Ceramide inhibition of chondrocyte proliferation and bone growth is IGF-I independent. *Journal of Endocrinology* **191**, 369-377.

MacRae,V.E., Farquharson,C. and Ahmed,S.F. (2006b). The restricted potential for recovery of growth plate chondrogenesis and longitudinal bone growth following exposure to pro-inflammatory cytokines. *Journal of Endocrinology* **189**, 319-328.

MacRae,V.E., Horvat,S., Pells,S.C., Dale,H., Collinson,R.S., Pitsillides,A.A., Ahmed,S.F. and Farquharson,C. (2009). Increased bone mass, altered trabecular architecture and modified growth plate organization in the growing skeleton of SOCS2 deficient mice. *Journal of Cellular Physiology* **218**, 276-284.

MacRae,V.E., Wong,S.C., Farquharson,C. and Ahmed,S.F. (2006c). Cytokine actions in growth disorders associated with pediatric chronic inflammatory diseases (Review). *International Journal of Molecular Medicine* **18**, 1011-1018.

MacRae,V.E., Wong,S.C., Smith,W., Gracie,A., McInnes,I., Galea,P., Gardner-Medwin,J., Farquharson,C. and Ahmed,S.F. (2007b). Cytokine profiling and in vitro studies of murine bone growth using biological fluids from children with juvenile idiopathic arthritis. *Clinical Endocrinology* **67**, 442-448.

Madsen,K., Friberg,U., Roos,P., Eden,S. and Isaksson,O. (1983). Growth hormone stimulates the proliferation of cultured chondrocytes from rabbit ear and rat rib growth cartilage. *Nature* **304**, 545-547.

- Magin,T.M., McWhir,J. and Melton,D.W. (1992). A new mouse embryonic stem cell line with good germ line contribution and gene targeting frequency. *Nucleic Acids Research* *20*, 3795-3796.
- Manolagas,S.C. (2000). Birth and death of bone cells: Basic regulatory mechanisms and implications for the pathogenesis and treatment of osteoporosis. *Endocrine Reviews* *21*, 115-137.
- Marine,J.C., McKay,C., Wang,D., Topham,D.J., Parganas,E., Nakajima,H., Pendeville,H., Yasukawa,H., Sasaki,A., Yoshimura,A. and Ihle,J.N. (1999a). SOCS3 is essential in the regulation of fetal liver erythropoiesis. *Cell* *98*, 617-627.
- Marine,J.C., Topham,D.J., McKay,C., Wang,D., Parganas,E., Stravopodis,D., Yoshimura,A. and Ihle,J.N. (1999b). SOCS1 deficiency causes a lymphocyte-dependent perinatal lethality. *Cell* *98*, 609-616.
- Martensson,K., Chrysis,D. and Sävendahl,L. (2004). Interleukin-1beta and TNF-alpha act in synergy to inhibit longitudinal growth in fetal rat metatarsal bones. *Journal of Bone and Mineral Research* *19*, 1805-1812.
- Matsumoto,T., Tsukazaki,T., Enomoto,H., Iwasaki,K. and Yamashita,S. (1994). Effects of interleukin-1 beta on insulin-like growth factor-I autocrine/paracrine axis in cultured rat articular chondrocytes. *Annals of the Rheumatic Diseases* *53*, 128-133.
- Mauras,N., George,D., Evans,J., Milov,D., Abrams,S., Rini,A., Welch,S. and Haymond,M.W. (2002). Growth hormone has anabolic effects in glucocorticosteroid-dependent children with inflammatory bowel disease: A pilot study. *Metabolism* *51*, 127-135.
- Melgar,S., Bjursell,M., Gerdin,A.K., Svensson,L., Michaelsson,E. and Bohlooly-Y,M. (2007). Mice with experimental colitis show an altered metabolism with decreased metabolic rate. *American Journal of Physiology-Gastrointestinal and Liver Physiology* *292*, G165-G172.
- Meraz,M.A., White,J.M., Sheehan,K.C.F., Bach,E.A., Rodig,S.J., Dighe,A.S., Kaplan,D.H., Riley,J.K., Greenlund,A.C., Campbell,D., Carver-Moore,K., DuBois,R.N., Clark,R., Aguet,M. and Schreiber,R.D. (1996). Targeted disruption of the Stat1 gene in mice reveals unexpected physiologic specificity in the JAK-STAT signaling pathway. *Cell* *84*, 431-442.
- Metcalf,D., Greenhalgh,C.J., Viney,E., Willson,T.A., Starr,R., Nicola,N.A., Hilton,D.J. and Alexander,W.S. (2000). Gigantism in mice lacking suppressor of cytokine signalling-2. *Nature* *405*, 1069-1073.
- Michaylira,C.Z., Ramocki,N.M., Simmons,J.G., Tanner,C.K., McNaughton,K.K., Woosley,J.T., Greenhalgh,C.J. and Lund,P.K. (2006a). Haplotype insufficiency for suppressor of cytokine signaling-2 enhances intestinal growth and promotes polyp formation in growth hormone-transgenic mice. *Endocrinology* *147*, 1632-1641.
- Michaylira,C.Z., Simmons,J.G., Ramocki,N.M., Scull,B.P., McNaughton,K.K., Fuller,C.R. and Lund,P.K. (2006b). Suppressor of cytokine signaling-2 limits intestinal growth and enterotrophic actions of IGF-I in vivo. *American Journal of Physiology - Gastrointestinal and Liver Physiology* *291*, G472-G481.
- Milward,A., Metherell,L., Maamra,M., Barahona,M.J., Wilkinson,I.R., Camacho-Hübner,C., Savage,M.O., Bidlingmaier,M., Clark,A.J., Ross,R.J. and Webb,S.M. (2004). Growth hormone (GH)

insensitivity syndrome due to a GH receptor truncated after Box1, resulting in isolated failure of STAT 5 signal transduction. *The Journal of Clinical Endocrinology & Metabolism* **89**, 1259-1266.

Minamoto,S., Ikegame,K., Ueno,K., Narazaki,M., Naka,T., Yamamoto,H., Matsumoto,T., Saito,H., Hosoe,S. and Kishimoto,T. (1997). Cloning and functional analysis of new members of STAT induced STAT inhibitor (SSI) family: SSI-2 and SSI-3. *Biochemical and Biophysical Research Communications* **237**, 79-83.

Minina,E., Kreschel,C., Naski,M.C., Ornitz,D.M. and Vortkamp,A. (2002). Interaction of FGF, Ihh/Pthlh, and BMP signaling integrates chondrocyte proliferation and hypertrophic differentiation. *Developmental Cell* **3**, 439-449.

Minina,E., Wenzel,H.M., Kreschel,C., Karp,S., Gaffield,W., McMahon,A.P. and Vortkamp,A. (2001). BMP and Ihh/PTHrP signaling interact to coordinate chondrocyte proliferation and differentiation. *Development* **128**, 4523-4534.

Mizushima,S. and Nagata,S. (1990). pEF-BOS, a powerful mammalian expression vector. *Nucleic Acids Research* **18**, 5322.

Morishima,A., Grumbach,M.M., Simpson,E.R., Fisher,C. and Qin,K. (1995). Aromatase deficiency in male and female siblings caused by a novel mutation and the physiological role of estrogens. *The Journal of Clinical Endocrinology and Metabolism* **80**, 3689-3698.

Mushtaq,T. and Ahmed,S.F. (2002). The impact of corticosteroids on growth and bone health. *Archives of Disease in Childhood* **87**, 93-96.

Mushtaq,T., Bijman,P., Ahmed,S.F. and Farquharson,C. (2004). Insulin-like growth factor-I augments chondrocyte hypertrophy and reverses glucocorticoid-mediated growth retardation in fetal mice metatarsal cultures. *Endocrinology* **145**, 2478-2486.

Mushtaq,T., Farquharson,C., Seawright,E. and Ahmed,S.F. (2002). Glucocorticoid effects on chondrogenesis, differentiation and apoptosis in the murine ATDC5 chondrocyte cell line. *Journal of Endocrinology* **175**, 705-713.

Naka,T., Matsumoto,T., Narazaki,M., Fujimoto,M., Morita,Y., Ohsawa,Y., Saito,H., Nagasawa,T., Uchiyama,Y. and Kishimoto,T. (1998). Accelerated apoptosis of lymphocytes by augmented induction of Bax in SSI-1 (STAT-induced STAT inhibitor-1) deficient mice. *Proceedings of the National Academy of Sciences of the United States of America* **95**, 15577-15582.

Naski,M.C., Colvin,J.S., Coffin,J.D. and Ornitz,D.M. (1998). Repression of hedgehog signaling and BMP4 expression in growth plate cartilage by fibroblast growth factor receptor 3. *Development* **125**, 4977-4988.

Nicholson,S.E., Willson,T.A., Farley,A., Starr,R., Zhang,J.G., Baca,M., Alexander,W.S., Metcalf,D., Hilton,D.J. and Nicola,N.A. (1999). Mutational analyses of SOCS proteins suggest a dual domain requirement but distinct mechanisms for inhibition of LIF and IL-6 signal transduction. *The EMBO Journal* **18**, 375-385.

Nilsson,A., Isgaard,J., Lindahl,A., Dahlström,A., Skottner,A. and Isaksson,O.G.P. (1986). Regulation by growth hormone of number of chondrocytes containing IGF-I in rat growth plate. *Science* **233**, 571-574.

- Nilsson,O., Chrysis,D., Pajulo,O., Boman,A., Holst,M., Rubinstein,J., Martin Ritzén,E. and Sävendahl,L. (2003). Localization of estrogen receptors- α and - β and androgen receptor in the human growth plate at different pubertal stages. *Journal of Endocrinology* 177, 319-326.
- Nilsson,O., Marino,R., De Luca,F., Phillip,M. and Baron,J. (2005). Endocrine regulation of the growth plate. *Hormone Research* 64, 157-165.
- Ohlsson,C., Bengtsson,B., Isaksson,O.G.P., Andreassen,T.T. and Słotweg,M.C. (1998). Growth hormone and bone. *Endocrine Reviews* 19, 55-79.
- Ohlsson,C., Nilsson,A., Isaksson,O. and Lindahl,A. (1992a). Growth hormone induces multiplication of the slowly cycling germinal cells of the rat tibial growth plate. *Proceedings of the National Academy of Sciences of the United States of America* 89, 9826-9830.
- Ohlsson,C., Nilsson,A., Isaksson,O.G.P. and Lindahl,A. (1992b). Effect of growth hormone and insulin-like growth factor-I on DNA synthesis and matrix production in rat epiphyseal chondrocytes in monolayer culture. *Journal of Endocrinology* 133, 291-300.
- Ornitz,D.M. (2005). FGF signaling in the developing endochondral skeleton. *Cytokine & Growth Factor Reviews* 16, 205-213.
- Owen,H.C., Ahmed,S.F. and Farquharson,C. (2009). Chondrocyte p21(WAF1/CIP1) expression is increased by dexamethasone but does not contribute to dexamethasone-induced growth retardation in vivo. *Calcified Tissue International* 85, 326-334.
- Öz,O.K., Millsaps,R., Welch,R., Birch,J. and Zerwekh,J.E. (2001). Expression of aromatase in the human growth plate. *Journal of Molecular Endocrinology* 27, 249-253.
- Parker,E.A., Hegde,A., Buckley,M., Barnes,K.M., Baron,J. and Nilsson,O. (2007). Spatial and temporal regulation of GH-IGF-related gene expression in growth plate cartilage. *Journal of Endocrinology* 194, 31-40.
- Parks,J.S., Brown,M.R. and Faase,M.E. (1997). The spectrum of growth-hormone insensitivity. *The Journal of Pediatrics* 131, S45-S50.
- Pass,C., MacRae,V.E., Ahmed,S.F. and Farquharson,C. (2009). Inflammatory cytokines and the GH/IGF-I axis: novel actions on bone growth. *Cell Biochemistry and Function* 27, 119-127.
- Pezet,A., Favre,H., Kelly,P.A. and Edery,M. (1999). Inhibition and restoration of prolactin signal transduction by suppressors of cytokine signaling. *The Journal of Biological Chemistry* 274, 24497-24502.
- Phornphutkul,C., Wu,K.Y., Yang,X., Chen,Q. and Gruppuso,P.A. (2004). Insulin-like growth factor-I signaling is modified during chondrocyte differentiation. *Journal of Endocrinology* 183, 477-486.
- Pizette,S. and Niswander,L. (2000). BMPs are required at two steps of limb chondrogenesis: Formation of prechondrogenic condensations and their differentiation into chondrocytes. *Developmental Biology* 219, 237-249.
- Rajaram,S., Baylink,D.J. and Mohan,S. (1997). Insulin-like growth factor-binding proteins in serum and other biological fluids: Regulation and functions. *Endocrine Reviews* 18, 801-831.

- Ram,P.A. and Waxman,D.J. (1999). SOCS/CIS protein inhibition of growth hormone-stimulated STAT5 signaling by multiple mechanisms. *The Journal of Biological Chemistry* 274, 35553-35561.
- Register,T.C., McLean,F.M., Low,M.G. and Wuthier,R.E. (1986). Roles of alkaline phosphatase and labile internal mineral in matrix vesicle-mediated calcification. *The Journal of Biological Chemistry* 261, 9354-9360.
- Reynolds,J.J., Hembry,R.M. and Meikle,M.C. (1994). Connective tissue degradation in health and periodontal disease and the roles of matrix metalloproteinases and their natural inhibitors. *Advances in Dental Research* 8, 312-319.
- Rico-Bautista,E., Flores-Morales,A. and Fernández-Pérez,L. (2006). Suppressor of cytokine signaling (SOCS) 2, a protein with multiple functions. *Cytokine & Growth Factor Reviews* 17, 431-439.
- Rico-Bautista,E., Greenhalgh,C.J., Tollet-Egnell,P., Hilton,D.J., Alexander,W.S., Norstedt,G. and Flores-Morales,A. (2005). Suppressor of cytokine signaling-2 deficiency induces molecular and metabolic changes that partially overlap with growth hormone-dependent effects. *Molecular Endocrinology* 19, 781-793.
- Rivera,C.A., Wheeler,M.D., Enomoto,N. and Thurman,R.G. (1998). A choline-rich diet improves survival in a rat model of endotoxin shock. *American Journal of Physiology - Gastrointestinal and Liver Physiology* 275, G862-G867.
- Rivkees,S.A., Bode,H.H. and Crawford,J.D. (1988). Long-term growth in juvenile acquired hypothyroidism: the failure to achieve normal adult stature. *The New England Journal of Medicine* 318, 599-602.
- Roach,H.I., Erenpreisa,J. and Aigner,T. (1995). Osteogenic differentiation of hypertrophic chondrocytes involves asymmetric cell divisions and apoptosis. *The Journal of Cell Biology* 131, 483-494.
- Roberts,A.W., Robb,L., Rakar,S., Hartley,L., Cluse,L., Nicola,N.A., Metcalf,D., Hilton,D.J. and Alexander,W.S. (2001). Placental defects and embryonic lethality in mice lacking suppressor of cytokine signaling 3. *Proceedings of the National Academy of Sciences of the United States of America* 98, 9324-9329.
- Rosenfeld,R.G., Kofoed,E., Buckway,C., Little,B., Woods,K.A., Tsubaki,J., Pratt,K.A., Bezrodnik,L., Jasper,H., Tepper,A., Heinrich,J.J. and Hwa,V. (2005). Identification of the first patient with a confirmed mutation of the JAK-STAT system. *Pediatric Nephrology* 20, 303-305.
- Salmon,W.D. and Daughaday,W.H. (1957). A hormonally controlled serum factor which stimulates sulfate incorporation by cartilage in vitro. *Journal of Laboratory and Clinical Medicine* 49, 825-836.
- Sävendahl,L., Underwood,L.E., Haldeman,K.M., Ulshen,M.H. and Lund,P.K. (1997). Fasting prevents experimental murine colitis produced by dextran sulfate sodium and decreases interleukin-1 beta and insulin-like growth factor I messenger ribonucleic acid. *Endocrinology* 138, 734-740.
- Scheven,B.A. and Hamilton,N.J. (1991). Longitudinal bone growth in vitro: effects of insulin-like growth factor I and growth hormone. *Acta Endocrinologica* 124, 602-607.

- Schipani,E., Ryan,H.E., Didrickson,S., Kobayashi,T., Knight,M. and Johnson,R.S. (2001). Hypoxia in cartilage: HIF-1 α is essential for chondrocyte growth arrest and survival. *Genes & Development* 15, 2865-2876.
- Schwartz,Z., Nasatzky,E., Ornoy,A., Brooks,B.P., Soskolne,W.A. and Boyan,B.D. (1994). Gender-specific, maturation-dependent effects of testosterone on chondrocytes in culture. *Endocrinology* 134, 1640-1647.
- Serra,R., Karaplis,A. and Sohn,P. (1999). Parathyroid hormone-related peptide (PTHrP)-dependent and -independent effects of transforming growth factor beta (TGF-beta) on endochondral bone formation. *The Journal of Cell Biology* 145, 783-794.
- Shapiro,I.M., Adams,C.S., Freeman,T. and Srinivas,V. (2005). Fate of the hypertrophic chondrocyte: Microenvironmental perspectives on apoptosis and survival in the epiphyseal growth plate. *Birth Defects Research (Part C)* 75, 330-339.
- Shen,W.H., Zhou,J.H., Broussard,S.R., Freund,G.G., Dantzer,R. and Kelley,K.W. (2002). Proinflammatory cytokines block growth of breast cancer cells by impairing signals from a growth factor receptor. *Cancer Research* 62, 4746-4756.
- Shi,H., Tzameli,I., Bjorbaek,C. and Flier,J.S. (2004). Suppressor of cytokine signaling 3 is a physiological regulator of adipocyte insulin signaling. *The Journal of Biological Chemistry* 279, 34733-34740.
- Shimizu,H., Yokoyama,S. and Asahara,H. (2007). Growth and differentiation of the developing limb bud from the perspective of chondrogenesis. *Development, Growth & Differentiation* 49, 449-454.
- Shimoaka,T., Kamekura,S., Chikuda,H., Hoshi,K., Chung,U.I., Akune,T., Maruyama,Z., Komori,T., Matsumoto,M., Ogawa,W., Terauchi,Y., Kadowaki,T., Nakamura,K. and Kawaguchi,H. (2004). Impairment of bone healing by insulin receptor substrate-1 deficiency. *The Journal of Biological Chemistry* 279, 15314-15322.
- Shoba,L.N., Newman,M., Liu,W. and Lowe,Jr.W.L. (2001). LY 294002, an inhibitor of phosphatidylinositol 3-kinase, inhibits GH-mediated expression of the IGF-I gene in rat hepatocytes. *Endocrinology* 142, 3980-3986.
- Siegel,S.A., Shealy,D.J., Nakada,M.T., Le,J., Woulfe,D.S., Probert,L., Kollias,G., Ghayeb,J., Vilcek,J. and Daddona,P.E. (1995). The mouse/human chimeric monoclonal antibody cA2 neutralizes TNF in vitro and protects transgenic mice from cachexia and TNF lethality in vivo. *Cytokine* 7, 15-25.
- Simon,D., Fernando,C., Czernichow,P. and Prieur,A.M. (2002a). Linear growth and final height in patients with systemic juvenile idiopathic arthritis treated with longterm glucocorticoids. *Journal of Rheumatology* 29, 1296-1300.
- Simon,D., Lucidarme,N., Prieur,A.M., Ruiz,J.C. and Czernichow,P. (2002b). Treatment of growth failure in juvenile chronic arthritis. *Hormone Research* 58, 28-32.
- Simon,D., Prieur,A.M., Quartier,P., Charles Ruitz,J. and Czernichow,P. (2007). Early recombinant human growth hormone treatment in glucocorticoid-treated children with juvenile idiopathic arthritis: a 3-year randomized study. *The Journal of Clinical Endocrinology and Metabolism* 92, 2567-2573.

- Sims,N.A., Clement-Lacroix,P., Da Ponte,F., Bouali,Y., Binart,N., Moriggl,R., Goffin,V., Coschigano,K., Gaillard-Kelly,M., Kopchick,J., Baron,R. and Kelly,P.A. (2000). Bone homeostasis in growth hormone receptor-null mice is restored by IGF-I but independent of Stat5. *The Journal of Clinical Investigation* *106*, 1095-1103.
- Sims,N.A. and Gooi,J.H. (2008). Bone remodeling: Multiple cellular interactions required for coupling of bone formation and resorption. *Seminars in Cells & Developmental Biology* *19*, 444-451.
- Sjögren,K., Liu,J.L., Blad,K., Skrtic,S., Vidal,O., Wallenius,V., LeRoith,D., Törnell,J., Isaksson,O.G.P., Jansson,J.O. and Ohlsson,C. (1999). Liver-derived insulin-like growth factor I (IGF-I) is the principal source of IGF-I in blood but is not required for postnatal body growth in mice. *Proceedings of the National Academy of Sciences of the United States of America* *96*, 7088-7092.
- Slonim,A.E., Bulone,L., Damore,M.B., Goldberg,T., Wingertzahn,M.A. and McKinley,M.J. (2000). A preliminary study of growth hormone therapy for crohn's disease. *The New England Journal of Medicine* *342*, 1633-1637.
- Smit,L.S., Meyer,D.J., Billestrup,N., Norstedt,G., Schwartz,J. and Carter-Su,C. (1996). The role of the growth hormone (GH) receptor and JAK1 and JAK2 kinases in the activation of Stats 1, 3, and 5 by GH. *Molecular Endocrinology* *10*, 519-533.
- Smith,E.P., Boyd,J., Frank,G.R., Takahashi,H., Cohen,R.M., Specker,B., Williams,T.C., Lubahn,D.B. and Korach,K.S. (1994). Estrogen resistance caused by a mutation in the estrogen-receptor gene in a man. *The New England Journal of Medicine* *331*, 1056-1061.
- Sommerfeldt,D.W. and Rubin,C.T. (2001). Biology of bone and how it orchestrates the form and function of the skeleton. *European Spine Journal* *10*, S86-S95.
- Spencer,G.S., Hodgkinson,S.C. and Bass,J.J. (1991). Passive immunization against insulin-like growth factor-I does not inhibit growth hormone-stimulated growth of dwarf rats. *Endocrinology* *128*, 2103-2109.
- St-Jaques,B., Hammerschmidt,M. and McMahon,A.P. (1999). Indian hedgehog signaling regulates proliferation and differentiation of chondrocytes and is essential for bone formation. *Genes & Development* *13*, 2072-2086.
- Stahl,N., Farruggella,T.J., Boulton,T.G., Zhong,Z., Darnell,J.E. and Yancopoulos,G.D. (1995). Choice of Stats and other substrates specified by modular tyrosine-based motifs in cytokine receptors. *Science* *267*, 1349-1353.
- Starr,R., Metcalf,D., Elefanty,A.G., Brysha,M., Willson,T.A., Nicola,N.A., Hilton,D.J. and Alexander,W.S. (1998). Liver degeneration and lymphoid deficiencies in mice lacking suppressor of cytokine signaling-1. *Proceedings of the National Academy of Sciences of the United States of America* *95*, 14395-14399.
- Starr,R., Willson,T.A., Viney,E.M., Murray,L.J.L., Rayner,J.R., Jenkins,B.J., Gonda,T.J., Alexander,W.S., Metcalf,D., Nicola,N.A. and Hilton,D.J. (1997). A family of cytokine-inducible inhibitors of signalling. *Nature* *387*, 917-921.
- Stevens,D.A., Hasserjian,R.P., Robson,H., Siebler,T., Shalet,S.M. and Williams,G.R. (2000). Thyroid hormones regulate hypertrophic chondrocyte differentiation and expression of parathyroid

hormone-related peptide and its receptor during endochondral bone formation. *Journal of Bone and Mineral Research* *15*, 2431-2442.

Stratikopoulos,E., Szabolcs,M., Dragatsis,I., Klinakis,A. and Efstratiadis,A. (2008). The hormonal action of IGF1 in postnatal mouse growth. *Proceedings of the National Academy of Sciences of the United States of America* *105*, 19378-19383.

Strle,K., Broussard,S.R., McCusker,R.H., Shen,W.H., Johnson,R.W., Freund,G.G., Dantzer,R. and Kelley,K.W. (2004). Proinflammatory cytokine impairment of insulin-like growth factor I-induced protein synthesis in skeletal muscle myoblasts requires ceramide. *Endocrinology* *145*, 4592-4602.

Suda,K., Iguchi,G., Yamamoto,M., Handayaningsih,A.E., Nishizawa,H., Takahashi,M., Okimura,Y., Kaji,H., Chihara,K. and Takahashi,Y. (2011). A case of gigantism associated with a missense mutation in the *SOCS2* gene. *Endo 2011: The 93rd Annual Meeting & Expo*.

Suntornsaratoon,P., Wongdee,K., Krishnamra,N. and Charoenphandhu,N. (2010). Possible chondroregulatory role of prolactin on the tibial growth plate of lactating rats. *Histochemistry and Cell Biology* *134*, 483-491.

Takeda,K., Noguchi,K., Shi,W., Tanaka,T., Matsumoto,M., Yoshida,N., Kishimoto,T. and Akira,S. (1997). Targeted disruption of the mouse *Stat3* gene leads to early embryonic lethality. *Proceedings of the National Academy of Sciences of the United States of America* *94*, 3801-3804.

Takeda,S., Bonnamy,J.P., Owen,M.J., Ducey,P. and Karsenty,G. (2001). Continuous expression of *Cbfa1* in nonhypertrophic chondrocytes uncovers its ability to induce hypertrophic chondrocyte differentiation and partially rescues *Cbfa1*-deficient mice. *Genes & Development* *15*, 467-481.

Teglund,S., McKay,C., Schuetz,E., van Deursen,J.M., Stravopodis,D., Wang,D., Brown,M., Bodner,S., Grosveld,G. and Ihle,J.N. (1998). *Stat5a* and *Stat5b* proteins have essential and nonessential, or redundant, roles in cytokine responses. *Cell* *93*, 841-850.

Teitelbaum,S.L. (2000). Bone resorption by osteoclasts. *Science* *289*, 1504-1508.

Tilg,H., Moschen,A.R., Kaser,A., Pines,A. and Dotan,I. (2008). Gut, inflammation and osteoporosis: basic and clinical concepts. *Gut* *57*, 684-694.

Tiulpakov,A., Rubtsov,P., Dedov,I., Peterkova,V., Bezlepkina,O., Chrousos,G.P. and Hochberg,Z. (2005). A novel C-terminal growth hormone receptor (GHR) mutation results in impaired GHR-STAT5 but normal STAT-3 signaling. *The Journal of Clinical Endocrinology & Metabolism* *90*, 542-547.

Tollet-Egnell,P., Flores-Morales,A., Stavreus-Evers,A., Sahlin,L. and Norstedt,G. (1999). Growth hormone regulation of *SOCS-2*, *SOCS-3*, and *CIS* messenger ribonucleic acid expression in the rat. *Endocrinology* *140*, 3693-3704.

Tomizawa,M., Shinozaki,F., Sugiyama,T., Yamamoto,S., Sueishi,M. and Yoshida,T. (2010). Insulin-like growth factor-I receptor in proliferation and motility of pancreatic cancer. *World Journal of Gastroenterology* *16*,1854-1858.

Tordoff,M.G., Bachmanov,A.A. and Reed,D.R. (2007). Forty mouse strain survey of water and sodium intake. *Physiology & Behaviour* *91*, 620-631.

- Touati,G., Prieur,A.M., Ruiz,J.C., Noel,M. and Czernichow,P. (1998). Beneficial effects of one-year growth hormone administration to children with juvenile chronic arthritis on chronic steroid therapy. I. Effects on growth velocity and body composition. *The Journal of Clinical Endocrinology & Metabolism* *83*, 403-409.
- Treadwell,B.V. and Mankin,HJ. (1986). The synthetic processes of articular cartilage. *Clinical orthopaedics and related research* *213*, 50-61.
- Turnley,A.M. (2005). Role of SOCS2 in growth hormone actions. *Trends in Endocrinology and Metabolism* *16*, 53-58.
- Udy,G.B., Towers,R.P., Snell,R.G., Wilkins,R.J., Park,S.H., Ram,P.A., Waxman,D.J. and Davey,H.W. (1997). Requirement of STAT5b for sexual dimorphism of body growth rates and liver gene expression. *Proceedings of the National Academy of Sciences of the United States of America* *94*, 7239-7244.
- Ulici,V., Hoenselaar,K., Gillespie,J.R. and Beier,F. (2008). The PI3K pathway regulates endochondral bone growth through control of hypertrophic chondrocyte differentiation. *BMC Developmental Biology* *8*, 40.
- Uyttendaele,I., Lemmens,I., Verhee,A., De Smet,A.S., Vandekerckhove,J., Lavens,D., Peelman,F. and Tavernier,J. (2007). Mammalian protein-protein interaction trap (MAPPIT) analysis of STAT5, CIS, and SOCS2 interactions with the growth hormone receptor. *Molecular Endocrinology* *21*, 2821-2831.
- van der Eerden,B.C.J., Karperien,M. and Wit,J.M. (2003). Systemic and local regulation of the growth plate. *Endocrine Reviews* *24*, 782-801.
- Vega,R.B., Matsuda,K., Oh,J., Barbosa,A.C., Yang,X., Meadows,E., McAnally,J., Pomajzl,C., Shelton,J.M., Richardson,J.A., Karsenty,G. and Olson,E.N. (2004). Histone deacetylase 4 controls chondrocyte hypertrophy during skeletogenesis. *Cell* *119*, 555-566.
- Veldehuis,J.D., Metsger,D.L., Martha,P.M.J., Mauras,N., Kerrigan,J.R., Keenan,B., Rogol,A.D. and Pincus,S.M. (1997). Estrogen and testosterone, but not a nonaromatizable androgen, direct network integration of the hypothalamo-somatotrope (growth hormone)-insulin-like growth factor I axis in the human: evidence from pubertal pathophysiology and sex-steroid hormone replacement. *The Journal of Clinical Endocrinology and Metabolism* *82*, 3414-3420.
- Vidal,O.M., Merino,R., Rico-Bautista,E., Fernandez-Perez,L., Chia,D.J., Woelfle,J., Ono,M., Lenhard,B., Norstedt,G., Rotwein,P. and Flores-Morales,A. (2007). In vivo transcript profiling and phylogenetic analysis identifies suppressor of cytokine signaling 2 as a direct signal transducer and activator of transcription 5b target in liver. *Molecular Endocrinology* *21*, 293-311.
- Vortkamp,A., Lee,K., Lanske,B., Segre,G.V., Kronenberg,H.M. and Tabin,C.J. (1996). Regulation of rate of cartilage differentiation by Indian hedgehog and PTH-related protein. *Science* *273*, 613-622.
- Walenkamp,M.J.E. and Wit,J.M. (2007). Genetic disorders in the GH IGF-I axis in mouse and man. *European Journal of Endocrinology* *157*, S15-S26.
- Wang,J., Zhou,J. and Bondy,C.A. (1999). IGF1 promotes longitudinal bone growth by insulin-like actions augmenting chondrocyte hypertrophy. *The FASEB Journal*. *13*, 1985-1990.

- Wang,J., Zhou,J., Cheng,C.M., Kopchick,J.J. and Bondy,C.A. (2004). Evidence supporting dual, IGF-I-independent and IGF-I-dependent, roles for GH in promoting longitudinal bone growth. *Journal of Endocrinology* *180*, 247-255.
- Waters,M.J., Hoang,H.N., Fairlie,D.P., Pelekanos,R.A. and Brown,R.J. (2006). New insights into growth hormone action. *Journal of Molecular Endocrinology* *36*, 1-7.
- Weise,M., De-Levi,S., Barnes,K.M., Gafni,R.I., Abad,V. and Baron,J. (2001). Effects of estrogen on growth plate senescence and epiphyseal fusion. *Proceedings of the National Academy of Sciences of the United States of America* *98*, 6871-6876.
- Williams,K.L., Fuller,C.R., Dieleman,L.A., DaCosta,C.M., Haldeman,K.M., Sartor,R.B. and Lund,P.K. (2001). Enhanced survival and mucosal repair after dextran sodium sulfate-induced colitis in transgenic mice that overexpress growth hormone. *Gastroenterology* *120*, 925-937.
- Wilsman,N.J., Farnum,C.E., Green,E.M., Lieferman,E.M. and Clayton,M.K. (1996a). Cell cycle analysis of proliferative zone chondrocytes in growth plates elongating at different rates. *Journal of Orthopaedic Research* *14*, 562-572.
- Wilsman,N.J., Farnum,C.E., Lieferman,E.M., Fry,M. and Barreto,C. (1996b). Differential growth by growth plates as a function of multiple parameters of chondrocytic kinetics. *Journal of Orthopaedic Research* *14*, 927-936.
- Woelfle,J., Billiard,J. and Rotwein,P. (2003a). Acute control of insulin-like growth factor-I gene transcription by growth hormone through Stat5b. *The Journal of Biological Chemistry* *278*, 22696-22702.
- Woelfle,J., Chia,D.J. and Rotwein,P. (2003b). Mechanisms of growth hormone (GH) action - Identification of conserved Stat5 binding sites that mediate GH-induced insulin-like growth factor-I gene activation. *The Journal of Biological Chemistry* *278*, 51261-51266.
- Wong,S.C., Hassan,K., McGrogan,P., Weaver,L.T. and Ahmed,S.F. (2007). The effects of recombinant growth hormone on linear growth in children with Crohn's disease and short stature. *Journal of Pediatric Endocrinology & Metabolism* *20*, 1315-1324.
- Wong,S.C., Kumar,P., Galloway,P.J., Blair,J.C., Didi,M., Dalzell,A.M., Hassan,K., McGrogan,P. and Ahmed,S.F. (2011). A preliminary trial of the effect of recombinant human growth hormone on short-term linear growth and glucose homeostasis in children with Crohn's disease. *Clinical Endocrinology* *74*, 599-607.
- Wong,S.C., Smyth,A., McNeill,E., Galloway,P.J., Hassan,K., McGrogan,P. and Ahmed,S.F. (2010). The growth hormone insulin-like growth factor 1 axis in children and adolescents with inflammatory bowel disease and growth retardation. *Clinical Endocrinology* *73*, 220-228.
- Yadav,A., Kalita,A., Dhillon,S. and Banerjee,K. (2005). JAK/STAT3 pathway is involved in survival of neurons in response to insulin-like growth factor and negatively regulated by suppressor of cytokine signaling-3. *The Journal of Biological Chemistry* *280*, 31830-31840.
- Yadav,M.C., Simão,A.M., Narisawa,S., Huesa,C., McKee,M.D., Farquharson,C. and Millán,J.L. (2011). Loss of skeletal mineralization by the simultaneous ablation of PHOSPHO1 and alkaline phosphatase function: a unified model of the mechanisms of initiation of skeletal calcification. *Journal of Bone and Mineral Research* *26*, 286-297.

- Yakar,S., Liu,J.L., Butler,A., Accili,D., Sauer,B. and LeRoith,D. (1999). Normal growth and development in the absence of hepatic insulin-like growth factor 1. *Proceedings of the National Academy of Sciences of the United States of America* 96, 7324-7329.
- Yakar,S., Rosen,C.J., Beamer,W.G., Ackert-Bicknell,C.L., Wu,Y., Liu,J.L., Ooi,G.T., Setser,J., Frystyk,J., Boisclair,Y.R. and LeRoith,D. (2002). Circulating levels of IGF-1 directly regulate bone growth and density. *Journal of Clinical Investigation* 110, 771-781.
- Yoon,B.S., Poque,R., Ovchinnikov,D.A., Yoshii,I., Mishina,Y., Behringer,R.R. and Lyons,K.M. (2006). BMPs regulate multiple aspects of growth-plate chondrogenesis through opposing actions on FGF pathways. *Development* 133, 4678.
- Yoshimura,A., Naka,T. and Kubo,M. (2007). SOCS proteins, cytokine signalling and immune regulation. *Nature Reviews Immunology* 7, 454-465.
- Yoshimura,A., Nishinakamura,H., Matsumura,Y. and Hanada,T. (2005). Negative regulation of cytokine signaling and immune responses by SOCS proteins. *Arthritis Research & Therapy* 7, 100-110.
- Zelzer,E., Glotzer,D.J., Hartmann,C., Thomas,D., Fukai,N., Soker,S. and Olsen,B.R. (2001). Tissue specific regulation of VEGF expression during bone development requires Cbfa1/Runx2. *Mechanisms of Development* 106, 97-106.
- Zeulak,K.M. and Green,H. (1986). The generation of insulin-like growth factor-1-sensitive cells by growth hormone action. *Science* 233, 551-553.
- Zong,C.S., Chan,J., Levy,D.E., Horvath,C., Sadowski,H.B. and Wang,L.H. (2000). Mechanism of STAT3 activation by insulin-like growth factor I receptor. *The Journal of Biological Chemistry* 275, 15099-15105.

CHAPTER 10

APPENDIX

10. Appendix

10.1. Appendix 1: Buffer Recipes

10.1.1. Cell Culture

Maintenance medium:

DMEM/F-12 (1:1) with GlutaMAX I, supplemented with 5% FBS, 3×10^{-8} M sodium selenite, 10 µg/ml human transferrin (Sigma), 1 mM sodium pyruvate, and 0.05 mg/ml gentamicin

Differentiation medium:

DMEM/F-12 (1:1) with GlutaMAX I containing 5% FBS, 1X insulin transferring selenium (ITS; Sigma), 1 mM sodium pyruvate and 0.05 mg/ml gentamicin

Freezing mix:

60% DMEM/F-12; 20% FBS; 20% dimethyl sulfoxide (DMSO).

10.1.2. *In Vivo* Studies

Lysis buffer (Promega):

0.3 M sodium acetate; 10 mM TrisHCl (pH 7.9); 1 mM EDTA (pH 8.0); 1% SDS; 200 µg/ml Proteinase K

Primary chondrocyte medium:

DMEM with 4.5 g/L glucose and L-Glutamine containing 10% FBS and 0.05 mg/ml gentamicin

Osteoblast medium:

α-MEM (Minimum Essential Medium, alpha) supplemented with 10% FBS and 0.05 mg/ml gentamicin

Metatarsal preparation medium:

Each aliquot contained: 0.8 ml αMEM medium (without ribonucleosides), 10.45 ml sterile PBS, 22.5 mg Bovine Serum Albumin (BSA; Fraction V)

Metatarsal medium:

αMEM medium (without ribonucleosides) supplemented with 0.2% BSA (Fraction V); 5 µg/ml L-ascorbic acid phosphate (Wako Pure Chemicals Ltd); 1 mM β-glycerophosphate; 0.05 mg/ml gentamicin; 1.25 µg/ml fungizone

10.1.3. Processing Tissue

DAB substrate:

DAB substrate buffer (20X), DAB chromogen solution (20X) and substrate solution (20X) all diluted approx. 1:20 in H₂O

Scott's tap water:

0.2% sodium hydrogen carbonate and 2% magnesium sulphate in dH₂O

STAT5 immunohistochemistry wash buffer:

0.1M TRIS-HCl, 0.15M NaCl, 0.05% Tween 20 in dH₂O; pH 7.5.

STAT5 immunohistochemistry blocking buffer:

0.1M TRIS-HCl, 0.15M NaCl, 0.5% Blocking Reagent (supplied with TSA kit, Perkin Elmer). The blocking reagent was added slowly to the buffer, in small volumes, with constant stirring. The solution was gradually heated to 60°C with stirring until the blocking reagent had fully dissolved. The solution was filtered using a syringe filter (0.45µm) and stored in aliquots at -20°C.

STAT5 immunohistochemistry Biotynyl Tyramide (Amplification Reagent) working solution

Biotynyl tyramide (provided with TSA kit, Perkin Elmer) was reconstituted in DMSO to provide a stock solution and stored at 4°C. Prior to use this was diluted 1:50 using 1X amplification diluent (supplied with TSA kit, Perkin Elmer) to make the working solution.

STAT5 immunohistochemistry DAB solution

30mg DAB, 50ml PBS, 50µl H₂O₂.

10.1.4. Transfecting ATDC5 cells

S.O.C. medium (Invitrogen):

2% tryptone, 0.5% yeast extract, 10mM NaCl, 2.5mM KCl (Potassium chloride), 10mM MgCl₂, 10mM MgSO₄ (Magnesium sulphate), 20mM glucose

LB agar:

1% tryptone, 0.5% yeast extract, 10mg/ml NaCl, pH 7.0; supplemented with 1.5% bacto-agar) ampicillin (100µg/ml

Miniprep resuspension buffer (Invitrogen):

50mM Tris-HCl, pH 8.0; 10mM EDTA, 20mg/ml RNase A). 250µl lysis buffer (200mM NaOH, 1% wt./vol. SDS

NEB buffer 4 (1X; New England Biolabs):

20mM Tris-acetate, 50mM potassium acetate, 10mM magnesium acetate, 1mM dithiothreitol; pH 7.9

SuRE/Cut buffer H (10X):

50mM Tris-HCl, 10mM MgCl₂, 100mM NaCl, 1mM dithioerythritol; pH 7.5

Maxiprep buffer P1 (Qiagen):

50mM Tris-Cl, pH8; 10mM EDTA; 100µg/ml RNase A; 0.1% LyseBlue as an indicator of optimum mixing

Maxiprep buffer P2 (Qiagen):

200mM NaOH, 1% SDS (wt./vol.)

Maxiprep buffer P3 (Qiagen):

3M potassium acetate, pH 5.5

Maxiprep medium-salt wash buffer QC (Qiagen):

1M NaCl; 50mM MOPS, pH 7.0; 15% isopropanol (wt./vol.)

Maxiprep high-salt buffer QN (Qiagen):

1.6M NaCl; 50mM MOPS, pH 7.0; 15% isopropanol

Maxiprep TE buffer (Qiagen):

10mM Tris-HCl, pH 8.0; 1mM EDTA

10.1.5. PCR

RT-PCR master mix:

11mM Ammonium Sulphate, 4.5mM MgCl₂, 45mM Tris-HCl (pH8.8), 4.5µM EDTA, 6.7mM 2-mercaptoethanol, and 1mM dNTP mix (Promega)

10.1.6. Western Blotting

RIPA buffer:

20mM Tris-HCl (pH8), 135mM NaCl, 10% Glycerol, 1% IGEPAL, 0.1% SDS, 0.5% Na Deoxycholate, 2mM EDTA

Transfer buffer:

100ml 10X transfer buffer, 200ml 98% Ethanol, 700ml dH₂O.

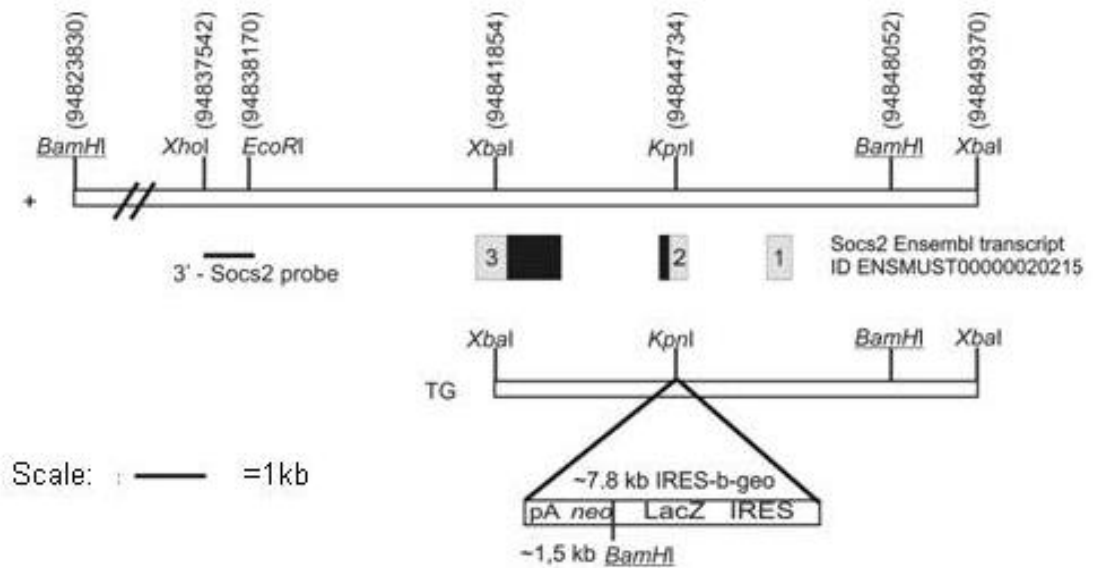
10X transfer buffer:

29.3mg/ml glycine, 58mg/ml Tris Base (trimethylamine), 18.8 μ l/ml 20% SDS (lauryl sulphate) in dH₂O

TBS/T:

Tris-buffered saline/Tween-20 consisting of 50mM Tris-HCl, 300mM NaCl, 0.1% Tween-20

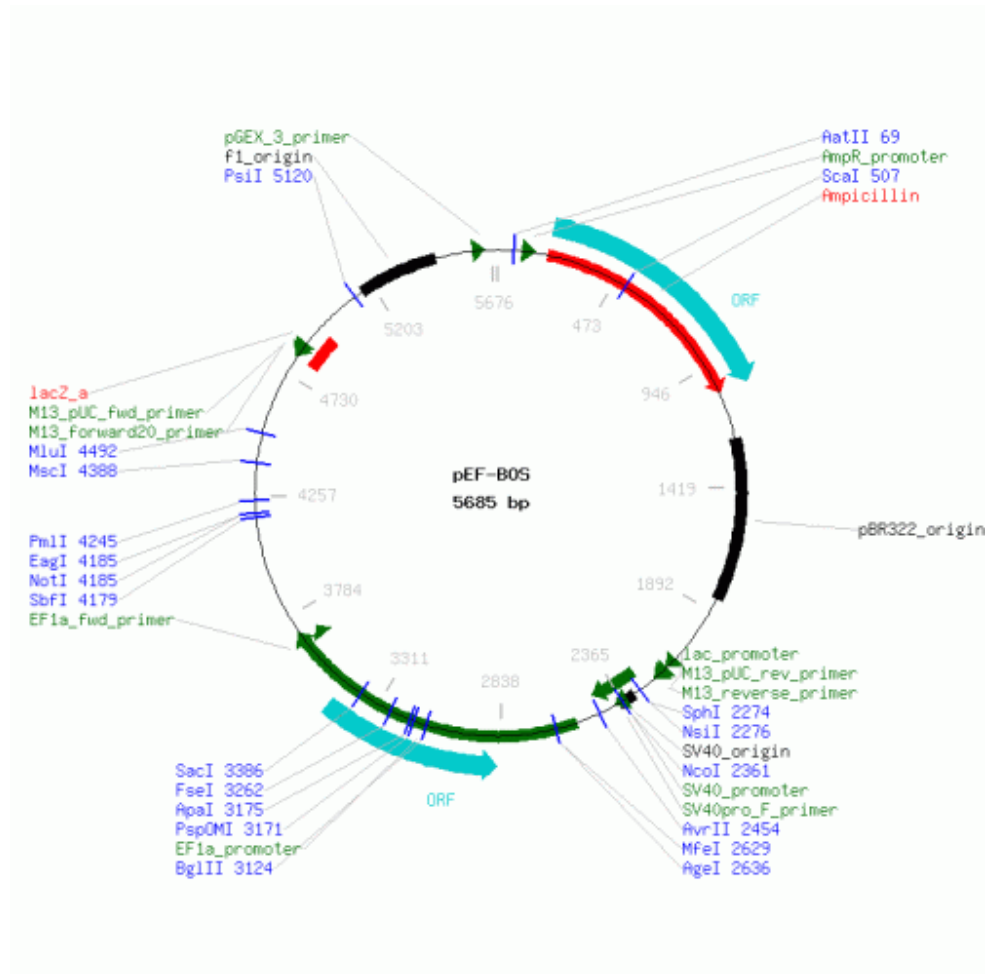
10.2. Appendix 2: Targeting for Construction SOCS2^{-/-} Mice



Targeting construct and wild-type (+) allele for creating SOCS2^{-/-} mice. A 7.8kb insert containing IRES-geo cassette has been inserted into exon 2 of the Socs2 transcript at the *KpnI* site (Ensembl ID ENSMUST00000020215; coding region in black). Positions within the mouse genome are indicated by numbers above the restriction sites (Ensembl release 45 - Jun 2007; <http://www.ensembl.org>).

10.3. Appendix 3: Plasmid Maps

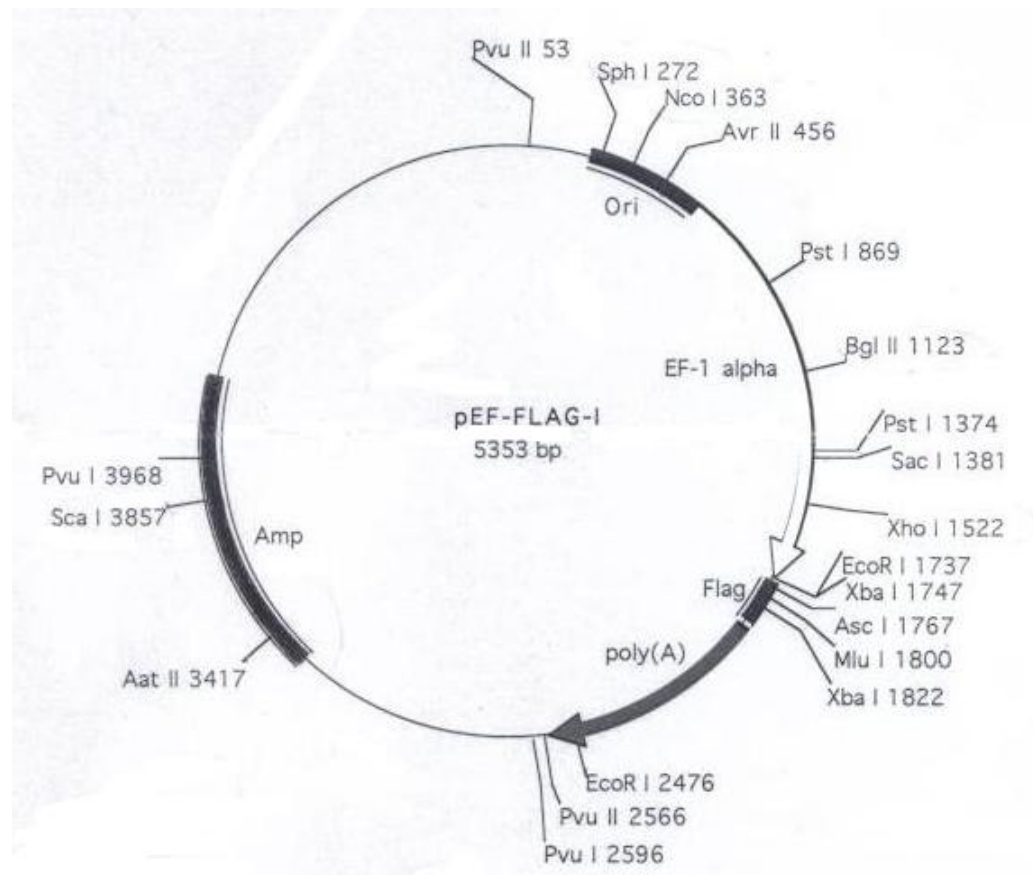
10.3.1. pEF-BOS Plasmid



Plasmid map of pEF-BOS, a mammalian non-viral plasmid that contains SV40ori, human EF-1alpha promoter, ampicillin resistance, poly-A from human G-CSF.

(www.lablife.org/p?a=vdb_view&old_id=5493&id=)

10.3.2. pEF-FLAG-I Plasmid



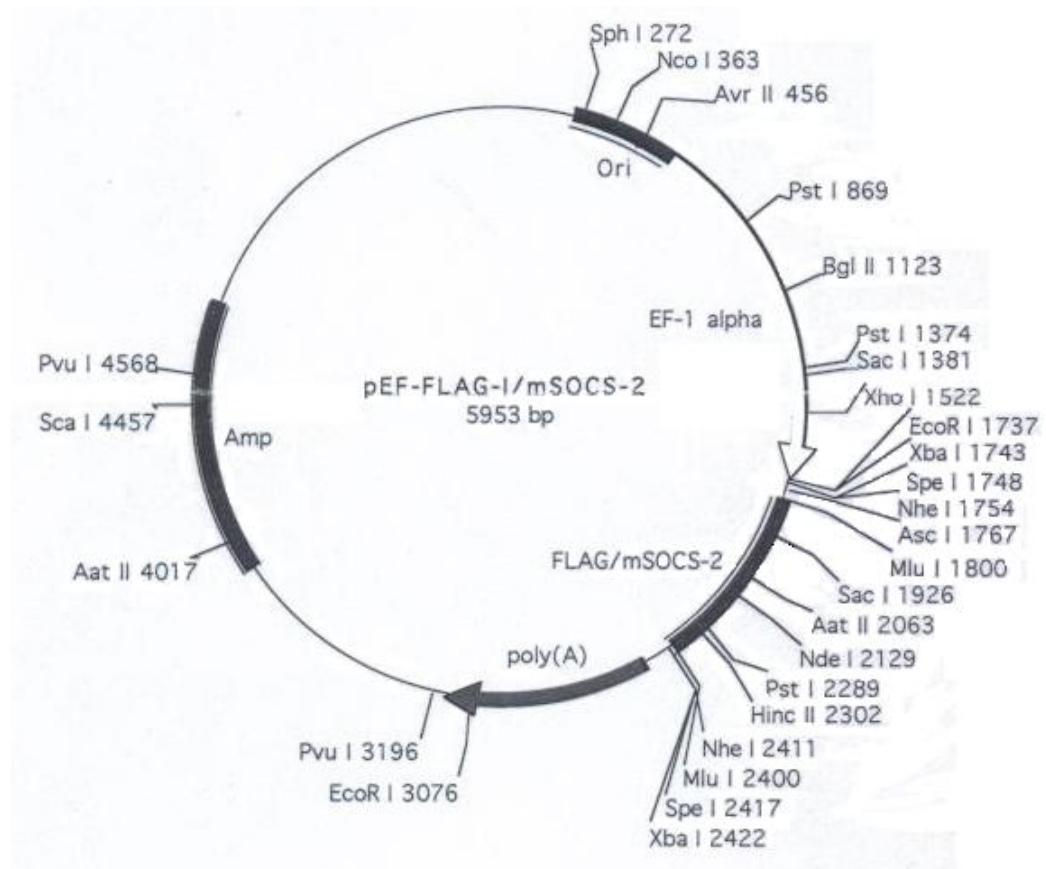
pEF-FLAG-I Expression Cassette:

TTCTTCCATTTTCAGGTGTCGTGAGGAATTCTCTAGACTAGTGCTAGCCACC M A R Q
 EcoRI Xba I Nhe I Asc I

D Y K D D D D K T R * *
 GAC TAC AAG GAC GAC GAT GAC AAG ACG CGT TAA TAG CTAGCACTAGTCTAGAGTGAG
 FLAG EPITOPE Mlu I Nhe I Xba I

GGTCCCCACCTGGGACCCTTGAGAGTATCAGGTCTCCCACGTGGGAGACAAGAAATCCCTGTTTAATA

10.3.3. pEF-FLAG-I/mSOCS2 Plasmid



pEF-FLAG-I/mSOCS2 Expression Cassette:

```

M A R Q D Y K D D D D K T R T L R C L E P S G
ATGGCGCGCCAGGACTACAAGGACGACGATGACAAGACGCGTACCCTGCGGTGCCTGGAGCCCTCCGGG
                FLAG                                mSOCS2 coding region

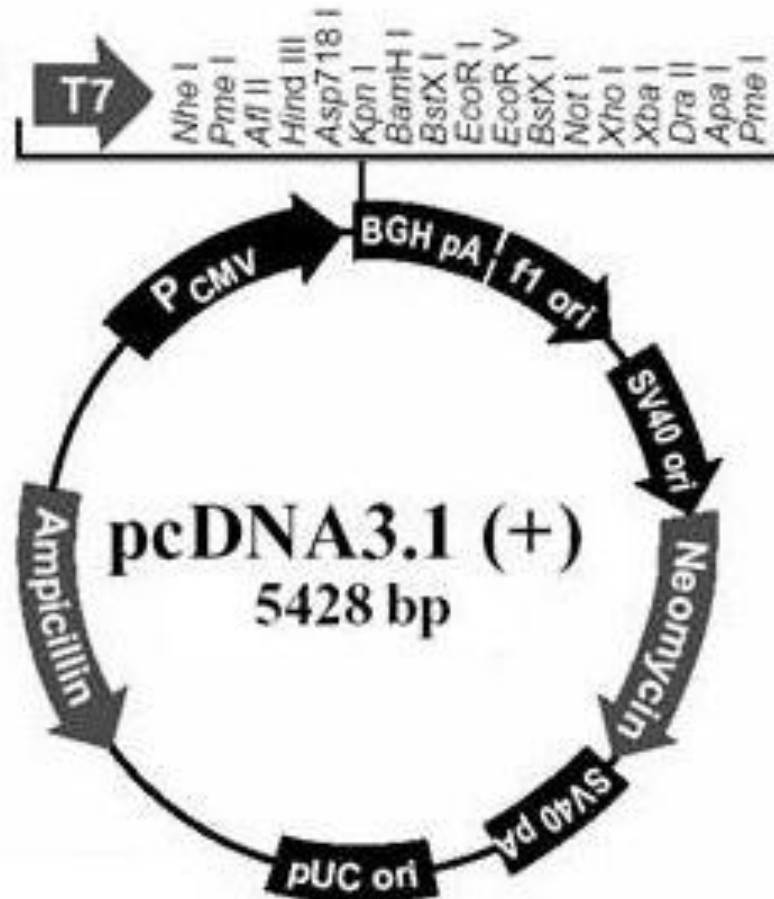
```

```

                P L P T R L K D Y L E E Y K F Q V *
.....CCTTTACCAACAAGACTAAAAGATTACTTGAAGAATATAAATCCAGGTATAA

```

10.3.4. pcDNA3.1(+) Plasmid



Comments for pcDNA3.1 (+)
5428 nucleotides

CMV promoter: bases 232-819

T7 promoter/priming site: bases 863-882

Multiple cloning site: bases 895-1010

pcDNA3.1/BGH reverse priming site: bases 1022-1039

BGH polyadenylation sequence: bases 1028-1252

f1 origin: bases 1298-1726

SV40 early promoter and origin: bases 1731-2074

Neomycin resistance gene (ORF): bases 2136-2930

SV40 early polyadenylation signal: bases 3104-3234

pUC origin: bases 3617-4287 (complementary strand)

Ampicillin resistance gene (*bla*): bases 4432-5428 (complementary strand)

ORF: bases 4432-5292 (complementary strand)

Ribosome binding site: bases 5300-5304 (complementary strand)

bla promoter (P3): bases 5327-5333 (complementary strand)

10.4. Appendix 4: Published Paper

The published review “Inflammatory cytokines and the GH/IGF-1 axis: novel actions on bone growth” follows this page.

Permission to reproduce this article has been granted by the publishers (John Wiley & Sons, Inc),
license number: 2744120316218.

Inflammatory cytokines and the GH/IGF-I axis: novel actions on bone growth

C. Pass^{1,2*}, V. E. MacRae¹, S. F. Ahmed² and C. Farquharson¹

¹*Bone Biology Group, Division of Developmental Biology, The Roslin Institute and Royal (Dick) School of Veterinary Studies, The University of Edinburgh, Roslin, Midlothian, UK*

²*Bone & Endocrine Research Group, Royal Hospital for Sick Children, Glasgow, UK*

Longitudinal bone growth is a tightly regulated process that relies on complex synchronized mechanisms at the growth plate. Chronic paediatric inflammatory diseases are well accepted to lead to growth retardation and this is likely due to raised inflammatory cytokine levels and reduced growth hormone (GH)/insulin-like growth factor-1 (IGF-I) signalling. The precise cellular mechanisms responsible for this inhibition are unclear and therefore in this article, we will review the potential interactions between inflammatory cytokines and the GH/IGF-I axis in the regulation of bone growth. In particular, we will emphasize the potential contribution of the suppressors of cytokine signalling (SOCS) proteins, and in particular SOCS2, in mediating this process. Copyright © 2009 John Wiley & Sons, Ltd.

KEY WORDS — GH; IGF-1; growth plate; chondrocytes; inflammatory cytokines; SOCS2

INTRODUCTION

Postnatal longitudinal bone growth is a tightly regulated process that relies on the growth plate¹. The actions of chondrocytes within the growth plate are controlled by various signalling pathways, including growth hormone (GH) and insulin-like growth factor-1 (IGF-1) signalling. Inhibition of these signalling pathways will result in growth retardation, as seen in a number of clinical disorders of the GH/IGF axis².

Impaired linear growth is commonly encountered in children suffering from chronic inflammatory conditions such as inflammatory bowel disease (IBD). In these children, maintenance of growth is a complex process that is influenced by a number of different mechanisms, including not only the administration of anti-inflammatory drugs but also other factors such as the disease process, and in the case of IBD, the malabsorption of nutrients^{3,4}. Clinical studies have shown that growth and skeletal development are reversibly impaired during periods of intensive therapy and especially during treatment with prednisolone and dexamethasone⁵. However, it is widely recognized that a contributing factor to the growth retardation observed in IBD and other inflammatory conditions is the raised levels of

inflammatory cytokines such as interleukin-1 β (IL-1 β), interleukin-6 (IL-6) and tumour necrosis factor α (TNF α)^{6,7}. The mechanisms by which these inflammatory cytokines inhibit the actions of the growth plate chondrocytes are poorly understood but an involvement of members of the suppressor of cytokine signalling (SOCS) family have been proposed. Although definitive studies have yet to be completed, SOCS2 may be central to this process, as SOCS2 knockout mice display an overgrowth phenotype and SOCS2 has been shown to inhibit GH signalling^{8,9}. Therefore, during chronic inflammation, raised levels of inflammatory cytokines may induce SOCS2 expression resulting in an inhibition of GH signalling and growth retardation.

ENDOCHONDRAL GROWTH: THE GROWTH PLATE AND CHONDROCYTES

Postnatal linear bone growth occurs as a result of endochondral ossification at the epiphyseal growth plate (Figure 1)^{10–12}. Growth plates are thin layers of cartilage found situated near the ends of all long bones and consist of both chondrocytes and their extracellular matrix^{11,13}. The matrix comprises of collagens, proteoglycans and a variety of other non-collagenous proteins¹⁴. The chondrocytes, which are arranged in columns that parallel the longitudinal axis of the bone, proceed through a series of differentiation and maturation stages whilst maintaining their spatially fixed locations^{6,11,15}.

* Correspondence to: C. Pass, Division of Developmental Biology, The Roslin Institute and R(D)SVS, The University of Edinburgh, Roslin, Midlothian, EH25 9PS, UK. Tel: 0131 5274244. Fax: 0131 440 0434. E-mail: chloe.pass@roslin.ed.ac.uk

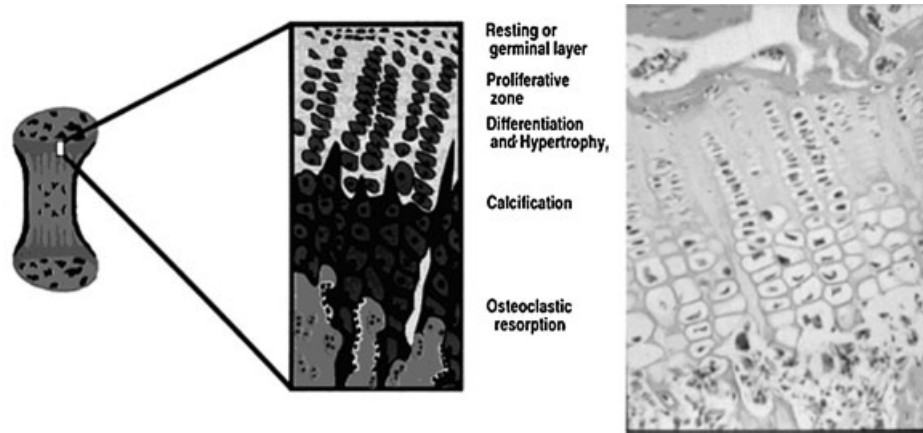


Figure 1. The growth plate. Schematic representation (left) and mouse growth plate (right), illustrating the position and organization of the growth plate, showing the different stages of chondrocyte maturation

The first layer (Zone I or germinal layer) consists of resting chondrocytes, with low proliferation levels, thought to store nutrients for later zones^{10,15}. Zone II is a proliferating zone, where the chondrocytes undergo proliferation to become flattened, forming clusters in longitudinal columns^{15,16}. The third zone consists of maturing chondrocytes, also known as pre-hypertrophic chondrocytes, similar in morphology to those in Zone II but with minimal DNA synthesis^{10,17}. The chondrocytes then become hypertrophic in Zone IV, increasing cell volume and height, with greater synthesis of extracellular matrix^{13,15,16}. Matrix components produced in Zone IV include type X collagen, osteonectin and chondrocalcin, with a reduction in collagen type II synthesis^{12,13,15}. The matrix of the longitudinal septae of the hypertrophic zone mineralizes through the formation of calcium phosphate crystals and the deposition of hydroxyapatite^{10,15}. The chondrocytes then enter the final terminal zone (Zone V), and the matrix is resorbed during vascular invasion to allow invasion of blood vessels, osteoblast precursors and osteoclasts^{12,15}. The fate of the terminally differentiated chondrocyte is likely to involve both apoptosis and autophagy, however, the transdifferentiation of chondrocytes into the osteogenic phenotype has yet to be established^{12,18–20}. In Zone V, the mineralized cartilage remaining after vascular invasion acts as a scaffold for bone deposition by the invading osteoblasts^{15,17}.

The rate of endochondral bone growth is determined by a complex interplay of proliferative kinetics, size of the proliferative pool, matrix production and hypertrophic chondrocyte enlargement²¹. The precise control of these processes is still a matter of debate and any perturbation of these synchronized variables may underlie the growth modulatory effects of external agents such as inflammatory cytokines. The width of the growth plate decreases with age, due to a reduction in cell proliferation and eventually growth stops completely. Rising oestrogen levels are associated with increased mineralization and bone formation within the growth plate leading to eventual replacement of the growth plate by bone and epiphyseal fusion^{11,22}.

GH AND IGF-1 SIGNALLING AND ENDOCHONDRAL GROWTH

Many factors contribute to the rate of bone growth such as hypertrophic cell volume and proliferation rates^{13,16,23}. There are also a number of mediators of bone growth that act to regulate the actions of chondrocytes, including transcription factors such as Sox9 and growth factors including bone morphogenetic proteins^{24,25}. This review will focus on the systemic growth factor GH and the autocrine/paracrine factor IGF-1.

It has long been recognized that GH plays an important role in postnatal, but not embryonic, bone growth. GH deficiency results in impaired postnatal growth, with growth retardation in GH receptor (GHR) knockout mice after 2 weeks of age, while excess GH causes gigantism^{26,27}. Indeed, recombinant human GH (rhGH) is widely used to treat a diverse group of conditions that are associated with short stature and poor growth and range from GH deficiency to conditions such as Prader–Willi syndrome and Turner's syndrome²⁸. Therapy with rhGH has also been used in humans with chronic inflammatory diseases and has shown variable extent of improvement in growth and even disease^{29–31}. IGF-1 deficiency inhibits growth both pre- and postnatal, with IGF-1 knockout mice exhibiting growth retardation and IGF-1 receptor (IGF-1R) deficient mice dying shortly after birth^{26,32}. Furthermore, in humans with GH insensitivity due to a GHR defect, growth retardation and osteoporosis that are the result of IGF-1 deficiency are observed.³³ More recently, abnormalities of STAT5b, the IGF-1 receptor gene itself and the binding proteins that influence bioavailability of IGF-1 at the tissue level have all been reported to be associated with a variable extent of short stature in humans².

The original model implicating GH and IGF-1 as central regulators of bone growth was termed the somatomedin hypothesis³⁴. It proposed that GH exerted its effects on the growth plate by stimulating production of hepatic IGF-1 (previously known as somatomedin), which would in turn

stimulate target tissues including bone and the growth plate^{26,34,35}. The somatomedin hypothesis has been questioned by experiments reporting that low concentrations of GH directly infused into the growth plate stimulated longitudinal growth in comparison to the contralateral limb³⁶. The somatomedin hypothesis has been further challenged with the recent observation that whilst IGF-1 knockout mice are growth retarded, targeted removal of hepatic IGF-1 alone does not affect growth, demonstrating that although the majority of IGF-1 is produced by the liver it is not required for postnatal growth³⁷. Furthermore, growth of complete IGF-1 knockout mice do not respond to GH administration whereas hepatic IGF-1 knockout mice do³⁷. It is now thought that GH can act independently on the growth plate to increase chondrocyte proliferation, as well as stimulating local production of IGF-1²². In combination with other similar studies, these observations have led to an alternative hypothesis termed the dual effector theory, where GH acts directly on germinal zone precursors of the growth plate to stimulate the differentiation of chondrocytes and the amplification of local IGF-1 secretion. This locally produced IGF-1, in turn, stimulates both chondrocyte clonal expansion and hypertrophy and consequently bone growth in an autocrine/paracrine manner^{36,38–40}. Thus, although liver-derived IGF-1 is the main determinant of systemic IGF-1 levels, it is locally derived IGF-1 that appears more important for postnatal growth^{41,42}. In fact, it is likely that GH and IGF-1 have both dual and overlapping functions on chondrocytes, as both GHR and IGF-1 mutant mice show reduced growth which is more severe in double GHR/IGF-1 mutants^{26,43}. However, it is yet unclear if GH mediates any IGF-1 independent effects on chondrocytes. Data on GH actions on chondrocyte proliferation have so far been largely conflicting; with some authors showing strong proliferative effects of GH while others show little or none^{44–46}.

The GHR is a member of the class I cytokine receptor superfamily, and contains an extracellular domain (ECD) consisting of two fibronectin type III sandwich domains, which is connected to a helical transmembrane domain leading to the intracellular domain (ICD) consisting of two box motifs^{47,48}. GH signalling follows GH activation of the GHR with dimerization of the ECD, leading to phosphorylation of the ICD⁴⁹. This allows binding and phosphorylation of the tyrosine (Tyr) kinase Janus kinase 2 (JAK2) at Box 1 in the ICD, which, in turn, phosphorylates specific Tyr residues on the associated ICD^{48–50}. These phosphorylated residues create binding sites for Src homology 2 (SH2) domain proteins, including signal transduction and activators of transcription (STAT)1, STAT3 and STAT5 proteins^{48,49}. STAT proteins often have two isoforms, for example STAT5a and STAT5b, thought to have separate and related functions^{51,52}. The identity of which GHR Tyr residues STAT5 preferentially binds is unclear, with evidence for stronger binding at Tyr534, Tyr566 and Tyr627, and weaker binding to Tyr595 and Tyr487⁵⁰. The STAT proteins are phosphorylated by JAK2 at the specific Tyr and/or serine residues, leading to homo- or heterodimerization and migration to the nucleus, activating gene

transcription^{48,49,52–54}. Although GH signalling through STAT proteins is the primary signalling pathway (Figure 2) there are elements of this signalling cascade that are not yet fully defined, leading to different models. For example, the mechanisms by which GH activates its receptor is debated, and may involve GH activating GHR dimerization as described above; GH binding causing GHR to internalize and auto-phosphorylate or GH stimulating conformational change of a constitutively dimerized GHR^{43,48,50}. The latter model is becoming more favoured, and has been supported by the hypothesis that upon ligand binding the cytoplasmic domains of the two GHR subunits constitutively bind JAK2 kinases, permitting the receptor subunits to rotate to allow aligned JAK2 proteins to activate each other⁴⁹. GH may regulate the phosphorylation of a range of STATs and this may depend on the cell type; for example, STAT5 is activated by GH in adipocytes but not in adherent epithelial cells⁵³. To date, it is unclear which STATs are utilized by GH signalling in growth plate chondrocytes. STAT5 null mice show growth retardation, with narrower growth plate proliferating zones and reduced circulating IGF-1, but their phenotype is slightly different to GHR knockout mice^{49,55}. Growth retardation of STAT5 null mice appears earlier and is less severe than in GHR null mice and appears to be due to an endochondral ossification fault as opposed to the premature growth plate senescence observed in GHR null mice^{49,55}. Also, STAT5 null mice show normal bone remodelling, whereas GHR null mice have lowered levels of bone remodelling⁴³. These different phenotypes suggest GH actions on chondrocytes have STAT5 independent effects. Interestingly, growth retardation and reduced circulating IGF-1 are observed in STAT5b null mice but not STAT5a null mice, suggesting that STAT5b may be the important isoform in GH signalling in bones⁵². STAT3 null mice are embryonic lethal, while STAT1 null mice are of normal size^{56–58}. In humans, mutations in STAT5b are associated with GH insensitivity and severe short stature⁵⁹.

One of the outcomes of GH signalling is induction of IGF-1 gene expression, the mechanisms of which are poorly understood⁵². Most evidence suggests that GH signalling through STAT5b leads directly to IGF-1 induction although other transcription factors may also be involved^{52,60,61}. IGF-1 signalling can occur both dependently and independently of GH. Prenatally, IGF-1 signalling is considered to be GH independent whereas postnatally, IGF-1 signalling is partly or fully GH dependent⁶². IGF-1 can be found in the circulation bound in a complex with IGF binding proteins such as IGF binding protein-3 (IGFBP-3) and the acid-labile subunit (ALS)^{63,64}. These complexes increase the half-life of circulating IGF-1 and target the ligand to its receptor.⁶⁵ Other binding proteins, such as IGFBP-1, inhibit IGF-1 bioactivity due to their greater affinity for IGF-1 than the IGF-1R^{65,66}.

In chondrocytes, IGF-1 signalling (Figure 3) involves IGF-1 binding a cell surface receptor Tyr kinase (IGF-1R) to induce IGF-1R conformational change (dimerization), leading to autophosphorylation of the receptor intracellular

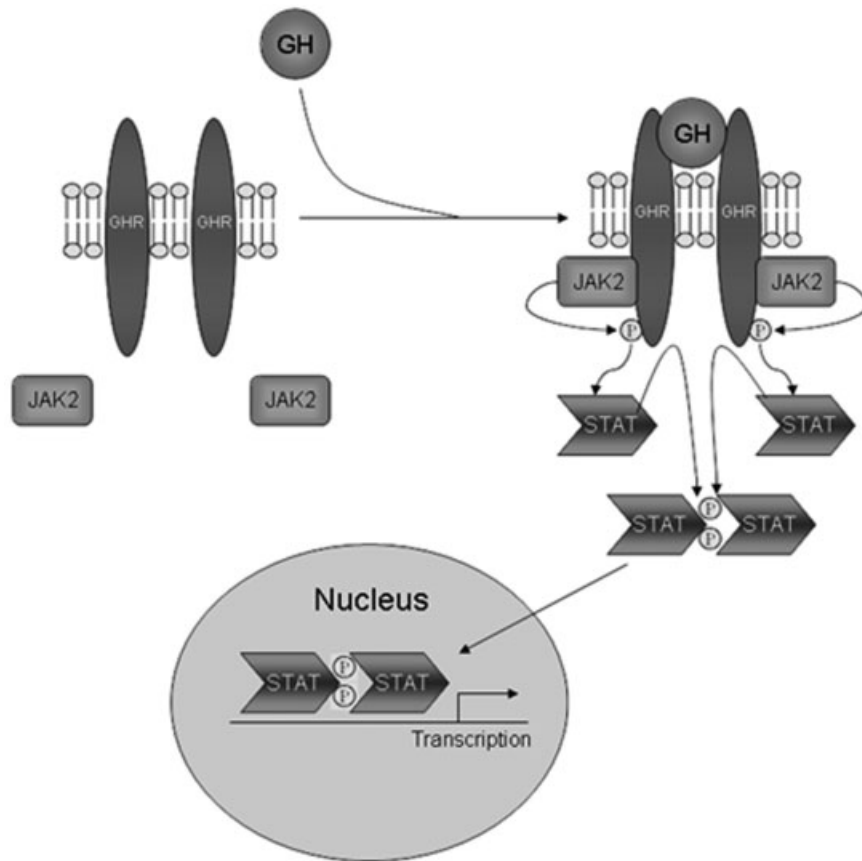


Figure 2. GH signalling via the JAK/STAT pathway. A representation of how GH may signal through JAK/STAT proteins in the cell, leading to gene transcription. Briefly, GH binds its receptor, leading to JAK2 and STAT activation. STAT proteins can then dimerize and translocate to the nucleus to initiate gene transcription

domain⁶². The receptor then phosphorylates immediate downstream substrates, insulin receptor substrate-1 (IRS-1) and Shc, which activate downstream pathways important for anti-apoptosis and proliferative effects^{7,67,68}. For example, IRS-1 provides binding sites for phosphoinositide 3-kinase (PI3K) that causes downstream signalling through other molecules including Akt^{7,52,67}. It is worth noting that as IGF-1R does not contain specific Tyr based motifs recognized by STATs, IGF-1 is not thought to signal via the JAK/STAT pathway^{54,69}. Despite this, there is a small amount of evidence of IGF-1 stimulation of STAT3 via JAK1, which clearly warrants more in depth investigation^{70,71}. IRS-1 has been shown to be vital to bone growth as chondrocytes in IRS-1 knockout mice have lower levels of proliferation, which undergo faster apoptosis and the growth plate closes early^{43,67}. This results in decreased bone turnover and reduced animal growth and weight^{43,67}. IRS-1 null mice also show impaired fracture healing, which can be restored by overexpression of IRS-1 in transgenic mice⁷². The addition of the PI3K inhibitor, LY294002, restricts the IGF-1 mediated increases in chondrocyte proliferation and metatarsal growth, suggesting that the PI3K pathway is crucial in chondrocyte responses to IGF-1^{7,73}. IGF-1 induces somatostatin which inhibits GH release and thereby forms a classical negative feedback loop⁴³.

INHIBITION OF BONE GROWTH BY INFLAMMATORY CYTOKINES

Many chronic childhood inflammatory diseases, such as IBD and juvenile idiopathic arthritis (JIA), are associated with growth retardation coupled with elevated levels of inflammatory cytokines such as IL-6, TNF α and IL-1 β ^{6,7,74}. Growth retardation in these patients is further exacerbated by the use of anti-inflammatory glucocorticoids such as dexamethasone that are known to inhibit bone growth and development⁵. Patients with inflammatory conditions have unchanged levels of GH but reduced levels of circulating IGF-1, indicating GH resistance^{75,76}. They also show lower concentrations of IGFBP-3^{75,76}. Treatment with relatively high doses of recombinant human GH has been shown to improve growth in children with JIA^{77,78}.

Mice overexpressing IL-6 or TNF α exhibit growth retardation, with IL-6 overexpression resulting in reduced IGF-1 and IGFBP-3 levels, as observed in patients^{75,79-81}. The IL-6 growth defect can be completely abolished by IL-6 neutralization⁸². Treatment with IL-1 β results in reduced plasma levels of IGF-1 and ALS^{83,84}. There is also evidence that IL-1 β stimulates IGFBP-1 protein expression, which will inhibit IGF-1 activity⁸⁵⁻⁸⁷.

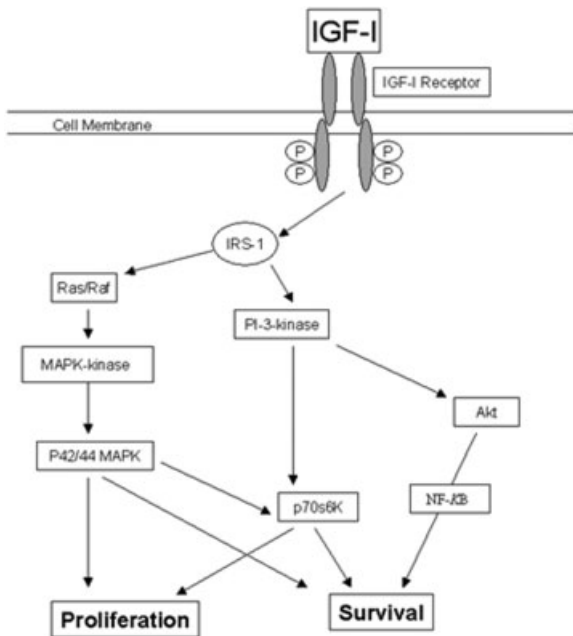


Figure 3. The IGF-1 signalling pathways, showing how IGF-1 signals through IRS-1 to activate downstream molecules important for cell survival. Image adapted from MacRae *et al.*¹³⁵

Few studies have reported the effects of inflammatory cytokines on the growth plate. Elevated levels of IL-1 β , TNF α and IL-6 during inflammatory synovitis lead to local destruction of the growth plate⁸⁸. IL-1 β and TNF α decrease both the width of the proliferating zone and the rate of endochondral bone growth; a possible consequence of altered chondrocyte proliferation and apoptosis rates^{89–91}. Furthermore, IL-1 β and TNF α reduce chondrocyte expression of proteoglycans including aggrecan and collagen types II and X^{89,92,93}. IL-6, in combination with IL-6 receptor, has been shown to inhibit articular chondrocyte differentiation, but IL-6 appears to have little effect on growth plate chondrocytes^{90,94}. Some of these effects, in particular those that result in destruction of the growth plate are likely to be a consequence of increased production of matrix metalloproteinase (MMPs)⁸⁴. The catabolic actions of MMPs on cartilage are well recognized and will counteract the anabolic actions of the GH/IGF-I axis⁹⁵. This topic is not covered further in this review as these actions are likely to be independent of SOCS2 function.

It is likely that one of the cellular mechanisms through which inflammatory cytokines act on the growth plate is by inhibiting IGF-1 signalling^{96,97}. Neither TNF α nor IL-1 β appear to affect IGF-1 signalling at its receptor level although this has been poorly investigated in chondrocytes^{6,98–100}. Alternatively, inflammatory cytokines may disrupt signalling downstream of the IGF-1R, for example, IRS phosphorylation, MAPK signalling or PI3K signalling. It has been suggested that IL-1 β is likely to inhibit the proliferative effect of IGF-1 on chondrocytes via the PI3K pathway⁷. TNF α and IL-1 β inhibit IRS-1 phosphorylation in myoblasts, and TNF α has been shown to inhibit Akt phosphorylation and MAPK-kinase phosphorylation in

neuronal cells^{96,97,100}. It is also possible that inflammatory cytokines act on GH signalling but to date little knowledge of the effects of inflammatory cytokines on STAT signalling in chondrocytes exists. IL-6 and oncostatin M has been shown to activate JAK2, STAT1 and STAT3 (IL-6 only) in chondrocytes, leading to down-regulation of matrix components^{94,101}. IL-1 β has been shown to antagonize GH signalling through STAT5 in hepatocytes, and has been shown to activate STAT3 in mouse kidney tumour cells^{102,103}. There is also evidence that IL-1 β , IL-6 and TNF α can induce the expression of SOCS proteins, which act to inhibit GH signalling^{104,105}.

ACTIONS OF SOCS2

Cytokine signalling is negatively controlled by a variety of proteins including protein Tyr phosphatases and SOCS⁸. There have been eight SOCS molecules identified to date, namely, CIS and SOCS1–7, all of which are involved in negatively regulating cytokine signalling. SOCS proteins consist of a conserved C-terminal motif named the SOCS box, a central SH2 domain and a variable N-terminal domain^{8,106}. SOCS proteins act to inhibit JAK/STAT signalling pathways thus down-regulating cytokine and growth factor signalling⁸.

Expression of SOCS is normally stimulated by the very cytokines they inhibit, thereby creating a negative feedback loop^{8,107}. GH signalling is inhibited by CIS, SOCS1, 2 and 3, but more information is available on the actions of SOCS2 on growth as SOCS1 and SOCS3 knockout mice die prematurely albeit with retarded growth^{108–110}. In contrast, SOCS2 knockout mice are viable and exhibit an overgrowth phenotype from 3 weeks of age⁹. Inhibition of GH signalling by SOCS1 and 3 is complete, whereas SOCS2 and CIS only cause partial inhibition and it is difficult to reconcile these actions with the observed growth of the transgenic mice^{111–113}. Clearly, other interactions are important, possibly involving the other SOCS proteins (4–7) but their role in growth regulation are unknown to date.

The overgrowth phenotype of SOCS2 knockout (SOCS2^{-/-}) mice has led to confirmation that the key pathway regulated by SOCS2 is the GH/IGF-1 axis although SOCS2 also regulates other pathways including prolactin signalling^{8,9,114}. Adult male SOCS2^{-/-} mice are 40% heavier than their wild-type littermates and are more severely affected than females. However, adult females still reach the same size as wild-type males⁹. The increased body weight of SOCS2^{-/-} is not as a result of any increase in fatty tissue, but rather a proportional increase in size of most internal organs, muscle and bones, due to hyperplasia and not hypertrophy⁹. Consistent with increased bone size, SOCS2^{-/-} mice have longer longitudinal bones (femur, tibia, radius and humerus) as well as increased body length^{9,115}. Consistent with this, the growth plates in SOCS2^{-/-} mice are wider, with wider proliferative and hypertrophic zones¹¹⁵. Some studies have shown reduced trabecular and cortical bone mineral density (BMD) in SOCS2^{-/-} bones, which is not consistent with the enhanced

GH/IGF-1 signalling observed in the SOCS2^{-/-} mice^{8,116}. More recent studies using high resolution analyses of trabecular bone architecture and cortical bone geometry has found that SOCS2^{-/-} mice exhibit no BMD difference compared to wild type littermates, coupled with increased trabecular bone volume¹¹⁵. SOCS2^{-/-} mice display elevated IGF-1 mRNA in some tissues, but interestingly circulating IGF-1 levels are not increased^{115,117}. Greenhalgh *et al.* demonstrated firm evidence that SOCS2 acts on the GH pathway by crossing SOCS2^{-/-} mice with Ghrhr^{lit/lit} mice, which are GH deficient due to a point mutation in the GH-releasing hormone^{118,119}. Both the double knockout mice and the Ghrhr^{lit/lit} mice exhibited a similar 60% growth retardation^{118,119}. Furthermore, administration of GH to these double knockout mice caused an increase of growth to a size indistinguishable from SOCS2^{-/-} mice^{118,119}. An interaction between SOCS2 and GH signalling in regulating growth is consistent with the temporal increased expression of the GHR and the overgrowth phenotype with both occurring at around 3-weeks of age⁹. Moreover, prolonged STAT5 activation in response to GH has been observed in hepatocytes cultured from SOCS2^{-/-} mice, which may result in increased IGF-1 activation^{107,118,120}. When SOCS2^{-/-} mice are crossed with STAT5b^{-/-} mice the overgrowth phenotype is attenuated, with normal growth observed^{47,118,120}.

It has been well documented that GH signalling stimulates SOCS2 expression, in a dose and concentration dependant manner, with the maximum affect observed after 24 h treatment with 0.5–5.0 µg GH /mL¹⁰⁶. Furthermore, it is thought that SOCS2 production is regulated by GH signalling through STAT5b, which is consistent with the importance of STAT5b for growth¹²¹. This confirms the hypothesis that SOCS2 acts in a negative feed back loop to control and regulate GH signalling under physiological conditions and offers a plausible explanation for the overgrowth phenotype of SOCS2^{-/-} mice¹⁰⁶. High SOCS2 expression has been found in the liver, a major source of circulating IGF-1, and in the heart¹⁰⁶.

The precise mechanism by which SOCS2 regulates GH signalling is unclear. The strongest evidence indicates that SOCS2 may bind the SHP2-binding sites on the GHR (Tyr595 and Tyr487), which will prevent STAT5b activation^{50,119,122}. It has also been demonstrated that SOCS2 binds elongins B and C, suggesting this complex may then bind cullin-2 and act as an E3 ubiquitin ligase to degrade the GHR or the GHR-JAK2 complex^{8,117,123}. Furthermore, it has been demonstrated that the SOCS2 SH2 domain directly binds a Tyr in the activation loop of JAK2, inhibiting JAK2 Tyr phosphorylation and activation of STATs^{8,47}. Interestingly, SOCS2 actions may not be confined to regulating GH signalling. SOCS2 directly binds the IGF-1R and therefore it is possible that SOCS2 also regulates IGF-1 signalling although IGF-1 does not induce SOCS2 expression^{117,124,125}.

Similar phenotypes to the SOCS2^{-/-} mice have been observed in high growth (hg) mice, a phenotype that occurs following a spontaneous mutation in mouse chromosome 10

that has been mapped to a genetic interval of 100–103 cM from the top of human chromosome 12^{126–128}. Again, these mice demonstrate 30–50% increases in postnatal growth and the identification of the SOCS2^{-/-} mouse phenotype has led to SOCS2 being mapped to the hg region^{126,127}. The only recognized difference between hg and SOCS2^{-/-} mice is that hg mice have high plasma IGF-1, possibly due to another gene deletion in the hg region¹²⁶.

Intriguingly, overexpression of SOCS2 using a human ubiquitin promoter does not limit growth as may be expected, but in fact results in a similar phenotype to SOCS2^{-/-} mice^{107,129}. Transgenic expression of SOCS2 in male mice causes a 13–15% increase in body weight, with significant increases in female mice also¹²⁹. It is, therefore, likely that the effects of SOCS2 on GH signalling is dose dependant, with dual effects^{47,107,129}. It has been proposed that, at physiological levels, SOCS2 inhibits GH signalling by blocking sites of STAT activation on the GHR, but at higher doses it inhibits signalling of other, more potent GH inhibiting SOCS (SOCS1 and 3)^{107,129,130}. This could be through association with SOCS3 binding sites on the GHR, thus blocking SOCS3 action, or by binding the other SOCS themselves and suppressing them by proteasomal degradation⁵⁰.

Glucocorticoids, including dexamethasone, are thought to desensitize GH signalling and thus suppress growth by up-regulating SOCS2^{8,106}. Estrogen inhibition of GH signalling, through JAK2 inhibition, is also thought to be mediated by SOCS2¹³¹. The effects of inflammatory cytokines on SOCS2, however, have been poorly investigated with evidence that some interleukins induce SOCS2 gene expression in specific cell types (IL-2, -3, -4, -5, -6)^{132,133}. For example, IL-1β has been shown to stimulate SOCS2 in tonsillar cells and B-lymphoma cells whereas it does not increase SOCS2 expression in hepatic liver cells^{102,134}. Furthermore, TNFα stimulates SOCS2 expression in chondrocytes¹¹⁵. There is evidence that IL-1β, TNFα and IL-6 induce expression of SOCS3 in certain cell types^{104,105}.

There are still many aspects on the actions of SOCS2 that have yet to be investigated. The precise mechanism by which SOCS2 alters GH/IGF-I signalling have yet to be fully determined as are the resultant cellular events that occur at the growth plate and are responsible for normal growth. It is also unclear if SOCS2 mediates the deleterious effects of inflammatory cytokines on linear bone growth.

CONCLUSIONS

Inflammatory cytokines may play a key role in mediating growth retardation frequently observed in patients with chronic inflammatory diseases such as JIA and IBD. Such growth disorders are likely to be multifactorial involving a myriad of pathways and mechanisms such as MMP driven catabolic effects and poor nutrition in IBD patients. Growth is further compromised by the use of glucocorticoids as anti-inflammatory agents. However, other mechanisms involving the mediatory actions of SOCS proteins on GH/IGF-1 signalling may be implicated. By examining further the effects of inflammatory cytokines and of SOCS proteins, in

particular SOCS2, on growth plate chondrocytes we will gain a better understanding of the mechanisms behind growth retardation in chronic paediatric diseases, which may lead to enhanced clinical interventions and outcomes.

ACKNOWLEDGEMENTS

We are grateful to the Biotechnology and Biological Sciences Research Council (BBSRC) for studentship funding (CP) and also BBSRC ISPG funding.

REFERENCES

- Kronenberg HM. Developmental regulation of the growth plate. *Nature* 2003; **423**: 332–336.
- Walenkamp MJE, Wit JM. Genetic disorders in the GH IGF-I axis in mouse and man. *Eur J Endocrinol* 2007; **157**: S15–S26.
- Mushtaq T, Ahmed SF. The impact of corticosteroids on growth and bone health. *Arch Dis Child* 2002; **87**: 93–96.
- Vagianos K, Bector S, McConnell J, et al. Nutrition assessment of patients with inflammatory bowel disease. *JPEN J Parenter Enteral Nutr* 2007; **31**: 311–319.
- Ahmed SF, Tucker P, Mushtaq T, et al. Short-term effects on linear growth and bone turnover in children randomized to receive prednisolone or dexamethasone. *Clinical Endocrinol* 2002; **57**: 185–191.
- Macrae VE, Wong SC, Farquharson C, et al. Cytokine actions in growth disorders associated with pediatric chronic inflammatory diseases (Review). *Int J Mol Med* 2006; **18**: 1011–1018.
- Macrae VE, Ahmed SF, Mushtaq T, et al. IGF-I signalling in bone growth: inhibitory actions of dexamethasone and IL-1[β]. *Growth Horm IGF Res* 2007; **17**: 435–439.
- Rico-Bautista E, Flores-Morales A, Fernández-Pérez L. Suppressor of cytokine signaling (SOCS) 2, a protein with multiple functions. *Cytokine Growth Factor Rev* 2006; **17**: 431–439.
- Metcalfe D, Greenhalgh CJ, Viney E, et al. Gigantism in mice lacking suppressor of cytokine signalling-2. *Nature* 2000; **405**: 1069–1073.
- Mackie EJ, Ahmed YA, Tatarczuch L, et al. Endochondral ossification: How cartilage is converted into bone in the developing skeleton. *Int J Biochem Cell Biol* 2008; **40**: 46–62.
- Kember NF, Sissons HA. Quantitative histology of the human growth plate. *J Bone Joint Surg Br* 1976; **58-B**: 426–435.
- Farnum CE, Wilsman NJ. Morphologic stages of the terminal hypertrophic chondrocyte of growth plate cartilage. *Anat Rec* 1987; **219**: 221–232.
- Farnum CE, Wilsman NJ. Determination of proliferative characteristics of growth plate chondrocytes by labeling with bromodeoxyuridine. *Calcif Tissue Int* 1993; **52**: 110–119.
- Ballock RT, O'Keefe RJ. The biology of the growth plate. *J Bone Joint Surg Am* 2005; **85**: 715–726.
- Hunziker EB, Schenk RK, Cruz-Orive LM. Quantitation of chondrocyte performance in growth-plate cartilage during longitudinal bone growth. *J Bone Joint Surg Am* 1987; **69**: 162–173.
- Hunziker EB, Shenk RK. Physiological mechanisms adopted by chondrocytes in regulating longitudinal bone growth in rats. *J Physiol* 1989; **414**: 55–71.
- Farquharson C. *Bone growth*. In *Biology of Growth of Domestic Animals*, Scanes CG (ed). Iowa State Press: Iowa, 2003; 170–185.
- Roach HI, Erenpreisa J, Aigner T. Osteogenic differentiation of hypertrophic chondrocytes involves asymmetric cell divisions and apoptosis. *J Cell Biol* 1995; **131**: 483–494.
- Cancedda R, Cancedda FD, Castagnola P. Chondrocyte differentiation. *Int Rev Cytol* 1995; **159**: 265–358.
- Shapiro IM, Adams CS, Freeman T, et al. Fate of the hypertrophic chondrocyte: microenvironmental perspectives on apoptosis and survival in the epiphyseal growth plate. *Birth Defects Res C Embryo Today* 2005; **75**: 330–339.
- Breur GJ, VanEnkevort A, Farnum CE, et al. Linear relationship between the volume of hypertrophic chondrocytes and the rate of longitudinal bone growth in growth plates. *J Orthop Res* 1991; **9**: 348–359.
- Nilsson O, Marino R, De Luca F, et al. Endocrine regulation of the growth plate. *Horm Res* 2005; **64**: 157–165.
- Kember NF. Comparative patterns of cell division in epiphyseal cartilage plates in the rabbit. *J Anat* 1985; **142**: 185–190.
- Pizette S, Niswander L. BMPs are required at two steps of limb chondrogenesis: formation of prechondrogenic condensations and their differentiation into chondrocytes. *Dev Biol* 2000; **219**: 237–249.
- Akiyama H, Chaboissier MC, Martin JF, et al. The transcription factor Sox9 has essential roles in successive steps of the chondrocyte differentiation pathway and is required for expression of Sox5 and Sox6. *Genes Dev* 2002; **16**: 2813–2828.
- Lupu F, Terwilliger JD, Lee K, et al. Roles of growth hormone and insulin-like growth factor 1 in mouse postnatal growth. *Dev Biol* 2001; **229**: 141–162.
- Cuttler L, Jackson JA, Saeed uz-Zafar M, et al. Hypersecretion of growth hormone and prolactin in McCune-Albright syndrome. *J Clin Endocrinol Metab* 1989; **68**: 1148–1154.
- Hindmarsh PC, Dattani MT. Use of growth hormone in children. *Nat Clin Pract Endocrinol Metab* 2006; **2**: 260–268.
- Slonim AE, Bulone L, Damore MB, et al. A preliminary study of growth hormone therapy for Crohn's disease. *N Engl J Med* 2000; **342**: 1633–1637.
- Mauras N, George D, Evans J, et al. Growth hormone has anabolic effects in glucocorticosteroid-dependent children with inflammatory bowel disease: a pilot study. *Metabolism* 2002; **51**: 127–135.
- Wong SC, Hassan K, McGrogan P, et al. The effects of recombinant growth hormone on linear growth in children with Crohn's disease and short stature. *J Pediatr Endocrinol Metab* 2007; **20**: 1315–1324.
- Baker J, Liu JP, Robertson EJ, et al. Role of insulin-like growth factors in embryonic and postnatal growth. *Cell* 1993; **75**: 73–82.
- Parks JS, Brown MR, Faase ME. The spectrum of growth-hormone insensitivity. *J Pediatr* 1997; **131**: S45–S50.
- Daughaday WH. A personal history of the origin of the somatomedin hypothesis and recent challenges to its validity. *Perspect Biol Med* 1989; **32**: 194–211.
- Daughaday WH, Hall K, Raben MS, et al. Somatomedin: proposed designation for sulphation factor. *Nature* 1972; **235**: 107.
- Isaksson OGP, Jansson JO, Gause IAM. Growth hormone stimulates longitudinal bone growth directly. *Science* 1982; **216**: 1237–1239.
- Liu JL, Yakar S, LeRoith D. Conditional knockout of mouse insulin-like growth factor-1 gene using the Cre/loxP system. *Proc Soc Exp Biol Med* 2000; **223**: 344–351.
- Green H, Morikawa M, Nixon T. A dual effector theory of growth-hormone action. *Differentiation* 1985; **29**: 195–198.
- Zeulak KM, Green H. The generation of insulin-like growth factor-1-sensitive cells by growth hormone action. *Science* 1986; **233**: 551–553.
- Wang J, Zhou J, Bondy CA. IGF1 promotes longitudinal bone growth by insulin-like actions augmenting chondrocyte hypertrophy. *FASEB J* 1999; **13**: 1985–1990.
- Yakar S, Liu JL, Butler A, et al. Normal growth and development in the absence of hepatic insulin-like growth factor 1. *Proc Natl Acad Sci U S A* 1999; **96**: 7324–7329.
- Yakar S, Rosen CJ, Beamer WG, et al. Circulating levels of IGF-1 directly regulate bone growth and density. *J Clin Invest* 2002; **110**: 771–781.
- Giustina A, Mazziotti G, Canalis E. Growth hormone, insulin-like growth factors, and the skeleton. *Endocr Rev* 2008; **29**: 535–559.
- Madsen K, Friberg U, Roos P, et al. Growth hormone stimulates the proliferation of cultured chondrocytes from rabbit ear and rat rib growth cartilage. *Nature* 1983; **304**: 545–547.
- Livne E, Laufer D, Blumenfeld I. Comparison of *in vitro* response to growth hormone by chondrocytes from mandibular condyle cartilage of young and old mice. *Calcif Tissue Int* 1997; **61**: 62–67.
- Hutchinson MR, Bassett MH, White PC. Insulin-like growth factor-I and fibroblast growth factor, but not growth hormone, affect growth plate chondrocyte proliferation. *Endocrinology* 2007; **148**: 3122–3130.
- Flores-Morales A, Greenhalgh CJ, Norstedt G, et al. Negative regulation of growth hormone receptor signaling. *Mol Endocrinol* 2006; **20**: 241–253.

48. Brooks AJ, Wooh JW, Tunny KA, *et al.* Growth hormone receptor; mechanism of action. *Int J Biochem Cell Biol* 2008; **40**: 1984–1989.
49. Waters MJ, Hoang HN, Fairlie DP, *et al.* New insights into growth hormone action. *J Mol Endocrinol* 2006; **36**: 1–7.
50. Uyttendaele I, Lemmens I, Verhee A, *et al.* Mammalian protein-protein interaction trap (MAPPIT) analysis of STAT5, CIS, and SOCS2 interactions with the growth hormone receptor. *Mol Endocrinol* 2007; **21**: 2821–2831.
51. Smit LS, Meyer DJ, Billestrup N, *et al.* The role of the growth hormone (GH) receptor and JAK1 and JAK2 kinases in the activation of Stats 1, 3 and 5 by GH. *Mol Endocrinol* 1996; **10**: 519–533.
52. Herrington J, Smit LS, Schwartz J, *et al.* The role of STAT proteins in growth hormone signaling. *Oncogene* 2000; **19**: 2585–2597.
53. Han YL, Leaman DW, Watling D, *et al.* Participation of JAK and STAT proteins in growth hormone-induced signaling. *J Biol Chem* 1996; **271**: 5947–5952.
54. Decker T, Kovarik P. Serine phosphorylation of STATs. *Oncogene* 2000; **19**: 2628–2637.
55. Sims NA, Clement-Lacroix P, Da Ponte F, *et al.* Bone homeostasis in growth hormone receptor-null mice is restored by IGF-I but independent of Stat5. *J Clin Invest* 2000; **106**: 1095–1103.
56. Takeda K, Noguchi K, Shi W, *et al.* Targeted disruption of the mouse Stat3 gene leads to early embryonic lethality. *Proc Natl Acad Sci USA* 1997; **94**: 3801–3804.
57. Durbin JE, Hackenmiller R, Simon MC, *et al.* Targeted disruption of the mouse Stat1 gene results in compromised innate immunity to viral disease. *Cell* 1996; **84**: 443–450.
58. Meraz MA, White JM, Sheehan KCF, *et al.* Targeted disruption of the Stat1 gene in mice reveals unexpected physiologic specificity in the JAK-STAT signaling pathway. *Cell* 1996; **84**: 431–442.
59. Kofoed EM, Hwa, V, Little B, *et al.* Growth hormone insensitivity associated with a STAT5b mutation. *N Engl J Med* 2003; **349**: 1139–1147.
60. Woelfle J, Chia DJ, Rotwein P. Mechanisms of growth hormone (GH) action—Identification of conserved Stat5 binding sites that mediate GH-induced insulin-like growth factor-I gene activation. *J Biol Chem* 2003; **278**: 51261–51266.
61. Woelfle J, Billiard J, Rotwein P. Acute control of insulin-like growth factor-I gene transcription by growth hormone through Stat5b. *J Biol Chem* 2003; **278**: 22696–22702.
62. Klammt J, Pfäffle R, Werner H, *et al.* IGF signaling defects as causes of growth failure and IUGR. *Trends Endocrinol Metab* 2008; **19**: 197–205.
63. Baxter RC, Martin JL. Structure of the Mr 140,000 growth hormone-dependent insulin-like growth factor binding protein complex: determination by reconstitution and affinity-labeling. *Proc Natl Acad Sci U S A* 1989; **86**: 6898–6902.
64. Firth SM, Baxter RC. Cellular actions of the insulin-like growth factor binding proteins. *Endocr Rev* 2002; **23**: 824–854.
65. Rajaram S, Baylink DJ, Mohan S. Insulin-like growth factor-binding proteins in serum and other biological fluids: regulation and functions. *Endocr Rev* 1997; **18**: 801–831.
66. Jones JJ, D'Ercole AJ, Camacho-Hubner C, *et al.* Phosphorylation of insulin-like growth factor (IGF)-binding protein 1 in cell culture *in vivo*: effects on affinity for IGF-I. *Proc Natl Acad Sci U S A* 1991; **88**: 7481–7485.
67. Hoshi K, Ogata N, Shimoaka T, *et al.* Deficiency of insulin receptor substrate-1 impairs skeletal growth through early closure of epiphyseal cartilage. *J Bone Miner Res* 2004; **19**: 214–223.
68. Michaylira CZ, Ramocki NM, Simmons JG, *et al.* Haplotype insufficiency for suppressor of cytokine signaling-2 enhances intestinal growth and promotes polyp formation in growth hormone-transgenic mice. *Endocrinology* 2006; **147**: 1632–1641.
69. Stahl N, Farruggella TJ, Boulton TG, *et al.* Choice of STATs and other substrates specified by modular tyrosine-based motifs in cytokine receptors. *Science* 1995; **267**: 1349–1353.
70. Zong CS, Chan J, Levy DE, *et al.* Mechanism of STAT3 activation by insulin-like growth factor 1 receptor. *J Biol Chem* 2000; **275**: 15099–15105.
71. Yadav A, Kalita A, Dhillion S, *et al.* JAK/STAT3 pathway is involved in survival of neurons in response to insulin-like growth factor and negatively regulated by suppressor of cytokine signaling-3. *J Biol Chem* 2005; **280**: 31830–31840.
72. Shimoaka T, Kamekura S, Chikuda H, *et al.* Impairment of bone healing by insulin receptor substrate-1 deficiency. *J Biol Chem* 2004; **279**: 15314–15322.
73. Ulici V, Hoenselaar K, Gillespie JR, *et al.* The PI3K pathway regulates endochondral bone growth through control of hypertrophic chondrocyte differentiation. *BMC Dev Biol* 2008; **8**: 40.
74. Macrae VE, Burdon T, Ahmed SF, *et al.* Ceramide inhibition of chondrocyte proliferation and bone growth is IGF-I independent. *J Endocrinol* 2006; **191**: 369–377.
75. De Benedetti F, Meazza C, Oliveri M, *et al.* Effect of IL-6 on IGF binding protein-3: a study in IL-6 transgenic mice and in patients with systemic juvenile idiopathic arthritis. *Endocrinology* 2001; **142**: 4818–4826.
76. Davies UM, Jones J, Reeve J, *et al.* Juvenile rheumatoid arthritis. Effects of disease activity and recombinant human growth hormone on insulin-like growth factor 1, insulin-like growth factor binding proteins 1 and 3, and osteocalcin. *Arthritis Rheum* 1997; **40**: 332–340.
77. Touati G, Prieur AM, Ruiz JC, *et al.* Beneficial effects of one-year growth hormone administration to children with juvenile chronic arthritis on chronic steroid therapy. I. Effects on growth velocity and body composition. *J Clin Endocrinol Metab* 1998; **83**: 403–409.
78. Bechtold S, Ripperger P, Muhlbauer D, *et al.* GH therapy in juvenile chronic arthritis: results of a two-year controlled study on growth and bone. *J Clin Endocrinol Metab* 2001; **86**: 5737–5744.
79. De Benedetti F, Alonzi T, Moretta A, *et al.* Interleukin 6 causes growth impairment in transgenic mice through a decrease in insulin-like growth factor-I. A model for stunted growth in children with chronic inflammation. *J Clin Invest* 1997; **99**: 643–650.
80. Li P, Schwartz EM. The TNF-alpha transgenic mouse model of inflammatory arthritis. *Springer Semin Immunopathol* 2003; **25**: 19–33.
81. Siegel SA, Shealy DJ, Nakada MT, *et al.* The mouse/human chimeric monoclonal antibody cA2 neutralizes TNF *in vitro* and protects transgenic mice from cachexia and TNF lethality *in vivo*. *Cytokine* 1995; **7**: 15–25.
82. De Benedetti F, Pignatti P, Vivarelli M, *et al.* *In vivo* neutralization of human IL-6 (hIL-6) achieved by immunization of hIL-6-transgenic mice with a hIL-6 receptor antagonist. *J Immunol* 2001; **166**: 4334–4340.
83. Barreca A, Ketelslegers JM, Arvigo M, *et al.* Decreased acid-labile subunit (ALS) levels by endotoxin *in vivo* and by interleukin-1[beta] *in vitro*. *Growth Horm IGF Res* 1998; **8**: 217–223.
84. Delhanty PJD. Interleukin-1[beta] suppresses growth hormone-induced acid-labile subunit mRNA levels and secretion in primary hepatocytes. *Biochem Biophys Res Commun* 1998; **243**: 269–272.
85. Lang CH, Fan J, Cooney R, *et al.* IL-1 receptor antagonist attenuates sepsis-induced alterations in the IGF system and protein synthesis. *Am J Physiol Endocrinol Metab* 1996; **270**: E430–E437.
86. Lang CH, Nystrom GJ, Frost RA. Regulation of IGF binding protein-1 in Hep G2 cells by cytokines and reactive oxygen species. *Am J Physiol Gastrointest Liver Physiol* 1999; **276**: G719–G727.
87. Frost RA, Nystrom GJ, Lang CH. Stimulation of insulin-like growth factor binding protein-1 synthesis by interleukin-1[beta]: requirement of the mitogen-activated protein kinase pathway. *Endocrinology* 2000; **141**: 3156–3164.
88. de Hooge, ASK, van de Loo FAG, Bennink MB, *et al.* Growth plate damage, a feature of juvenile idiopathic arthritis, can be induced by adenoviral gene transfer of oncostatin M: a comparative study in gene-deficient mice. *Arthritis Rheum* 2003; **48**: 1750–1761.
89. Macrae VE, Farquharson C, Ahmed SF. The restricted potential for recovery of growth plate chondrogenesis and longitudinal bone growth following exposure to pro-inflammatory cytokines. *J Endocrinol* 2006; **189**: 319–328.
90. Martensson K, Chrysis D, Savendahl L. Interleukin-1beta and TNF-alpha act in synergy to inhibit longitudinal growth in fetal rat metatarsal bones. *J Bone Miner Res* 2004; **19**: 1805–1812.
91. Aizawa T, Kon T, Einhorn TA, *et al.* Induction of apoptosis in chondrocytes by tumor necrosis factor-alpha. *J Orthop Res* 2001; **19**: 785–796.
92. Horiguchi M, Akiyama H, Ito H, *et al.* Tumour necrosis factor-alpha up-regulates the expression of BMP-4 mRNA but inhibits chondrogenesis in mouse clonal chondrogenic EC cells, ATDC5. *Cytokine* 2000; **12**: 526–530.

93. Goldring MB, Birkhead J, Sandell LJ, *et al.* Interleukin 1 suppresses expression of cartilage-specific types II and IX collagens and increases types I and III collagens in human chondrocytes. *J Clin Invest* 1988; **82**: 2026–2037.
94. Legendre F, Dudhia J, Pujol JP, *et al.* JAK/STAT but not ERK1/ERK2 pathway mediates interleukin (IL)-6/soluble IL-6R down-regulation of type II collagen, aggrecan core, and link protein transcription in articular chondrocytes. *J Biol Chem* 2003; **278**: 2903–2912.
95. Reynolds JJ, Hembry RM, Meikle MC. Connective tissue degradation in health and periodontal disease and the roles of matrix metalloproteinases and their natural inhibitors. *Adv Det Res* 1994; **8**: 312–319.
96. Broussard SR, McCusker RH, Novakofski JE, *et al.* IL-1{beta} impairs insulin-like growth factor I-induced differentiation and downstream activation signals of the insulin-like growth factor I receptor in myoblasts. *J Immunol* 2004; **172**: 7713–7720.
97. Kenchappa P, Yadav A, Singh G, *et al.* Rescue of TNF-alpha-inhibited neuronal cells by IGF-1 involves Akt and c-Jun N-terminal kinases. *J Neurosci Res* 2004; **76**: 466–474.
98. Matsumoto T, Tsukazaki T, Enomoto H, *et al.* Effects of interleukin-1 beta on insulin-like growth factor-I autocrine/paracrine axis in cultured rat articular chondrocytes. *Ann Rheum Dis* 1994; **53**: 128–133.
99. Shen WH, Zhou JH, Broussard SR, *et al.* Proinflammatory cytokines block growth of breast cancer cells by impairing signals from a growth factor receptor. *Cancer Res* 2002; **62**: 4746–4756.
100. Strle K, Broussard SR, McCusker RH, *et al.* Proinflammatory cytokine impairment of insulin-like growth factor I-induced protein synthesis in skeletal muscle myoblasts requires ceramide. *Endocrinology* 2004; **145**: 4592–4602.
101. Li WQ, Dehnade F, Zafarullah M. Oncostatin M-induced matrix metalloproteinase and tissue inhibitor of metalloproteinase-3 genes expression in chondrocytes requires janus kinase/STAT signaling pathway. *J Immunol* 2001; **166**: 3491–3498.
102. Boisclair YR, Wang J, Shi J, *et al.* Role of the suppressor of cytokine signaling-3 in mediating the inhibitory effects of interleukin-1beta on the growth hormone-dependent transcription of the acid-labile subunit gene in liver cells. *J Biol Chem* 2000; **275**: 3841–3847.
103. Liu XB, Shi Q, Sigmund CD. Interleukin-1 beta attenuates renin gene expression via a mitogen-activated protein kinase kinase-extracellular signal-regulated kinase and signal transducer and activator of transcription 3-dependent mechanism in As4. 1 cells. *Endocrinology* 2006; **147**: 6011–6018.
104. Shi H, Tzamelis I, Bjorbaek C, *et al.* Suppressor of cytokine signaling 3 is a physiological regulator of adipocyte insulin signaling. *J Biol Chem* 2004; **279**: 34733–34740.
105. Denson LA, Held MA, Menon RK, *et al.* Interleukin-6 inhibits hepatic growth hormone signaling via upregulation of Cis and Socs-3. *Am J Physiol Gastrointest Liver Physiol* 2003; **284**: G646–G654.
106. Tollet-Egnell P, Flores-Morales A, Stavreus-Evers A, *et al.* Growth hormone regulation of SOCS-2, SOCS-3, and CIS messenger ribonucleic acid expression in the rat. *Endocrinology* 1999; **140**: 3693–3704.
107. Turnley AM. Role of SOCS2 in growth hormone actions. *Trends Endocrinol Metab* 2005; **16**: 53–58.
108. Starr R, Metcalf D, Elefanti AG, *et al.* Liver degeneration and lymphoid deficiencies in mice lacking suppressor of cytokine signaling-1. *Proc Natl Acad Sci U S A* 1998; **95**: 14395–14399.
109. Alexander WS, Starr R, Fenner JE, *et al.* SOCS1 is a critical inhibitor of interferon [gamma] signaling and prevents the potentially fatal neonatal actions of this cytokine. *Cell* 1999; **98**: 597–608.
110. Roberts AW, Robb L, Rakar S, *et al.* Placental defects and embryonic lethality in mice lacking suppressor of cytokine signaling 3. *Proc Natl Acad Sci U S A* 2001; **98**: 9324–9329.
111. Adams TE, Hansen JA, Starr R, *et al.* Growth hormone preferentially induces the rapid, transient expression of SOCS-3, a novel inhibitor of cytokine receptor signaling. *J Biol Chem* 1998; **273**: 1285–1287.
112. Hansen JA, Lindberg K, Hilton DJ, *et al.* Mechanism of inhibition of growth hormone receptor signaling by suppressor of cytokine signaling proteins. *Mol Endocrinol* 1999; **13**: 1832–1843.
113. Inaba M, Saito H, Fujimoto M, *et al.* Suppressor of cytokine signaling 1 suppresses muscle differentiation through modulation of IGF-I receptor signal transduction. *Biochem Biophys Res Commun* 2005; **328**: 953–961.
114. Rico-Bautista E, Greenhalgh CJ, Tollet-Egnell P, *et al.* Suppressor of cytokine signaling-2 deficiency induces molecular and metabolic changes that partially overlap with growth hormone-dependent effects. *Mol Endocrinol* 2005; **19**: 781–793.
115. Macrae VE, Horvat S, Pells SC, *et al.* Increased bone mass, altered trabecular architecture and modified growth plate organization in the growing skeleton of SOCS2 deficient mice. *J Cell Physiol* 2009; **218**: 276–284.
116. Lorentzon M, Greenhalgh CJ, Mohan S, *et al.* Reduced bone mineral density in SOCS-2-deficient mice. *Pediatr Res* 2005; **57**: 223–226.
117. Greenhalgh CJ, Alexander WS. Suppressors of cytokine signalling and regulation of growth hormone action. *Growth Horm IGF Res* 2004; **14**: 200–206.
118. LeRoith D, Nissley P. Knock your SOCS off! *J Clin Invest* 2005; **115**: 233–236.
119. Greenhalgh CJ, Rico-Bautista E, Lorentzon M, *et al.* SOCS2 negatively regulates growth hormone action *in vitro* and *in vivo*. *J Clin Invest* 2005; **115**: 397–406.
120. Greenhalgh CJ, Bertolino P, Asa SL, *et al.* Growth enhancement in suppressor of cytokine signaling 2 (SOCS-2)-deficient mice is dependent on signal transducer and activator of transcription 5b (STAT5b). *Mol Endocrinol* 2002; **16**: 1394–1406.
121. Vidal OM, Merino R, Rico-Bautista E, *et al.* *In vivo* transcript profiling and phylogenetic analysis identifies suppressor of cytokine signaling 2 as a direct signal transducer and activator of transcription 5b target in liver. *Mol Endocrinol* 2007; **21**: 293–311.
122. Yoshimura A, Naka T, Kubo M. SOCS proteins, cytokine signalling and immune regulation. *Nat Rev Immunol* 2007; **7**: 454–465.
123. Ram PA, Waxman DJ. SOCS/CIS protein inhibition of growth hormone-stimulated STAT5 signaling by multiple mechanisms. *J Biol Chem* 1999; **274**: 35553–35561.
124. Dey BR, Spence SL, Nissley P, *et al.* Interaction of human suppressor of cytokine signaling (SOCS)-2 with the insulin-like growth factor-I receptor. *J Biol Chem* 1998; **273**: 24095–24101.
125. Michaylira CZ, Simmons JG, Ramocki NM, *et al.* Suppressor of cytokine signaling-2 limits intestinal growth and enterotrophic actions of IGF-I *in vivo*. *Am J Physiol Gastrointest Liver Physiol* 2006; **291**: G472–G481.
126. Horvat S, Medrano JF. Lack of Socs2 expression causes the high-growth phenotype in mice. *Genomics* 2001; **72**: 209–212.
127. Horvat S, Medrano JF. Interval mapping of high growth (hg), a major locus that increases weight gain in mice. *Genetics* 1995; **139**: 1737–1748.
128. Horvat S, Medrano JF. A 500-kb YAC and BAC contig encompassing the high-growth deletion in mouse chromosome 10 and identification of the murine Raidd/Cradd gene in the candidate region. *Genomics* 1998; **54**: 159–164.
129. Greenhalgh CJ, Metcalf D, Thaus AL, *et al.* Biological evidence that SOCS-2 can act either as an enhancer or suppressor of growth hormone signaling. *J Biol Chem* 2002; **277**: 40181–40184.
130. Favre H, Benhamou A, Finidori J, *et al.* Dual effects of suppressor of cytokine signaling (SOCS-2) on growth hormone signal transduction. *FEBS Lett* 1999; **453**: 63–66.
131. Leung KC, Doyle N, Ballesteros M, *et al.* Estrogen inhibits GH signaling by suppressing GH-induced JAK2 phosphorylation, an effect mediated by SOCS-2. *Proc Natl Acad Sci U S A* 2003; **100**: 1016–1021.
132. Krebs DL, Hilton DJ. SOCS proteins: negative regulators of cytokine signaling. *Stem Cells* 2001; **19**: 378–387.
133. Starr R, Willson TA, Viney EM, *et al.* A family of cytokine-inducible inhibitors of signalling. *Nature* 1997; **387**: 917–921.
134. Dogusan Z, Hooghe-Peters EL, Berus D, *et al.* Expression of SOCS genes in normal and leukemic human leukocytes stimulated by prolactin, growth hormone and cytokines. *J Neuroimmunol* 2000; **109**: 34–39.
135. Macrae VE, Farquharson C, Ahmed SF. The pathophysiology of the growth plate in juvenile idiopathic arthritis. *Rheumatology* 2006; **45**: 11–19.